Report 4425

...ncephalographic Monitoring ...plex Mental Tasks

...Richard Montgomery,
...and Chris Hickey

NASA Contractor Report 4425

Electroencephalographic Monitoring of Complex Mental Tasks

Raul Guisado, Richard Montgomery,
Leslie Montgomery, and Chris Hickey
Center for Neurodiagnostic Study, Inc.
San Jose, California

Prepared for
Langley Research Center
under Contract NAS1-18847

National Aeronautics and
Space Administration

Office of Management

Scientific and Technical
Information Program

1992

INDEX

I. EXECUTIVE SUMMARY

This final report outlines the development of neurophysiological procedures to monitor operators during the performance of cognitive tasks. Our approach included use of electroencephalographic (EEG) and rheoencephalographic (REG) measures of cerebral function. EEG was used to determine changes in cortical function associated with cognition and REG was used to monitor changes in operator's state (fatigue, boredom, effects of learning). During the study period testing, analytical and display procedures for EEG and REG monitoring were developed, that extend the state of the art and provide a valuable tool for the study of cerebral circulatory and neural activity during cognition.

A two channel tetrapolar REG, a single channel forearm impedance plethysmograph, a Lead I electrocardiogram (ECG) and a 21 channel EEG were used to measure subject responses to various visual-motor cognitive tasks as administered by specially developed software. EEG and REG recordings were done sequentially in order to facilitate direct comparison between the two modalities.

It is expected that the analysis of cognitive EEG/REG test sequences will facilitate studies of learning and memory disorders, dementias and other encephalopathies. The near-real time capability of the recording equipment will facilitate monitoring of patients with a variety of neurological disorders and will allow researchers to obtain immediate feed-back of results to optimize experimental conditions during the recording session.

EEG METHODS

Our EEG methodology was influenced by the generally accepted view that certain regions of the cerebral cortex have specialized roles in cognition. For instance, the occipital cortex plays a major role in initial analysis of visually presented cognitive stimuli and may also facilitate visualization during later stages of reasoning; linguistic analysis draws more strongly on left hemispheric resources and so on.

This emphasis upon topographic sequences of cortical activation over the course of a cognitive task dictated two special objectives: 1) the development of computer graphical techniques for integrating separate electrode time traces into a 3-D picture of the evolving cortical electrical field and 2) development of data reduction procedures to enhance the spatial resolution of EEG data.

Both goals were attained by use of a least squares surface modeling technique that fitted a surface to the set of simultaneous electrode voltage readings at each instant. The

resulting surface displays, on a computer screen, the evolving pattern of cortical activation during cognition. The least squares equation for the voltage surface at each instant permits direct mathematical transformation of the data to increase spatial resolution.

This approach represents a departure from traditional EEG analysis techniques that rely on measurements of cortically-generated currents flowing through the skull and onto the scalp. These procedures assume that the recorded EEG voltage fluctuations are primarily due to the effects of the radiated cortical electrical field upon scalp surface charges, instead of conduction effects through the skull. This approach seems plausible considering the high resistivity of the skull.

REG METHODS

The REG methodology attempted to characterize cerebral hemodynamic responses by graphical analysis of pulse waveforms recorded during the performance of cognitive tasks, a procedure that required precise real-time coordination of multiple experimental parameters. This was accomplished by developing a control board and software capable of executing all monitoring, display and control functions to within a temporal resolution of 1 millisecond. A rheoencephalographic impedance trace scanning system (RHEOSYS) was developed to automate analysis of the impedance waveforms.

EXPERIMENTAL APPROACH

The experimental approach included these eight aspects: 1) the development of three distinct visual-motor cognitive tasks presented by means of a computer screen at three jury-selected levels of difficulty; 2) generation of ensemble averaged event-related potentials (ERPs) for each cognitive task; 3) development of analytical procedures to evaluate the whole-scalp shape of the cognitive ERP; 4) mathematical modeling of the scalp electrocortical field to increase the spatial resolution of the EEG signal; 5) correlation of electrocortical activity and indices of task performance; 6) development of prolonged cognitive tasks to assess the stability of the cognitive ERP over time; 7) simultaneous measure of EEG and REG signals and 8) measurement of hemodynamic changes induced by prolonged cognitive effort.

RESULTS

The following paragraphs summarize the outcome of each of these eight aspects:

a) Cognitive tasks: Three discrete visual-motor cognitive tasks were developed by modification of a standard cognitive protocol (Action and Crabtree, 1985; Shingledecker, 1984). During Phase I of this project

(Guisado, et. al., 1988) it was found that apparent monotonic changes in the ERP voltages in the occipital region with increasing levels of task difficulty could be related to physical changes in the nature of the cognitive stimulus. During Phase II of this project, the cognitive protocol was modified to correct these artifacts and prevent subtle mislabeling of the task levels.

The three cognitive tasks selected included arithmetic (MATH), semantic (VERB) and shape-recognition (SPAT) processing tasks. In addition a manual tracking task (TRACK) and a long term cognitive task (LONG) were used to test the stability of the findings. The cognitive stimulus protocol is described on pages 8-9 of this report.

b) Data analysis: Time-gated EEG segments from each cognitive task were ensemble averaged to obtain cognitive ERPs. A least squares estimate of the spatial distribution of scalp voltage levels was obtained, at each digital sampling point in the ensemble-averaged ERP. The Laplacian of the voltage distribution was then obtained by using the least-squares equation for the voltage surface. This produced a second surface that improved the spatial resolution of the EEG data, by reducing spatial smearing of the signal induced by volume conduction. A further improvement in the spatial resolution of the EEG data was obtained by estimating the potential energy of the electrical field imposed upon the scalp by the cortical electropotential field.

c) Correlation with performance: A procedure was developed for regressing task performance on EEG energy density. Task performance was represented by an "error rate" index which combines a subject's average reaction-time and percentage of mistakes in the responses included in the averaged cognitive ERP. Energy density was measured as an integral over a 40 msec period at a particular electrode site. A search procedure was carried out to find time windows and electrode locations for which the regression fit is optimal. It was then possible to relate performance differences (with very high statistical confidence) to differences in the energy density of the cortically-generated electrical field. At certain instants during the task and at certain cortical locations, more than 95% of the intersubject performance variation could be explained by a simple linear relationship to energy density.

d) Topographic display of cognitive ERP: In the regression of performance on energy density, very good fitting results were obtained at specific cortical (scalp) and instants during the task. This suggests that these are locations where cortical activity is specifically related to task performance in the sense that effective performance is critically related to either a high or low level of

cortical activity at that location at that instant during the task. The locus of this contingency relationship over the cortex during the task differs from one task to another and may provide valuable clues to the localization of cognitive function.

e) REG findings: Cerebral blood flow was found to increase in a graded fashion with degree of task difficulty when the cognitive stimulus was synchronized with cardiac cycle. The extent of this gradation was found to vary with cognitive task type (rather than level of difficulty within a task). In contrast, systemic circulation did not change significantly during any of the MATH, SPAT or VERB tasks. The CBF changes appeared to reflect the amount of arousal or "engagement" of cognitive resources required to perform a cognitive task, rather than the actual task content.

During the TRACK task, CBF increased during the first 20 - 30 min and returned towards control values after 45 -60 min. Forearm blood flow exhibited an opposite response (decreasing during the first half of the task and increasing during the last half) confirming the synergistic relationship between systemic and central blood flow.

CBF decreased in all quadrants during the first 90 min of the LONG cognitive task. After 100 minutes of continuous effort, CBF continued to decrease in the posterior head segments but increased in the anterior ones. The changes were more pronounced for some tasks but paralleled the degree of difficulty encountered by the subject during the performance of the task.

f) Correlation between REG parameters and EEG frequency spectral analysis: An attempt was made to determine the extent to which the REG parameters are reflected by neural activity. During the LONG cognitive task, the EEG PSD (Power Spectral Density function) magnitudes remained relatively constant during the first half of the task and increased dramatically in the anterior quadrants of the head during the last half of the task. These changes paralleled the CBF changes and were more pronounced for rhythms in the alpha range (8 -13 Hz).

In summary, changes in scalp EEG energy density measures show cortical areas that specifically relate to performance (and task difficulty). The REG changes appear to reflect the degree of arousal or changes in subjects' state during prolonged cognitive effort.

It is anticipated that these techniques can be expanded to shed light on the cognitive strategies used by individuals to solve certain cognitive tasks. For example, we have studied a

small group of subjects with dyslexia (and sex and age matched controls), using a semantic task. The major difference between normal and dyslexic subjects appear to be sequential activation of cortical areas and their relationship to cognitive performance.

The major advance provided by the REG technique is the ability to track changes in subjects' mental state, particularly during prolonged mental effort. These techniques can be expanded to explore mental state changes in operators engaged in more complex monitoring tasks.

Work done during this project led to the completion of a patent disclosure document describing the innovation. This document has been submitted to NASA for further processing. The present configuration of the innovation includes a computer based control system, commercial instrumentation for REG, EEG and systemic physiologic measurements. Proprietary software is used for subject testing and data analysis. In addition, the data obtained during the performance period has been used by CNDS to support the submission of research proposals to expand the application of the technique. CNDS is currently involved in preliminary conversations with venture capital groups for possible development and capital support of the innovation.

II. INTRODUCTION

NASA SBIR Contract NAS1-18847 allowed Center for Neuro-diagnostic Study, Inc (CNDS) to develop electroencephalo-graphic(EEG) and rheoencephalographic (REG) procedures to monitor human operators during the performance of complex cognitive tasks. In developing these procedures it was recognized that, to be most useful, physiological monitoring must supply data useful to predict human mental performance, since operator's cognitive performance may deteriorate before actual deterioration of task performance. Performance at routine tasks might remain adequate even though boredom, fatigue or other factors compromise the operator's ability to respond to a critical change. Hence, physiological monitoring would be a useful tool if it could monitor changes in subjects' state as well as behaviors associated with a given level of performance. The most useful device would be one that would help match personnel abilities to task characteristics.

II.1. Electroencephalography:

EEG has long be recognized as a potentially valuable tool to identify changes in cognitive state. EEG techniques may be useful for pre-selecting candidates for assignment to demanding cognitive tasks. If it could provide information not already obvious in conventional screening test scores, EEG might offer a means of identifying subjects who, though they perform well, do so only by extraordinary mental effort. Similarly, EEG techniques may help in designing work stations to match operator's natural skills or heuristic habits. While performance data itself will naturally be the most useful indicator of this fit, EEG data may reveal patterns of cognitive activity that are unique to certain individuals.

These considerations led us to expand the scope of ERP research in three respects: 1) to use topographic EEG recordings to quantify the shape of the whole electropotential field over the scalp; 2) to use more elaborate experimental protocols in order to identify subtle differences in EEG patterns elicited by a variety of cognitive and sensory-motor stimuli and 3) to perform cross-subject comparison of correlations between individual's cortical activity and their performance.

II.2. Rheoencephalography:

Rheoencephalography (Jenker, 1962; Hadjiev, 1968; Dekonink, 1982)) is a relatively simple way to continuously monitor changes in regional cerebral circulation for extended periods of time. The REG technique offers a number of advantages over other monitoring procedures. REG is non-invasive, offers increased (beat-by-beat) temporal resolution and can be repeated at will. Other techniques for measuring regional

cerebral blood flow, based on the intra-arterial injection or inhalation of radioactive isotopes, present a number of limitations in cognitive research: (1) intrarterial administration of radioisotopes is difficult to justify for use on normals, (2) the inherent radiation burden limits the frequency of administration so that few repeated observations can be made and (3) isotope procedures require equilibration times of 3 -5 minutes and thus yield only static, cross-sectional information about rCBF relative to cognitive tasks.

Rheoencephalography has been independently validated through comparative measurements of cerebral blood flow using xenon inhalation (Jacquy, 1974), venous dilution of 131-I (Hadjiev, 1968) and carotid doppler (Atefie, 1983) techniques. These studies show that the extent of correlation between REG measures and cerebral blood flow is very high, ranging from 0.75 to 0.92, depending upon the type and location of scalp electrodes.

Given the ease of application, the noninvasive nature of REG and the limitations of other techniques, rheoencephalography seems to be ideally suited for use in most experimental conditions. However, as with EEG data, analysis of the REG recordings requires graphical interpretation of the pulse waveforms (a tedious and time consuming process). I addition, it is difficult to manually select individual cardiac intervals, coincident with stimulus presentation, for direct comparison with EEG data. Therefore, procedures have been developed that overcome these two limitations by allowing semi-automated analysis of the REG data and by triggering task presentation based upon precise synchronization with the subjects' heart beat and peripheral blood flow.

III. Experimental Approach

The experimental approach consisted of three distinct test phases. Event-related potential (ERP) analysis was used during Test Phases I and III. On-going EEG analysis was used during Test Phase III. Rheoencephalography was used in all three Test Phases, and correlated with the EEG and ERP measures.

During Test Phase I, the cognitive stimulus consisted of three visual-motor cognitive tasks: arithmetic (MATH), semantic (VERB) and form-recognition (SPAT) processing tasks), administered at three jury-determined levels of difficulty (Low, Medium and High levels). The task types and difficulty criteria were modified from the Criterion Task Set protocol (Action and Crabtree, 1985, Shingledecker, 1984) and are described below. This protocol (Mixed cognitive task), was used to investigate short term ERP and REG changes to task level and task type. During Test Phase II, a continuous visual-motor tracking task (TRACK) was used to monitor on-going EEG and REG changes associated with sustained effort. During Test Phase III, LONG term (3 hours) arithmetic, semantic and form-recognition tasks (similar to Test Phase I) were administered to investigate the effects of fatigue and the stability of the REG and ERP findings over time. The EEG recording procedures were identical in all testing phases. The REG instrumentation and recording procedures were modified somewhat during the three Test Phases. These modifications are described under each Test Phase description.

Observations were made on eight right handed adult male subjects of similar educational background and free of any medical, psychiatric, or neurological conditions. All of the experimental trials were performed at the Center for Neurodiagnostic Study, Inc. (CNDS), in San Jose, CA.

III.1. Cognitive Stimuli

After instrumentation and checkout, each subject was given a computerized workload task for a preset period of time. Each test sequence consisted of a standardized MATH, VERB or SPAT task at empirically selected Low, Medium and High levels of difficulty. All cognitive stimuli were presented in sequential order of difficulty on a computer screen within a large circle to avoid corner fixation and provide a constant background. The subject's response was provided by pressing one of two buttons on a key pad using the right hand. Each response automatically triggered presentation of the next stimulus after a delay of two seconds.

During the MATH task a string of four digits separated by "+" or "-" operators were presented via a computer screen (Figure 1). The different difficulty levels were determined by the

number of "0s" in the string. Thus the Low difficulty level presented two digits (and two zeros), the Medium level three digits (and one zero) and the High level four digits. This format was chosen to keep the length of the string (and thus the magnitude of the visual stimulus) constant between the different levels. The subject was required to determine if the product of the string was greater or less than 0.

The SPAT task consisted of two simultaneously presented groups of horizontal bars resembling a standard histogram bar chart. One group, shown on the left portion of the crt display, (Figure 2) was drawn with a common baseline and served as the control diagram. The second group of horizontal bars were presented on the right side of the screen in a disjointed display. The subject was required to specify whether or not the disjointed bars could be made to form the same pattern as shown in the control diagram. Task difficulty was determined by using 2, 4, or 6 bars in each display.

The VERB task consisted of word-pairs randomly presented on the computer screen from a list of 300 pairs, with jury-determined "easy", "moderate" and "difficult" pairs equally represented in the list. The words were presented in a large, easy-to-read format (Figure 3) and the two words were spaced beside each other in a manner that maintained a constant visual angle from one pair to the next. The subject was instructed to decide whether the words were synonyms or antonyms and responded by pressing the appropriate key.

Subject performance was measured and recorded during each test sequence. Reaction times for correct and incorrect responses, percentage of correct, incorrect, and missed responses and mean correct response times were computed for each stimuli by the experimental control computer. These measures were used to determine an "error rate" index of poor performance for each task by the formula:

Error Rate (ER) = (Average Reaction Time) x (1+Percentage Wrong)

in which the "percentage wrong" is the number of wrong responses divided by total number of responses x 100.

III.2. Mixed Task

During the mixed task, Low, Medium and High difficulty stimuli were given sequentially for a total of 150 stimuli (fifty Low, fifty Medium and fifty High difficulty stimuli). MATH, VERB and SPAT tasks were given in separate recording sessions. Thirty-two two-second stimulus-gated artifact-free EEG response montages were averaged for each task level to create a multielectrode event related potential (ERP) for each level.

REG recordings during the Mixed Task were obtained continuously for three minutes (independent of the number of stimuli presented) on six subjects. Right and left hemisphere REG, forearm impedance plethysmography (IPG) and EKG signals were obtained in all subjects. Presentation of the cognitive stimuli was synchronized to the cardiac cycle (by the control computer) so that each stimulus was presented during diastole. Due to the time required by the control computer to process the on-line physiologic signals, subject movement, respiratory artifacts and eye blinks, only 10-15 Low, Medium and High stimuli were presented during the three minute test period, with a delay of 3-5 seconds between stimuli.

REG, IPG and EKG data traces were recorded on a CODAS data acquisition system. The stored REG pulses were visually inspected by an Advanced CODAS play-back system. The triggering REG pulse and the one immediately following were saved in ASCII format and catalogued according to task level and time of occurrence. Four paired pulses were then selected for each task level to represent the first, last and two equally spaced intermediate time periods.

III.3. Tracking Task

The experiments described above were designed to raise the signal to noise ratio of cognitive potentials and to increase the statistical power of the analysis procedures. However, it was speculated that EEG and REG analysis might also facilitate monitoring of subject state during a continuous task. A continuous tracking task was designed to explore that possibility.

The tracking stimulus presented a computer display consisting of two vertical bars (Figure 4). A "target bar" was controlled by the computer so that its height changed by random increments; the subject controlled the height of the "response bar" via a joystick and attempted to keep the bars at the same height. The computer recorded a continuous record of the height of both bars. Separate trials were conducted for EEG and REG to exclude the possibility of interference between the EEG and REG instrumentation.

Five consecutive two second epochs of 21-channel EEG data were selected starting at the beginning of each minute indicated below:

Five minute control period (No change in target)

Minutes 1, 2, 3, 4, 5
(5x5=25 two second epochs)

Fifty-three minute test period

Minutes 3, 8, 13, 18, 23, 28, 33, 38, 43, 48, 53

(5x11=55 two second epochs)

REG instrumentation and procedures were identical to the ones used during the Mixed Task. Task presentation was independent of EKG cycle. Each test sequence consisted of a five minute control period and a one hour continuous tracking test period. Left and right hemisphere REG, ECG and forearm blood flow records were obtained at times -5, -3 and -1 minutes during the last 5 minutes of a non-tracking control period during which the subjects were looking at a blank but lit computer screen. The same parameters were recorded at 3, 18, 36 and 54 minutes during the tracking task. Subjects were not aware of the recording periods during the continuous task.

Subject performance was assessed by the length of time it took them to match a given step change in the target bar and the percent time they kept the response bar within 80% of the target bar following a maximal target bar step change.

A tracking response index (TRI) was calculated to measure subject performance. The TRI represents the average deviation between the target bar height Ht (cm) and the response bar Hr (cm), following a maximum positive or negative target bar height change. This deviation is measured over the N sample points between the start of the maximum excursion until the next target bar height change:

$$TRI = (\text{Sum } |Ht - Hr|)/N$$

III.4. Long MATH, VERB, SPAT Task

This Test Phase was designed to test the value of REG monitoring of changes in subject's state during a prolonged cognitive task and to explore the value of the EEG energy density regression procedure when applied to a single subject's longitudinal data rather than to cross subject data. Three adult, right handed males, of similar educational background were tested with the same three types of cognitive tasks (MATH, VERB and SPAT) discussed in Section III.1. MATH, VERB and SPAT tasks were given in separate recording sessions. Twenty-five Low, twenty-five Medium and twenty-five High difficulty stimuli were given sequentially and repeated six times for a total of 450 stimuli (25 x 18 = 450), followed by the presentation of an unrelated task, used to distract and further stress the subject. This "Multi-Attribute Task (MAT)" (Arnegard and Comstock, 1990), was developed at NASA Langley Research Center to provide a continuous task that simulates many of the cognitive activities found in the flight deck. The MAT consists of a combination of manual tracking, resource (fuel) management, and monitoring tasks displayed on a computer screen simultaneously.

The entire experimental sequence was presented to three

subjects in one un-interrupted sequence according to the following protocol:

RECORDING	DURATION OF RECORDING	NUMBER OF STIMULI	ELAPSED TIME
REG MIXED TASK	5 MIN	85	5 MIN
EEG MIXED TASK	30 MIN	450	35 MIN
REG MIXED TASK	5 MIN	85	40 MIN
MAT TASK	30 MIN	--	70 MIN
REG MIXED TASK	5 MIN	85	75 MIN
EEG MIXED TASK	30 MIN	450	105 MIN
REG MIXED TASK	5 MIN	85	110 MIN
MAT TASK	30 MIN	--	140 MIN
REG MIXED TASK	5 MIN	85	145 MIN
EEG MIXED TASK	30 MIN	450	175 MIN
REG MIXED TASK	5 MIN	85	180 MIN

REG records were obtained immediately prior to and following each EEG and MAT task periods. No physiological recording was done during the MAT task. Stimulus presentation was independent of cardiac cycle, and each Low, Medium and High stimulus was separated by a 3 second delay. During the EEG recording periods, Low, Medium and High stimuli were presented in sequences of 25 stimuli.

Sixteen artifact-free two-second EEG records were selected from each 25 stimuli sequence and then averaged to obtain a cognitive ERP. Each EEG Mixed Task recording yielded 18 ERPs (six LOW, six MEDIUM and six HIGH ERPs) for a total of fifty-four ERPs for each subject ([three task levels] x [six ERPs] x [three EEG Mixed Task recordings]). Task difficulty was "rotated" so that these ERPs would represent, in sequence, task levels L, M, H, L, M, H etc. This was done to assure equal exposure to each level, which is not a certainty with random generation of task levels.

Each triplet of L,M,H ERPs was then averaged, thus reducing the data to eighteen 48-response ERPs ([three task levels] x [sixteen responses]), arrayed in time as follows:

ERP 1 - 6: Cognitive task (MATH, VERB, SPAT)

MAT task

7 - 12: Cognitive task

MAT task

13 - 18: Cognitive task

In order to facilitate comparison with REG data, those ERPs closest to REG recording periods were singled out for particular attention. These were the first and last ERPs in

each of the three cognitive task sessions shown above.

REG pulses were selected from the start, mid-point and end of each REG Mixed Task test period for analysis. Subject performance was assessed using the Error index described above. Overall hemodynamic and performance results were plotted as functions of time throughout the testing session.

FIGURE III-1

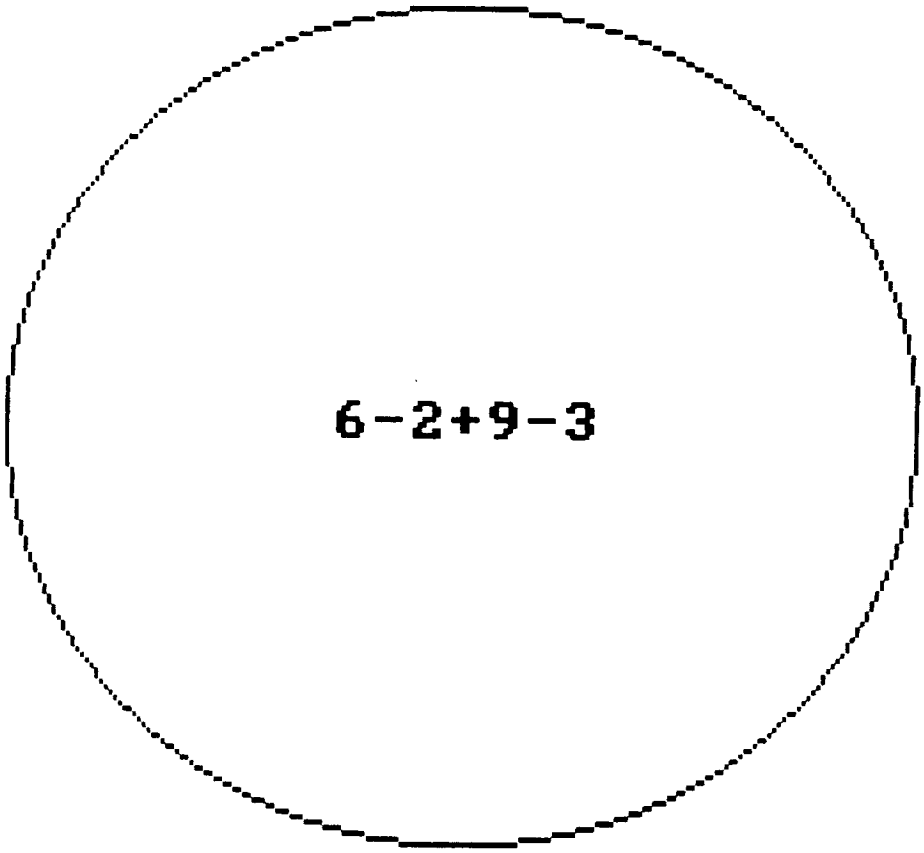

FIGURE III-2

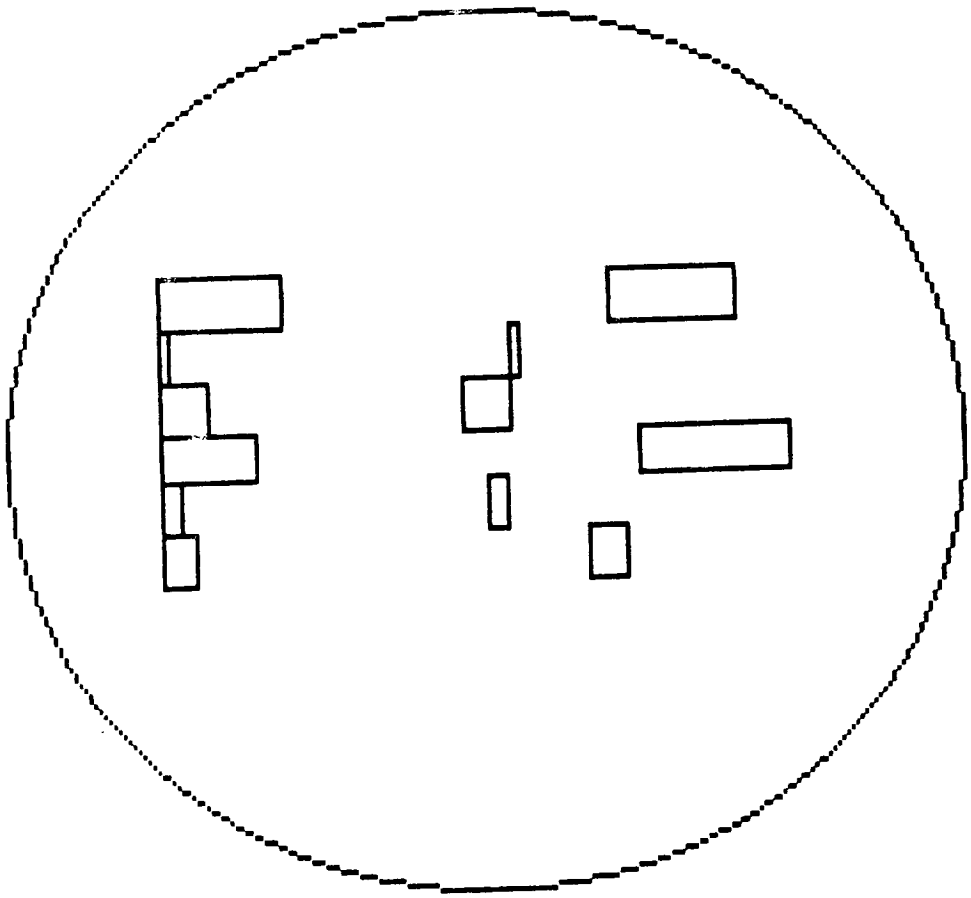

FIGURE III-3

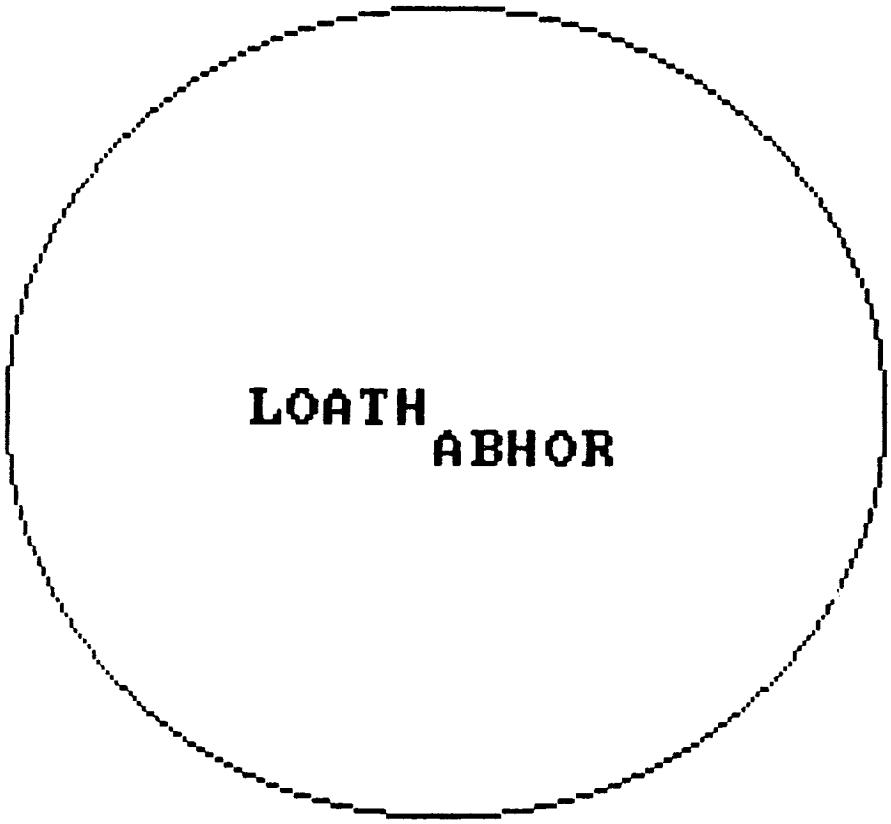

FIGURE III-4

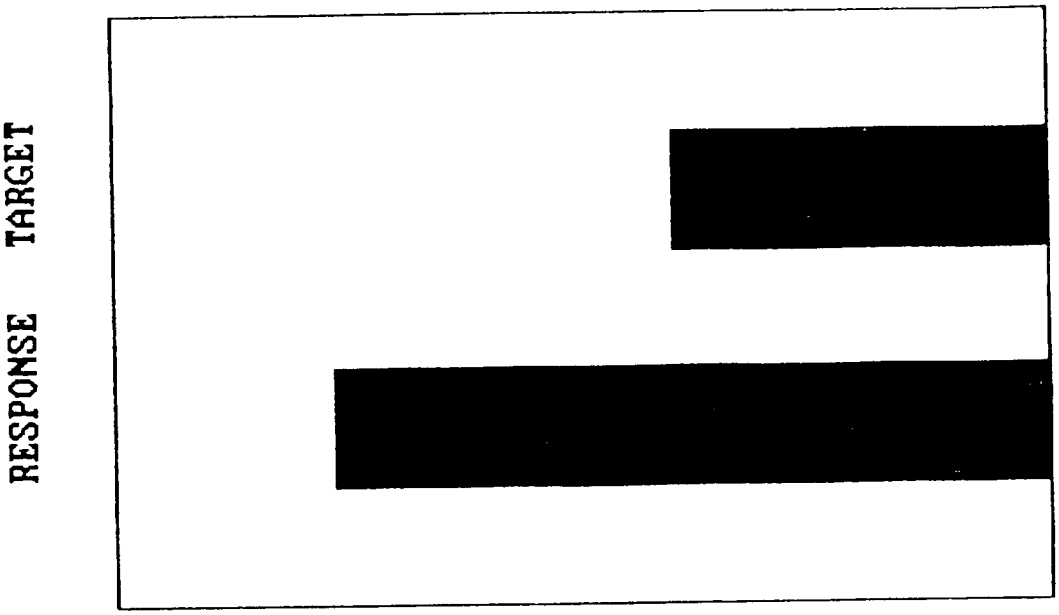

IV. Instrumentation.

The experimental recording system included a computer based control system and commercial instrumentation for REG, EEG and systemic physiologic measurements. The functional characteristics of the computer based control system are described below. This section is followed by a description of the instrumentation used to obtain and record REG/EEG signals during each test sequence. Procedures and programs used for post-test REG/EEG analysis are also described in this report.

IV.1. Computer Based Control System

The experimental approach required a system capable of real-time coordination of multiple experimental parameters, in order to time the selection of REG and EEG segments to the time of presentation of the cognitive stimulus. The control functions of this system included: a) analysis of select features of the forearm electrical impedance pulse waveform and the precordial electrocardiograph (ECG); b) presentation of cognitive tasks; c) monitoring and assessment of subject response times and d) the simultaneous insertion of timing signals into the EEG and REG records. Scanned channels included the derivative of the REG waveform (dR/dt), a single analog channel of the subject ECG and the analog output of a keyboard used by the subject to respond to each cognitive task. The required coordination and control of these experimental events was assessed in detail and a computer-driven real-time system was designed to support these functions. This System Control Computer is described in detail in Appendix A.

IV.2. Electroencephalographic Recording

Scalp EEG recordings were obtained from twenty-one silver-chloride cup electrodes applied to the scalp according to the International 10-20 system referenced to linked earlobes. A Brain Atlas III system (Biologic Inc., Mundelein, Ill.) was used to digitize and store scalp potentials with a sampling rate of 128 Hz per channel (20,000 gain, 30 Hz high filter, 1 Hz low filter, and electrode impedances less than 2,000 ohms).

The three frontal-most electrodes were used for eye-blink monitoring. A software-generated timing mark was introduced into the Oz electrode position by the system control computer to denote the start and end of each problem presentation.

IV.3. Rheoencephalographic Recording

Two different rheoencephalographic systems were employed during testing. A two channel system was used during the Mixed and Tracking Tasks to monitor right and left hemisphere

hemodynamics, and a four channel system was used to monitor four quadrants of the head during the extended Mixed/MAT test.

REG Configuration for Mixed and Tracking Tasks: A UFI, Inc. two channel tetrapolar rheoencephalograph (REG) was used to obtain intracranial blood flow measures during each subject test. Disposable ECG type electrodes were placed in the center of the forehead and at the back of the neck to serve as current input electrodes. EEG electrodes placed on each side of the subject's head at positions F7, F8, O1 and O2 are shared by the REG and EEG recording systems and used to record the impedance waveform during each cardiac cycle from right and left hemispheres. These positions provide the maximal field for monitoring intracranial circulation.

The REG introduces a high-frequency (50 KHz), low amperage (0.1 mA rms) constant current between the two input electrodes. Base resistances and pulsatile impedance waveforms are recorded between the two sets of detecting electrodes. These signals were digitized at an A/D conversion rate of 250 Hz to a 12 bit resolution and recorded on a dedicated data acquisition system for processing and analysis.

A standard lead I electrocardiogram and forearm blood flow, was measured by a single channel UFI, Inc. impedance plethysmograph and a UFI Model 2121 EKG Bio-amplifier. These signals were used to assess the subject's systemic response to mental processing and to trigger the presentation of each problem by the control computer.

The signals were also digitized at an A/D rate of 250 Hz to a 12 bit resolution and recorded on a dedicated data acquisition system for later processing.

REG configuration for the Long Task: A four channel UFI, Inc. (Model 2994) tetrapolar rheoencephalograph was used to measure hemodynamic responses in four quadrants of the head. EKG electrodes were applied to the forehead and nape of the neck for use as current input sites, as described above. The Cz position was shared as a pick-up electrode by all four REG quadrants. The F4, O2, F3 and O1 positions were used as the second pick-up electrode for the right anterior, right posterior, left anterior and left posterior head segments.

V. Data Analysis

The following sections describe the computer programs used to analyze REG and EEG data.

V.1. **Electroencephalographic Data Analysis**

The multichannel EEG signal was analyzed to obtain the regional distribution of charge and energy densities as explained in the following paragraphs. These techniques may be applied to both on-going EEG and ensemble averaged cognitive ERPs.

Thirty-two artifact-free stimulus-gated 2-second response epochs were ensemble averaged, producing an "Event Related Potential" (ERP) in the form of a single 2-second 21-electrode montage. Each ERP record is thus represented by a single 21 (electrodes) by 256 (number of sample points in 2 seconds) data matrix.

At each digital time sample point in the ERP data matrix a least-squares estimate of the spatial distribution of scalp voltage levels was obtained by fitting the following equation to the 21 simultaneous voltage values

$$V = (a + bX + cY + dXY)^3 .$$

Where:

V = voltage at the electrode identified by the coordinates x,y

X = side-to-side direction in a flattened scalp electrode grid,

Y = front-to-back direction in the grid.

When expanded, this equation is linear in 16 terms, each of which is a combination of various powers of X and Y:

$$V = b_1 + b_2 X + b_3 X^2 + \ldots + b_{15} X^2 Y^3 + b_{16} X^3 Y^3 .$$

The least squares algorithm finds optimal values of the 16 b-coefficients -- optimal in the sense of minimizing the sum, over all electrode sites, of the squared differences between the value of voltage predicted by the equation, for each site, and the actual EEG-recorded value.

Figure 1 shows the least squares procedure for one instant (200 milliseconds) in a visual VERB ERP. The electrode grid is flattened and oriented with the front of the subject's head to the viewer's right. The height of each vertical spike is proportional to the ERP voltage at that instant for that particular electrode site. The corner position voltage values

are averages of adjacent electrodes. Figure 2 illustrates how a series of these fitted surfaces can be used to represent the sequence of voltage profiles at each time point throughout the 2 second ERP. The quality of the least-squares estimate can be evaluated by comparing the actual data with pseudo time-traces recorded at the various electrode sites from the series of fitted surfaces. Such a comparison is shown in Figure 3 , where the actual data is the solid line and the least-squares estimates produced the dotted line. For this figure, a raw, unfiltered montage was used instead of an ERP, in order to demonstrate a more severe test for the least-squares procedure. (The raw data contains high frequency components and abrupt discontinuities which would not be present in an ERP). With raw data traces, the least-squares estimate typically has an electrode-average R-squares value in excess of .92; that is, on average for the 21 electrodes, at least 92% of the variation of the raw data is accounted for by the fitted equation.

Initially during this project, we explored the possibility of obtaining a better estimate of the shape of the scalp voltage distribution by use of additional electrodes. It was thought possible that, even though 21 electrodes produce a good fit, spatial peaks might occur between the electrode sites and hence fail to appear in the data. To test this concept, a cap containing 32 electrodes was custom fabricated by Electro-Cap International, Inc. and a data acquisition system capable of recording 32 electrodes was used to obtain a 32-channel ERP.

Figure 4 shows the resulting fit, using the same electrode positions shown in Figure 3. As can be seen, the quality of the estimate actually falls, probably due to multicollinearity. The spatial distance between the 32 electrodes is so small that voltage fluctuations recorded at adjacent electrodes are too highly correlated to be consistent with the requirements underlying the least-squares method, that the independent variables be independent (cf. the Gauss-Markov theorem, eg. in Wonnacott & Wonnacott, 1970). It is conceivable that the multicollinearity problem could be overcome by appropriate respecification of the equation to be fitted as a model for the voltage surface (cf. Farrar and Glauber, 1967). However, the added complexity of the estimation procedures would outweigh the marginal gain in information.

In summary, evidence of multicollinearity in the empirical test and rapid increase in the expense and complexity of data acquisition and reduction as a function of additional electrodes led us to abandon the 32-electrode approach. Twenty-one electrodes were deemed sufficient for the technical purposes.

EEG Energy Density Distribution:

An interpolation procedure such as cubic-splines or Coon's patches (Lord and Wilson, 1986) could have been used instead, of the least-squares method, if the objective was merely to produce a 3-D picture of scalp voltage (the usual approach in EEG topographic analysis). However, the objective of this step was to produce a single equation to represent the voltage distribution, which could then be manipulated mathematically in subsequent analysis steps. Of particular importance is the ease of computing the second spatial derivatives of each function and hence obtain the "Laplacian" of each EEG surface.

At each time sample point the fitted equation is differentiated twice with respect to X (assuming Y constant) and twice with respect to Y (assuming X constant), to obtain the Laplacian of the fitted surface, i.e., the sum of the second partial spatial derivatives:

$$L(X,Y) = Dxx\{V(X,Y)\} + Dyy\{V(X,Y)\}.$$

Where:

$L(X,Y)$ = Laplacian operator at X,Y,

$Dxx(V)$ = second partial derivative of V with respect to X,

$Dyy(V)$ = same, with respect to Y.

Mathematically, it has been shown that the Laplacian of a electropotential field shows the charge density underlying the field (Hjorth, 1975, 1980; Murray and Cobb, 1980; Nunez, 1981, 1989).

Resolution of the EEG data can be improved even more by taking a second step: at each X,Y coordinate location, an estimate of the potential energy of the electrical field at that location is obtained by forming the product of voltage and the negative of the Laplacian:

$$U(X,Y) = -V(X,Y)\ L(X,Y)$$

U(X,Y) is the local potential energy of the cortically generated electrical field i.e., "surface energy density" which in the MKSA system has units of Joules per square centimeter.

The result of this manipulation is a third surface for each sample point, which by its height shows the relative spatial distribution of potential energy.

Figure 4 shows the voltage surface, the (negative of the) Laplacian surface and the energy density surface for one given instant in an ERP obtained as the subject performed a word-pair task. Comparison of these three surfaces shows how

much better the energy density surface reveals cortical localization of electrical activity.

Figures 5 and 6 show how this treatment also improves the frequency resolution of continuous EEG data. Both figures are derived from the same record, a two-second segment recorded from the left occipital electrode as the subject fixed his gaze on a distant point. The top panels of both figures show the actual time traces. Comparison of the Digital Fourier Transforms (DFTs) in each figure shows improved definition of the frequency band peaks with energy density derivation. The DFTs are obtained by a radix-2, in place, decimation in time, Fast Fourier Transform (FFT) algorithm; input data shuffling, natural order output.

The conversion of EEG voltages to potential energy yields a discrete numerical value that, unlike voltage, can be integrated over time and location. Thus, it is possible to "add-up" the energy levels shown for a particular cortical region over a period of time and thereby quantify the energy density changes imposed on that region during a given experimental protocol.

V.2. **Rheoencephalographic Data Analysis**

In the past, the pulsatile impedance data had to be analyzed by hand due to the fact that it was usually recorded on paper strip charts and not available for computer manipulation. The segmental blood flow data obtained during the performance of this project was digitized and recorded using a computer data acquisition system. This made it possible to automate most of the data analysis procedure using RHEOSYS (RHEOencephalographic impedance trace scanning SYStem), developed by CNDS during the course of this project. The RHEOSYS program is described in detail in Appendix B.

RHEOSYS also provided an opportunity to assess the utility of various REG indices currently used to quantify different aspects of cerebral circulation. A thorough literature search revealed approximately 30 parameters that can be calculated from a subject's REG waveform, segmental base resistance and electrocardiogram. Different combinations of these parameters were found to be useful during the performance of the different experimental procedures, as follows: cerebral blood flow (RHEOSYS parameter No. P25), segmental volume (P26, P27), pulse volume (P4-6, P9-12, P27), pulse transit time (P18-21), arterial and venous tone (P7, P8), regional vasomotor reflexes (P1, P2, P22-24), and cardiodynamics (P3, P15-17).

FIGURE V-1

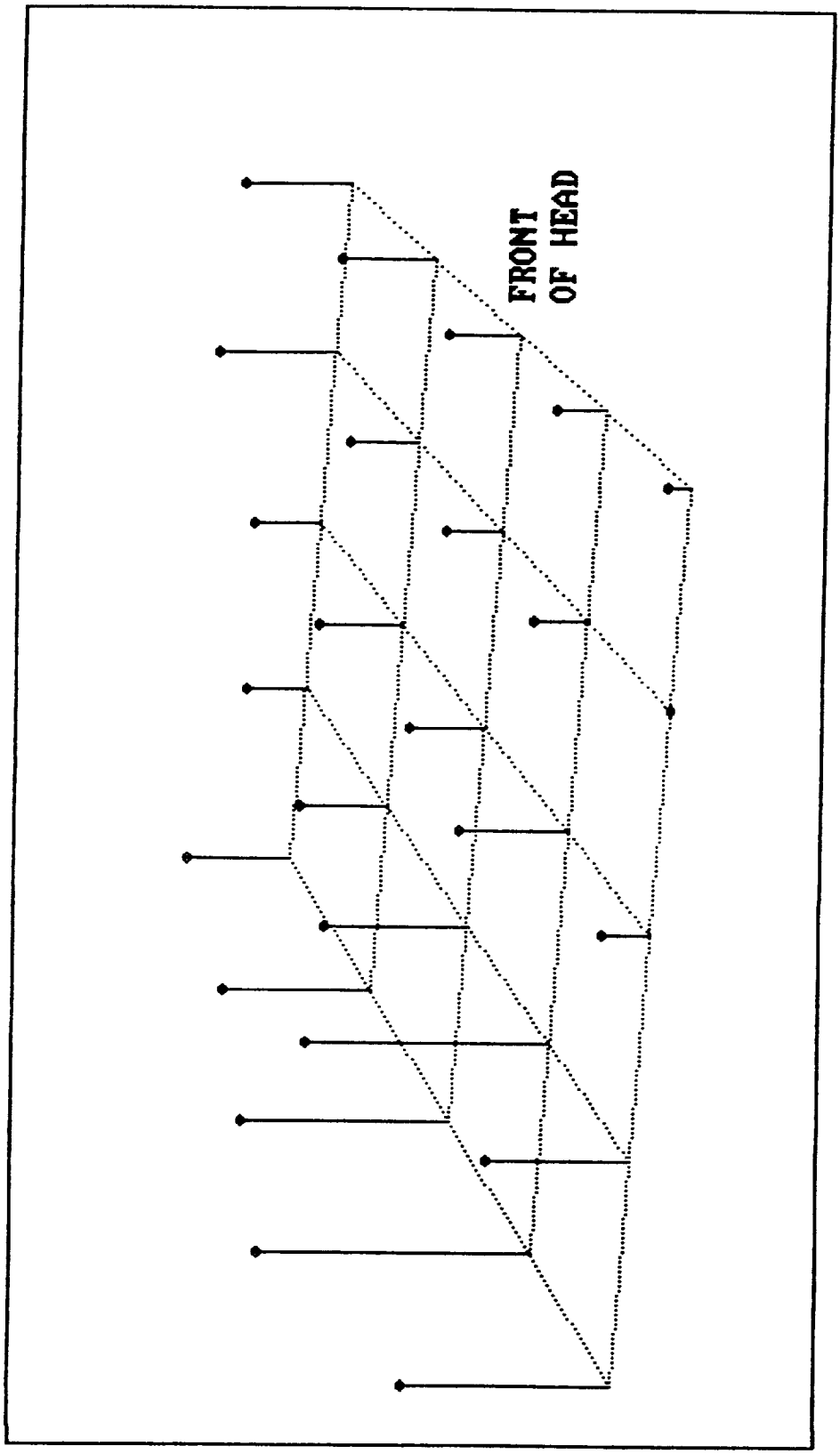

VOLTAGE VALUES AT 200 MILLISECONDS

FIGURE V-2

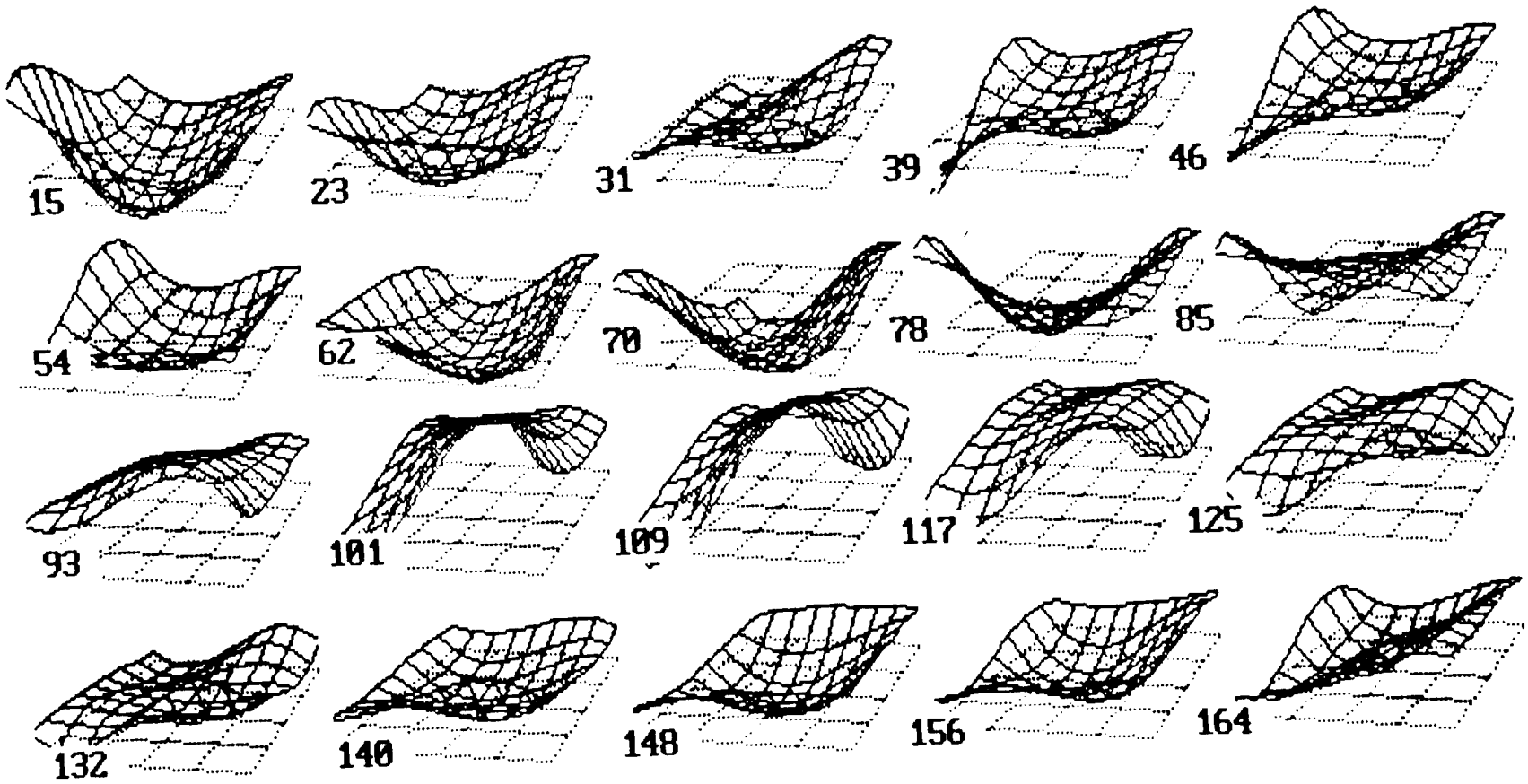

EVOLUTION OF VOLTAGE SURFACE

FIGURE V-3

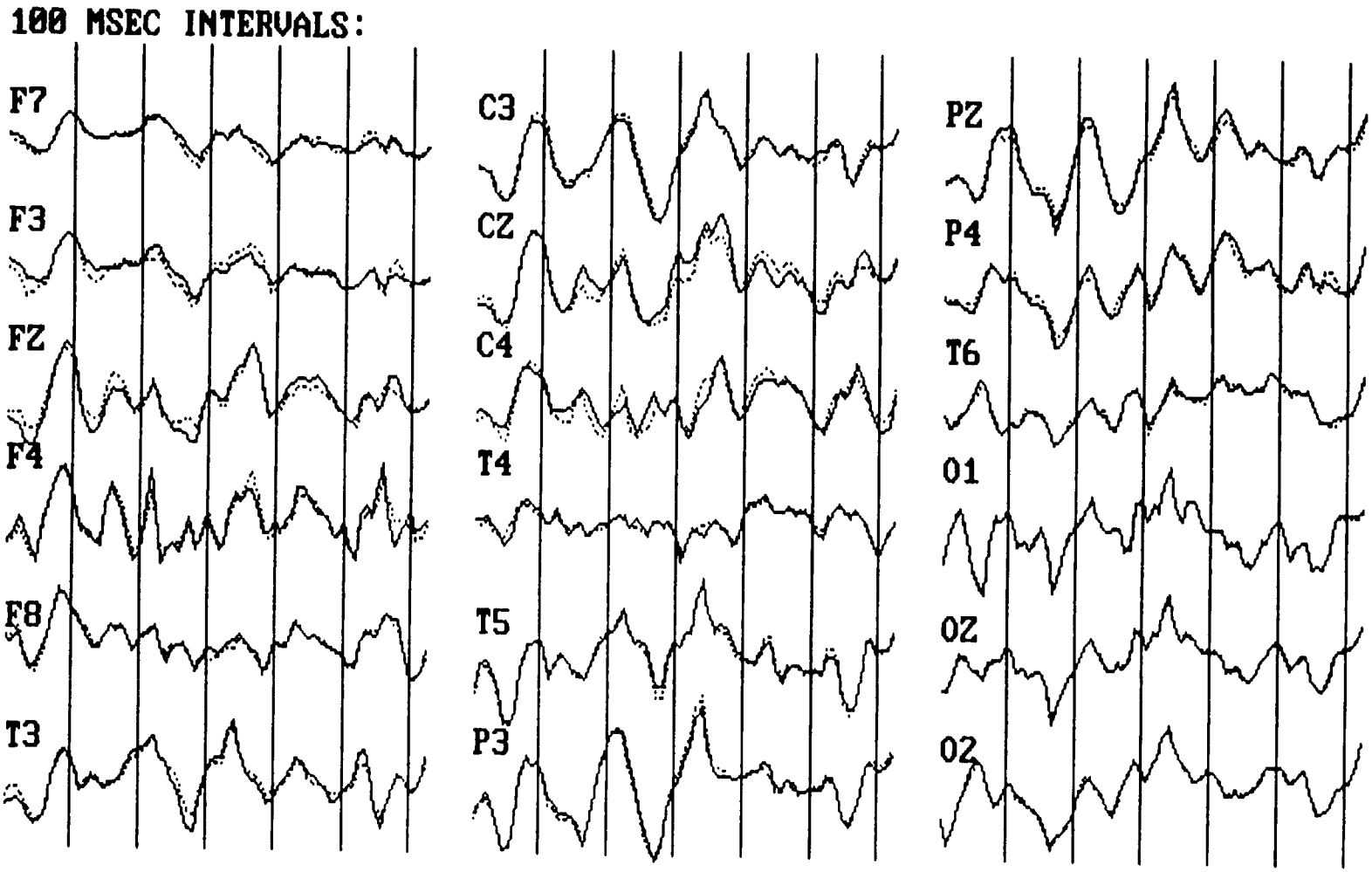

RAW DATA (SOLID LINE) VS. ESTIMATE (DOTTED LINE)

FIGURE V-4

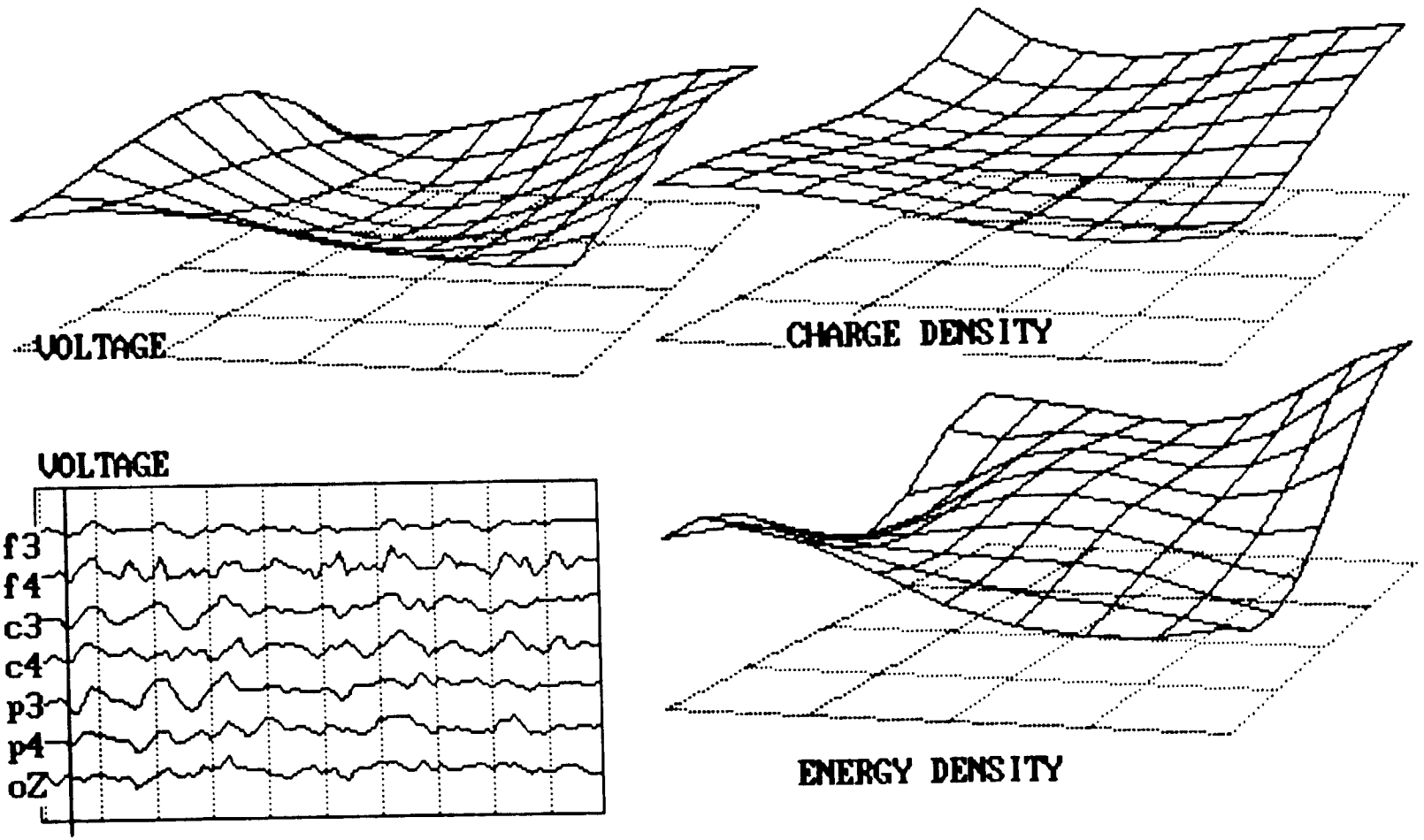

SURFACES AT 54 MILLISECONDS

FIGURE V-5

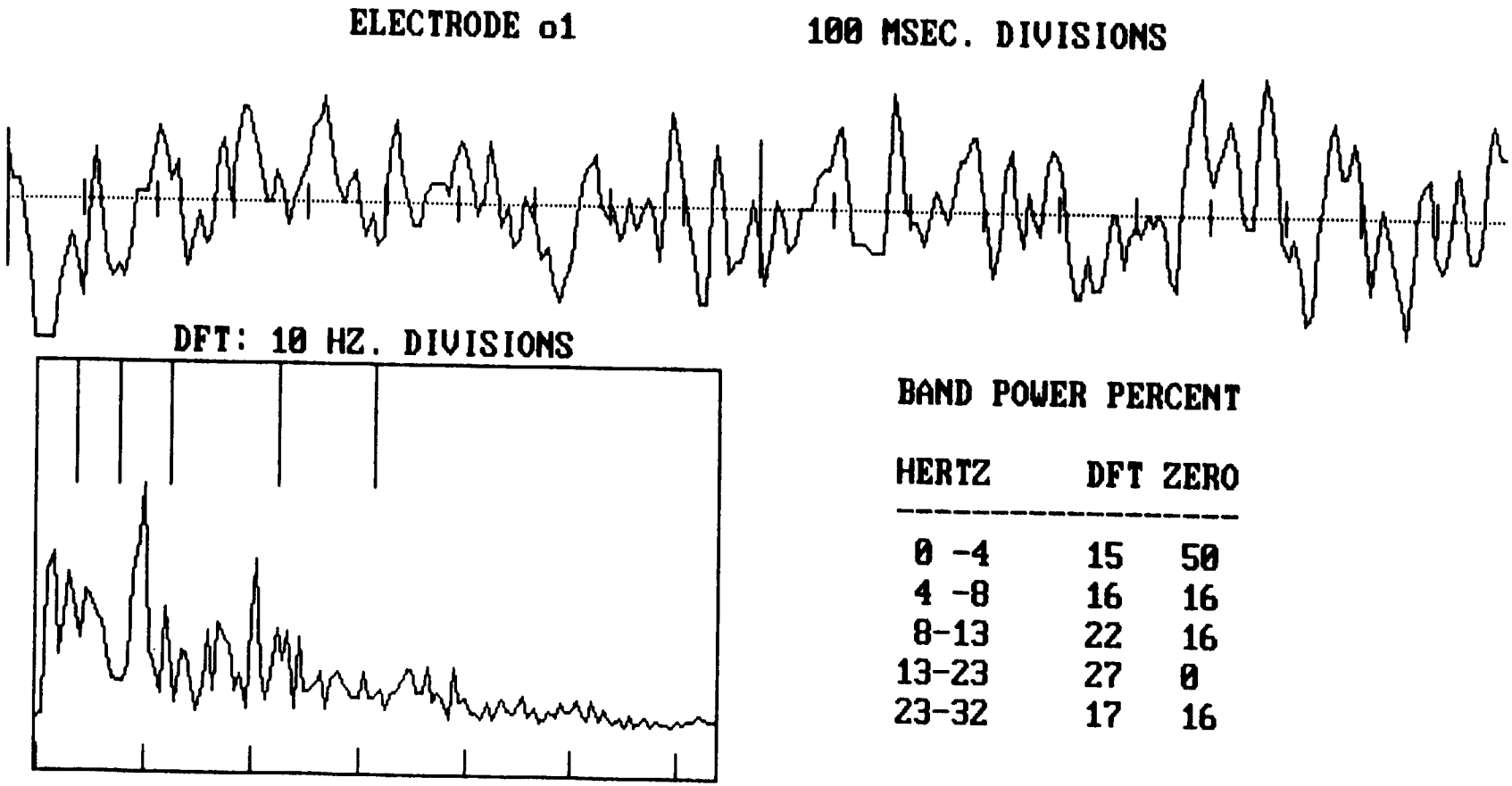
ELECTRODE o1
100 MSEC. DIVISIONS
DFT: 10 HZ. DIVISIONS
BAND POWER PERCENT
HERTZ DFT ZERO
0 -4 15 50
4 -8 16 16
8-13 22 16
13-23 27 0
23-32 17 16
VOLTAGE TRACE

FIGURE V-6

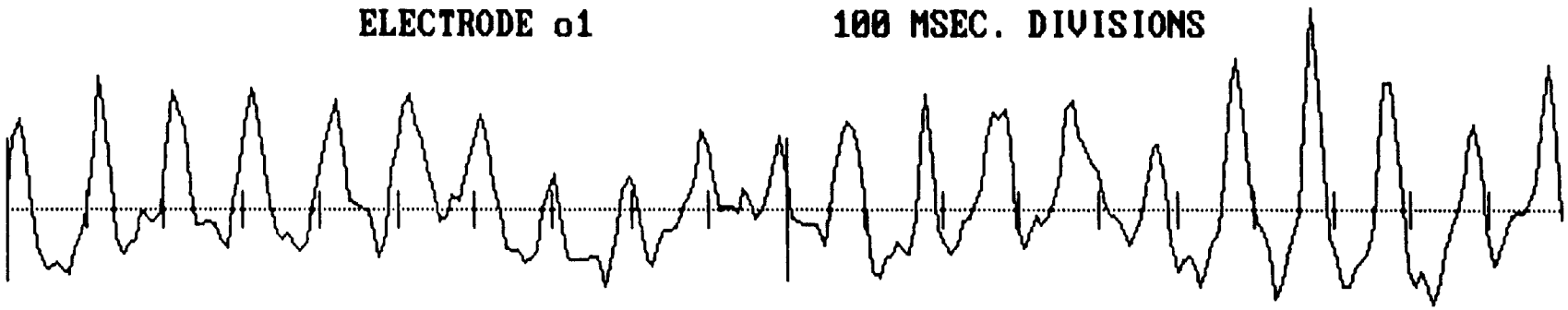

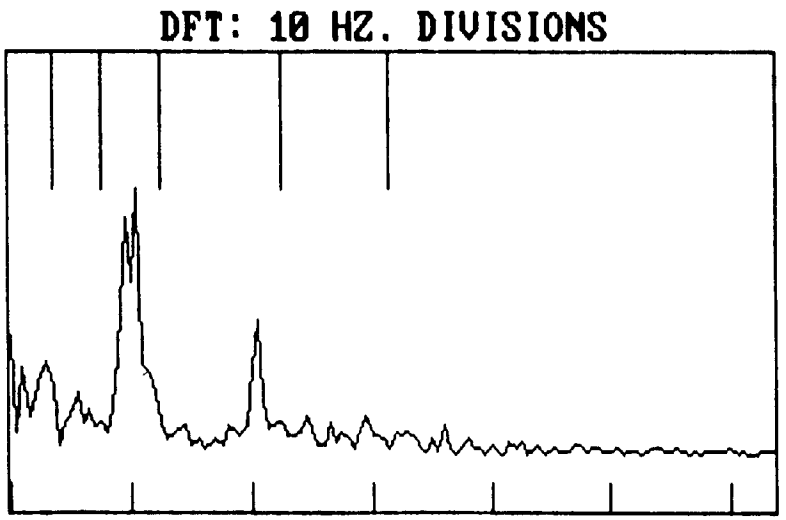

BAND POWER PERCENT

HERTZ	DFT	ZERO
0 -4	18	0
4 -8	11	82
8-13	36	8
13-23	21	0
23-32	12	8

ENERGY DENSITY TRACE

VI. RESULTS

VI.1. EEG RESULTS

VI.1.1. Mixed Task.

VI.1.1.1. Subjects' performance results (Figures VI.1.1.1 -1 through VI.1.1.1 -3)

Figures 1 through 3 (and Table I, Appendix C) show the reaction time, percent wrong and error index for the three cognitive tasks, respectively, and the respective Low, Medium and High difficulty levels. The error index was calculated as:

Error Index = (1 + % wrong) x Reaction time

Table II (also located in Appendix C) shows the average and standard error for the pooled subject population.

The reaction time, by itself, tends to be monotonically graded by task level. However the Low-vs-Medium and Medium-vs-High separations are hardly more than one standard error of the mean, so they are not statistically significant. The other basic measure, percentage wrong, increases monotonically only for the VERB task. For the MATH task, subjects actually did best for the "high" level and performance was practically constant for all levels of the SPAT task.

FIGURE VI.1.1.1-1

PERFORMANCE DATA FOR MENTAL ARITHMETIC TASK

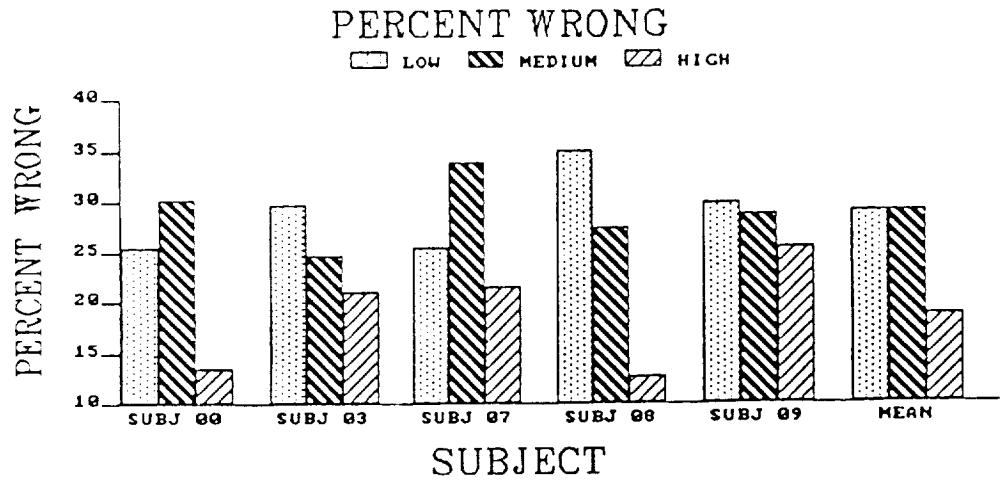

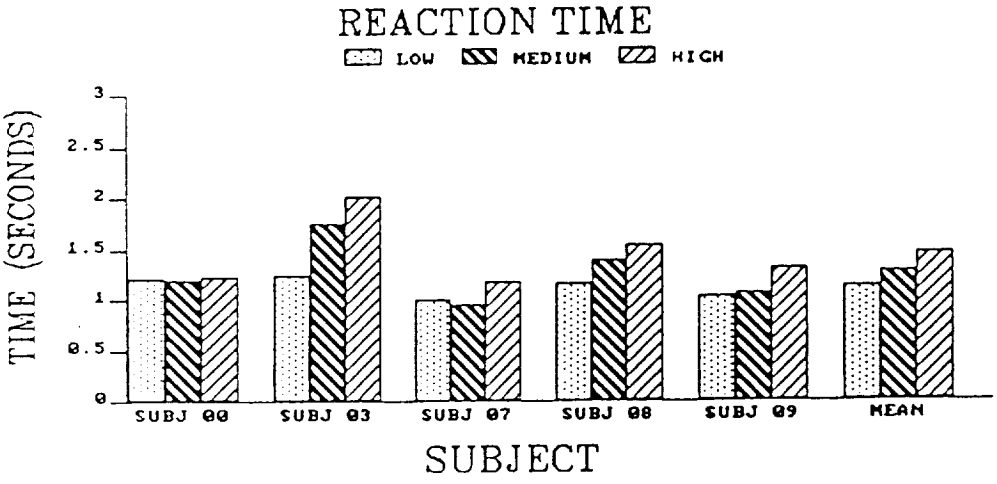

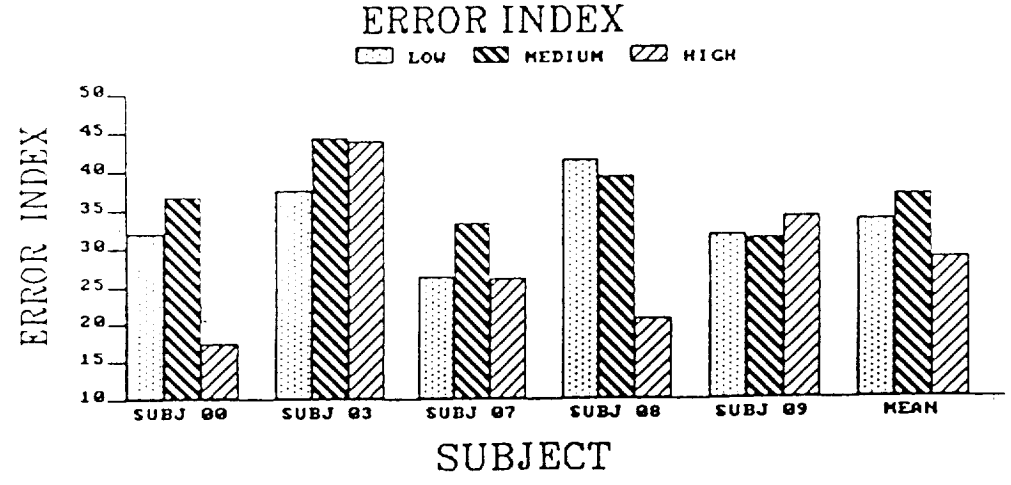

FIGURE VI.1.1.1-2

PERFORMANCE DATA FOR WORD PAIR TASK

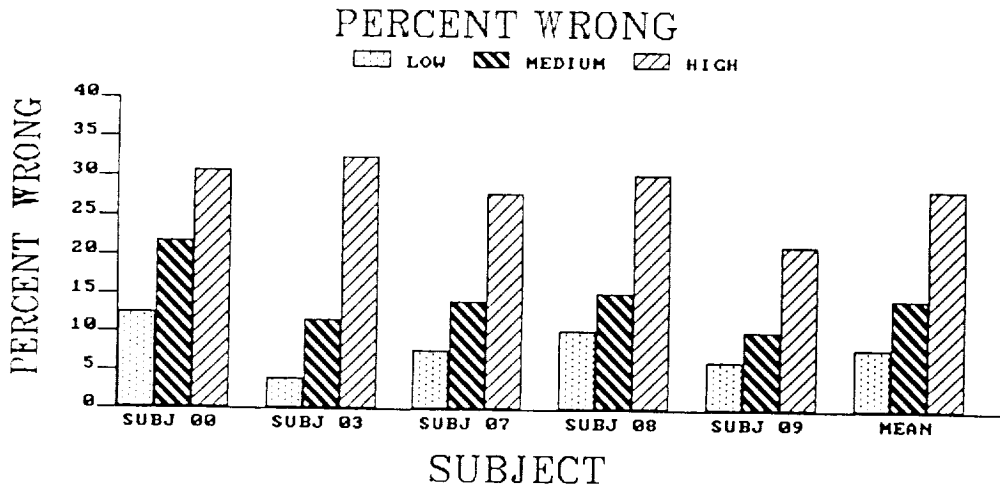

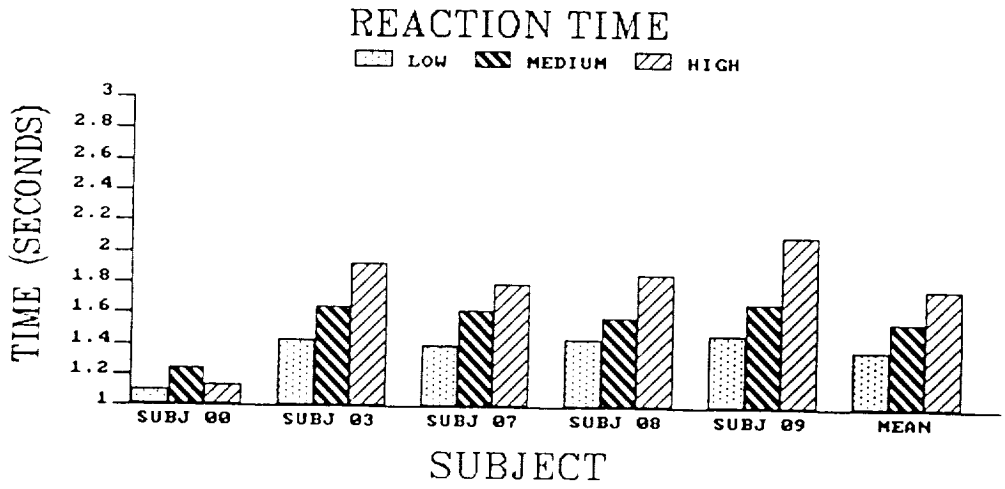

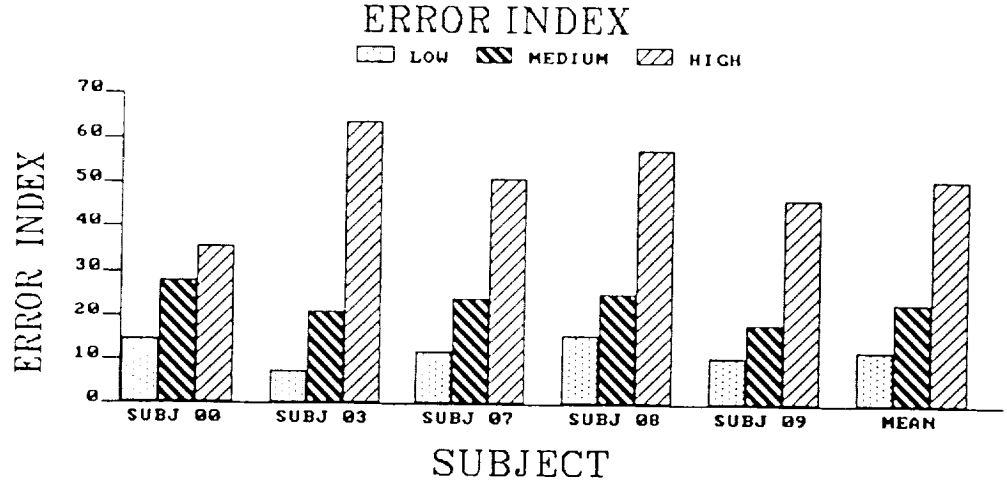

FIGURE VI.1.1.1-3

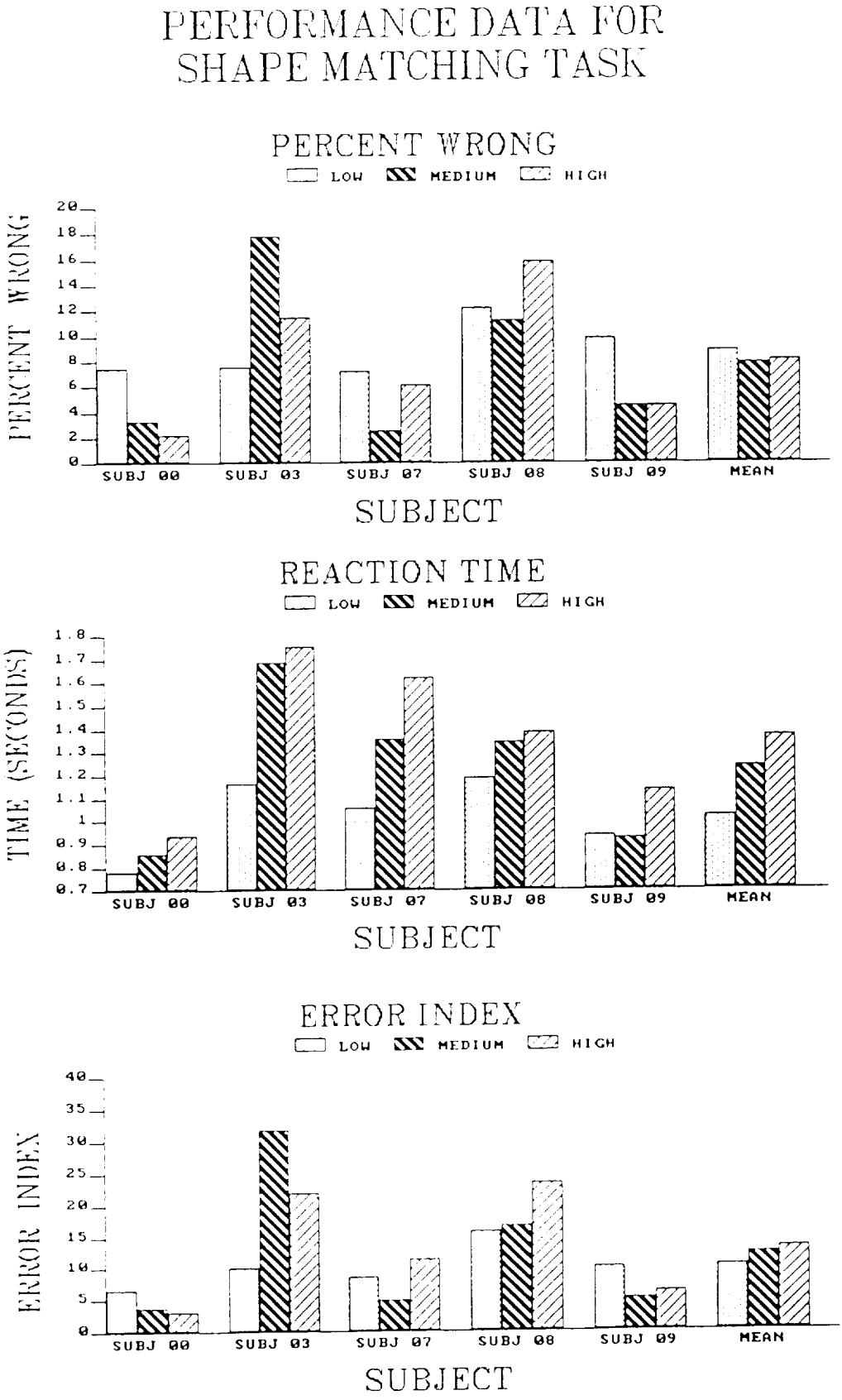

VI.1.1.2. Voltage ERP. (Figures VI.1.-1 through VI.1.-18)

Figures 1 through 15 show the voltage ERP for the Mixed task experiment. Each multichannel ERP was constructed by averaging 32 artifact-free stimulus-gated EEG recordings. In these figures, the ERPs for the Low, Medium and High levels of difficulty are overlayed for each electrode. To avoid crowding the figures, only 18 of the 21 electrode traces are shown; the 3 frontal-most electrodes (used for artifact rejection) are omitted. An upward deflection of the trace represents a "+" activity. The heavy vertical lines are separated by 100 msec.

In order to understand the charts in Sections VI.1.1.2, VI.1.1.3, and VI.1.3 it is essential to know the file name convention. Using the file "AM03L.EEG" as an example, the convention is as follows:

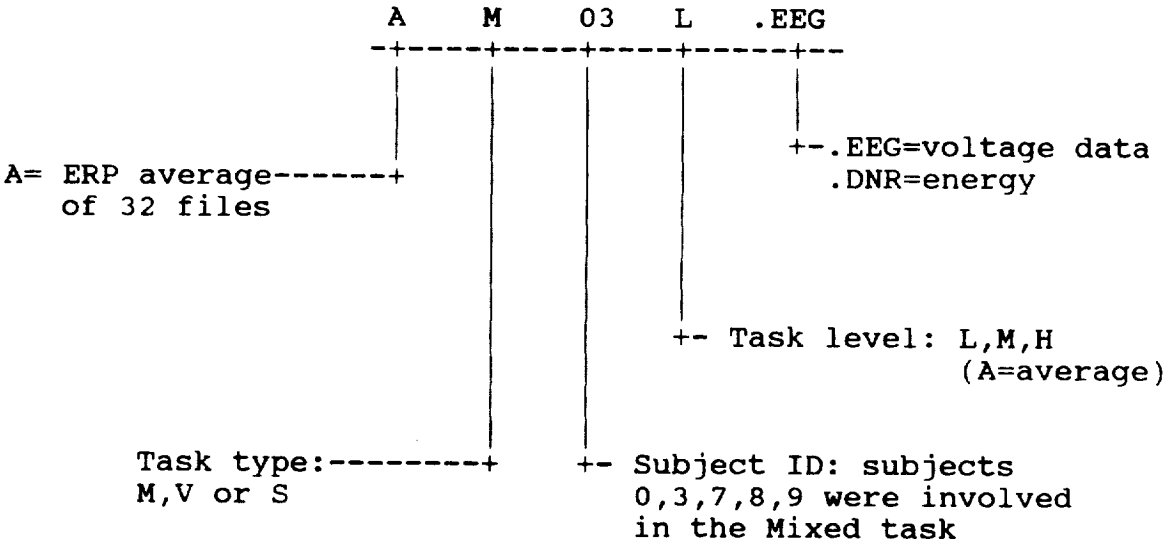

In general, the traces are remarkably similar for all task levels and for all subjects, with minor qualitative differences. For all task types, a series of positive and negative peaks can be identified in the frontal/temporal region, central parietal, posterior temporal and occipital areas. The most prominent peaks occur at about 150 and 350 msec in the frontal temporal area, at 150 and 400 msec in the parietal region and at 350 msec in the occipital region. A negative occipital peak at 350 msec is followed by a ramp-like positivity lasting approximately 250 msec.

The traces for the separate task level traces are also very similar. Clearly there are instances where there is an amplitude difference between the overlayed traces. T-value traces were constructed to determine the significance of the amplitude difference between the traces. As an example, Figures 16 and 17 show t-value curves for a t-test of statistical difference between the Low, Medium and High

traces for two subjects (00 and 03) for the Math task. For each electrode, at each instant, the electrode value is a mean of 32 individual observations and the t-test evaluates the difference between the mean values for the two ERPs relative to the variance among the underlying observations. Performing this test at each instance (for each electrode) produces the t-value traces.

The horizontal dotted and dashed lines in Figures 16 and 17 show the t-value required for rejecting the null hypothesis at the .05 level. Although significant amplitude differences between task levels are seen, these differences are not monotonically graded nor generalizable: significant differences fail to occur at the same electrode site and time period for the subjects tested. Figure 18 overlays the t-value traces for the two subjects used in this example, in order to show that, even if monotonicity were not an issue, it is difficult to find electrode/time combinations for which the Low-Medium separation is statistically significant for both subjects.

The negative results with respect to task level comparisons in the EEG data might be interpreted as symptomatic of lack of validity of the task level construct. An example of this problem was discovered when the Phase I data was re-examined (Guisado et al, 1988). During Phase I, on-going EEG and ERPs were obtained from ten subjects performing a mathematical processing task as presented by the USAF Criterion Task Set (CTS) Cognitive battery (Action and Crabtree, 1985). ERP voltages in the occipital region were found to be co-variant with levels of difficulty of the task (numbers of terms of the mental arithmetic problem). Further analysis however, revealed that since the three levels of the task used progressively longer arithmetic expressions (progressively longer character strings on the computer screen) this implied progressively higher luminosity and wider visual scanning. These effects, by themselves, could have accounted for the ERP gradations.

That particular problem was corrected by modifying the stimulus package. A similar problem was the possibility that arithmetic expressions could, at random, contain repeated numbers which make the arithmetic problem easier than intended. The "High" difficulty problem 2+2+2+2 is rather trivial but it could be labeled as being in the same category as 2+6+9-5. Another example is "cancelling", as in 3+9-9. Many checks were built into the Phase II stimulus program to prevent subtle mislabeling of task levels.

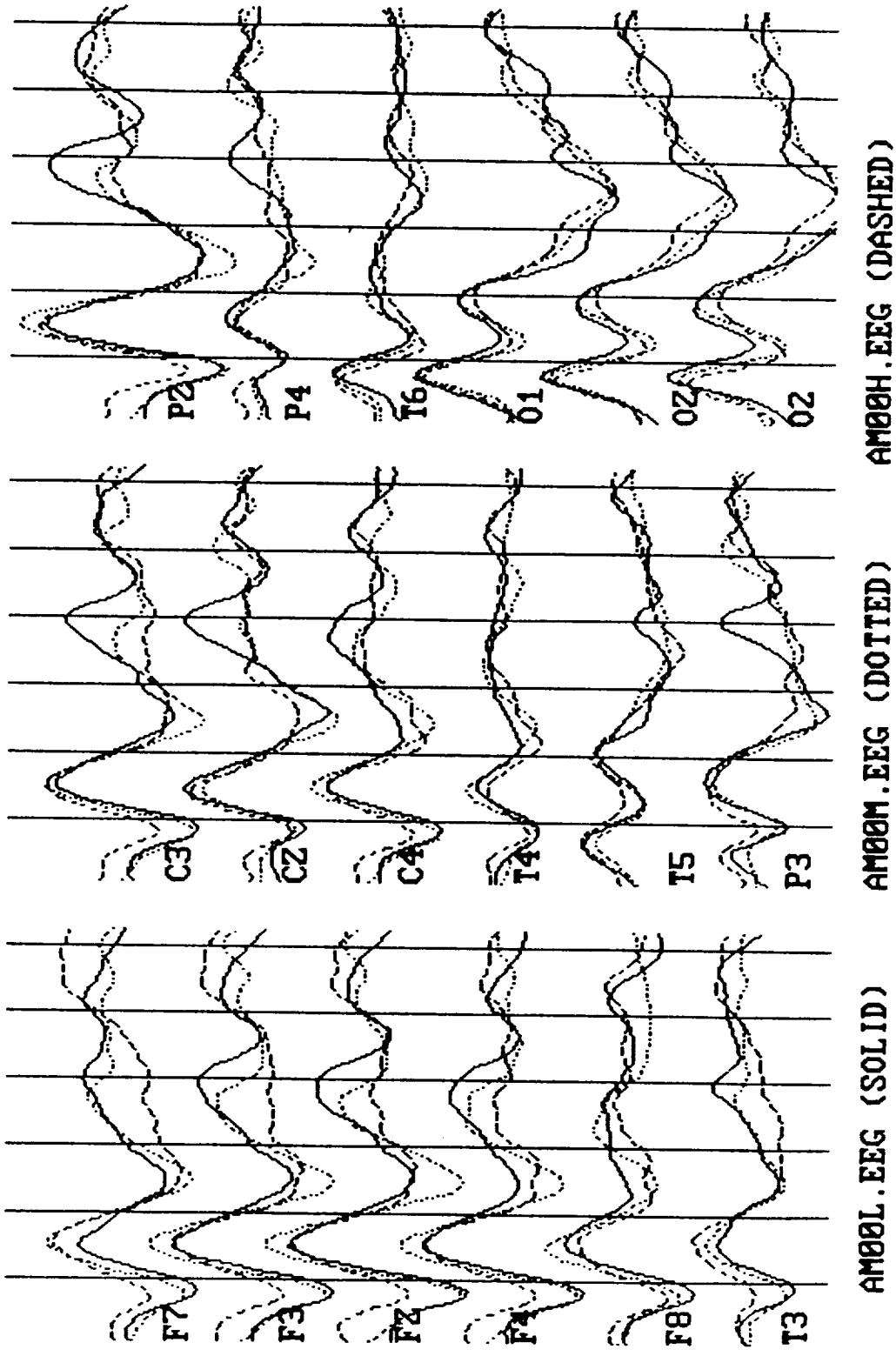
F7
F3
FZ
F4
F8
T3
C3
C2
C4
T4
T5
P3
P2
P4
T6
O1
OZ
O2
AM00L.EEG (SOLID)
AM00M.EEG (DOTTED)
AM00H.EEG (DASHED)

FIGURE VI.1.-1

FIGURE VI.1.-2

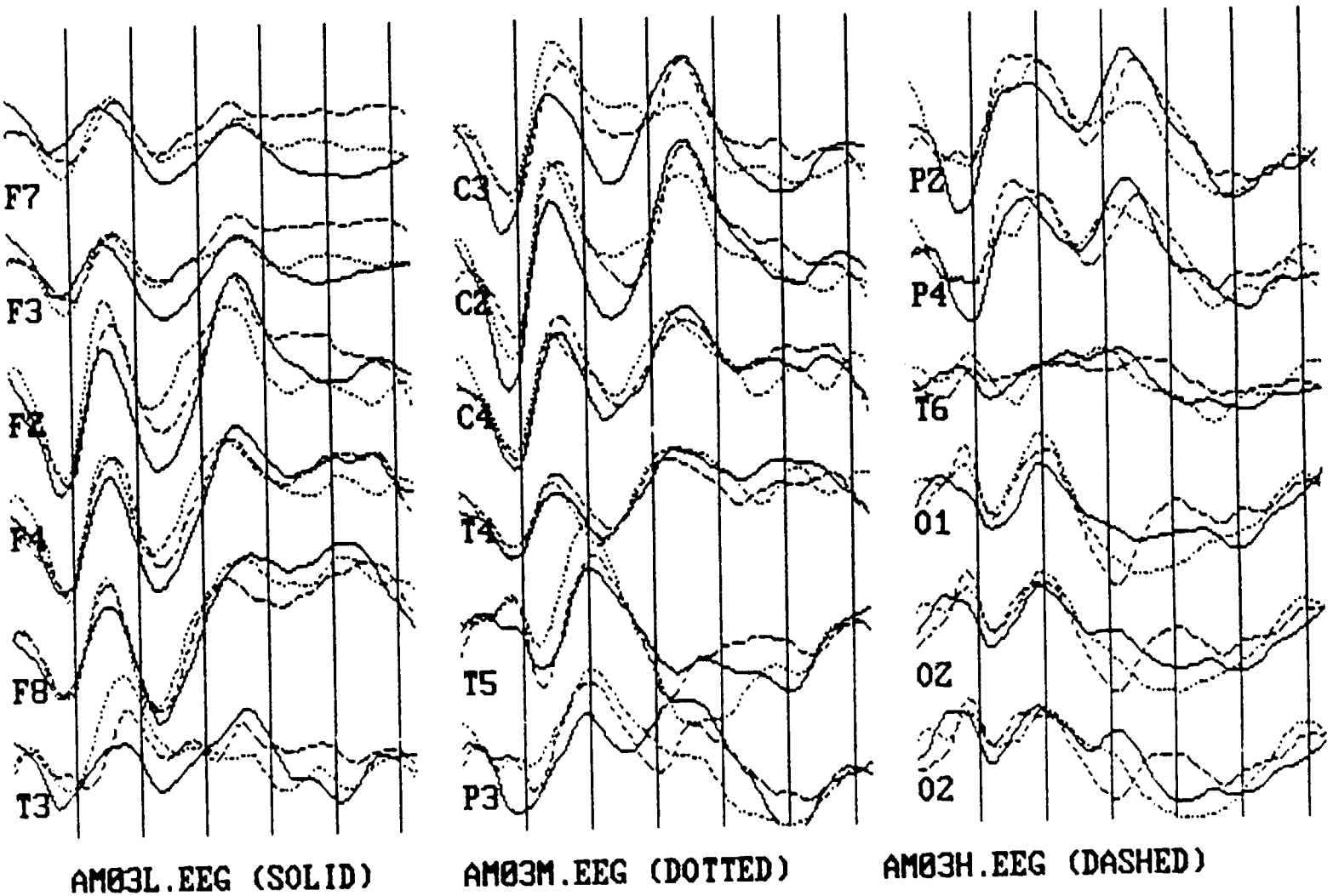
F7
F3
FZ
F4
F8
T3
C3
CZ
C4
T4
T5
P3
PZ
P4
T6
01
OZ
02
AM03L.EEG (SOLID)
AM03M.EEG (DOTTED)
AM03H.EEG (DASHED)

FIGURE VI.1.-3

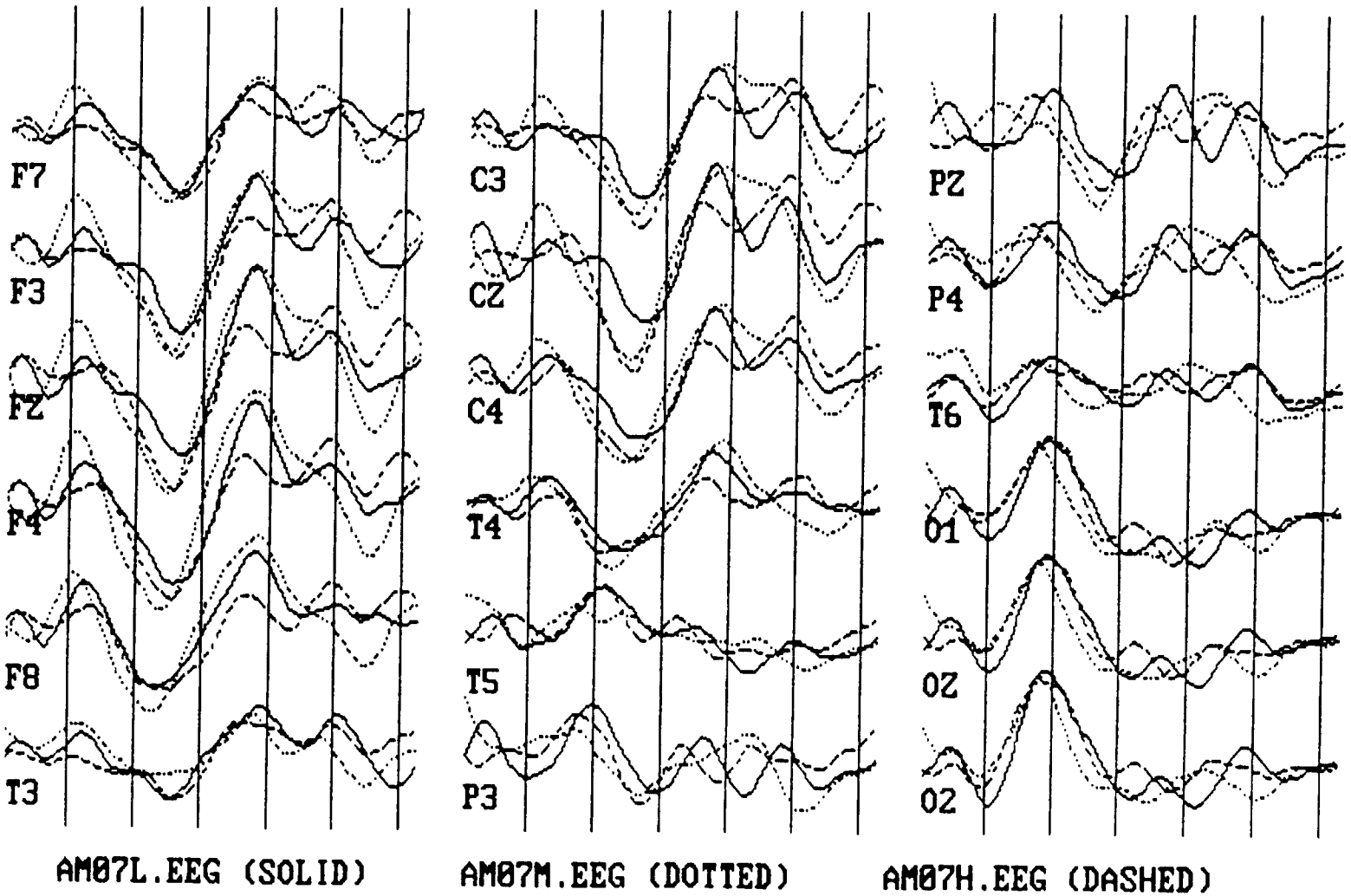
F7
F3
FZ
F4
F8
T3
C3
CZ
C4
T4
T5
P3
PZ
P4
T6
01
OZ
02
AM07L.EEG (SOLID)
AM07M.EEG (DOTTED)
AM07H.EEG (DASHED)

FIGURE VI.1.-4

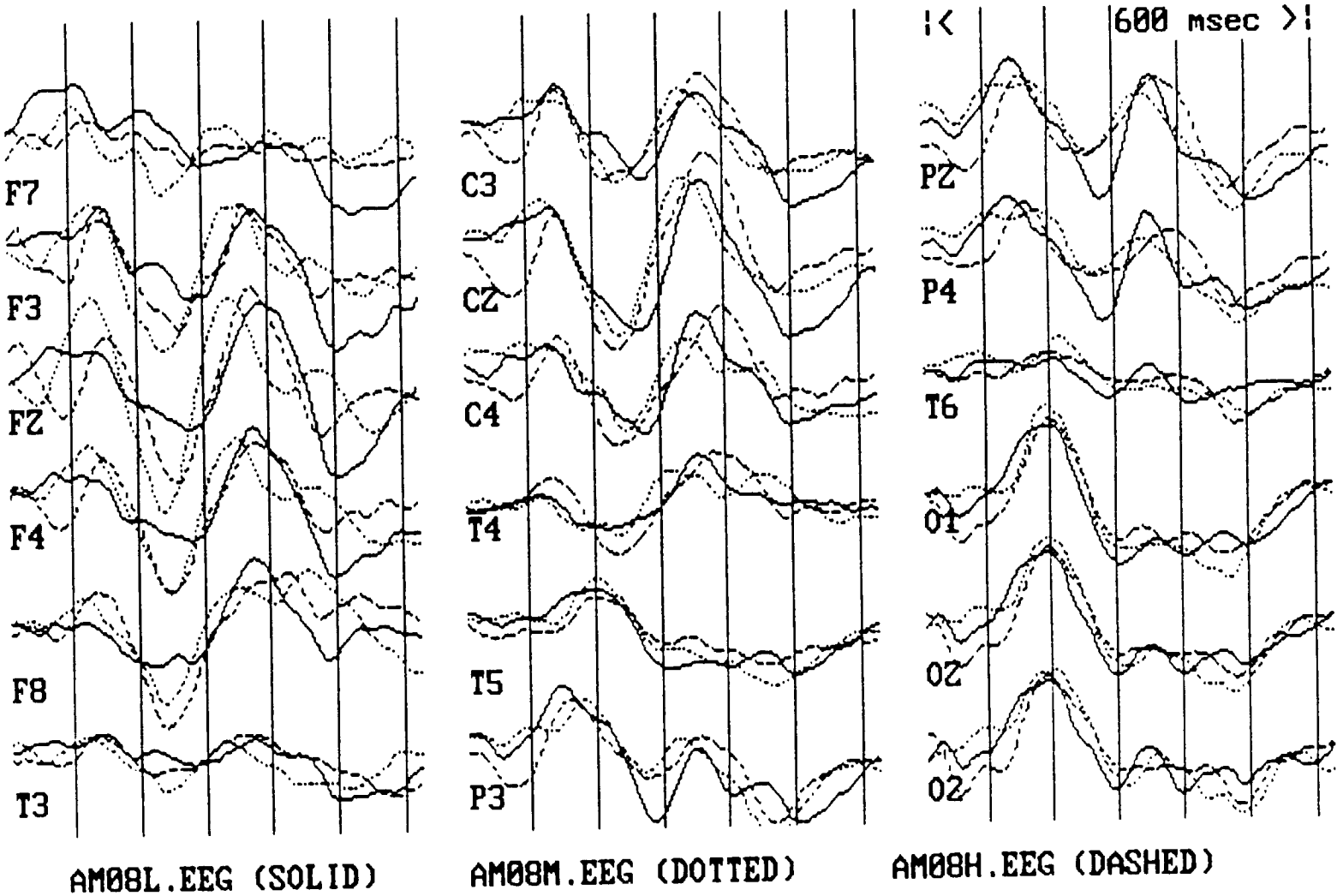
F7
F3
FZ
F4
F8
T3
C3
CZ
C4
T4
T5
P3
PZ
P4
T6
O1
O2
02
|< 600 msec >|
AM08L.EEG (SOLID)
AM08M.EEG (DOTTED)
AM08H.EEG (DASHED)

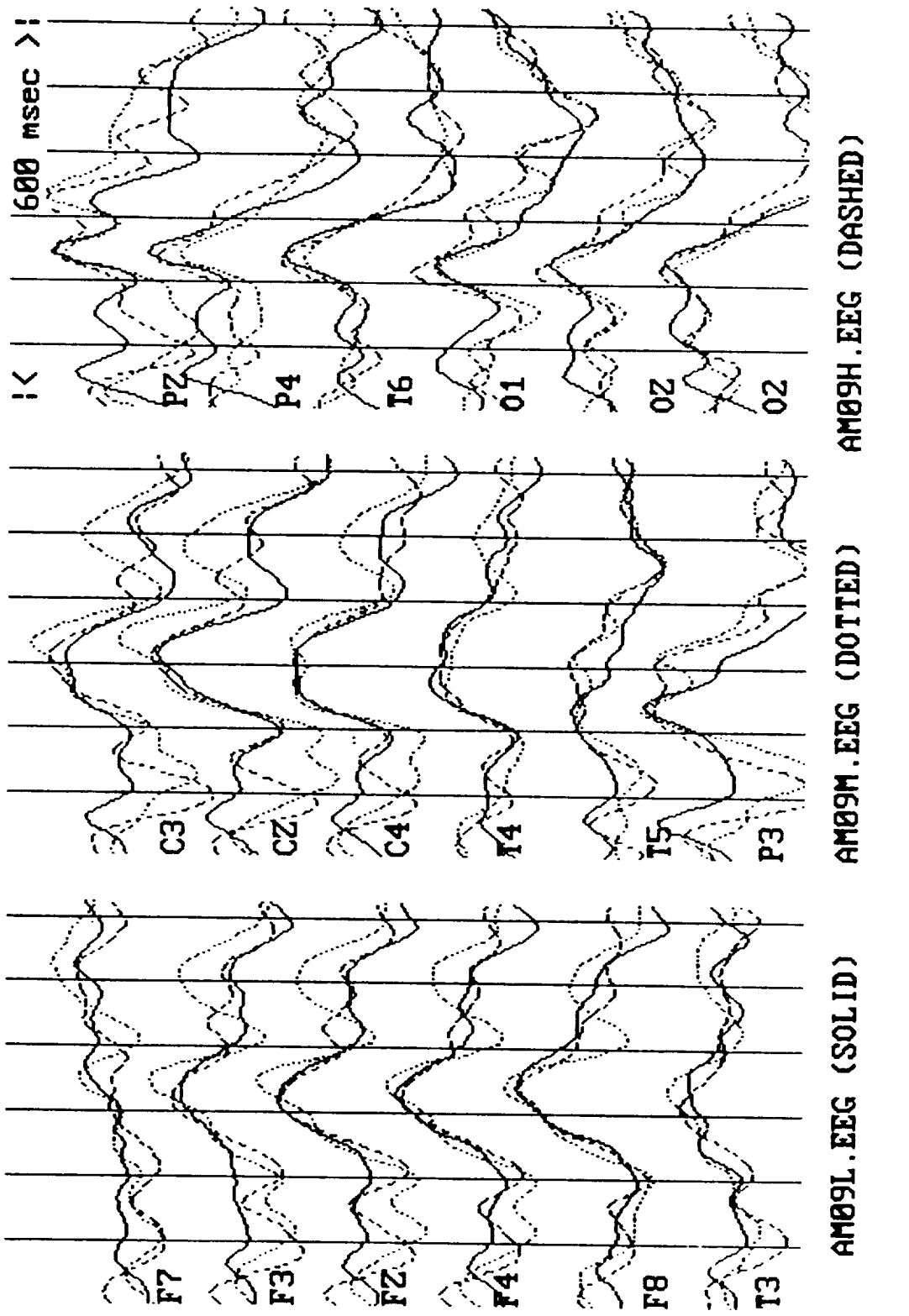
600 msec
F7
F3
FZ
F4
F8
T3
C3
CZ
C4
T4
T5
P3
PZ
P4
T6
O1
OZ
O2
AM09L.EEG (SOLID)
AM09M.EEG (DOTTED)
AM09H.EEG (DASHED)

FIGURE VI.1.-5

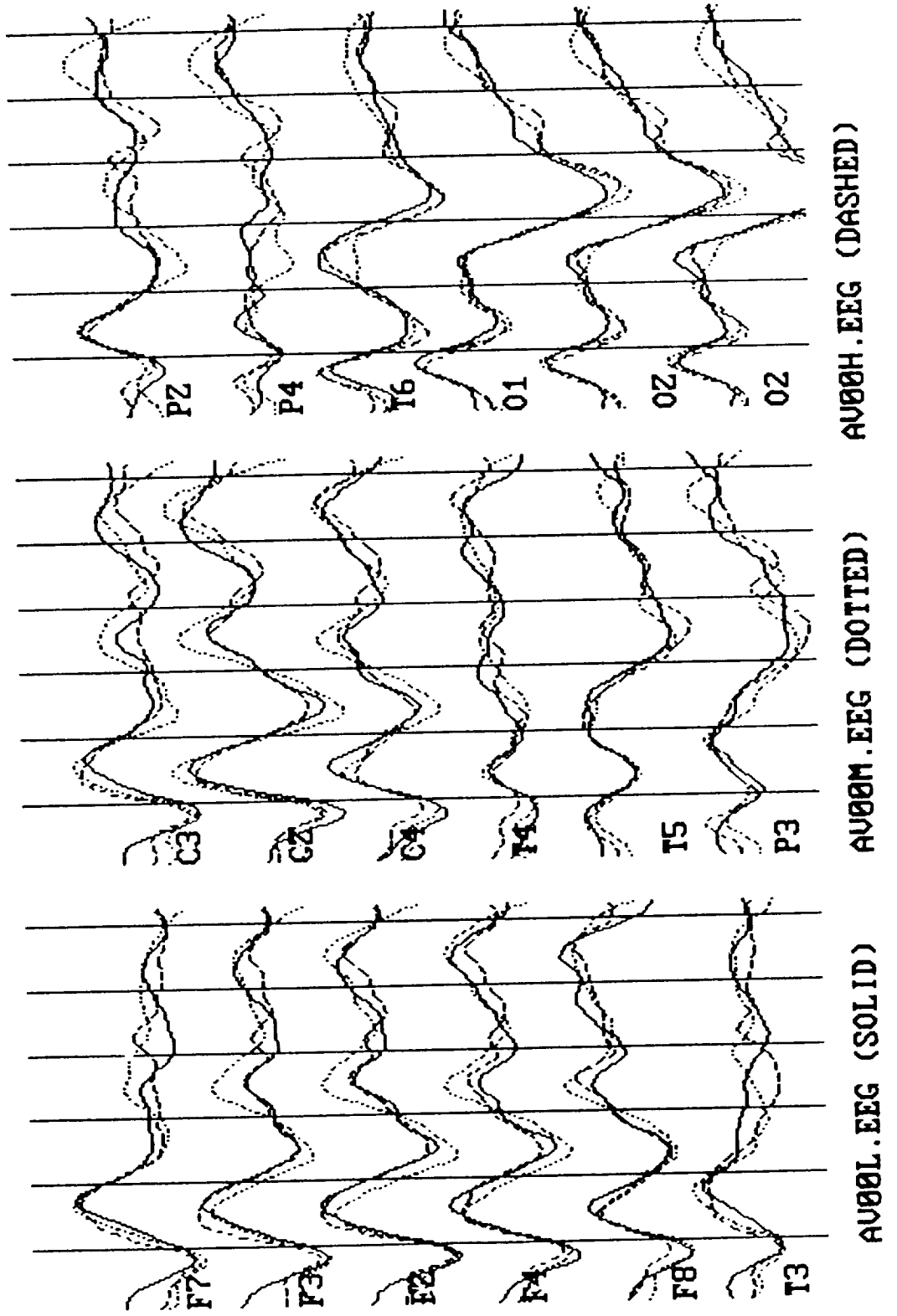
F7
F3
E2
F4
F8
T3
C3
CZ
C4
T4
T5
P3
PZ
P4
T6
O1
OZ
O2
AV00L.EEG (SOLID)
AV00M.EEG (DOTTED)
AV00H.EEG (DASHED)

FIGURE VI.1.-6

FIGURE VI.1.-7

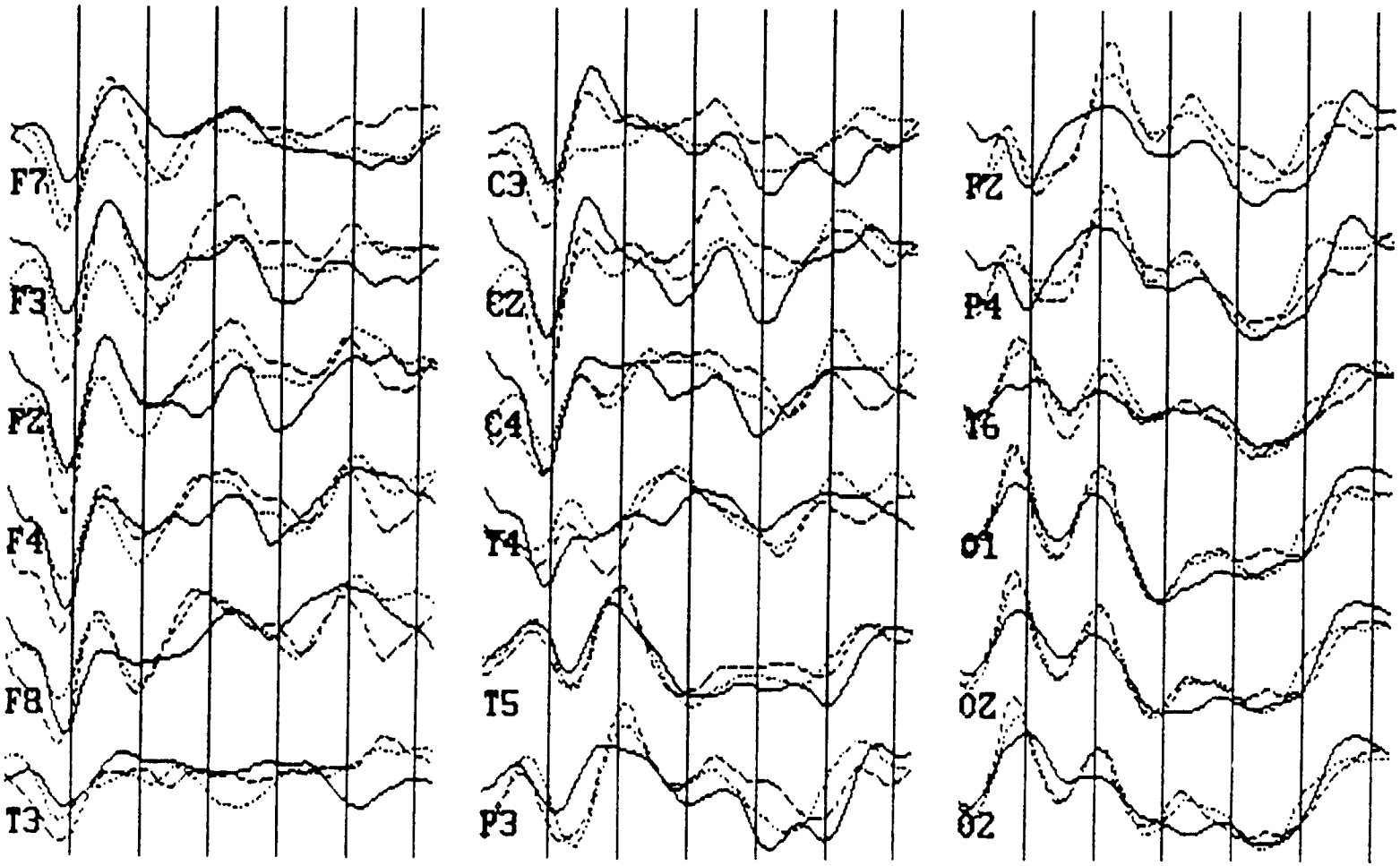
F7
F3
FZ
F4
F8
T3
C3
CZ
C4
T4
T5
P3
PZ
P4
T6
O1
OZ
O2
AV03L.EEG (SOLID)
AV03M.EEG (DOTTED)
AV03H.EEG (DASHED)

FIGURE VI.1.-8

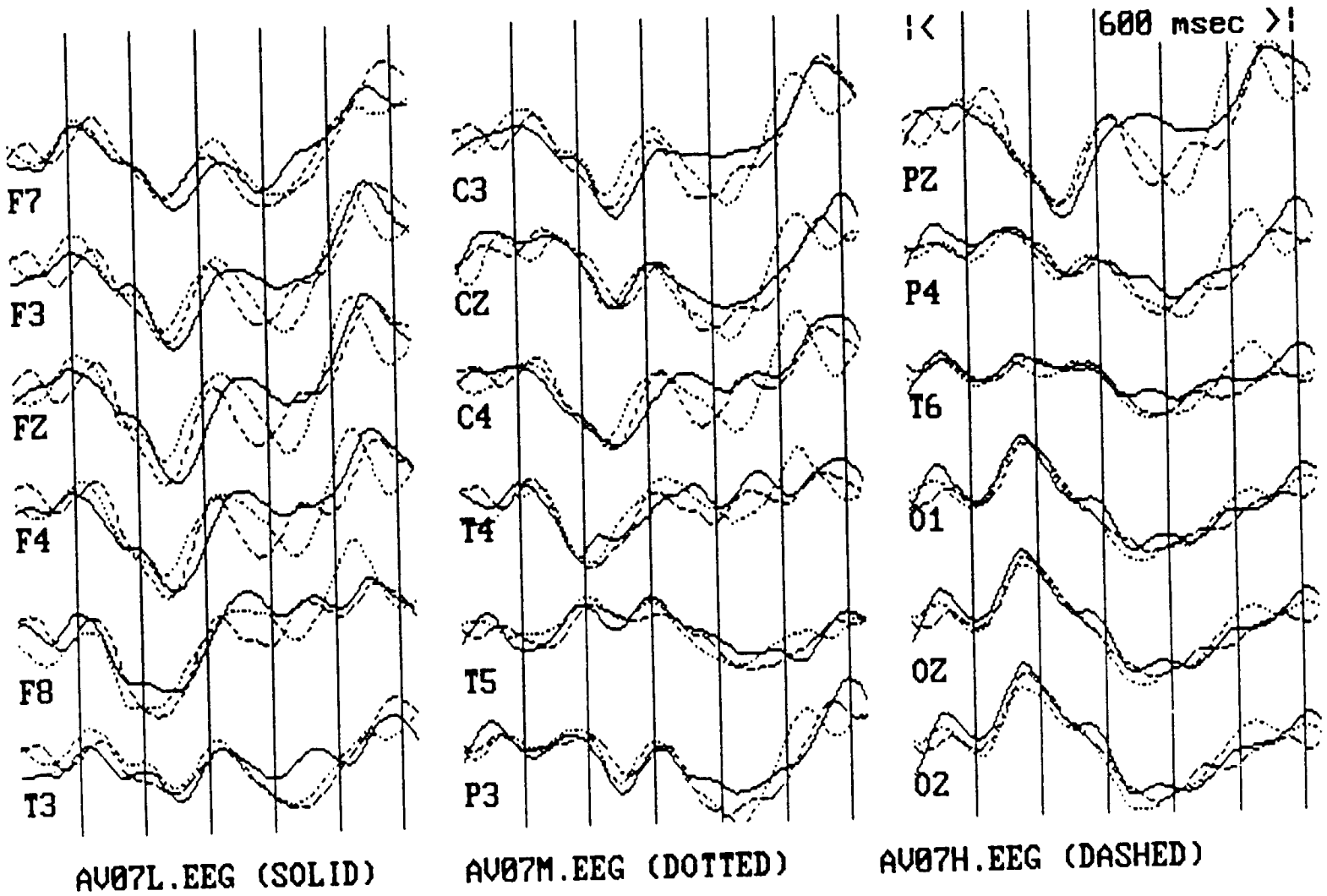
F7
F3
FZ
F4
F8
T3
C3
CZ
C4
T4
T5
P3
PZ
P4
T6
O1
OZ
O2
|< 600 msec >|
AV07L.EEG (SOLID)
AV07M.EEG (DOTTED)
AV07H.EEG (DASHED)

FIGURE VI.1.-9

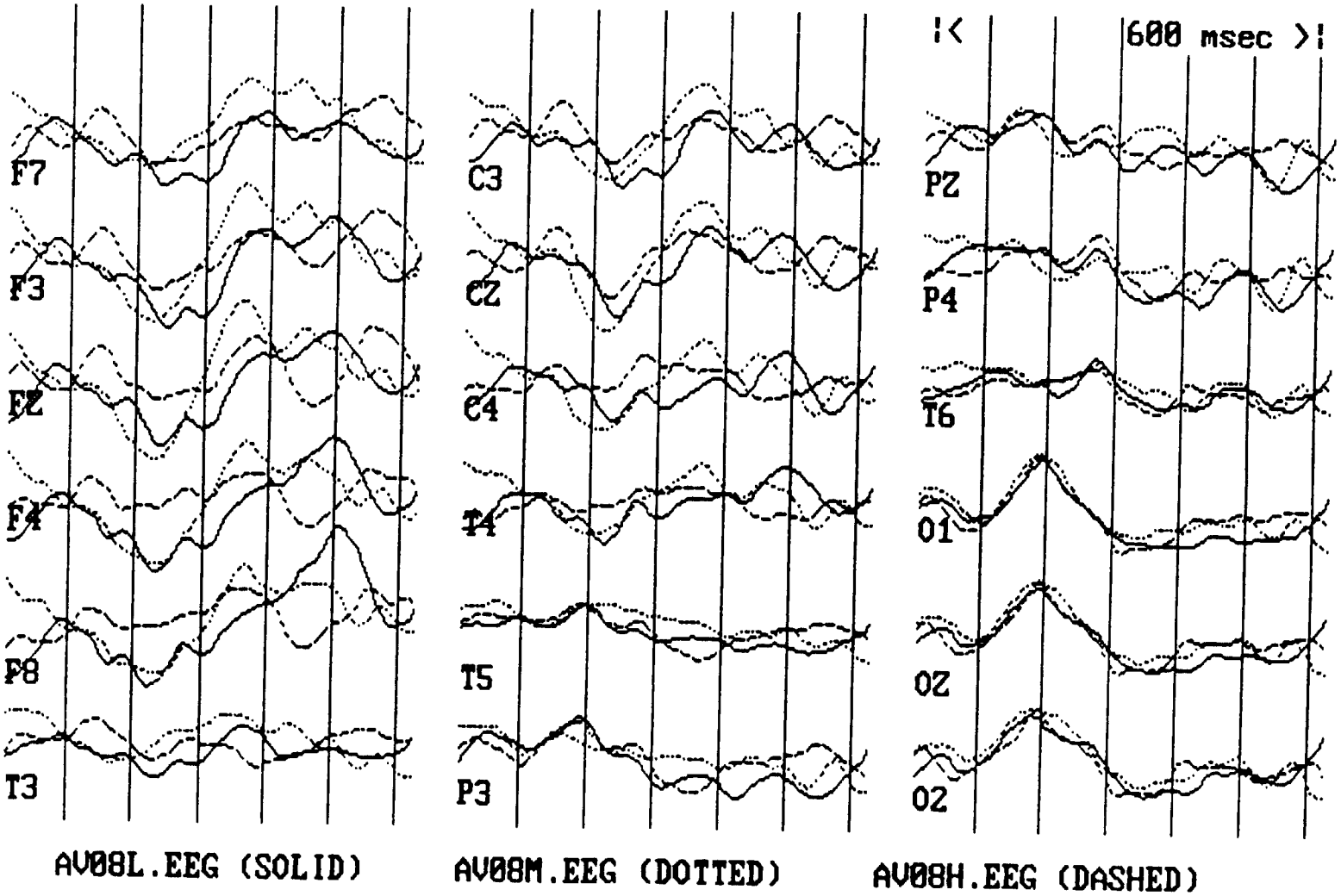
F7
F3
FZ
F4
F8
T3
C3
CZ
C4
T4
T5
P3
PZ
P4
T6
O1
OZ
O2
|< 600 msec >|
AV08L.EEG (SOLID)
AV08M.EEG (DOTTED)
AV08H.EEG (DASHED)

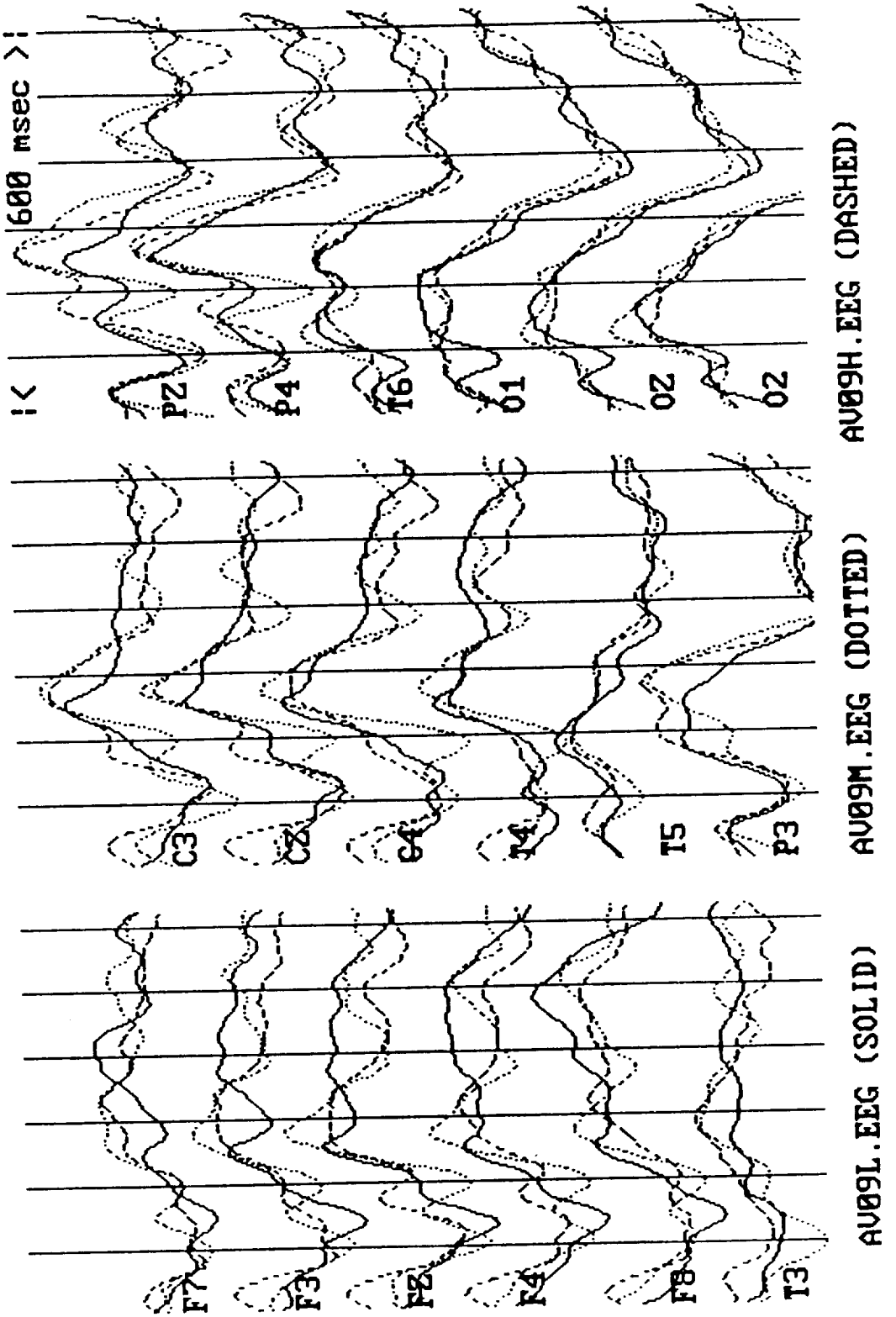

FIGURE VI.1.-10

FIGURE VI.1.-11

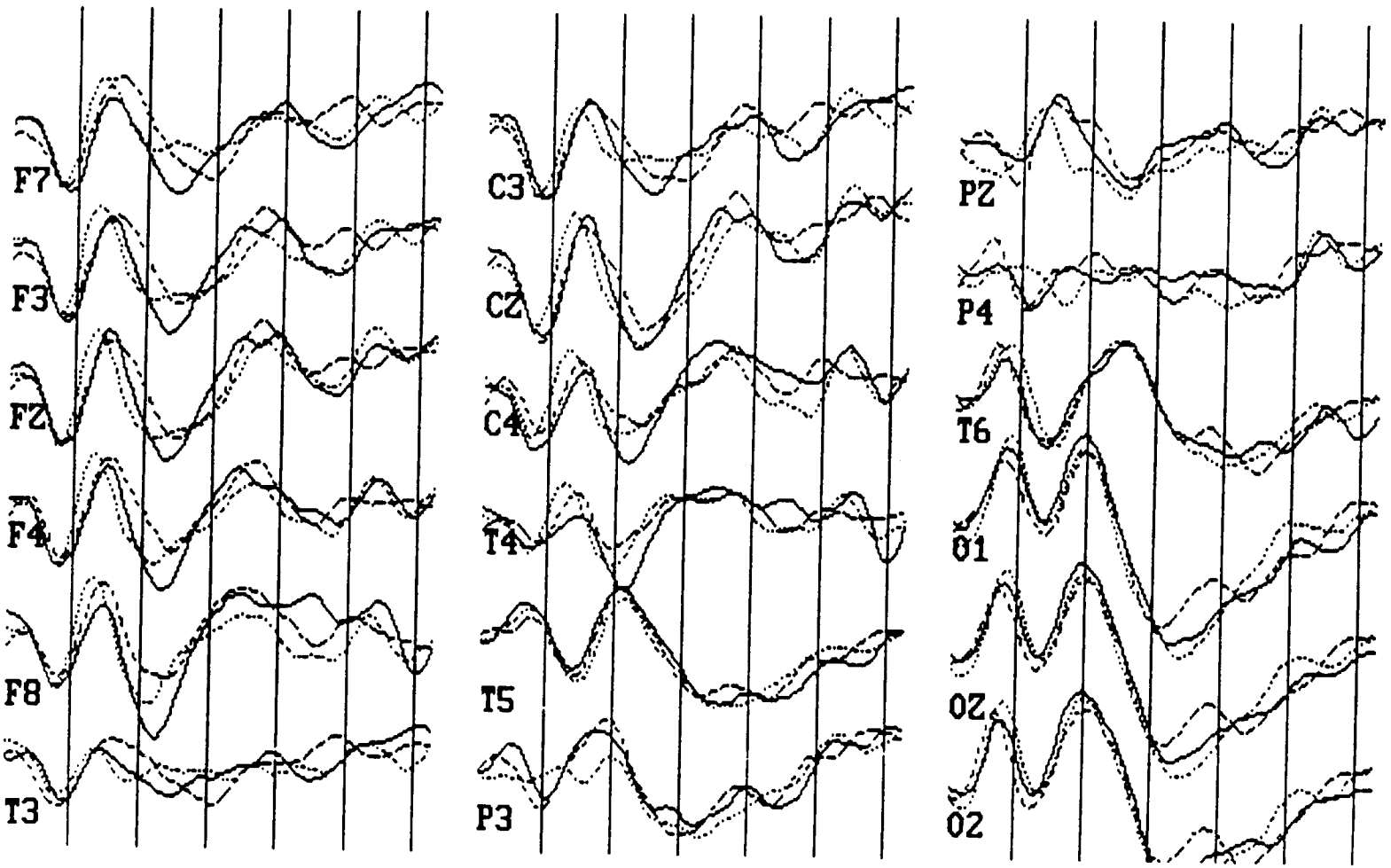

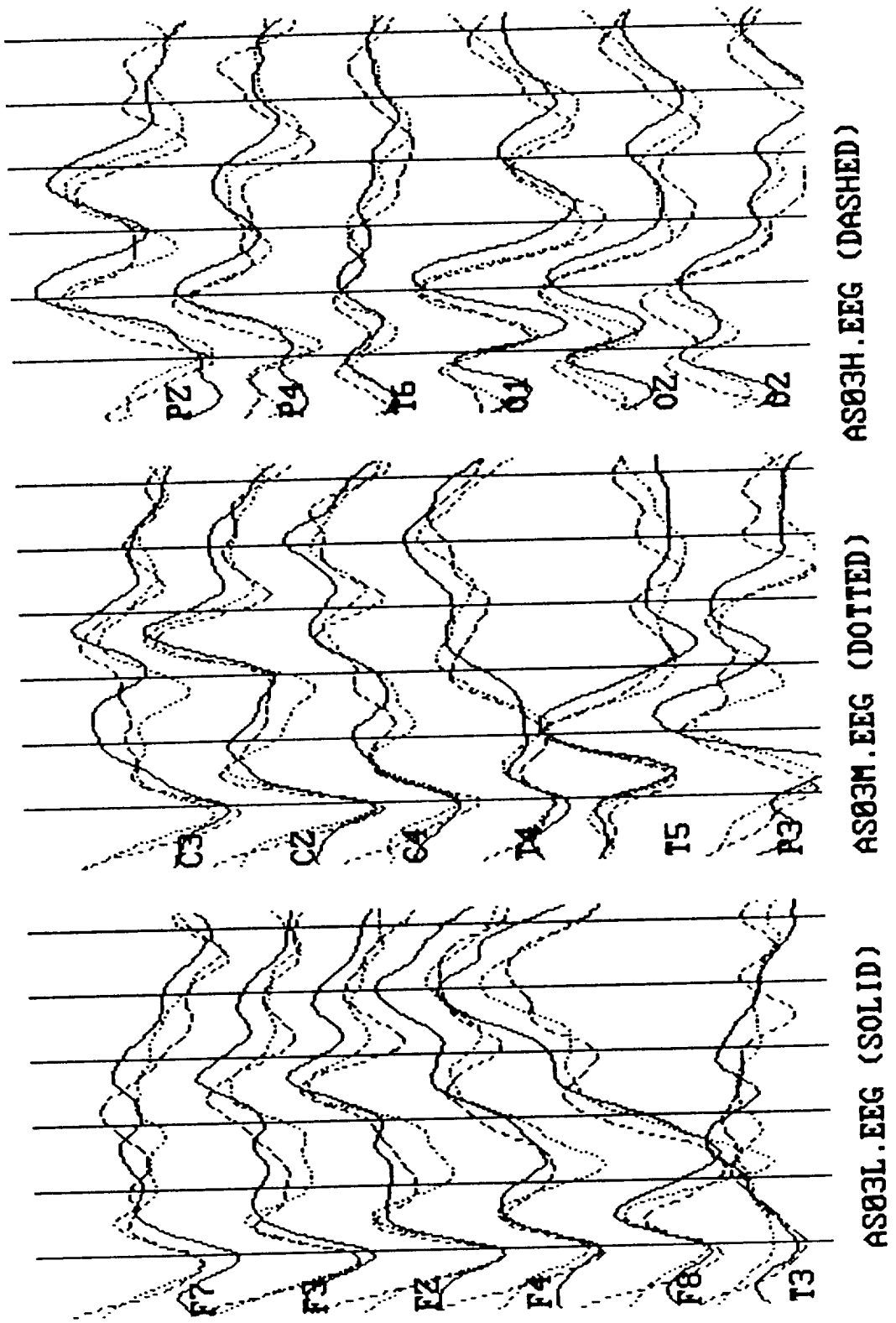

FIGURE VI.1.-12

FIGURE VI.1.-13

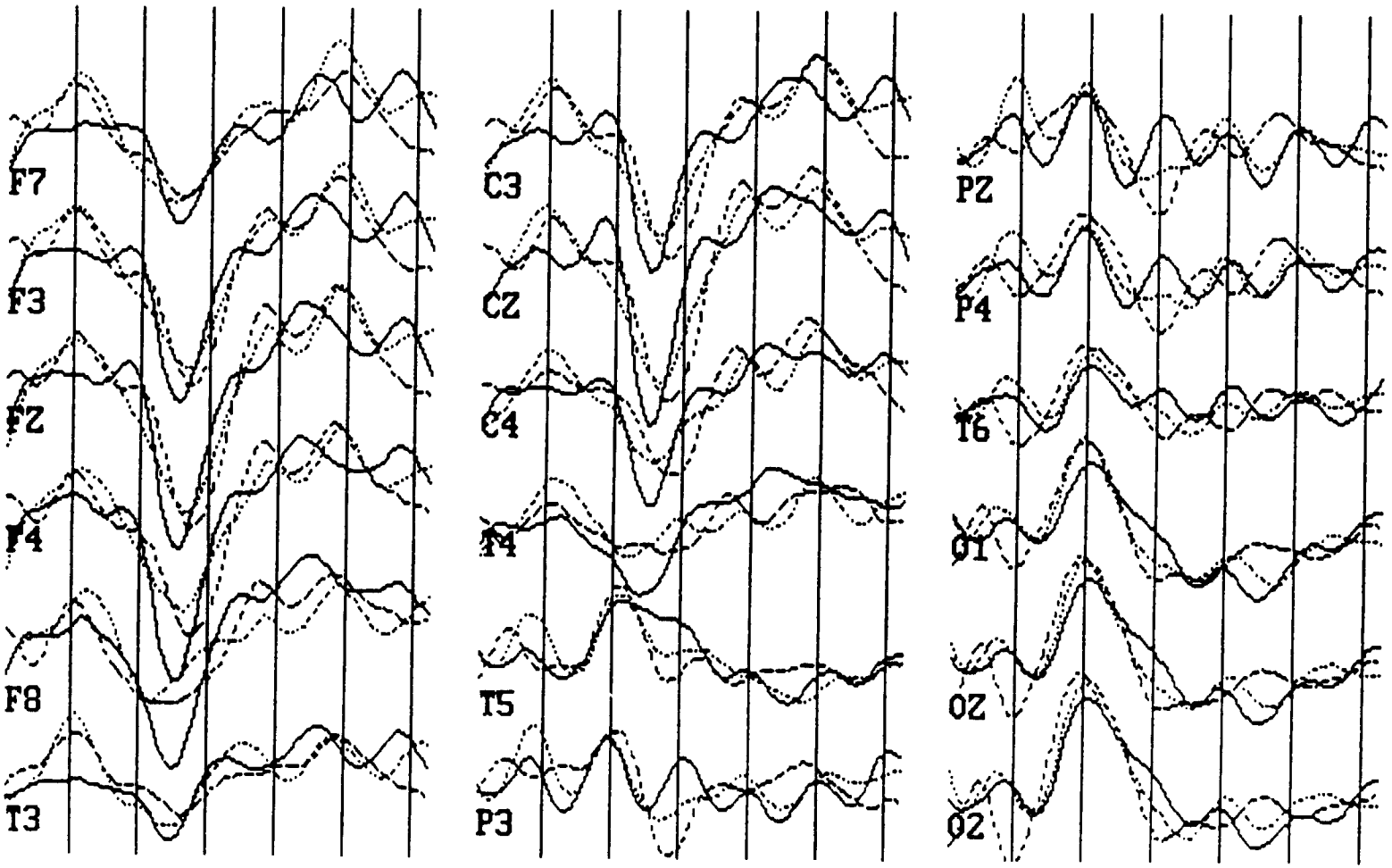

FIGURE VI.1.-14

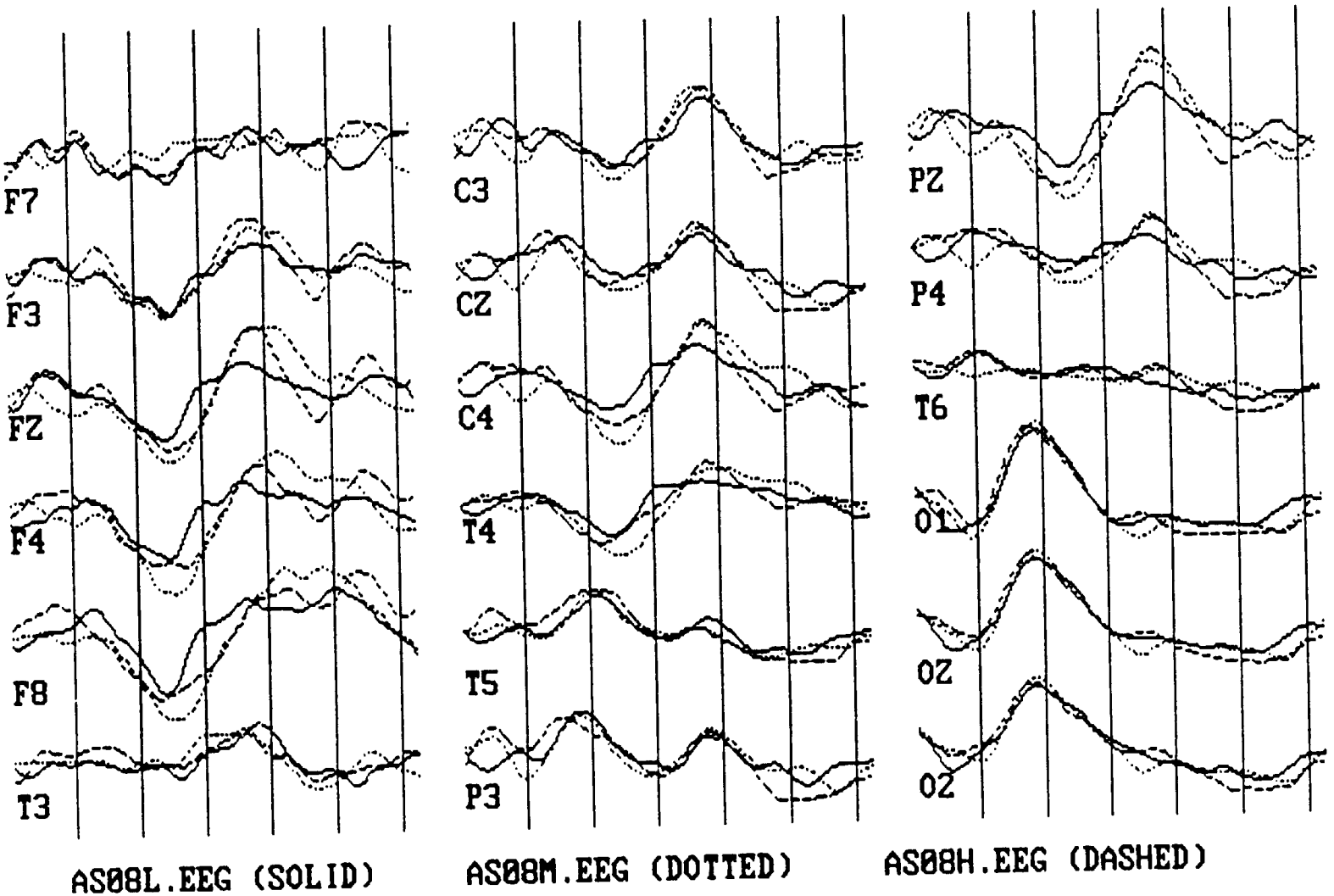

FIGURE VI.1.-15

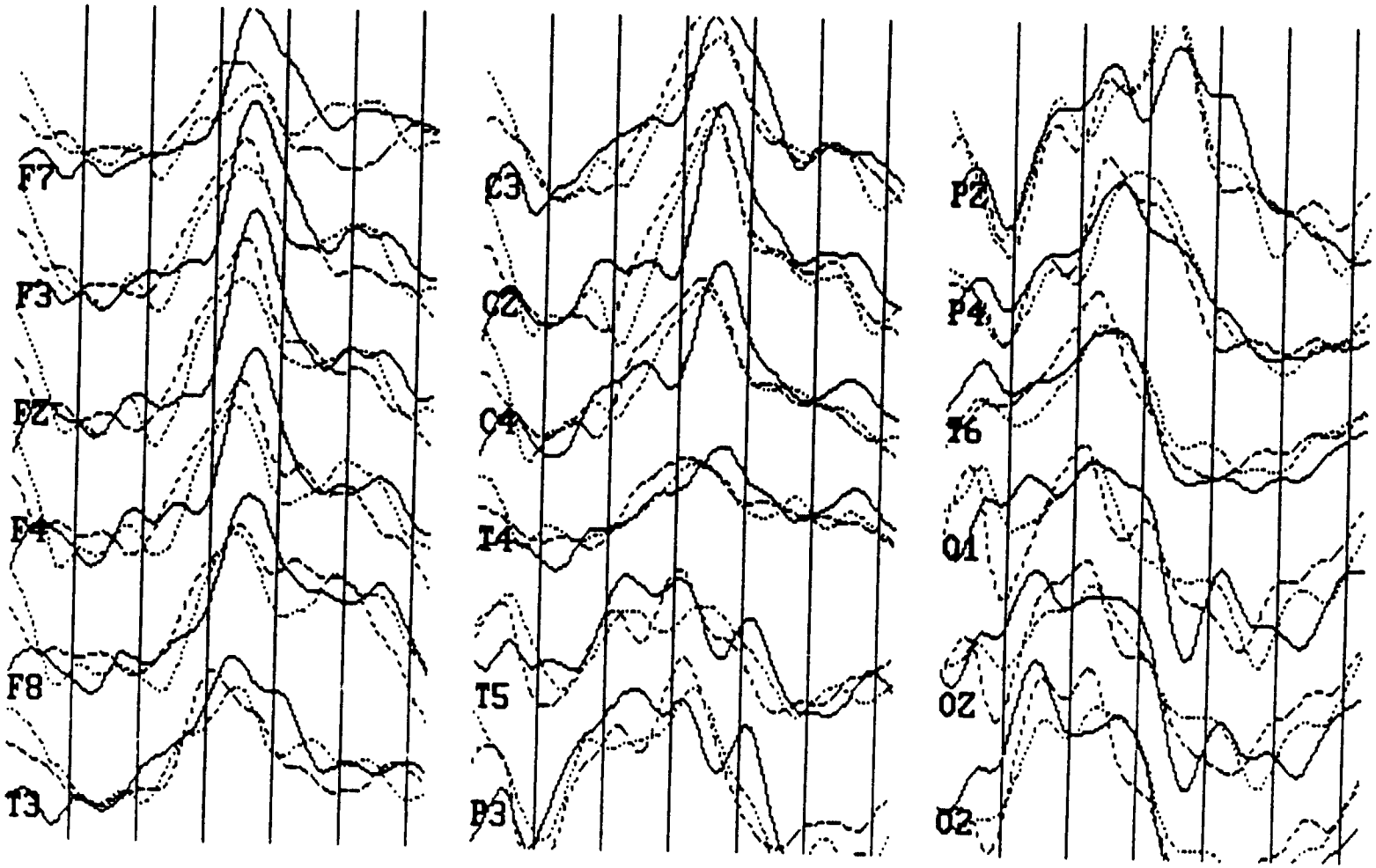

AS09L.EEG (SOLID) AS09M.EEG (DOTTED) AS09H.EEG (DASHED)

FIGURE VI.1.-16

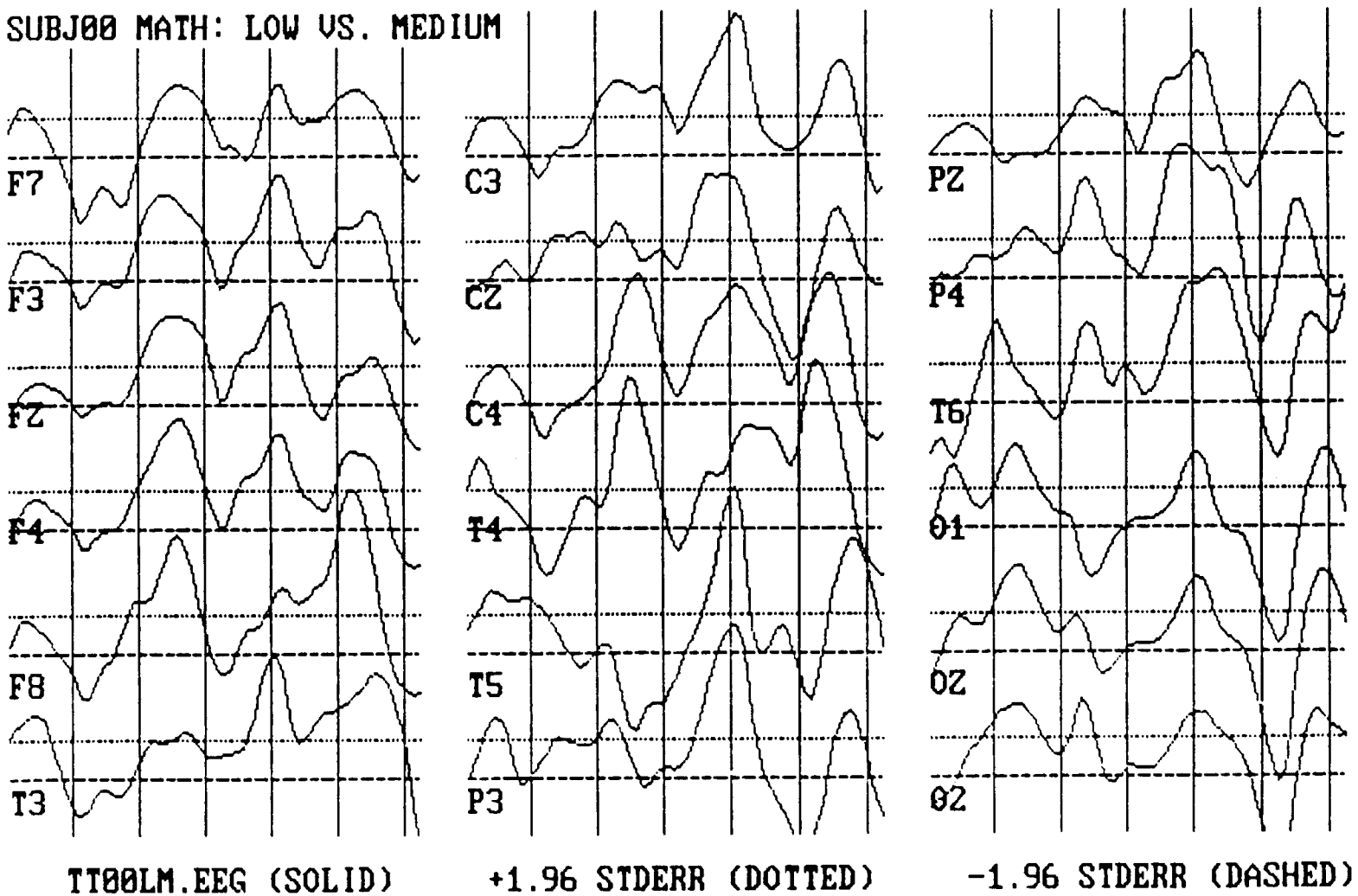

FIGURE VI.1.-17

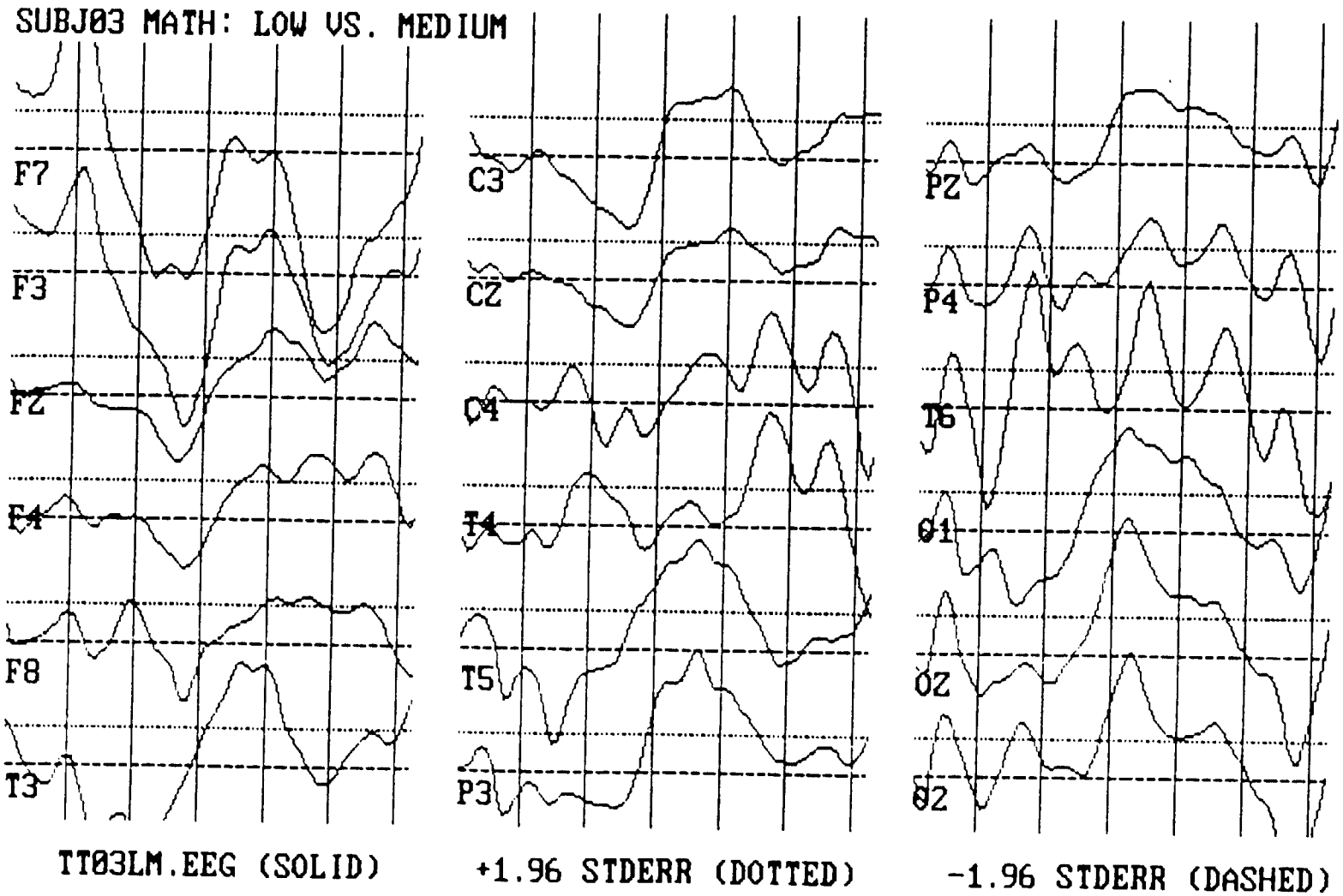

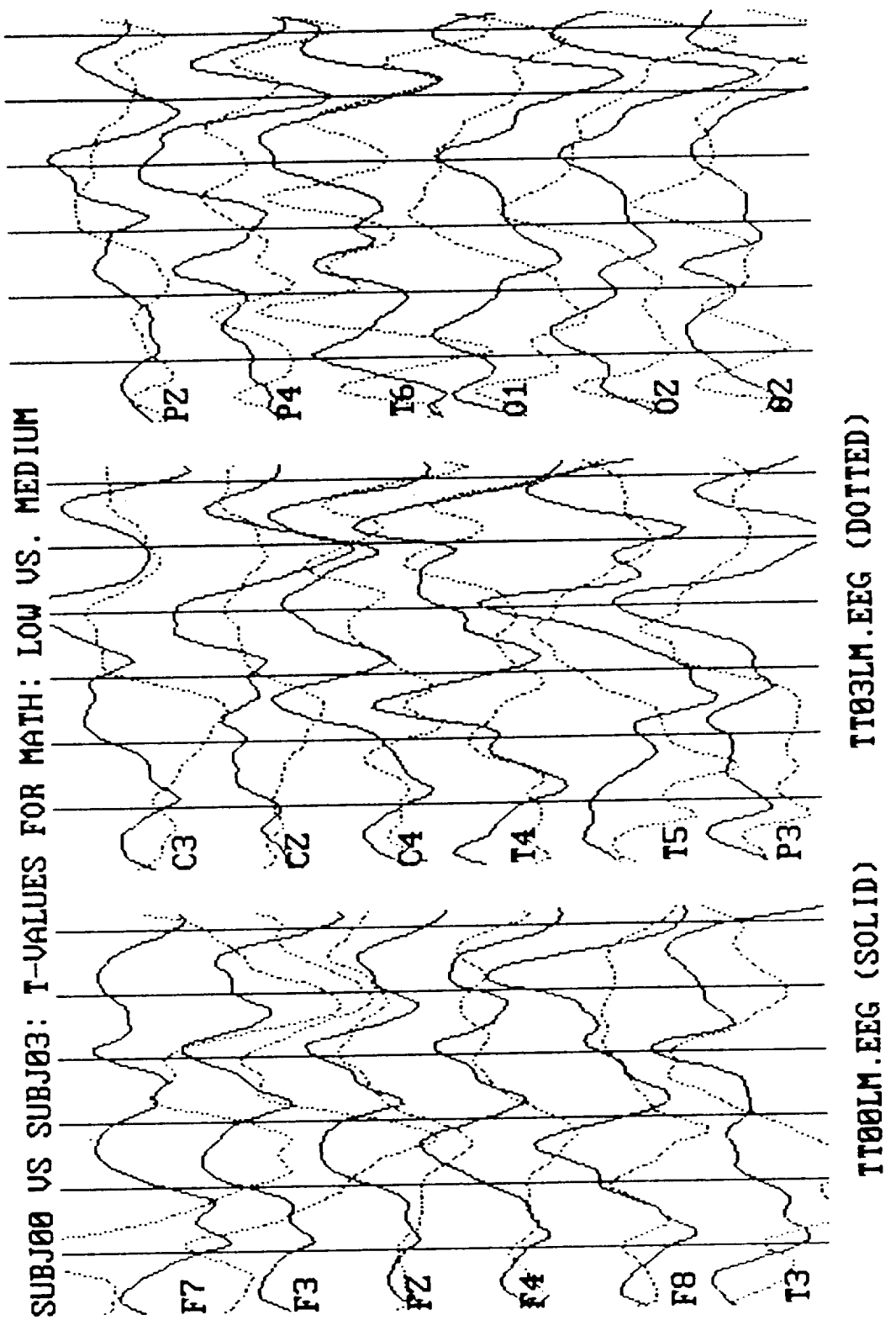

FIGURE VI.1.-18

VI.1.1.3. Energy ERP. (Figures VI.1.-19 through VI.1.-39)

The task level comparison proved to be just as problematic for the energy density data as for the raw voltage ERPs. Cases of statistically significant task level differences do occur, but no cases survive both the tests of monotonicity and generalizability. This demonstrates that, even when resolution is enhanced by the energy transformation, direct time trace analysis is not the best method to monitor cognition.

Figures 19 through 33 show the energy density ERPs for the Mixed task, with Low, Medium and High task level ERPs overlaid for each subject. Again, distinct peaks of activity can be defined during the first 600 msec after task presentation. The energy density transform results in fewer but better defined peaks than seen for the voltage ERP. The ERPs remain remarkably stable across task level. There are, however, distinct qualitative differences between task types and between subjects. In general, the most constant activity peaks appear at 150 msec over the frontal, central and temporal region and between 350-400 msec over the frontal and central regions. A distinct biphasic activity peak is present over the occipital region at 150-200 msec.

Unlike voltage however, energy density is a quantity that can be integrated. Figures 34 through 39 show the results, for the L-M-H comparison, of integrating energy density over electrode fields. "Right hemisphere electrodes" are represented by F4,F8,C4,T4,P4,T6 and O2 electrodes. "Left hemisphere electrodes" are represented by F3,F7,C3,T3,P3,T5 and O1 electrodes. "Front electrodes" are represented by F3,F7,Fz,F4,F8,T3,C3,Cz,C4 and T4 electrodes. "Back electrodes" are represented by T5,P3,Pz,P4,T6,O1,Oz and O2 electrodes.

Although for any given subject there are shifts in the front to back or left to right relationships that seem graded with task level, it is difficult to generalize these themes across subjects.

FIGURE VI.1.-19

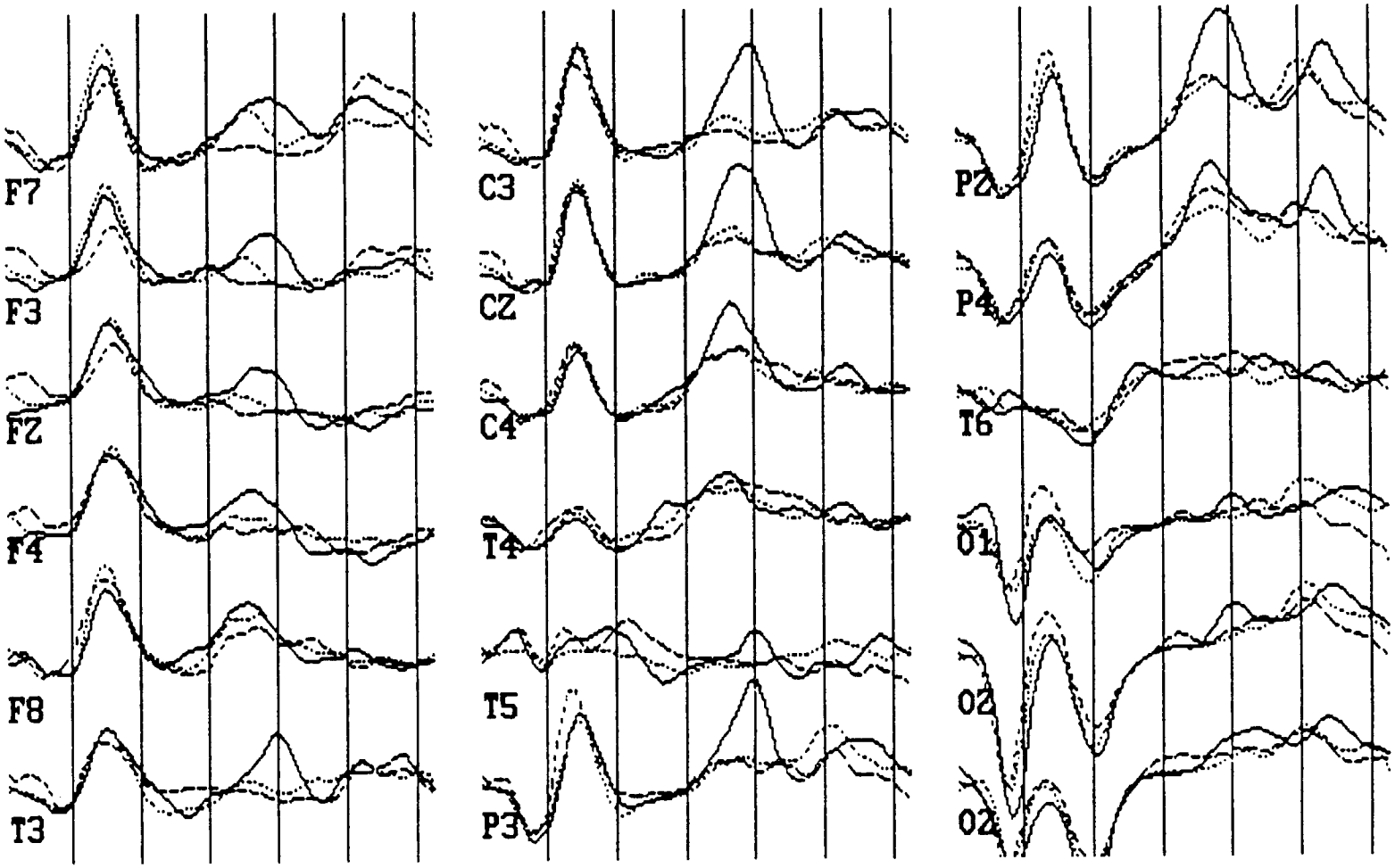

FIGURE VI.1.-20

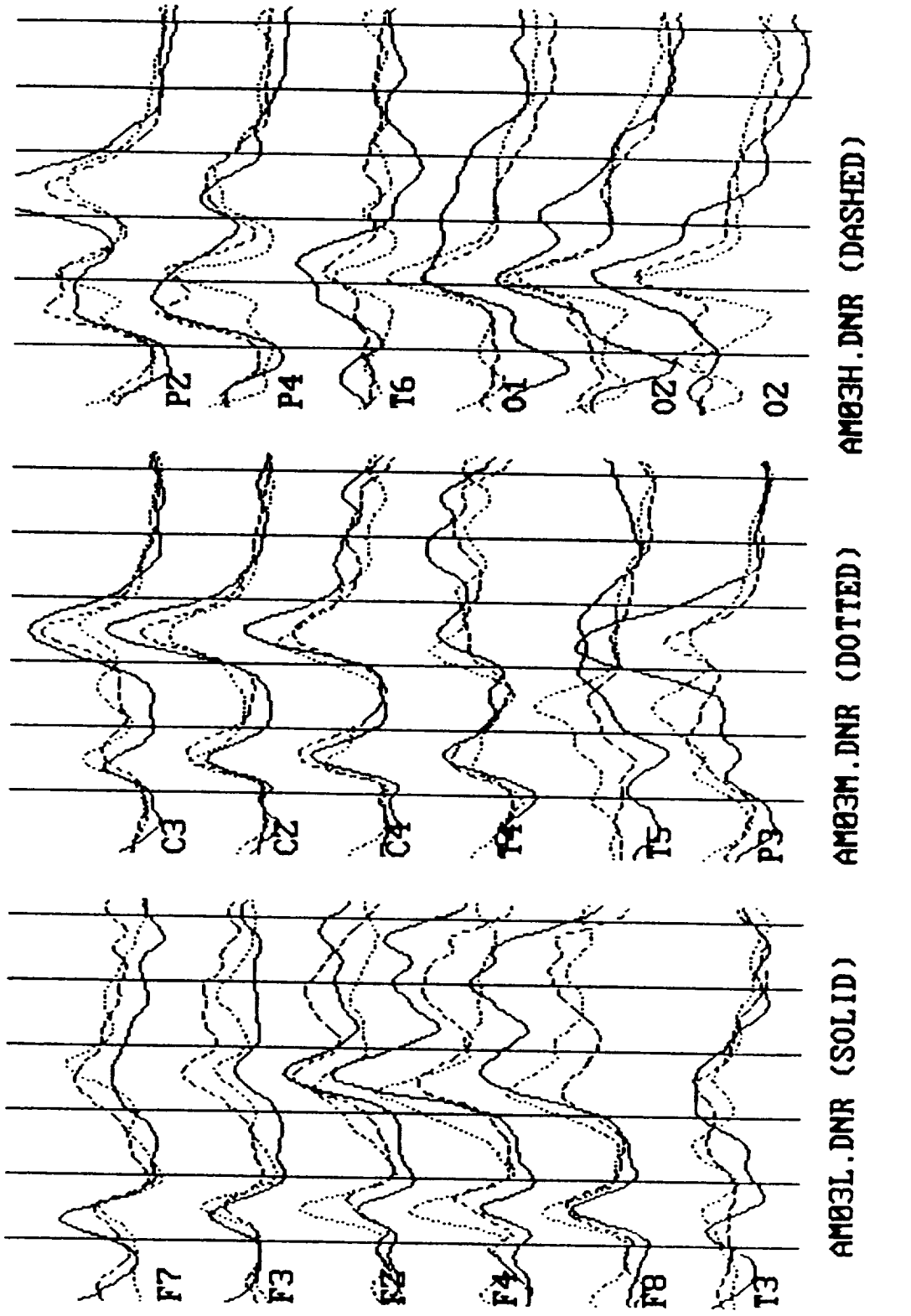

FIGURE VI.1.-21

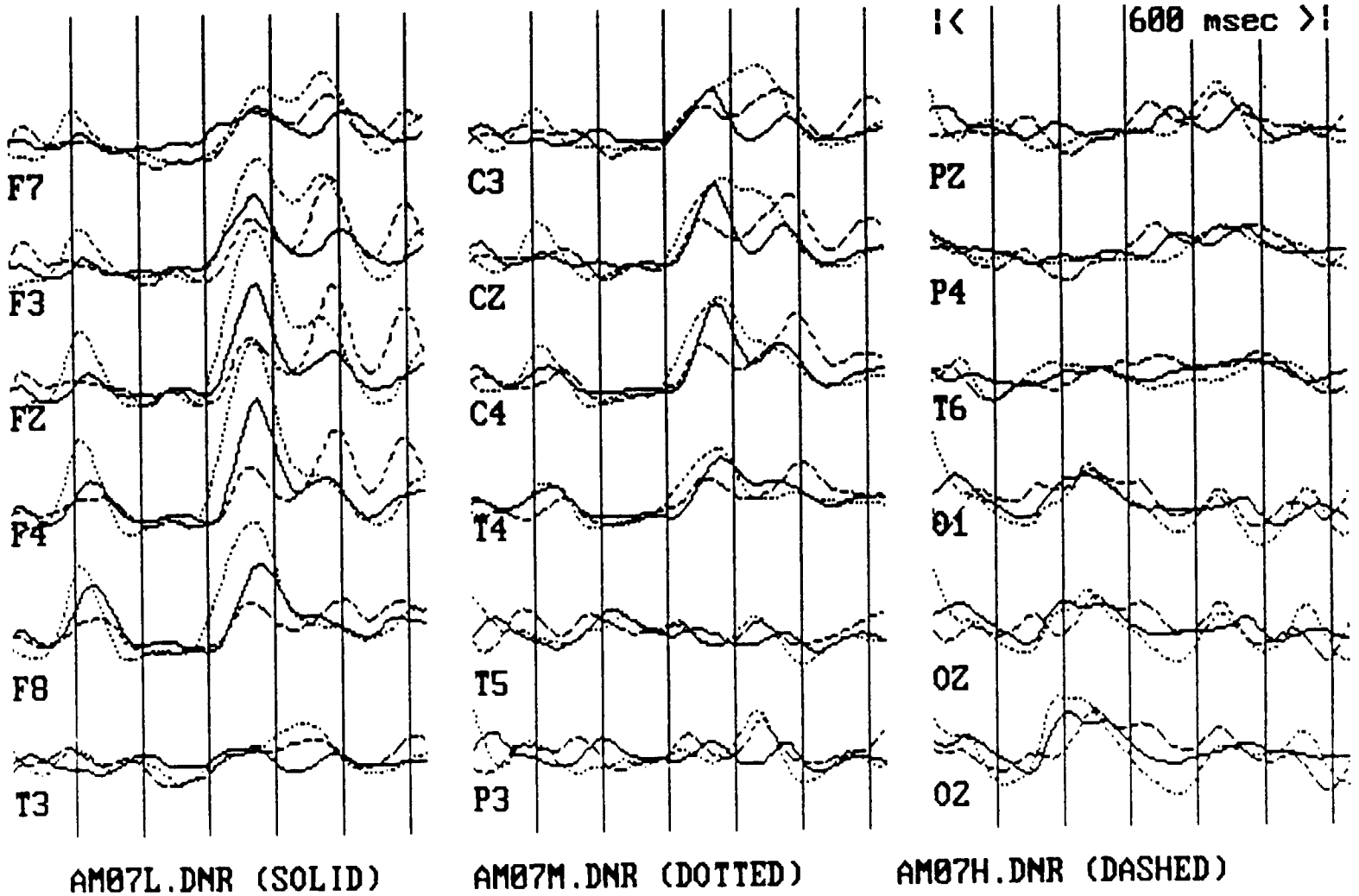

FIGURE VI.1.-22

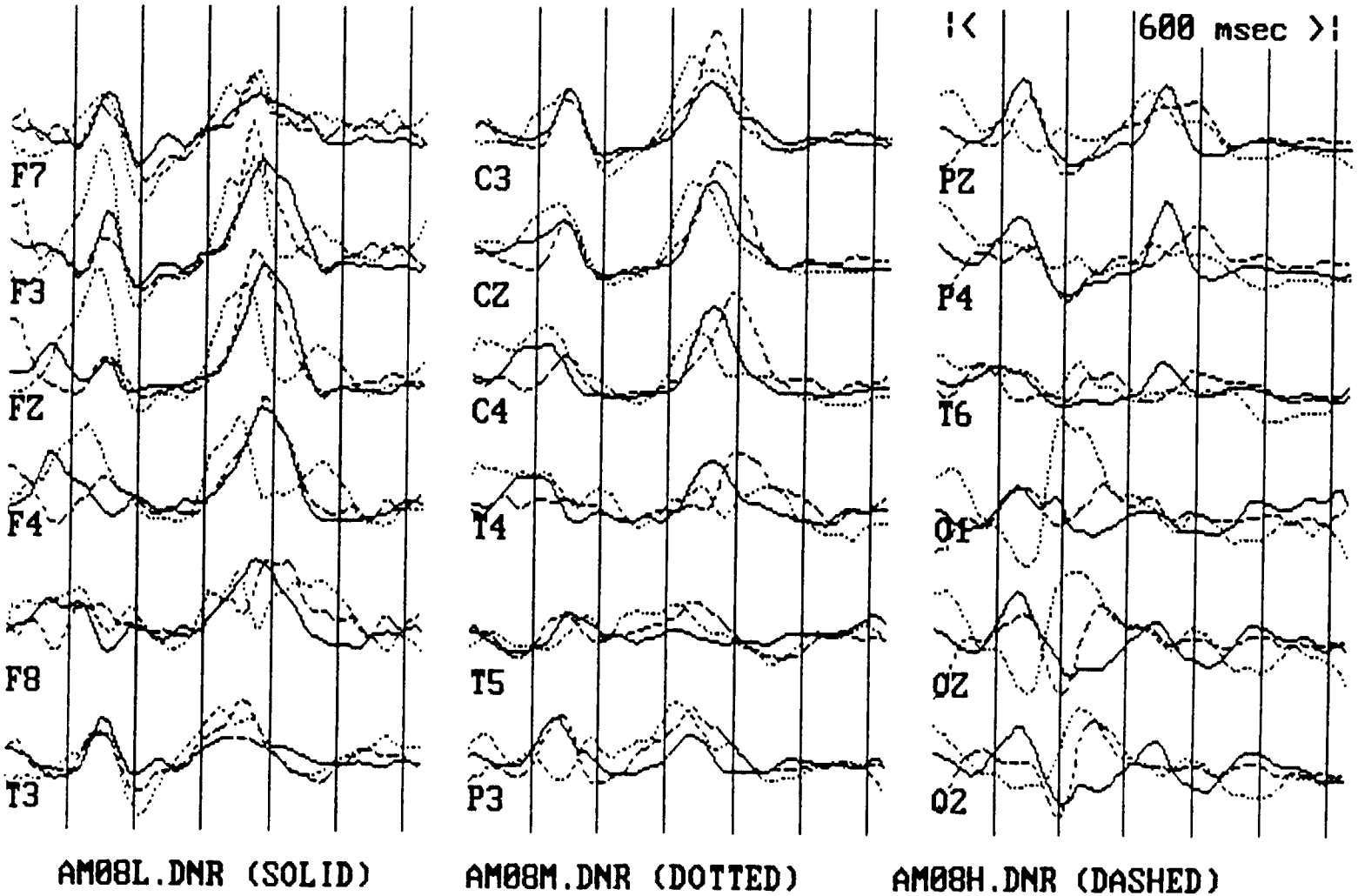

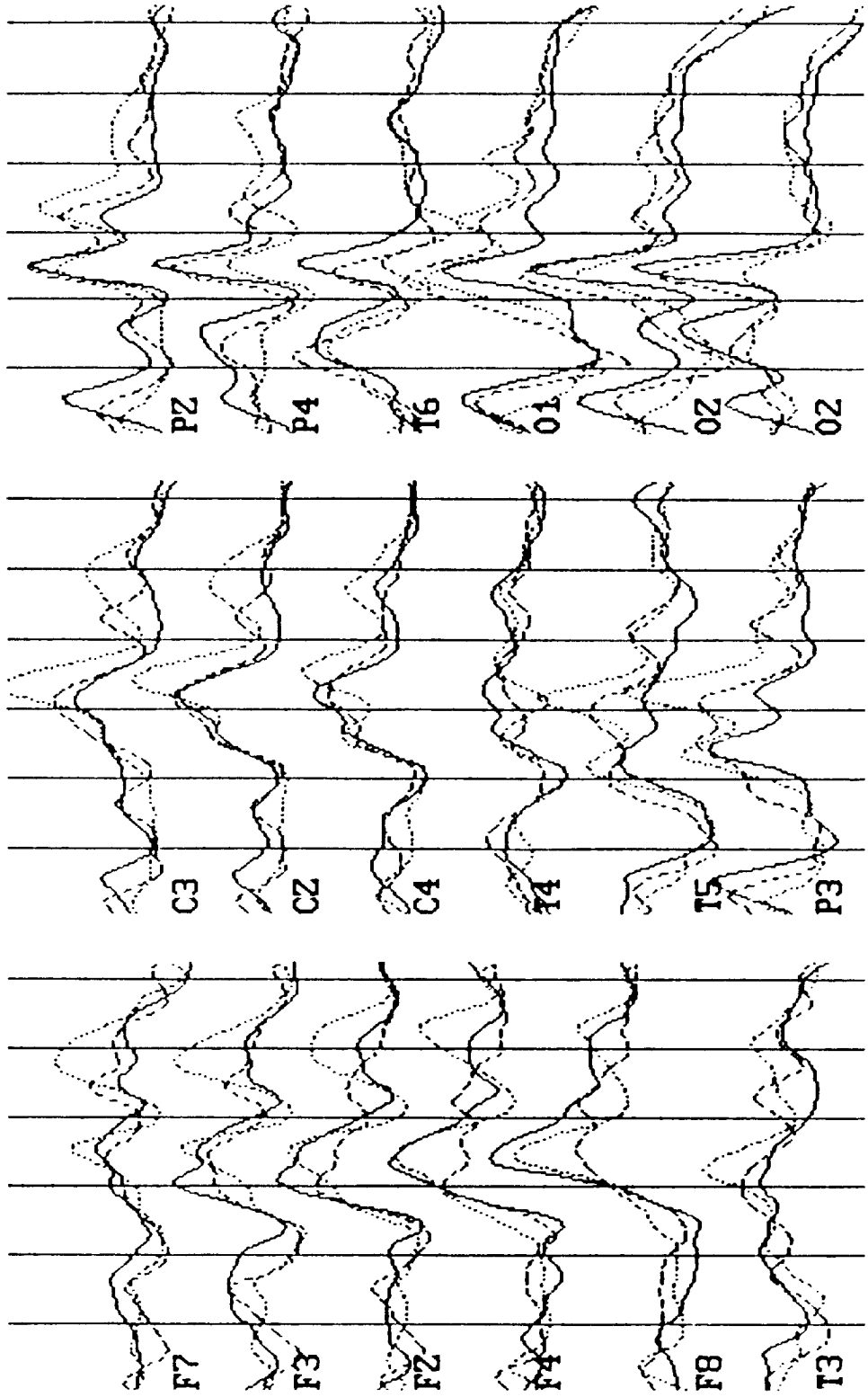

FIGURE VI.1.-23

FIGURE VI.1.-24

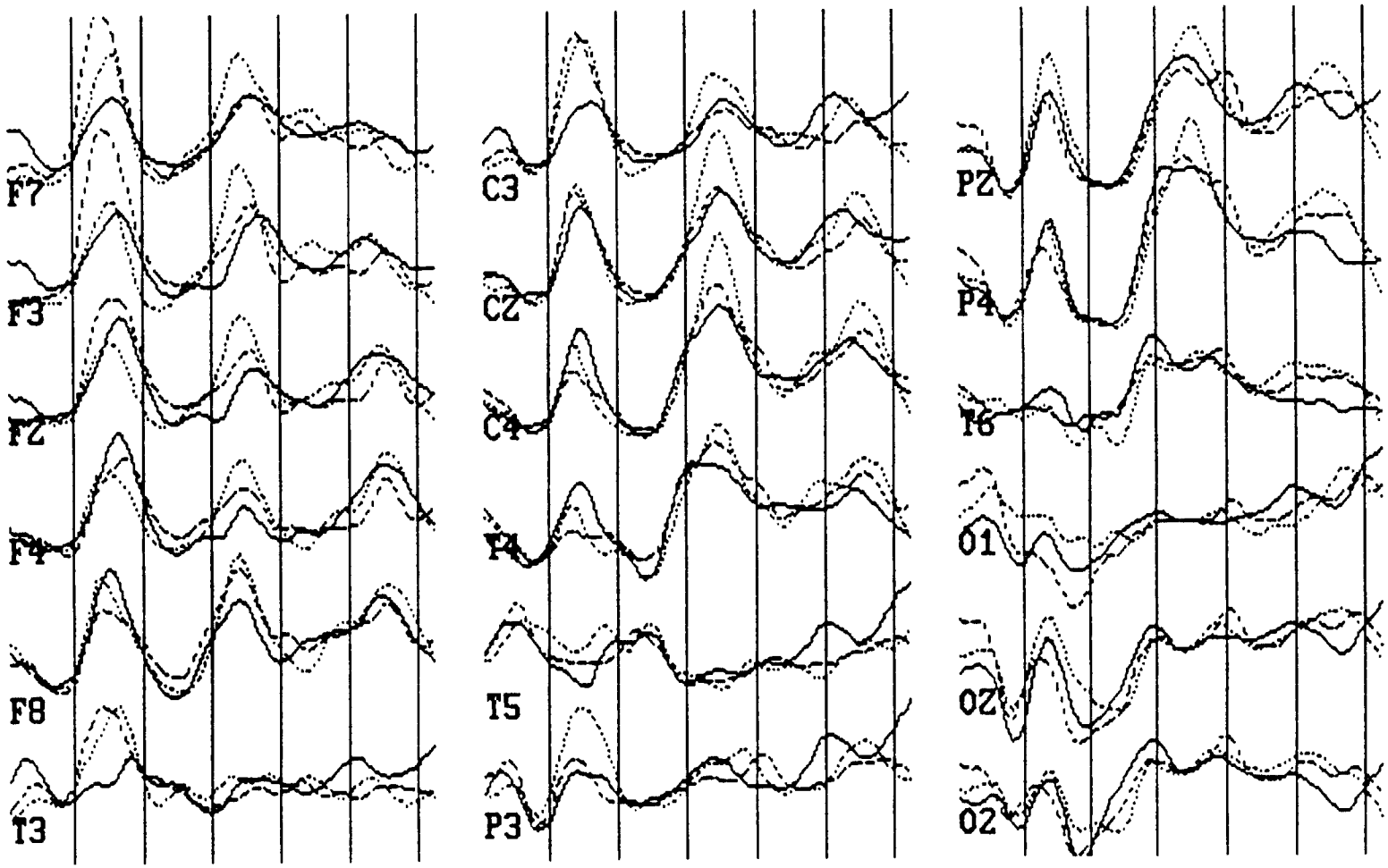

FIGURE VI.1.-25

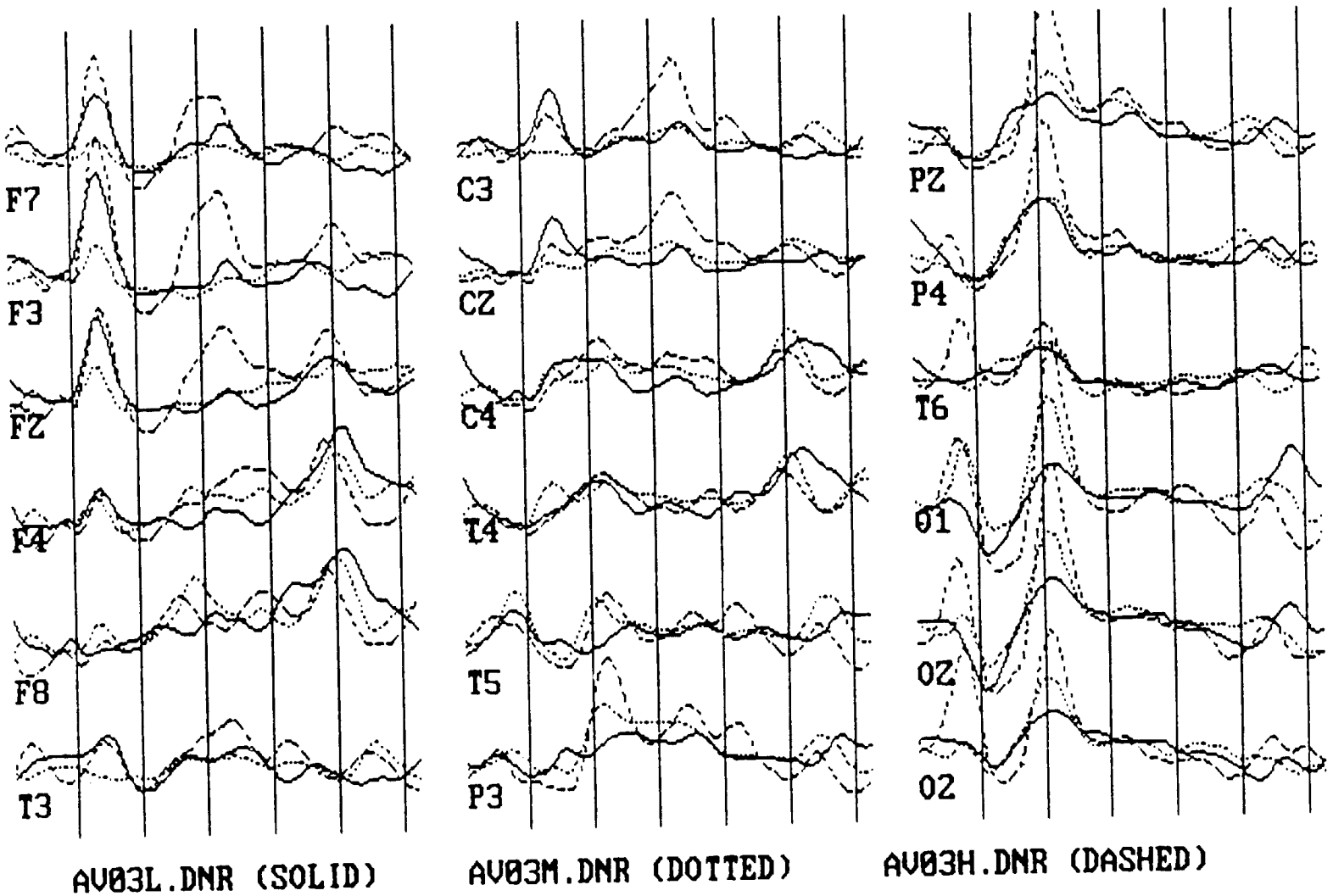

FIGURE VI.1.-26

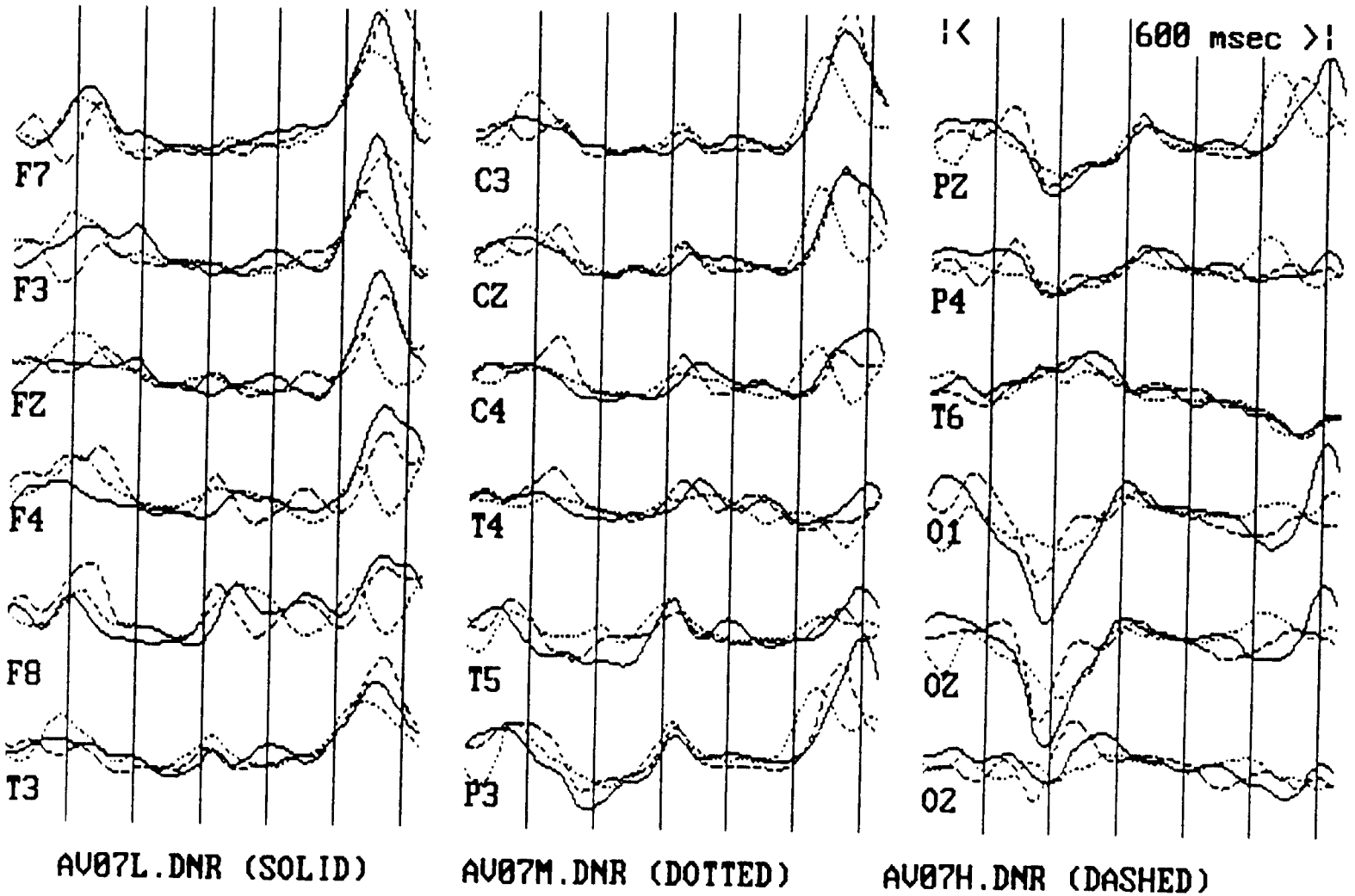

FIGURE VI.1.-27

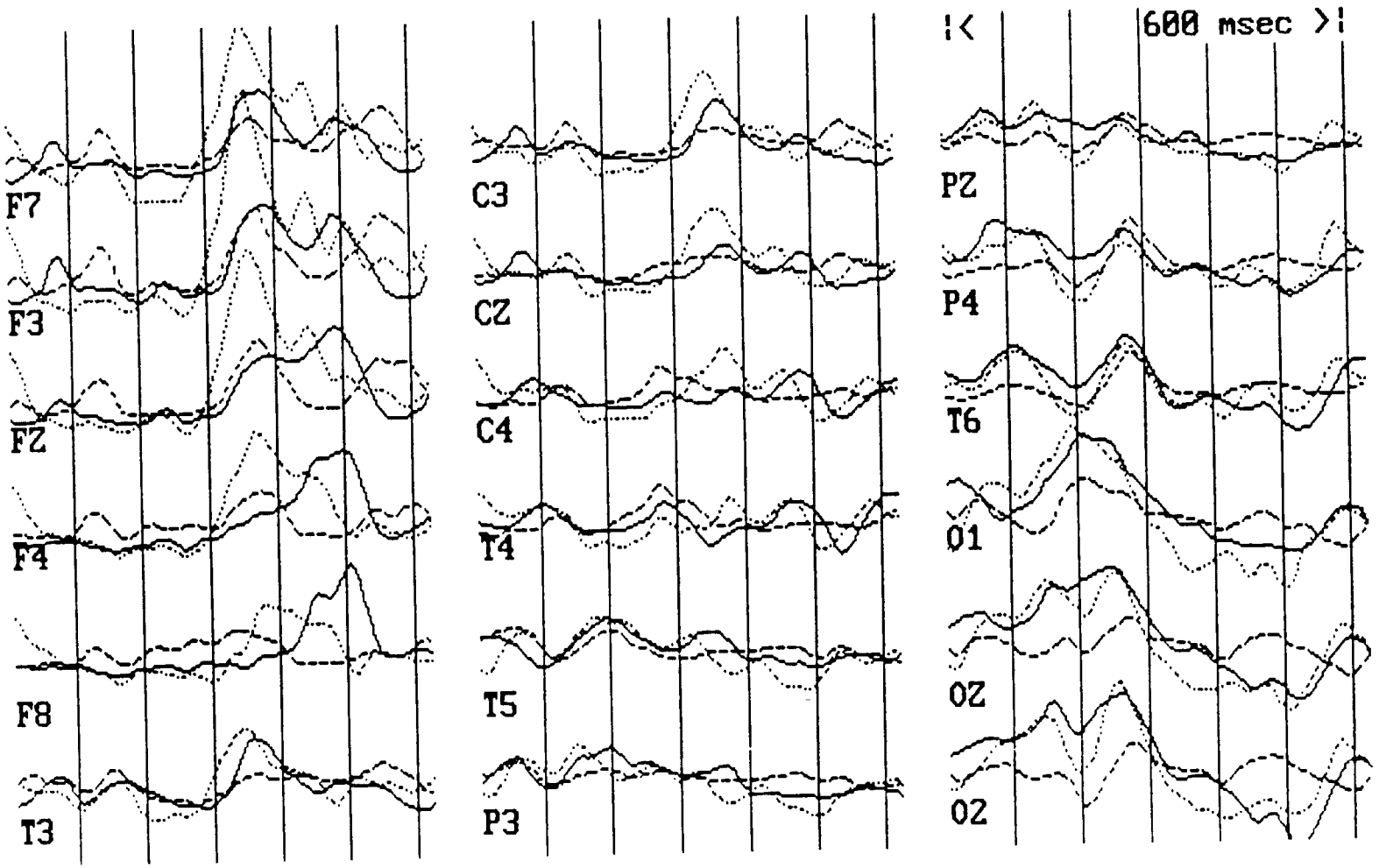

FIGURE VI.1.-28

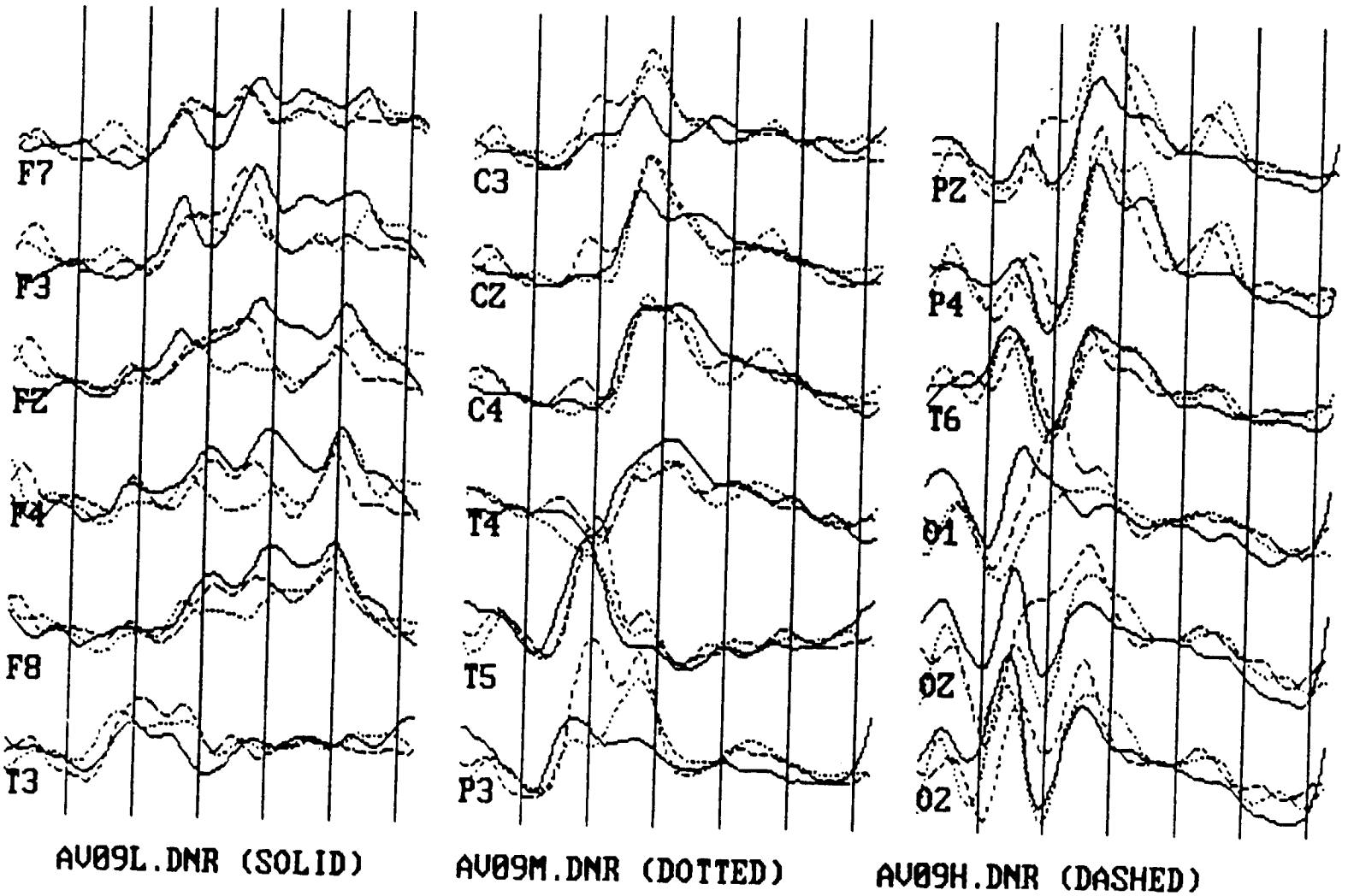

FIGURE VI.1.-29

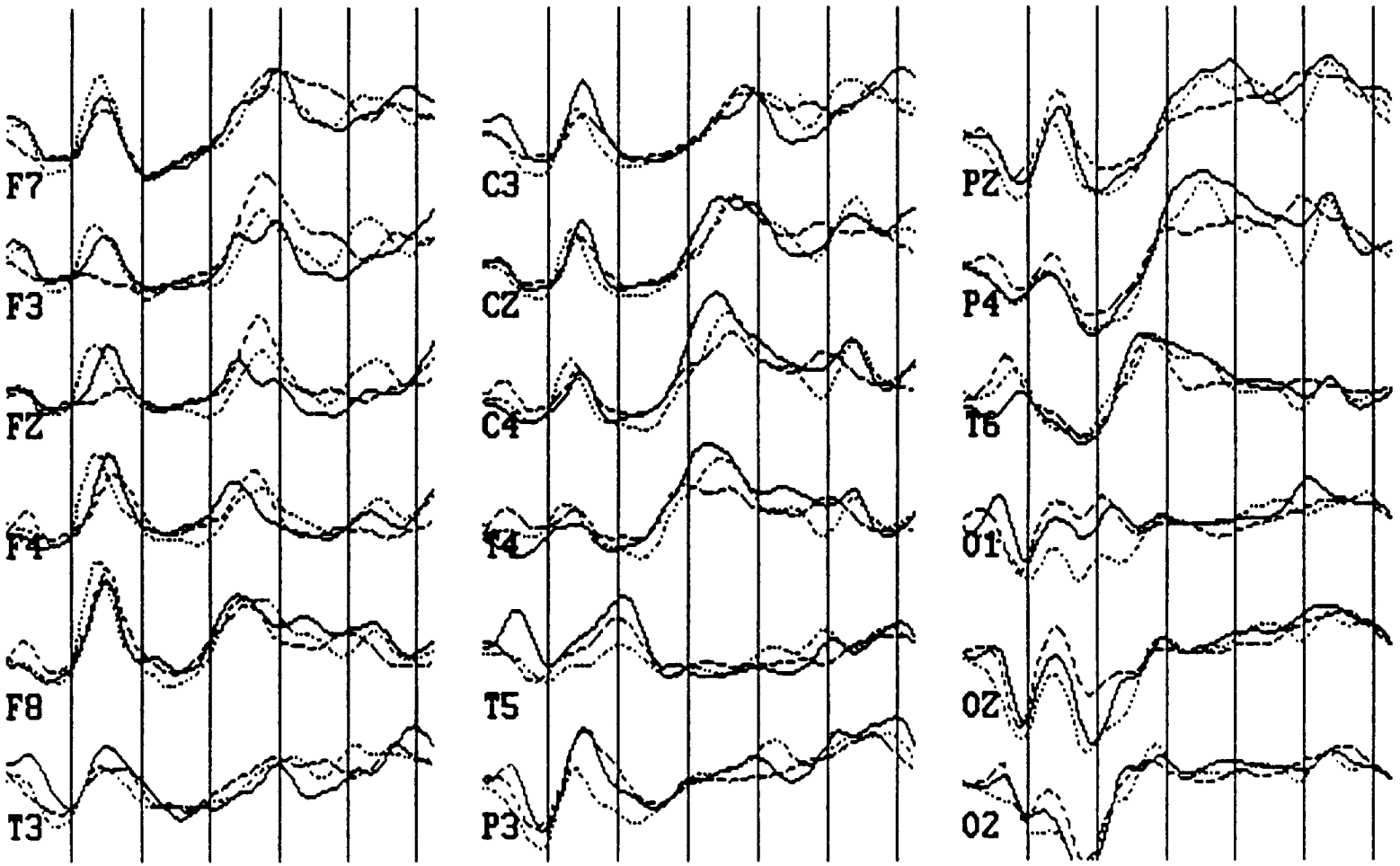

FIGURE VI.1.-30

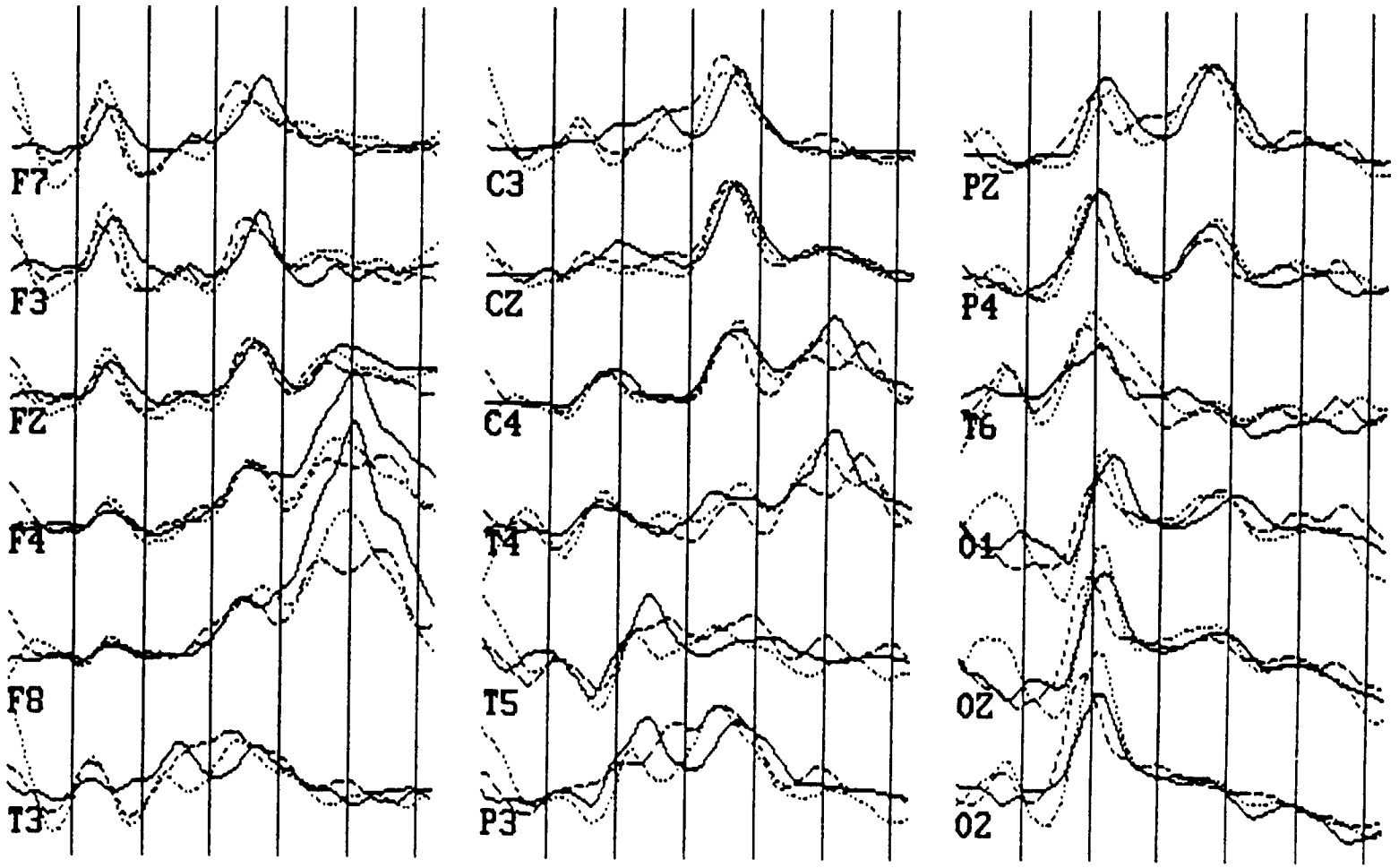

FIGURE VI.1.-31

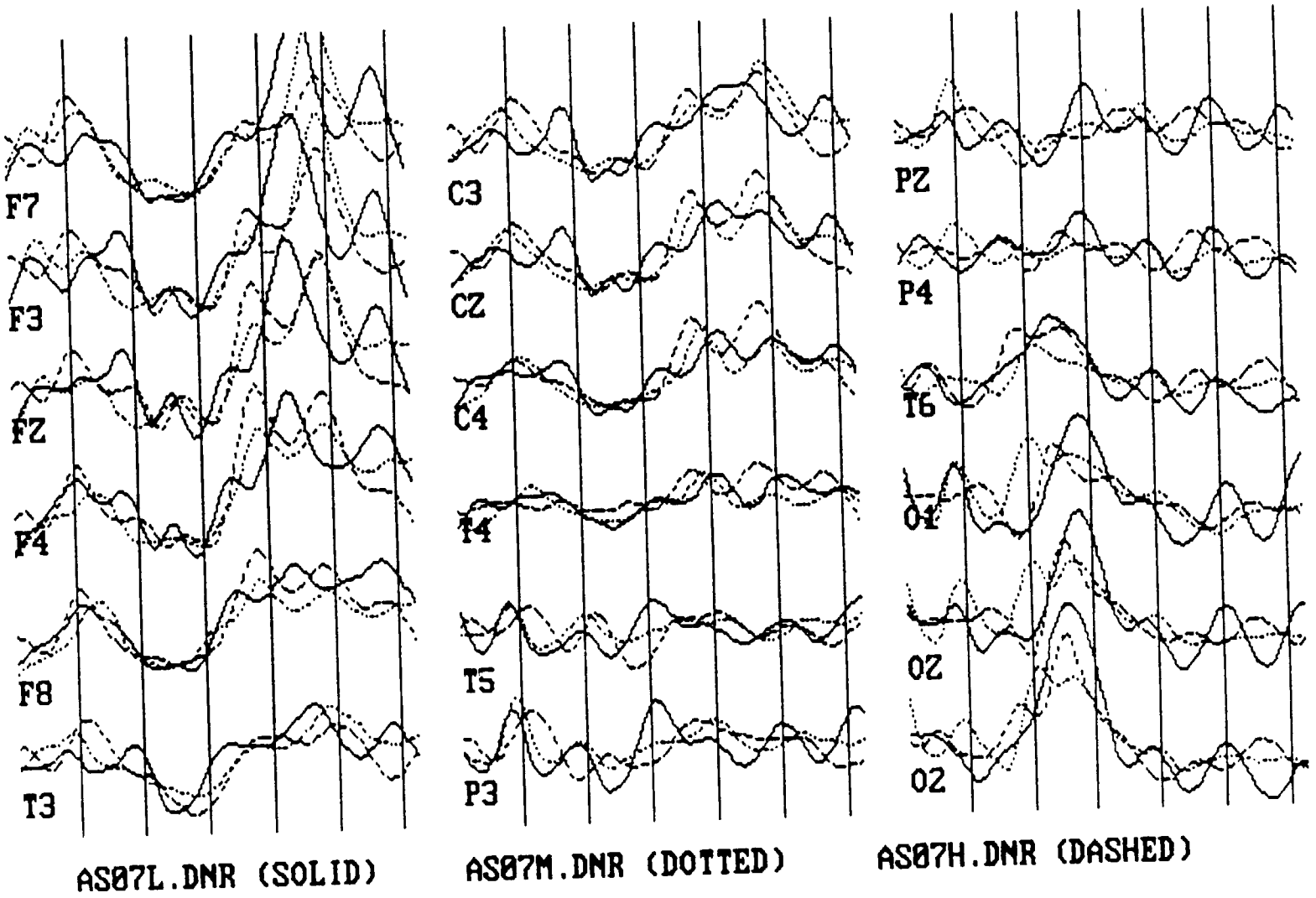

FIGURE VI.1.-32

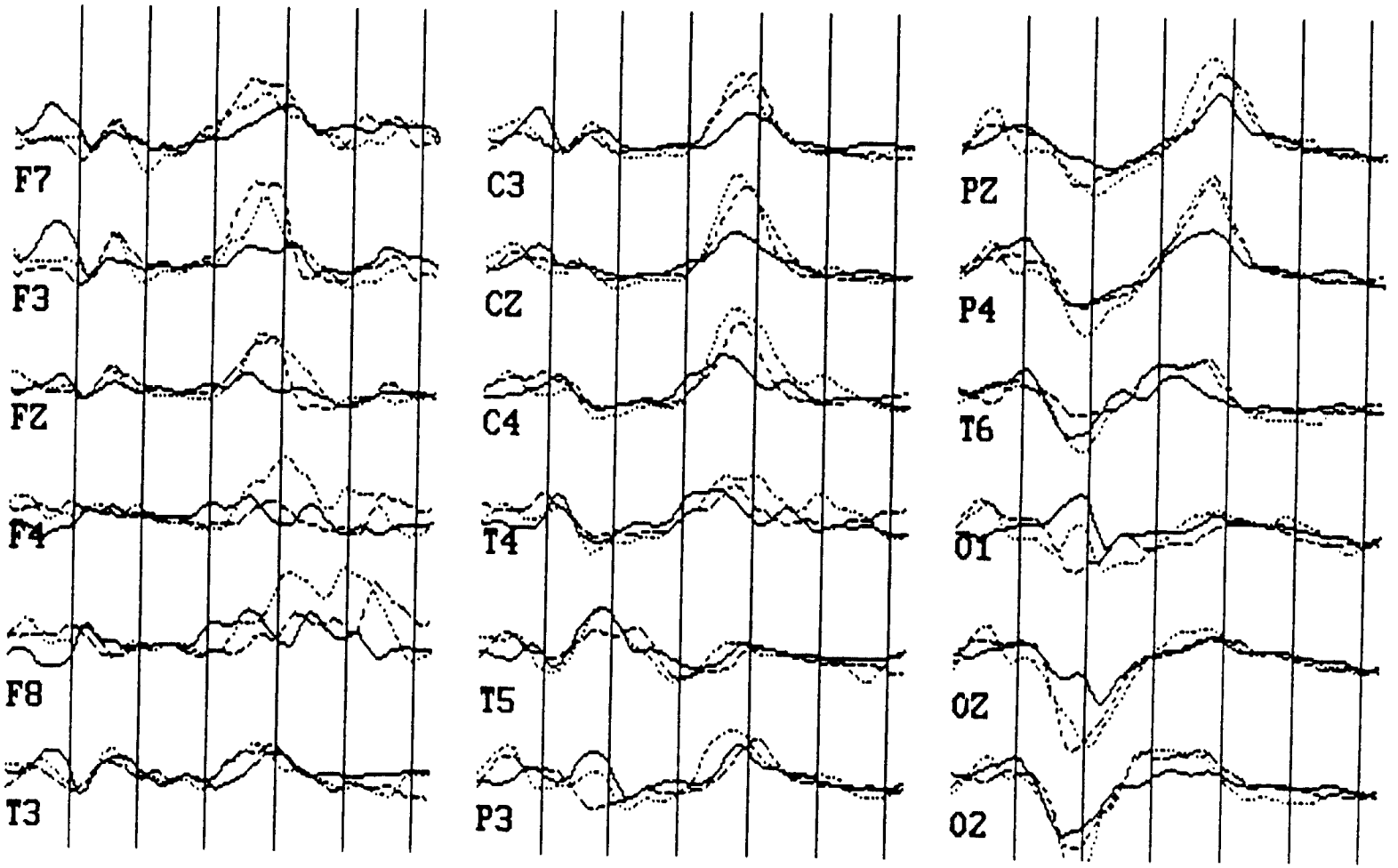

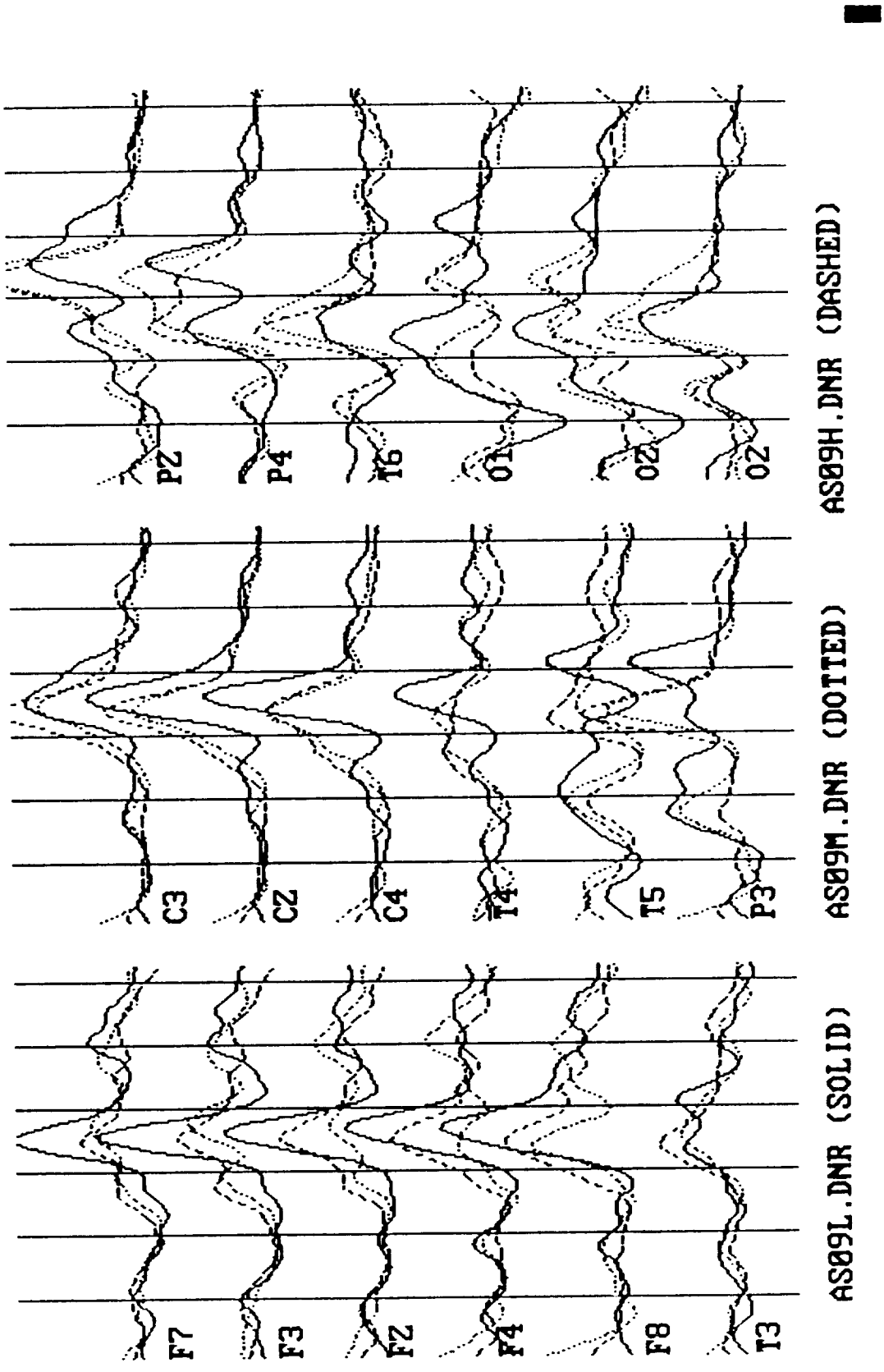

FIGURE VI.1.-33

FIGURE VI.1.-34

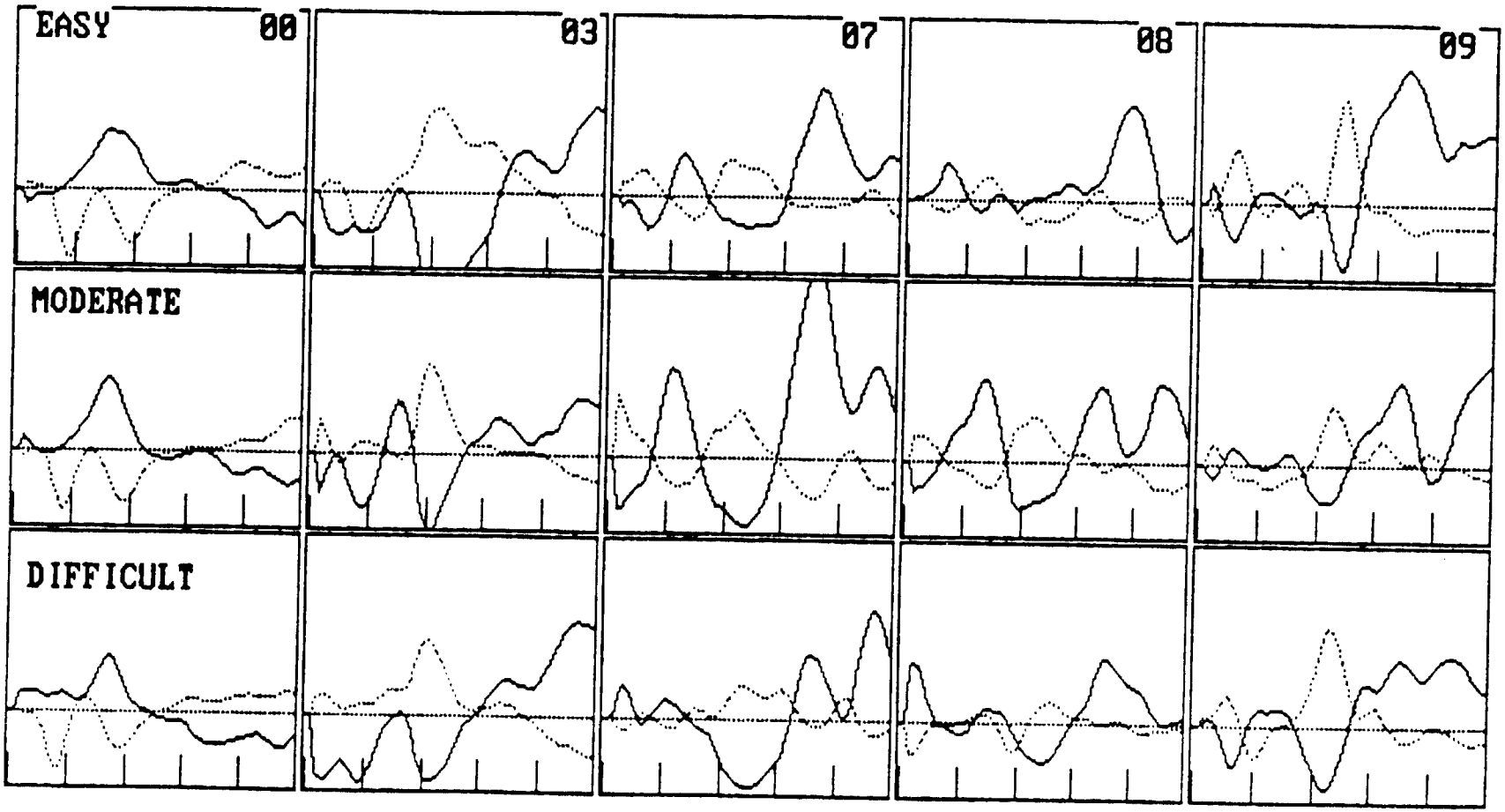

CHANGE IN SCALP POTENTIAL ENERGY: MENTAL ARITHMETIC
ELECTRODE GROUP: FRONT (SOLID), BACK (DOTTED)

FIGURE VI.1.-35

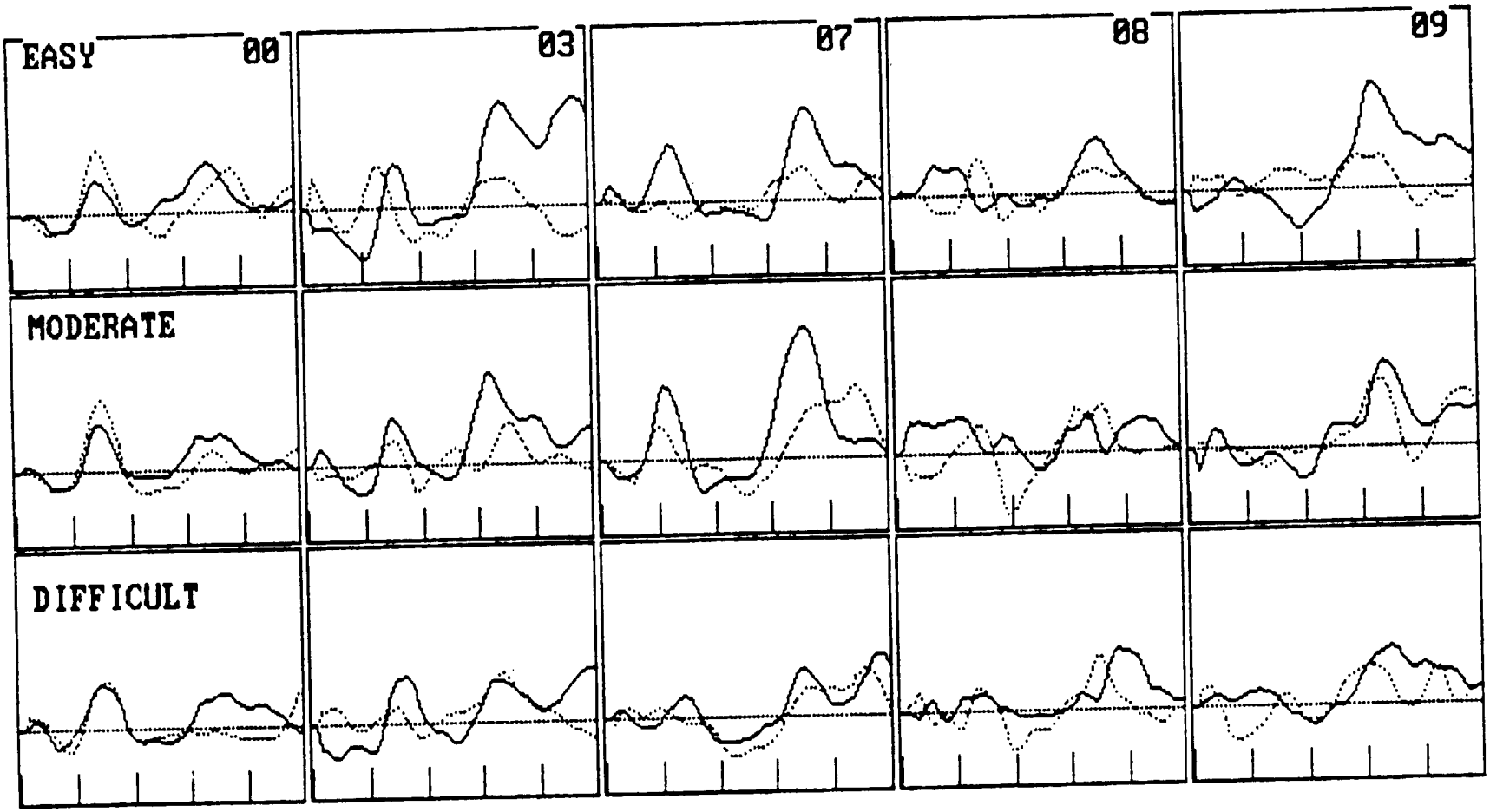

CHANGE IN SCALP POTENTIAL ENERGY: MENTAL ARITHMETIC
ELECTRODE GROUP: RIGHT (SOLID), LEFT (DOTTED)

FIGURE VI.1.-36

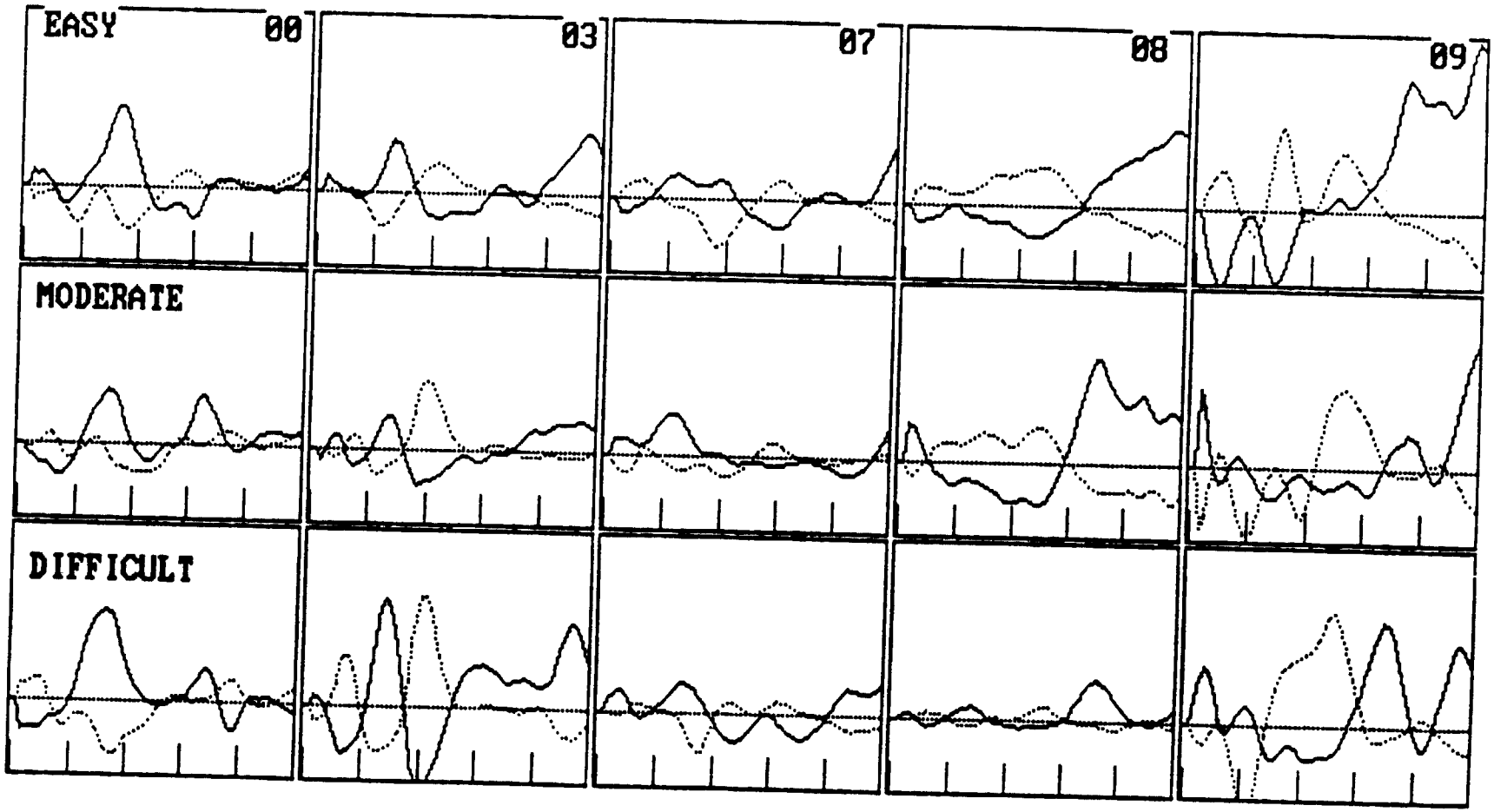

CHANGE IN SCALP POTENTIAL ENERGY: WORD RECOGNITION
ELECTRODE GROUP: FRONT (SOLID), BACK (DOTTED)

FIGURE VI.1-37

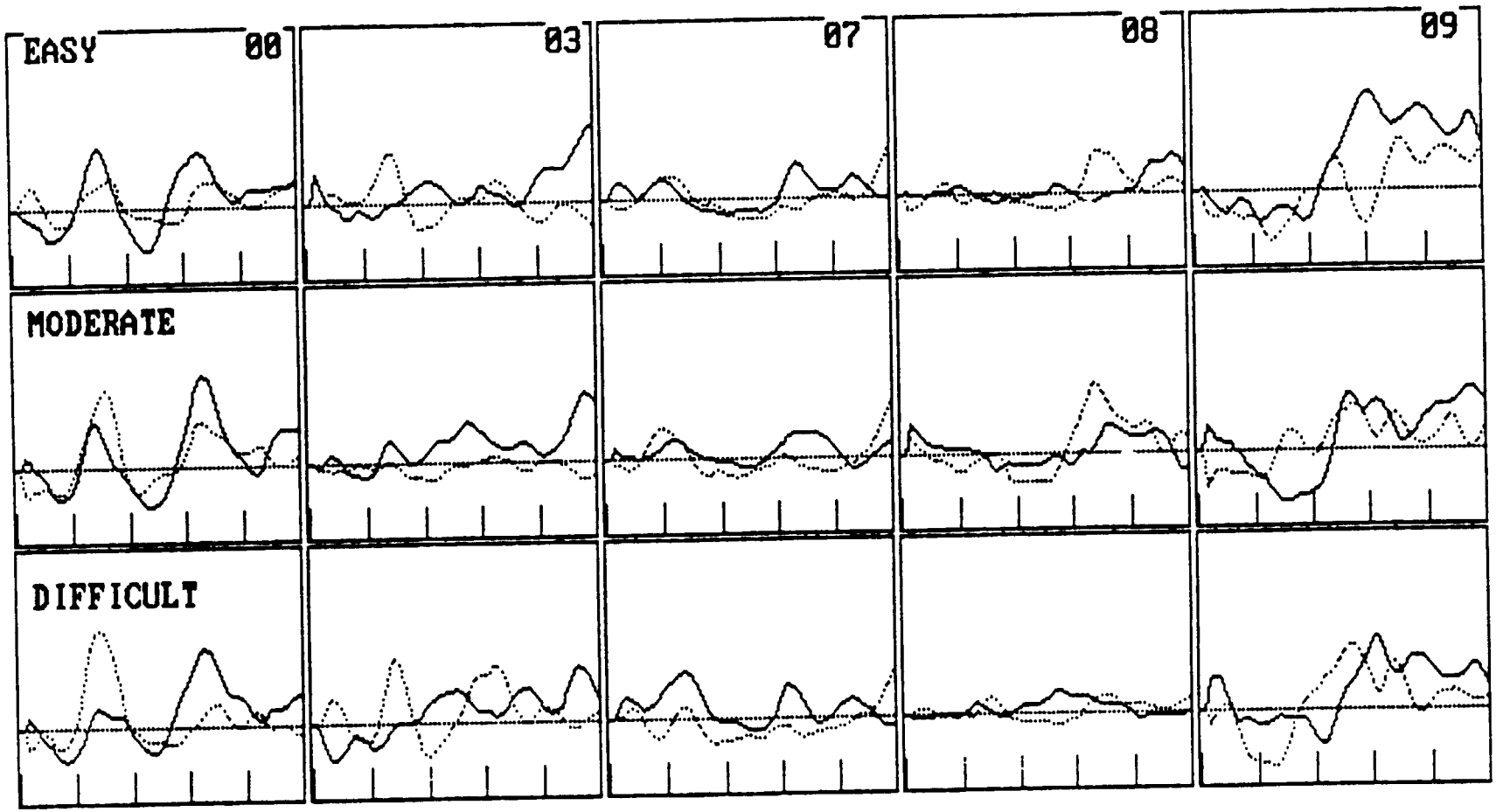

CHANGE IN SCALP POTENTIAL ENERGY: WORD RECOGNITION
ELECTRODE GROUP: RIGHT (SOLID), LEFT (DOTTED)

FIGURE VI.1.-38

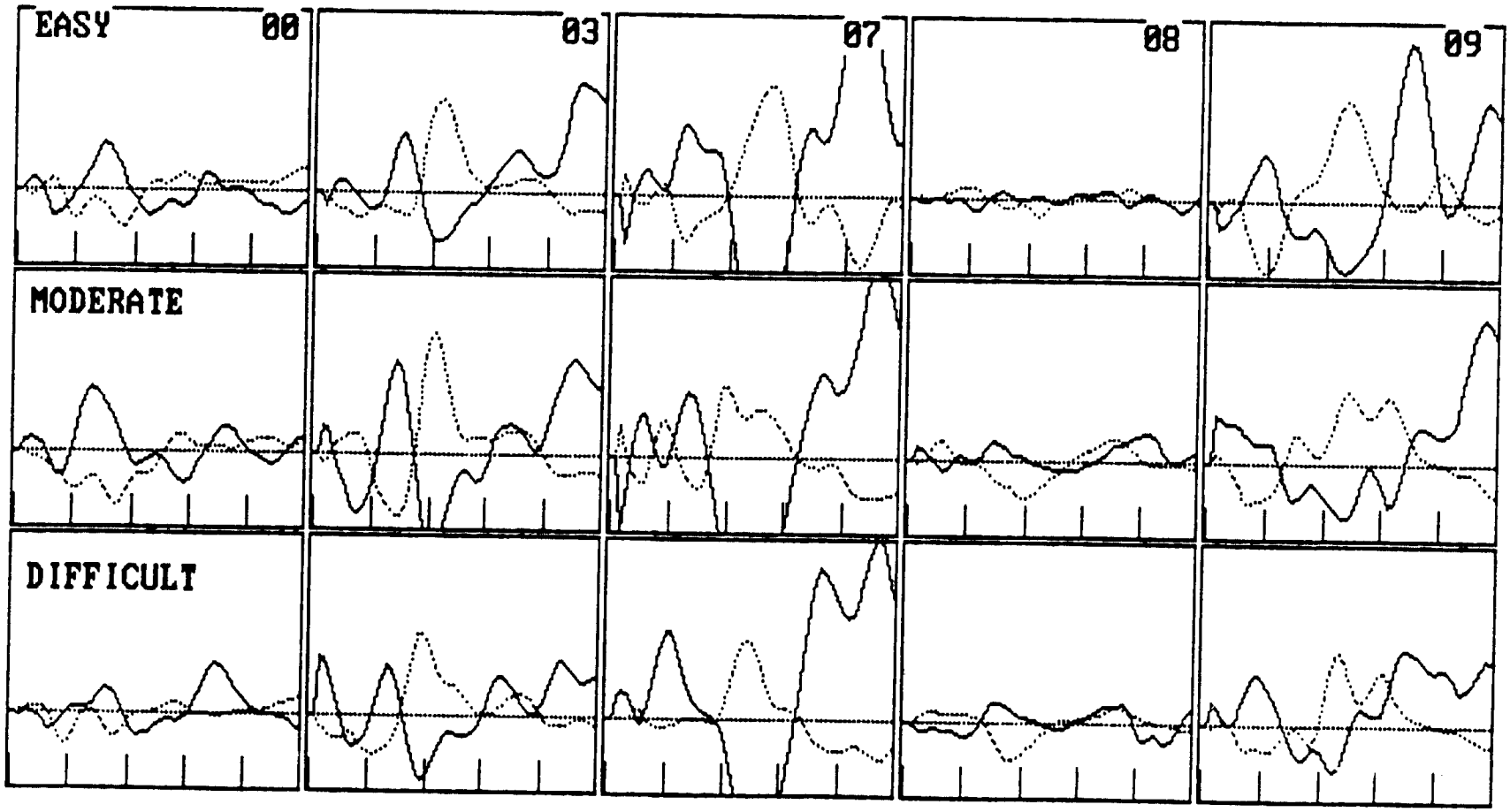

CHANGE IN SCALP POTENTIAL ENERGY: SPATIAL PERCEPTION
ELECTRODE GROUP: FRONT (SOLID), BACK (DOTTED)

FIGURE VI.1.-39

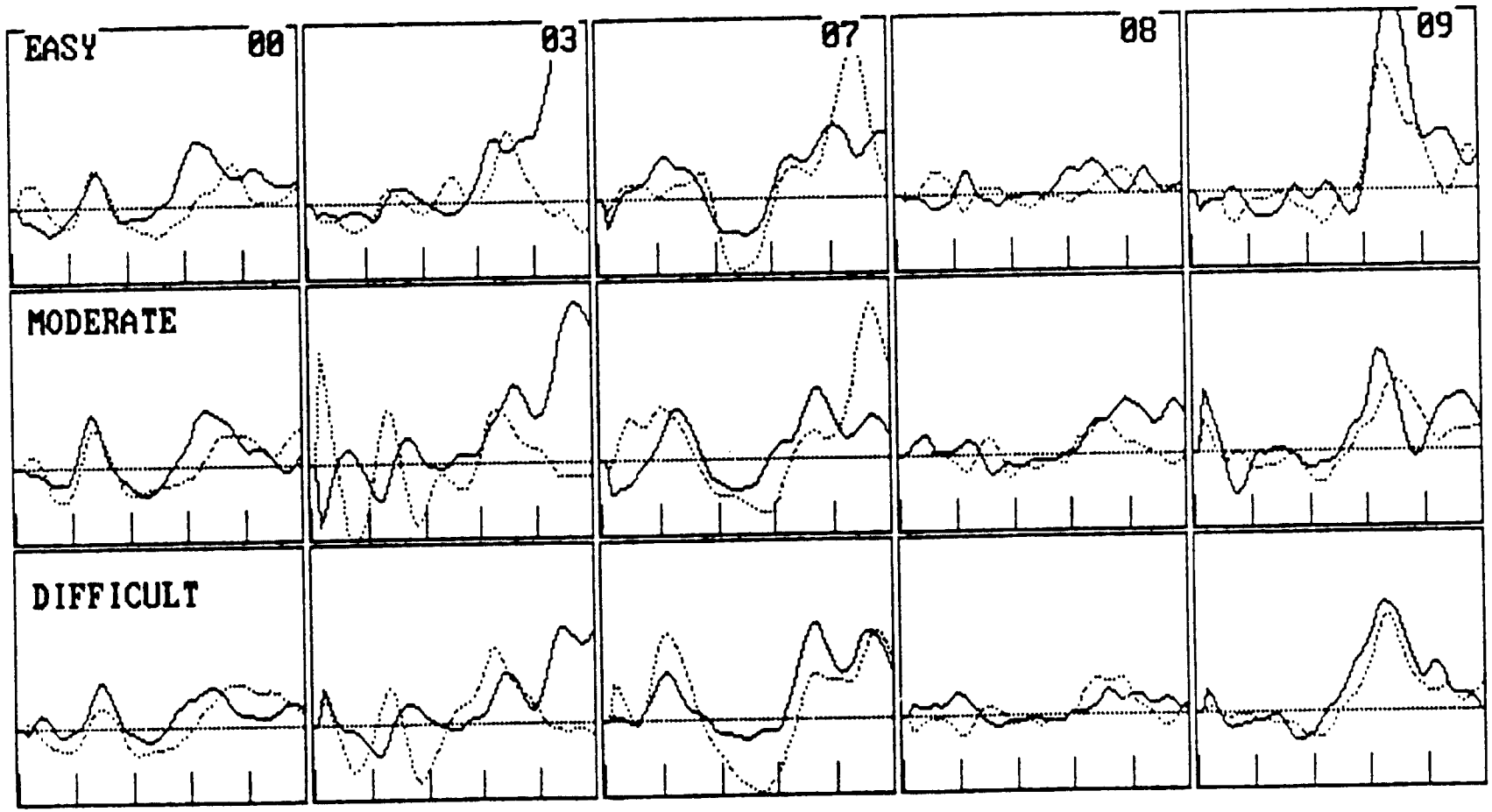

CHANGE IN SCALP POTENTIAL ENERGY: SPATIAL PERCEPTION
ELECTRODE GROUP: RIGHT (SOLID), LEFT (DOTTED)

VI.1.1.4. Cross-subject regression analysis. (Figures VI.1.-40 through VI.1.- 45)

The most prominent conclusion of the ERP analysis for individual subjects is that the five subjects' cortical response patterns are too different to allow cross-subject generalization. The Low, Medium and High (LMH) difficulty ERPs, however, were so remarkably similar for each individual subject, that these levels cannot be reliably distinguished.

However, the main EEG tool developed in this project is a technique to circumvent this limitation: the use of regression analysis to relate EEG differences to a criterion variable. A procedure was developed for regressing task performance on cortical energy density. Task performance was represented by the "error rate" index (see page 9) which combines subjects' average reaction time and percentage of errors for the responses included in the LMH-averaged ERP. Energy density was measured as an integral over a brief (39 msec) period at a particular electrode site. A search procedure finds time windows and electrode locations for which the regression fit is optimal.

Figures 40 through 45 are scatterplots showing the regressions for the two time and site combinations producing the best fitting results for each of the three tasks. Each "case" is identified by a letter (M= MATH, V= VERB, S= SPAT) and a single digit that identifies each of five subjects. In each case there are five data points, corresponding to the five subjects' ERPs and error indices. For each task (MATH, VERB and SPAT) a list is presented of those site and time combinations that produced a the best fit (Tables III, IV and V).

These scatterplots reveal that performance differences among subjects can be related (with very high statistical confidence) to differences in the energy density of their cortically generated electrical field. At certain instants during the task and at certain cortical locations, more than 95 % of the intersubject performance variation can be explained by a simple linear relationship between performance and energy density.

FIGURE VI.1.-40

CASE	INDEX	ENERGY
M0	28.59	346.09
M7	28.62	280.33
M9	32.34	366.45
M8	35.08	431.37
M3	42.92	603.58

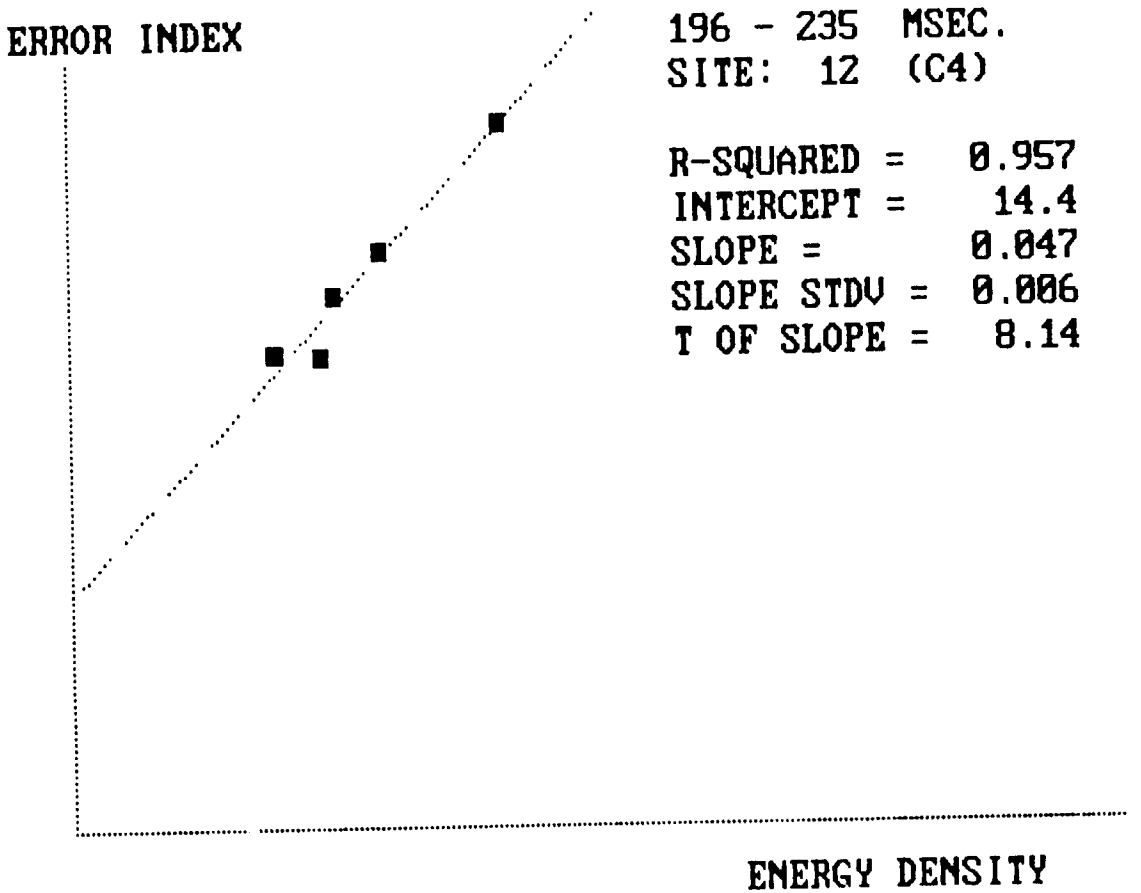

196 - 235 MSEC.
SITE: 12 (C4)

R-SQUARED = 0.957
INTERCEPT = 14.4
SLOPE = 0.047
SLOPE STDV = 0.006
T OF SLOPE = 8.14

MENTAL ARITHMETIC (5 SUBJECTS)

FIGURE VI.1.-41

CASE	INDEX	ENERGY
M0	28.59	610.14
M7	28.62	626.93
M9	32.34	596.58
M8	35.08	416.50
M3	42.92	149.22

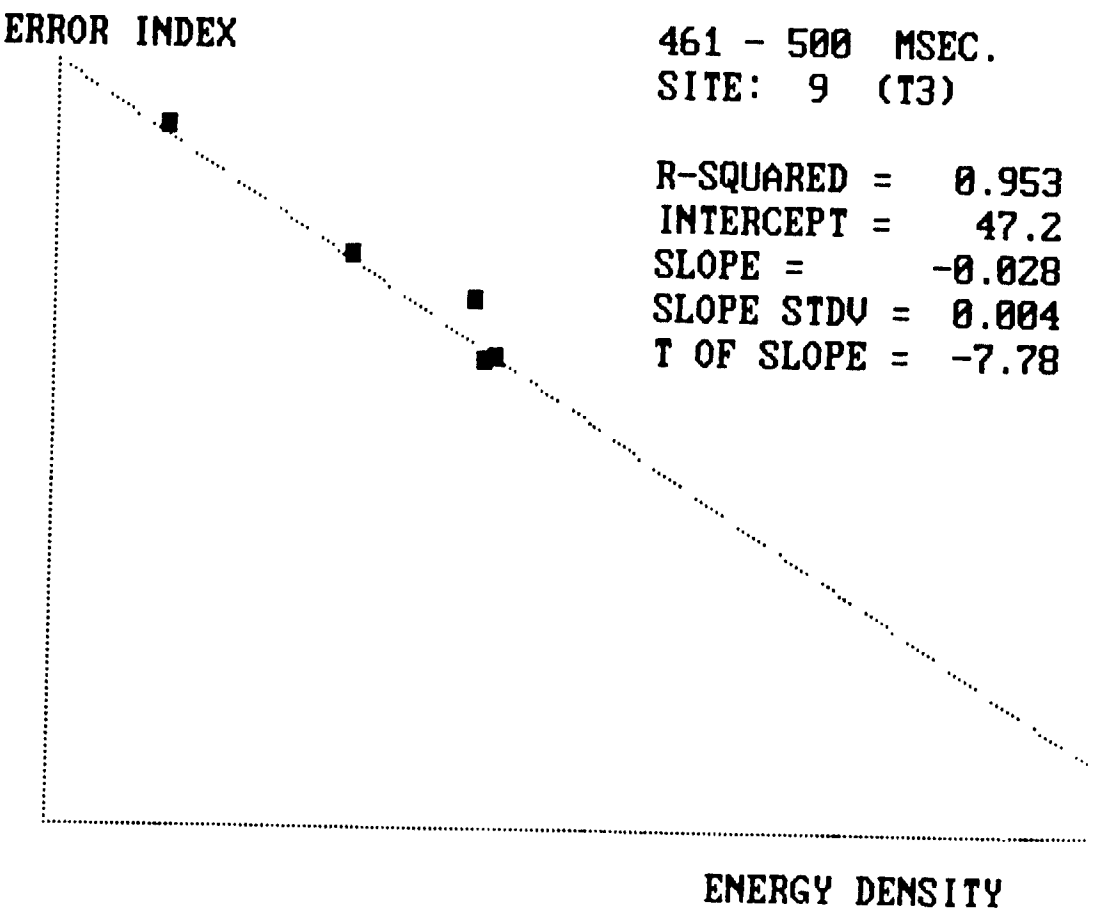

MENTAL ARITHMETIC (5 SUBJECTS)

FIGURE VI.1.-42

CASE	INDEX	ENERGY
V9	23.31	744.93
V0	25.69	652.01
V7	27.47	570.50
V3	27.92	523.94
V8	31.18	401.69

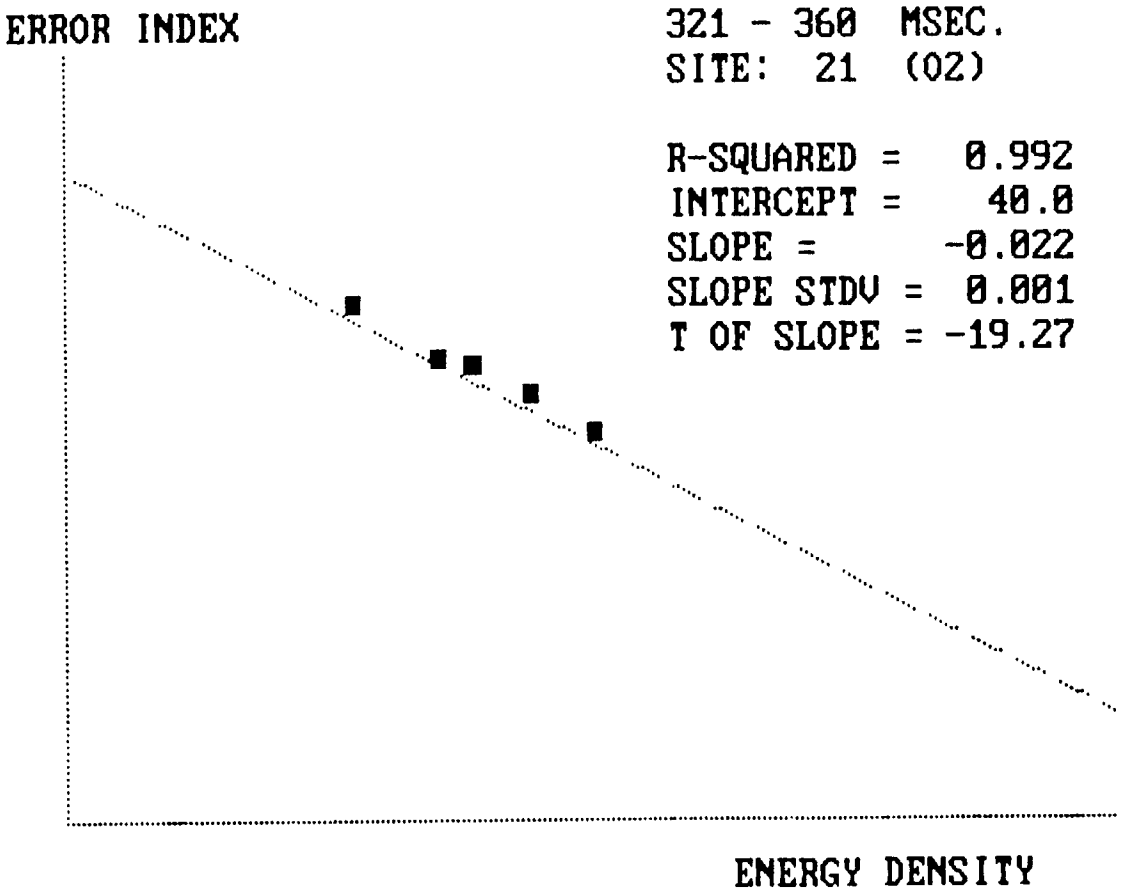

WORDPAIR TASK (5 SUBJECTS)

FIGURE VI.1.-43

CASE	INDEX	ENERGY
V9	23.31	529.19
V0	25.69	495.48
V7	27.47	474.53
V3	27.92	459.50
V8	31.18	380.74

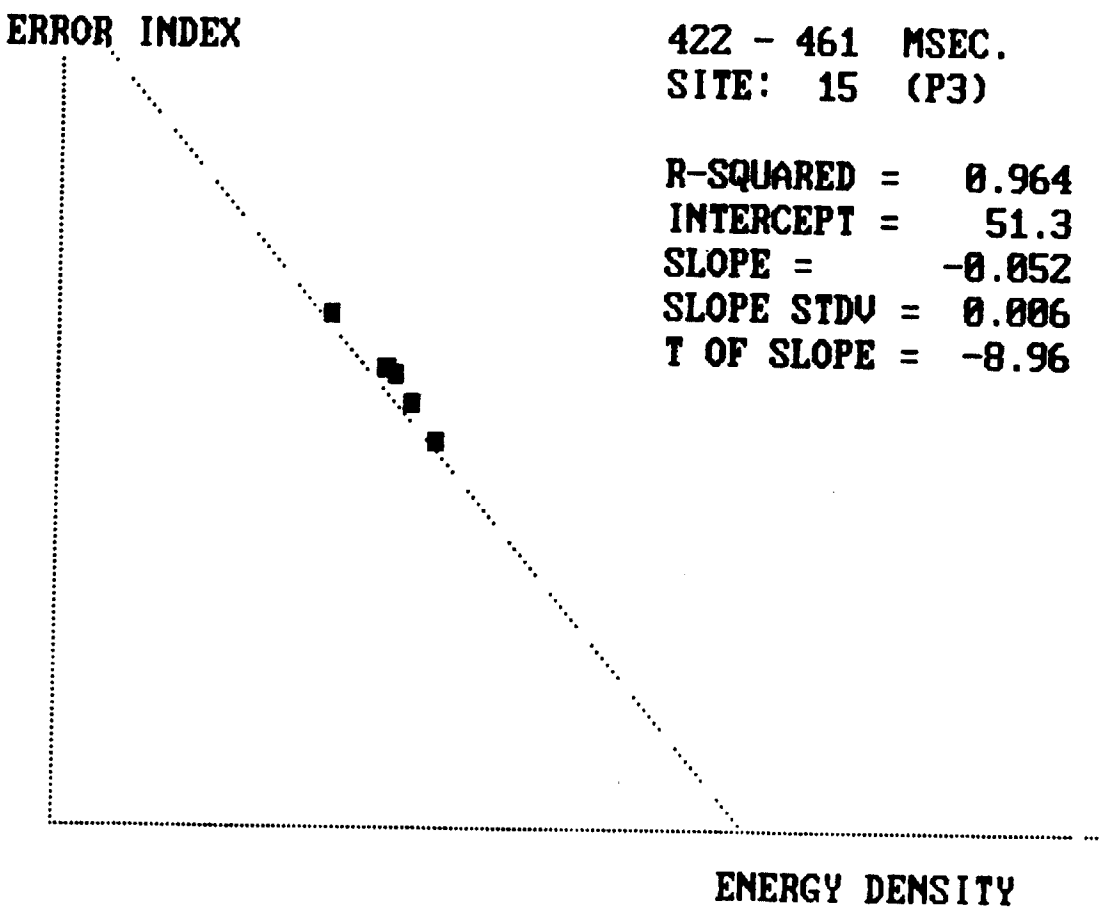

WORDPAIR TASK (5 SUBJECTS)

FIGURE VI.1.-44

CASE	INDEX	ENERGY
S0	4.41	357.48
S9	7.07	409.98
S7	8.18	392.82
S8	18.28	451.61
S3	20.19	471.32

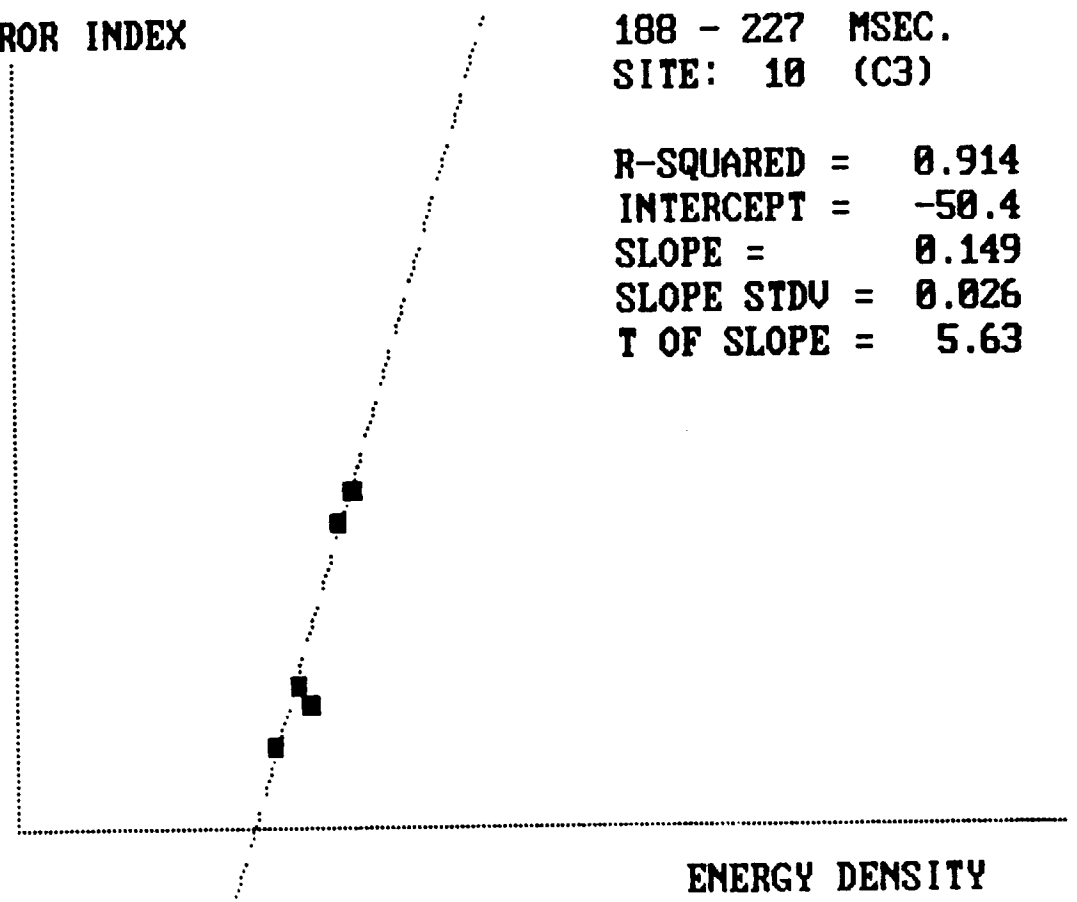

188 - 227 MSEC.
SITE: 10 (C3)

R-SQUARED = 0.914
INTERCEPT = -50.4
SLOPE = 0.149
SLOPE STDV = 0.026
T OF SLOPE = 5.63

SHAPE MATCHING TASK (5 SUBJECTS)

FIGURE VI.1.-45

CASE	INDEX	ENERGY
S0	4.41	1209.83
S9	7.07	1192.19
S7	8.18	1078.57
S8	18.28	943.61
S3	20.19	918.27

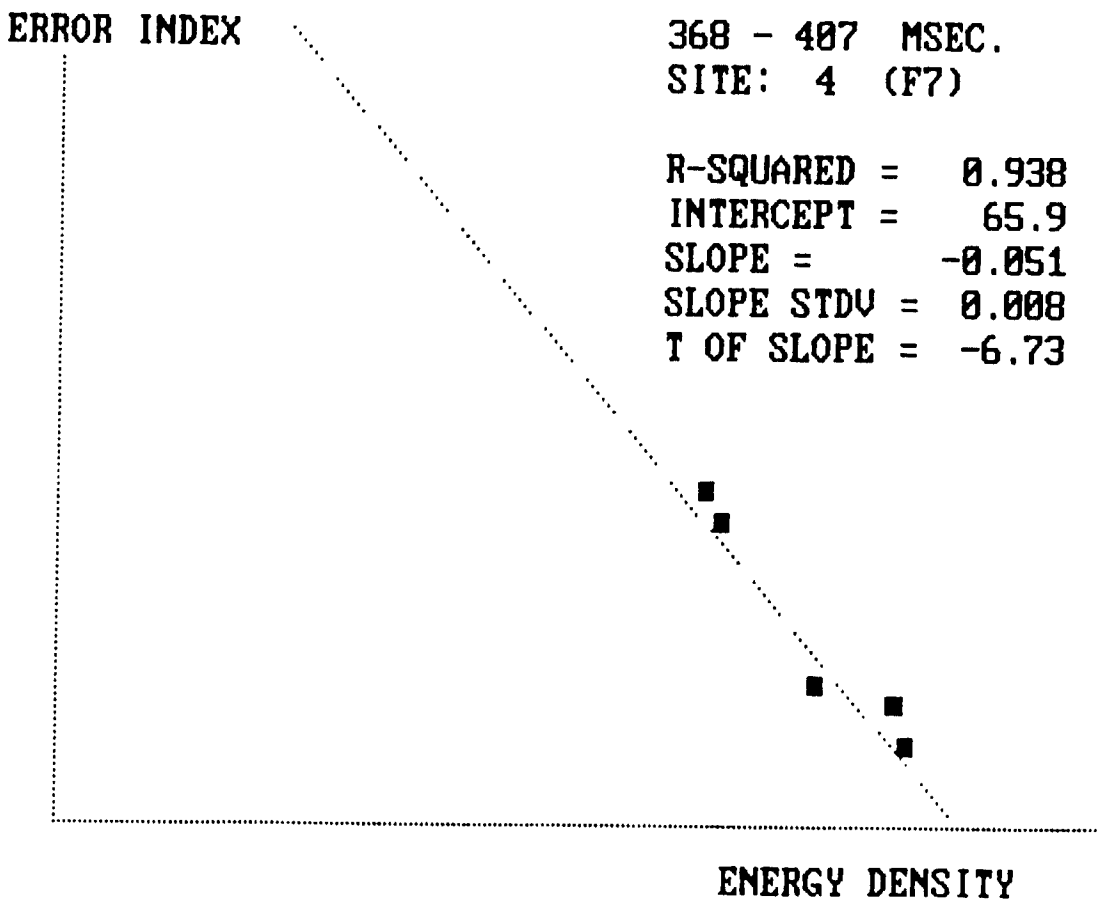

SHAPE MATCHING TASK (5 SUBJECTS)

TABLE III

ERROR INDEX VS. ENERGY DENSITY:
MIXED TASK SUBJS 00 03 07 08 09 (ARITHMETIC)

ELECTRODE	PERIOD	R-SQUARE	T-VALUE	SLOPE
T5	47 - 86	0.913	-5.624	-0.058
T5	55 - 94	0.948	-7.402	-0.061
Fpz	94 - 133	0.897	-5.122	-0.030
Fpz	102 - 141	0.891	-4.946	-0.032
P4	157 - 196	0.882	4.740	0.025
T5	172 - 211	0.914	-5.637	-0.149
C4	188 - 227	0.889	4.908	0.067
C4	196 - 235	0.957	8.138	0.094
Fz	227 - 266	0.899	-5.180	-0.116
T5	344 - 383	0.896	5.077	0.082
T3	454 - 493	0.925	-6.092	-0.057
T3	461 - 501	0.953	-7.779	-0.057

TABLE IV

ERROR INDEX VS. ENERGY DENSITY:
MIXED TASK SUBJS 00 03 07 08 09 (WORDPAIRS)

ELECTRODE	PERIOD	R-SQUARE	T-VALUE	SLOPE
O2	79 - 118	0.916	5.711	0.018
O2	86 - 126	0.984	13.623	0.020
O2	94 - 133	0.935	6.558	0.024
Fp1	243 - 282	0.888	-4.866	-0.039
F8	290 - 329	0.880	-4.697	-0.023
Pz	297 - 336	0.909	-5.459	-0.014
O2	313 - 352	0.952	-7.749	-0.038
O2	321 - 360	0.992	-19.272	-0.045
F8	344 - 383	0.884	-4.790	-0.031
Pz	399 - 438	0.913	-5.606	-0.029
Pz	407 - 446	0.913	-5.605	-0.028
Pz	415 - 454	0.896	-5.079	-0.028
P3	422 - 461	0.964	-8.957	-0.103
Pz	422 - 461	0.894	-5.038	-0.029

TABLE V

ERROR INDEX VS. ENERGY DENSITY:
MIXED TASK SUBJS 00 03 07 08 09 (SHAPES)

ELECTRODE	PERIOD	R-SQUARE	T-VALUE	SLOPE
F8	40 - 79	0.726	2.819	0.191
Pz	141 - 180	0.863	-4.347	-0.107
C3	188 - 227	0.914	5.629	0.298
C3	196 - 235	0.742	2.938	0.124
T6	266 - 305	0.766	-3.131	-0.040
T6	274 - 313	0.740	-2.923	-0.047
F7	368 - 407	0.938	-6.725	-0.102
F7	376 - 415	0.928	-6.208	-0.089

VI.1.1.5. Localization of cognitive function. (Figures VI.1.-46 through VI.1.-48)

In the regression of performance on energy density, the best fitting results were obtained at specific scalp locations and instants during the task. This suggests that these are locations where cortical activity is specifically related to task performance, such that effective performance is critically related to either a high or low level of cortical activity at that location, at that particular instant during the task.

Figures 46 through 48 show the cortical locus of the contingency relationship for each task. For each task, a series of brain outlines is presented, one for each 100 msec period during the ERP, with circles drawn to show the location and relative magnitude of peak R-square values occurring during these intervals.

The locus of this contingency relationship over the cortex during the task differs from one type of task to another, and we believe that it reveals sites of cortical localization for the particular types of cognitive function involved.

The best correlations between performance and R-square contingency was obtained for the MATH task, and these results correspond remarkably well to the localization pattern expected for a mental arithmetic task. Figure 46 shows areas of high correlation over the left parietal occipital region (300-500 milliseconds after task presentation), and the left and mid-frontal regions (within 200 milliseconds of task presentation). Primary acalculia is commonly seen in lesions of the left parietal occipital region (Luria, 1966). In addition, individuals with frontal lesions "experience difficulty during mental arithmetical operations involving the carrying over to the tens column, especially operations composed of several stages (for example, 31-17 or 12+9-6)" (Luria, 1966, page 289). Luria interpreted the role of the frontal lobes as critical for "planning" how to perform these more complicated calculations; frontal lobe lesions did not appear to impair the basic concept of number (1966; pages 270, 289, 290). On the other hand, Luria reports (1966; page 438) that patients with lesions of the left parietal-occipital regions manifest an apparent break-down in "categorical structure" of number.

In addition to the correlations mentioned above, Figure 46 reveals some "dynamic" aspects of cognition. Areas of "early" correlation (47-94 milliseconds) in the left posterior temporal region may represent a preparatory response (Jaynes, 1976) or a "planning stage", since it occurs before the visual stimulus is fully processed by primary and association visual cortex, and the subject is expecting to be presented with a series of mathematical tasks. Finally, areas of high

R-square contingency occurring in the right parietal region between 100-200 milliseconds of task presentation, may correspond to visual form analysis related to the subject's assessment of the locational significance of the terms and operators in the arithmetic expressions.

Figure 47, the correlation diagram for the VERB task, shows task performance to be predominantly correlated with cortical activation in the right parietal-occipital region. This would seem to conflict with the well known specialization of the left temporal-parietal region for speech. The VERB task, however, deals more with analogical reasoning than with pure verbal or speech processes. Even though verbal mechanisms were involved in recognizing the visually presented words, the main challenge of the task was to determine whether the word pairs were synonyms or antonyms. Most of the word pairs used (such as FOXY - CLEVER, HEARTLESS - COLD) can be classified as antonyms or synonyms only on the basis of metaphors. The role of the right hemisphere in the processing of metaphor-dependent or context-dependent cognitive tasks, is well known (Cook, 1986).

Figure 48 shows the correlation results for the "SPAT" or spatial (shape matching) task. The most noticeable feature of this figure is the general lack of instances of high correlations. This particular task in fact, made minimal demands upon spatial reasoning. It is indeed possible to solve most of the spatial tasks merely by noticing any single bar-length mismatch between the paired figures. It is usually not necessary to superimpose a mental image of one figure on the other (and it is never necessary to perform a rotation or a more complex transformation of a figure). There was consequently too little variation in subjects' performance to permit meaningful regression analysis (which finds R-square at each site at each instant).

It can be anticipated then, that the contingency locus will be helpful in "matching" individuals to particular cognitive tasks or even help in diagnosis of certain neurological conditions. Preliminary work done by CNDS has shown different contingency peak patterns between normal and dyslexic individuals, for example.

FIGURE VI.1.-46

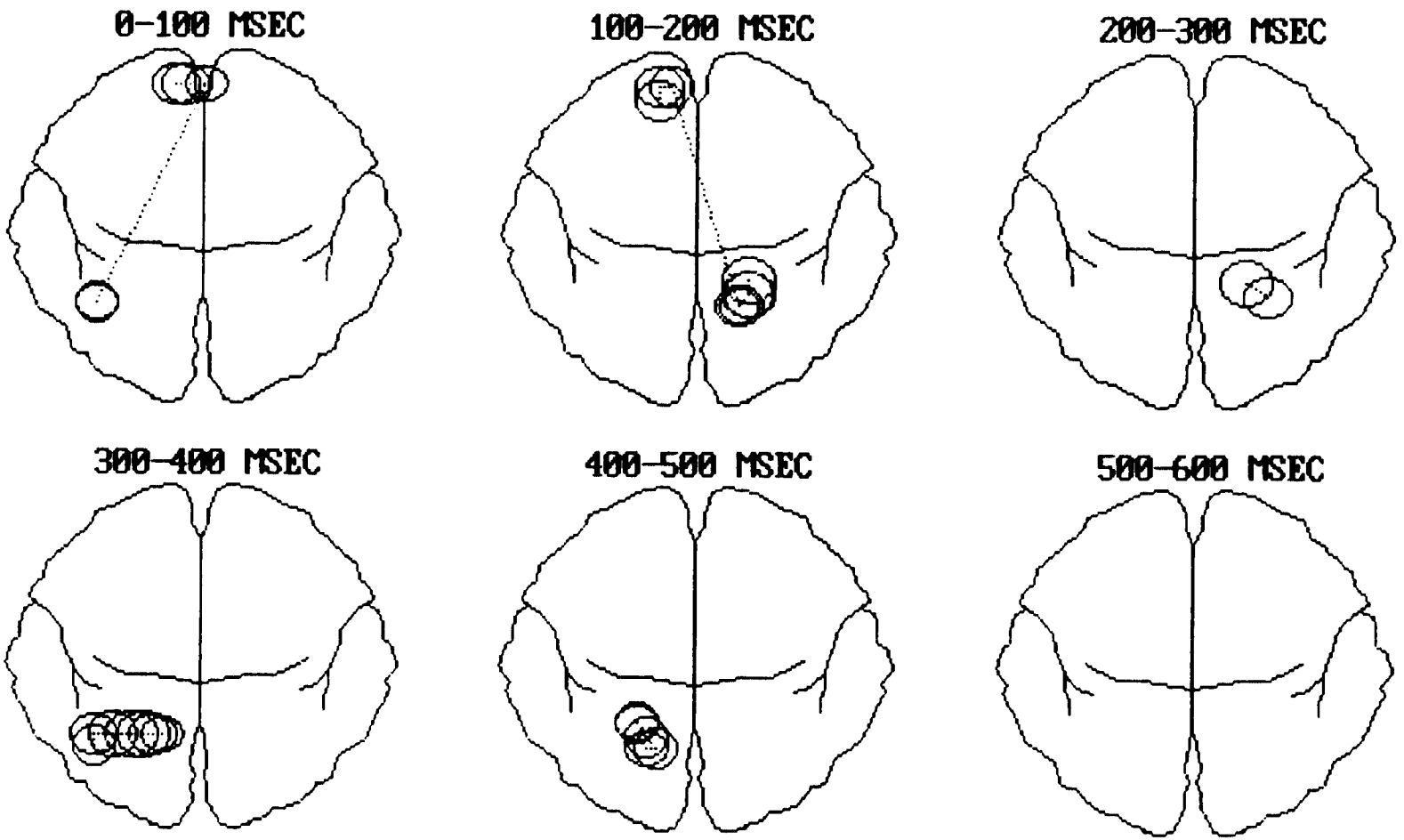

MENTAL ARITHMETIC TASK
CORRELATION OF PERFORMANCE WITH CORTICAL ENERGY

FIGURE VI.1.-47

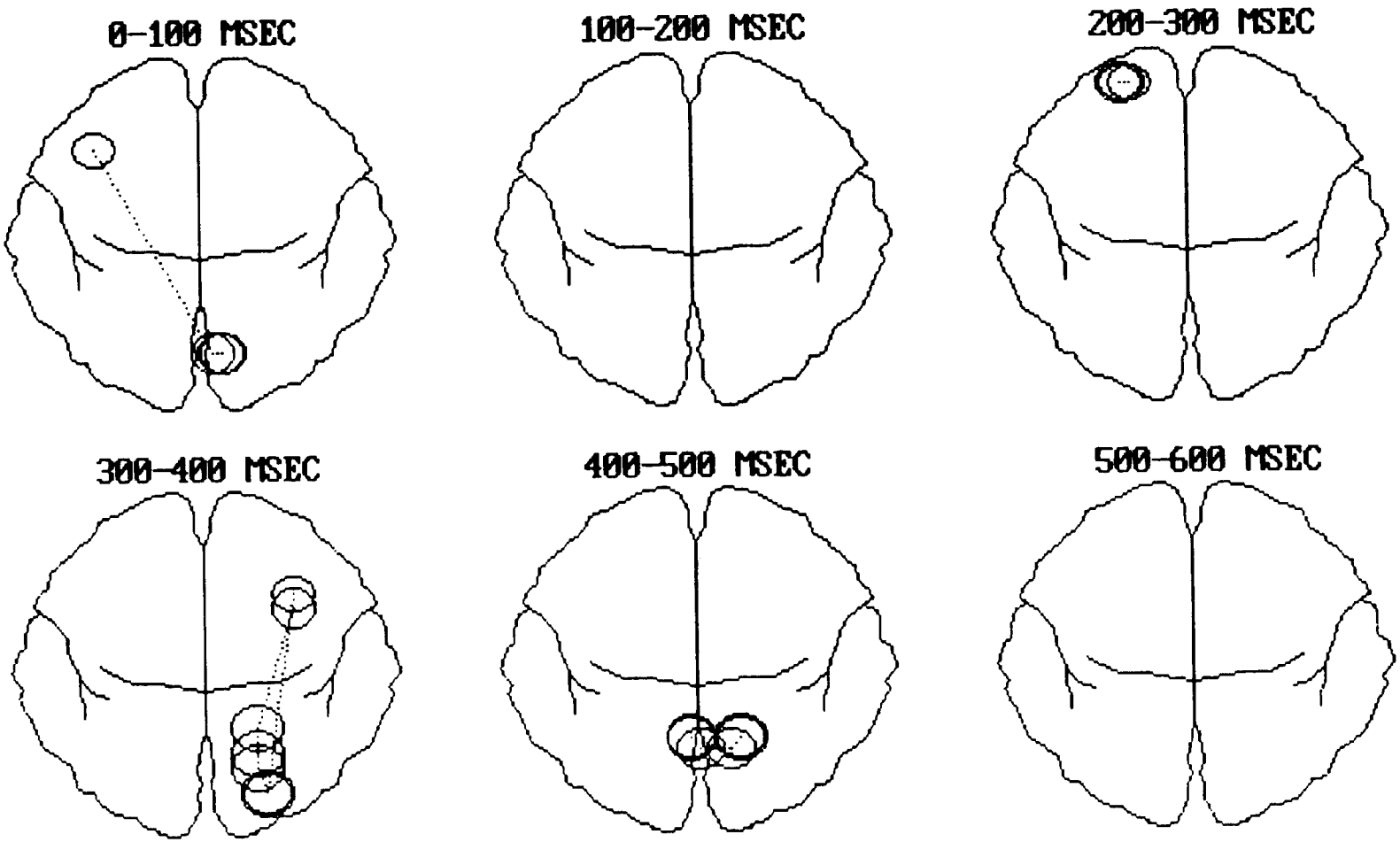

WORD PAIR TASK
CORRELATION OF PERFORMANCE WITH CORTICAL ENERGY

FIGURE VI.1.-48

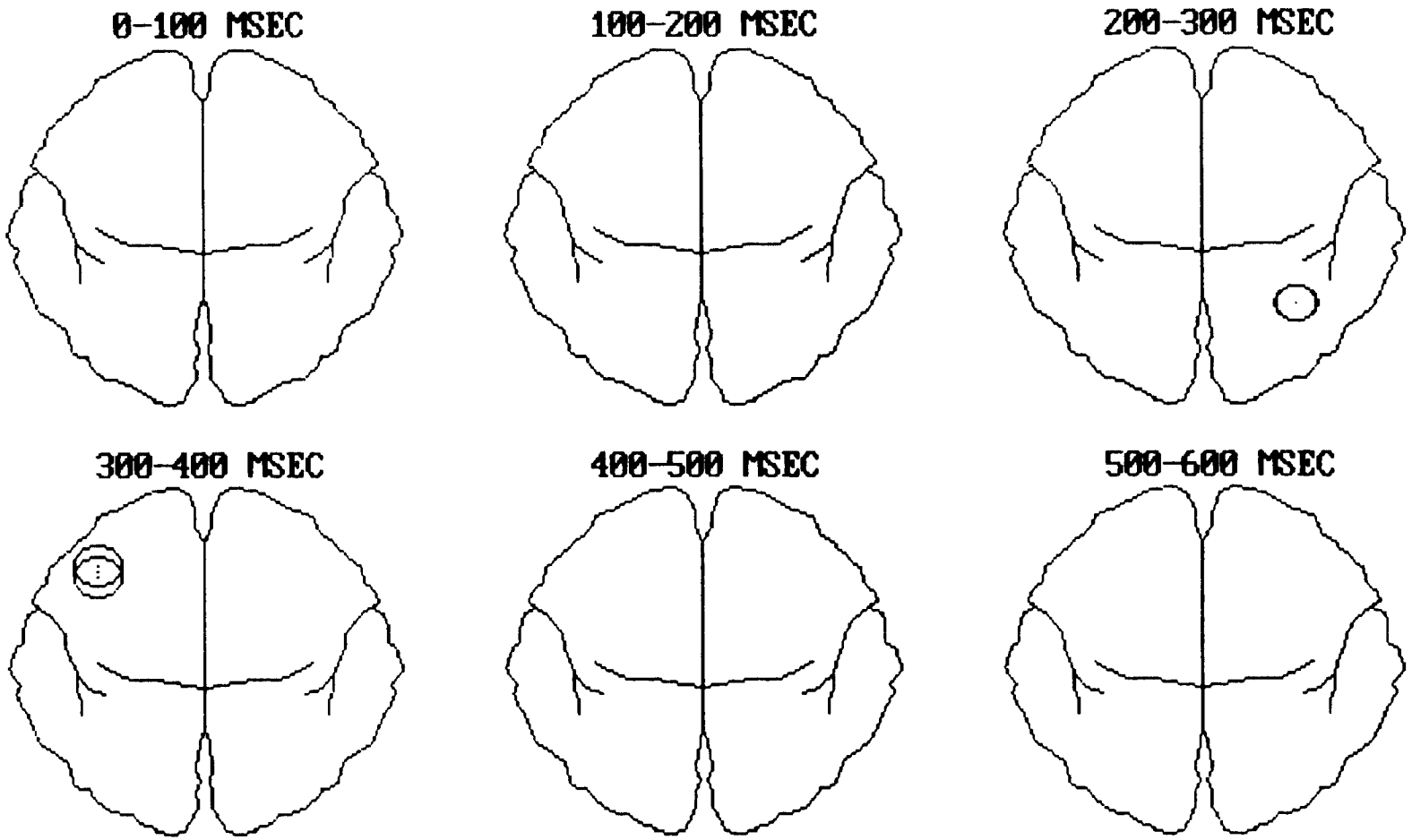

SHAPE MATCHING TASK
CORRELATION OF PERFORMANCE WITH CORTICAL ENERGY

VI.1.2. Tracking Task

VI.1.2.1. Energy density analysis. Figures VI.1.-49 through VI.1.-63.

It was hypothesized that subject fatigue would become evident in the changes in total energy of the scalp electrical field. Therefore, each two second EEG record was converted to energy density and the resulting traces were integrated over time. The integrals for all electrodes were summed over the left and right hemispheres individually as well as over the whole head.

The EEG results are displayed as summed 2-second integrals in Figures 49 to 63. For each subject there are three figures: one for the right hemisphere sum, one for the left hemisphere sum and one for the whole head. Each display contains 25 vertical bars for the control period and 55 for the test period. Tables VI-X (Appendix C) show the EEG results for each subject. The first 25 lines in each table correspond to the control period and the remainder are for the test period as per the protocol in page 10.

Visual inspection of these displays reveals no right-left difference. In three subjects however, there is a tendency for the integrals from the test period to be higher than those over the control period. There is no appreciable change in energy integral during task in the other two subjects.

FIGURE VI.1.-49

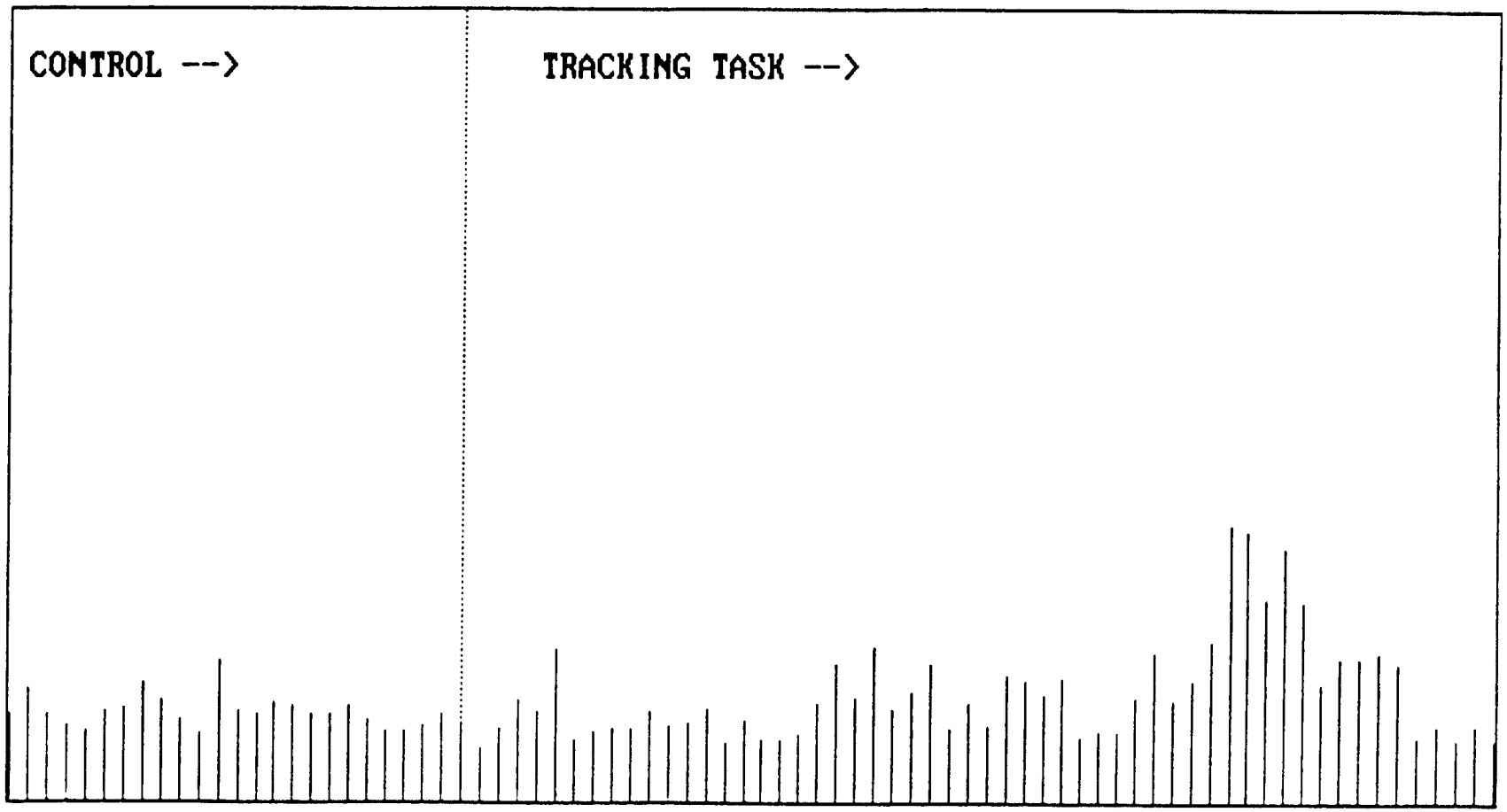

TRACKING TASK -->

2-SECOND RIGHT HEMISPHERE ENERGY INTEGRALS: C:TRAK-00.INT

FIGURE VI.1.-50

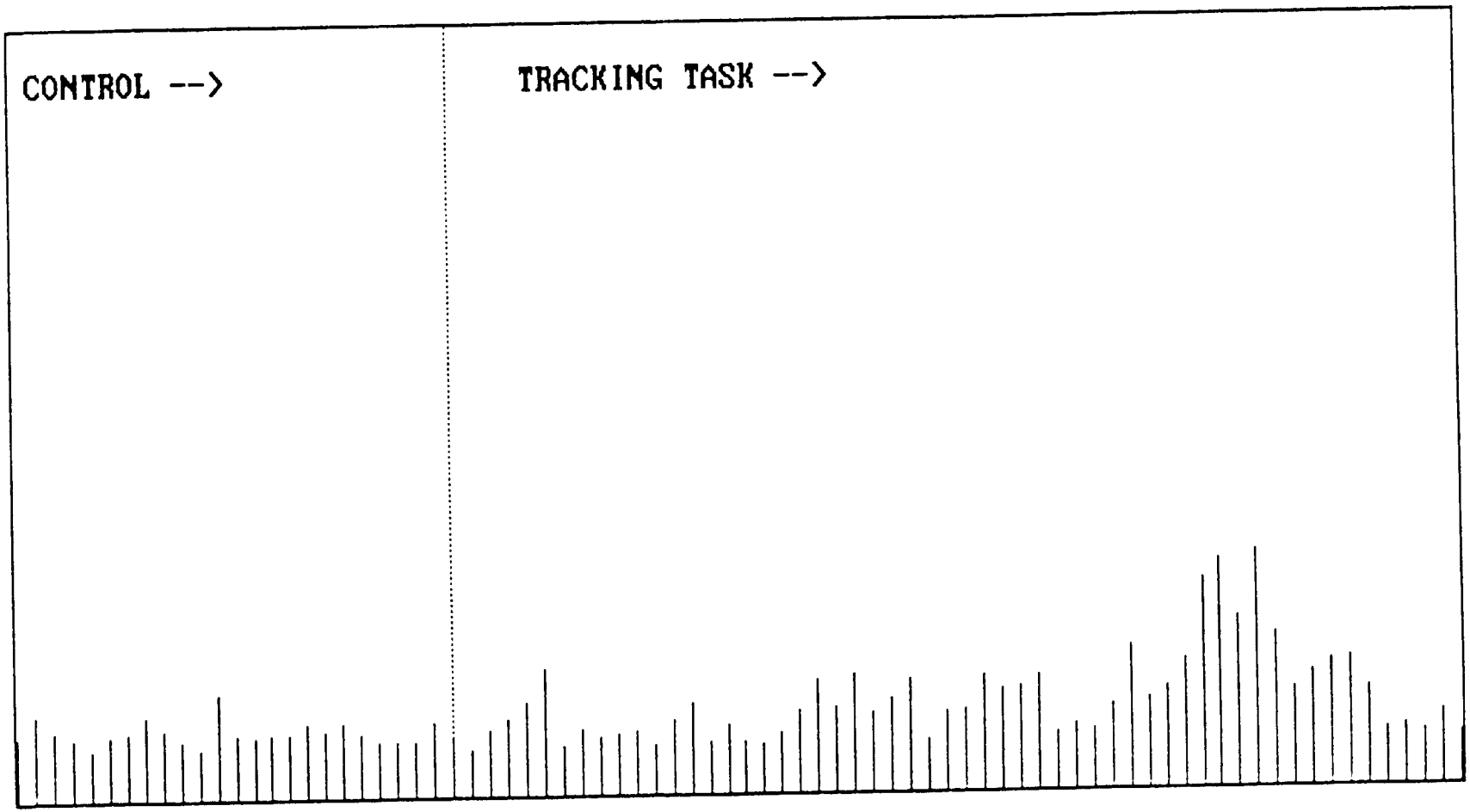

TRACKING TASK -->

2-SECOND LEFT HEMISPHERE ENERGY INTEGRALS: C:TRAK-00.INT

FIGURE VI.1.-51

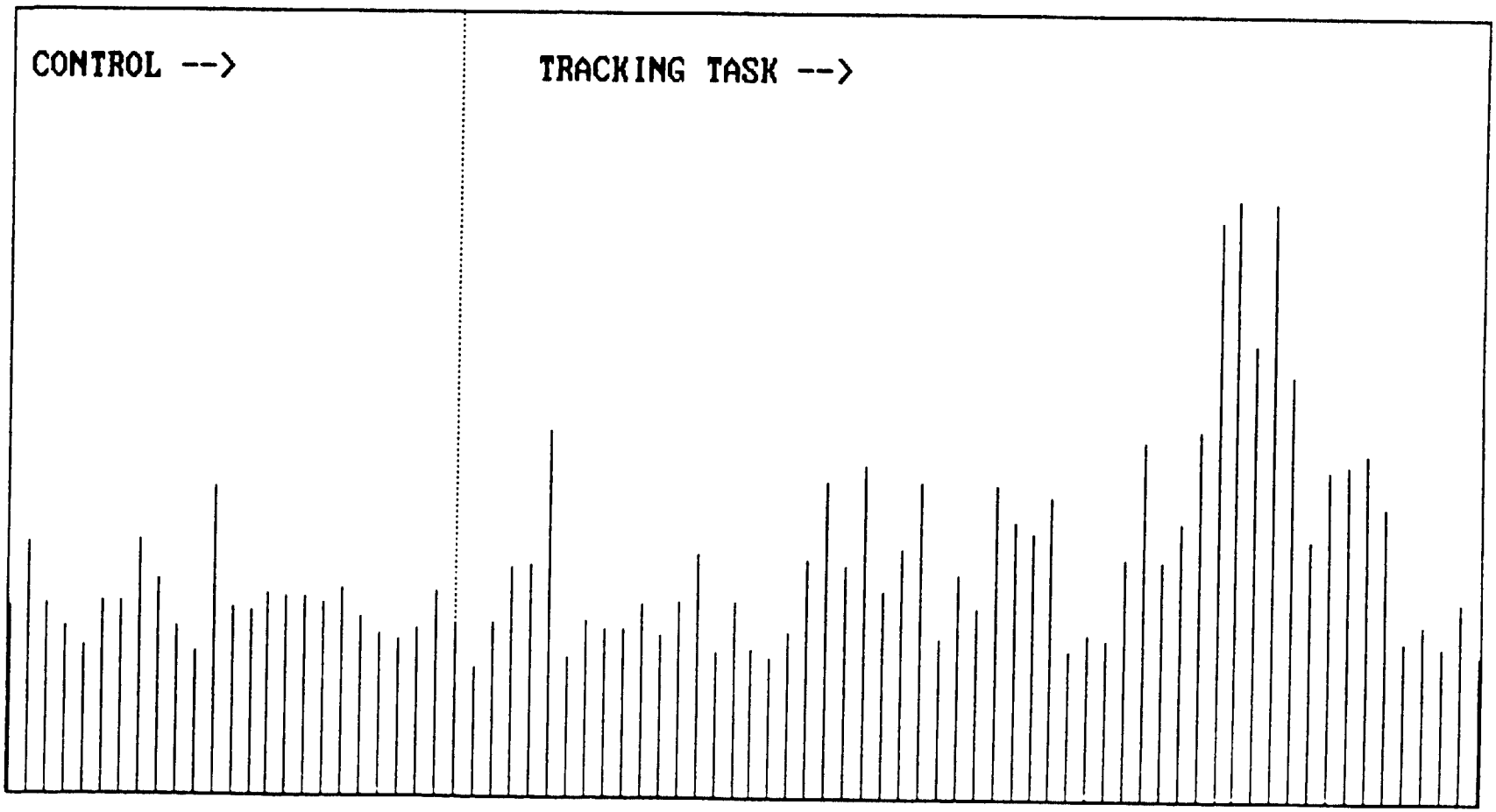

TRACKING TASK -->

2-SECOND WHOLE HEAD ENERGY INTEGRALS: C:TRAK-00.INT

FIGURE VI.1.-52

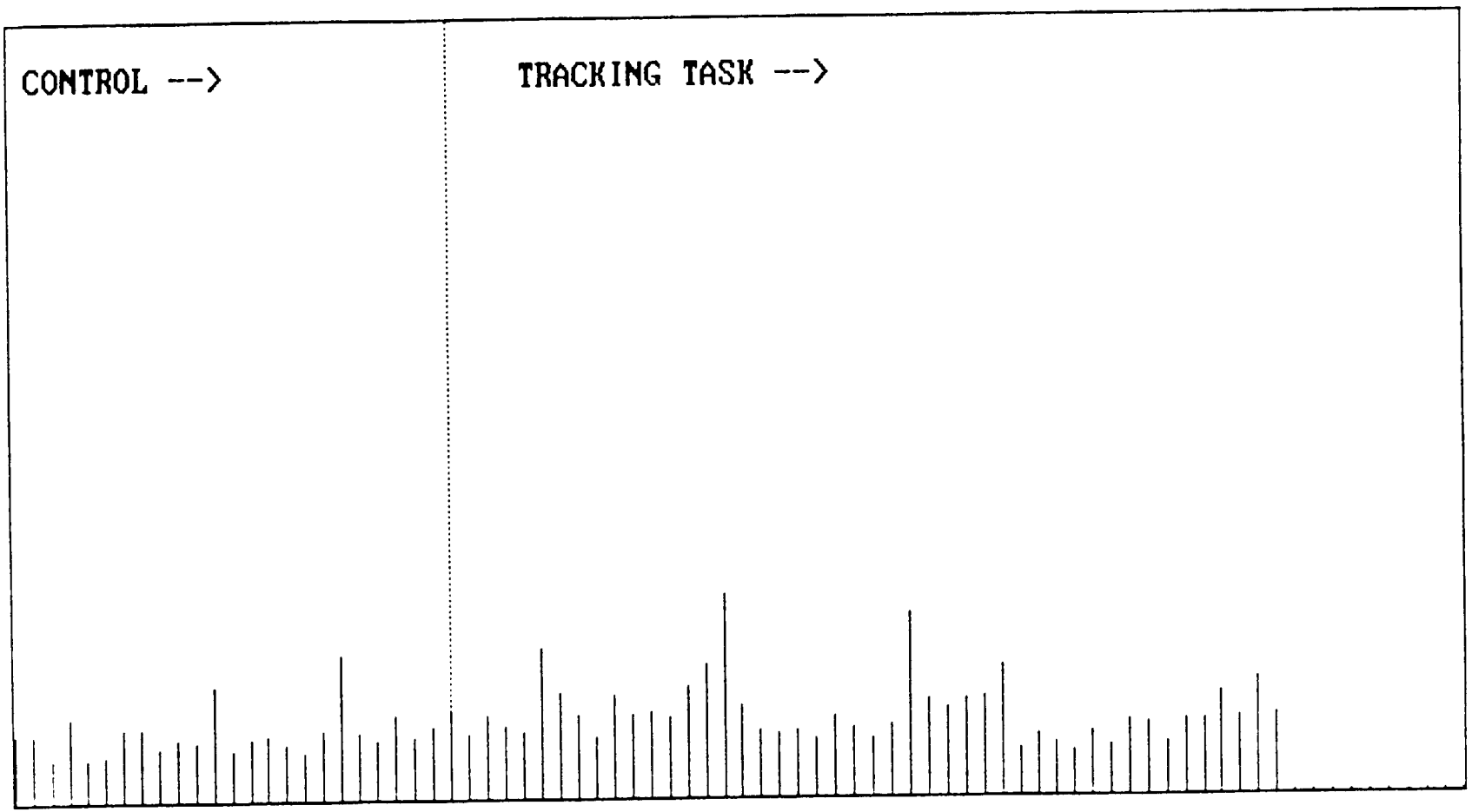

TRACKING TASK -->

2-SECOND RIGHT HEMISPHERE ENERGY INTEGRALS: C:TRAK-03.INT

FIGURE VI.1.-53

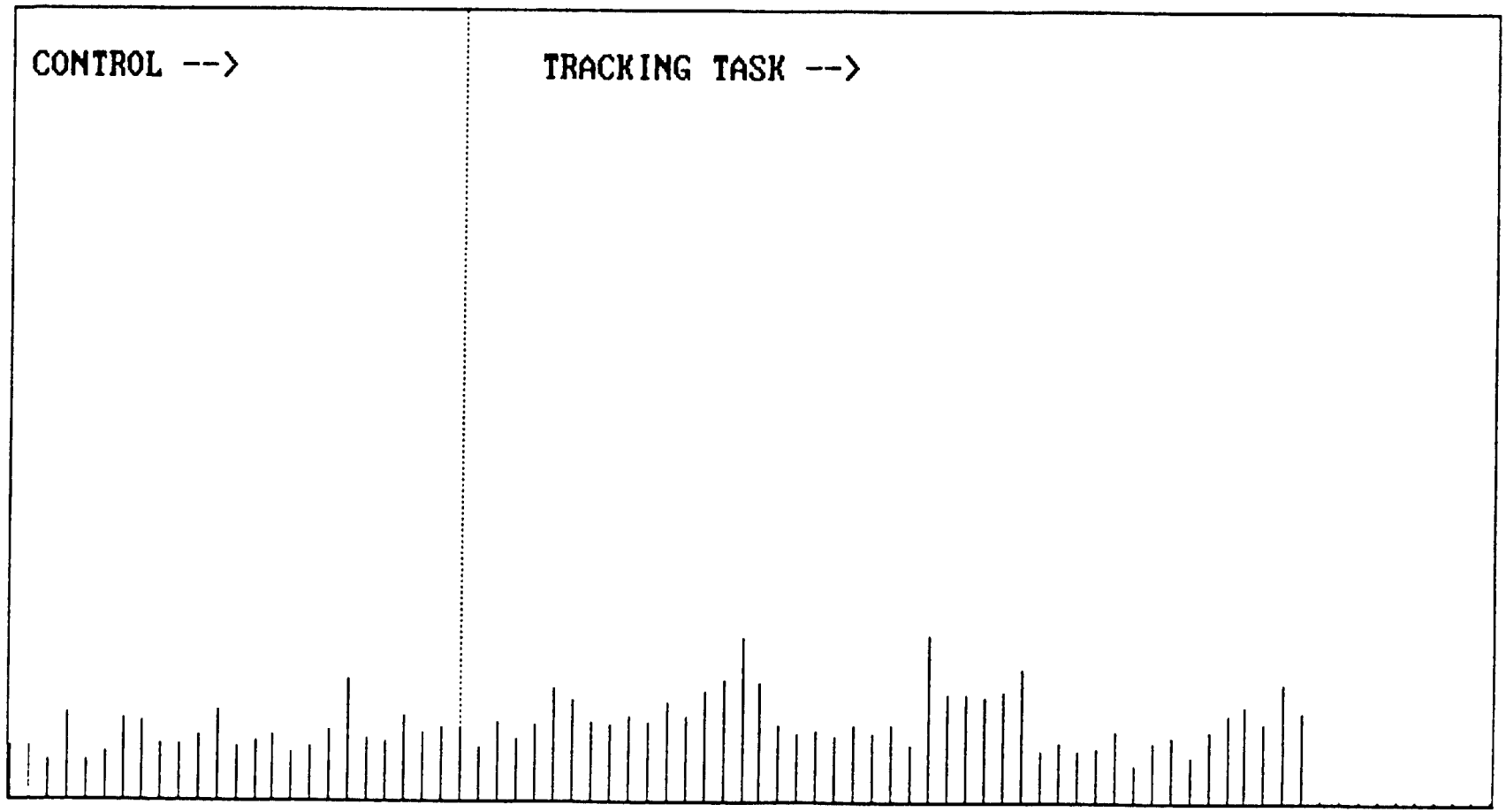

TRACKING TASK -->

2-SECOND LEFT HEMISPHERE ENERGY INTEGRALS: C:TRAK-03.INT

FIGURE VI.1.-54

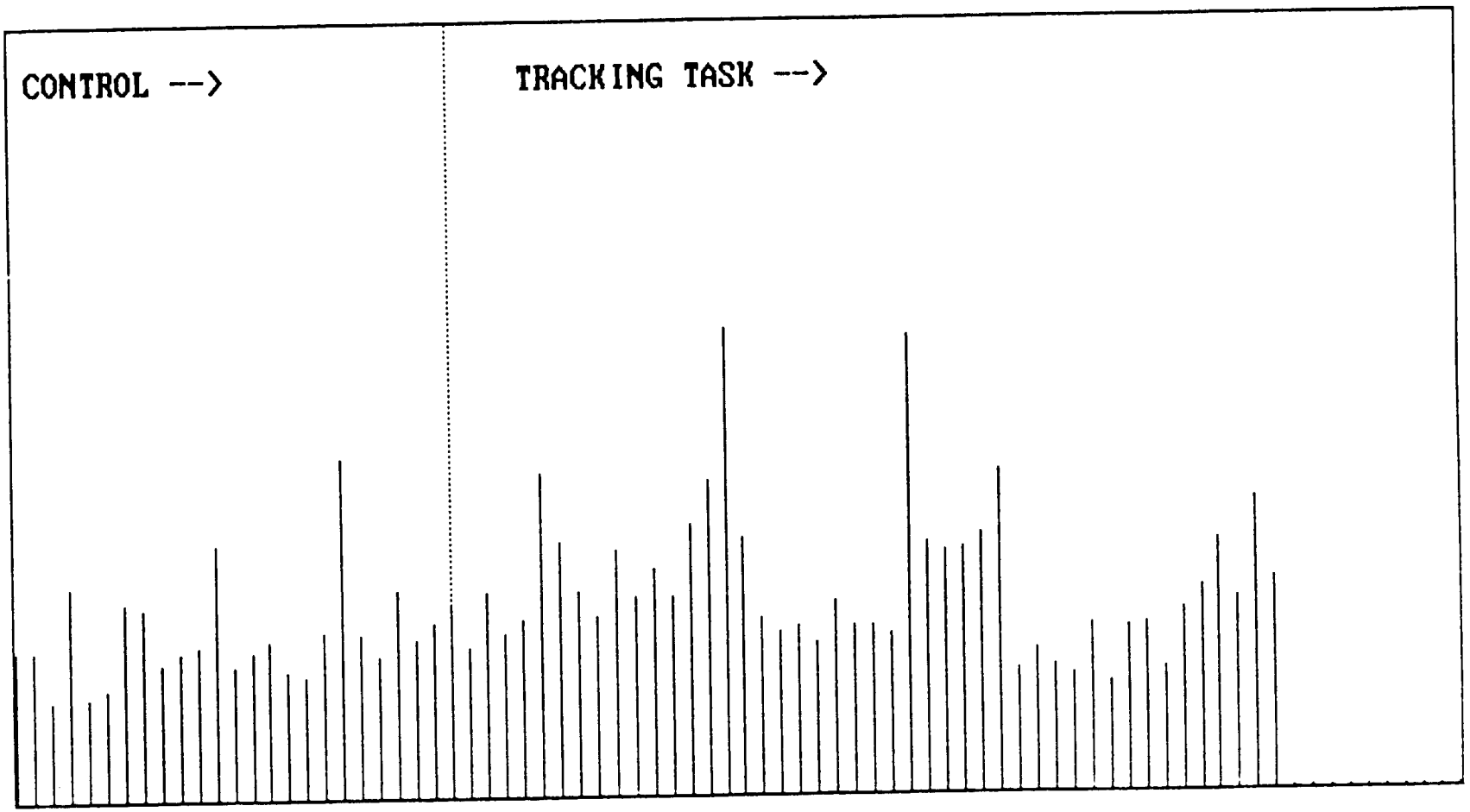

TRACKING TASK -->

2-SECOND WHOLE HEAD ENERGY INTEGRALS: C:TRAK-03.INT

FIGURE VI.1.-55

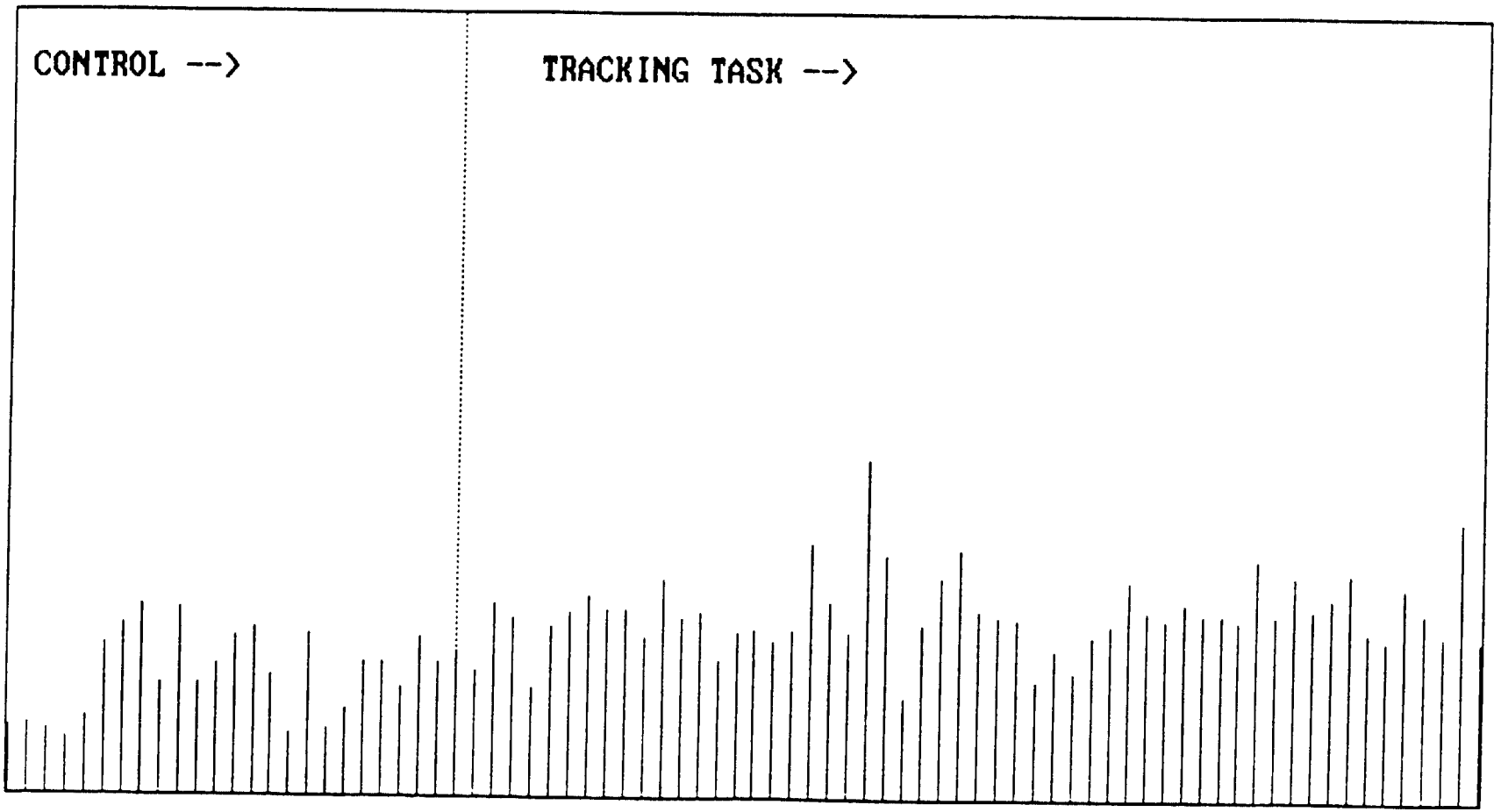

2-SECOND RIGHT HEMISPHERE ENERGY INTEGRALS: C:TRAK-07.INT

FIGURE VI.1.-56

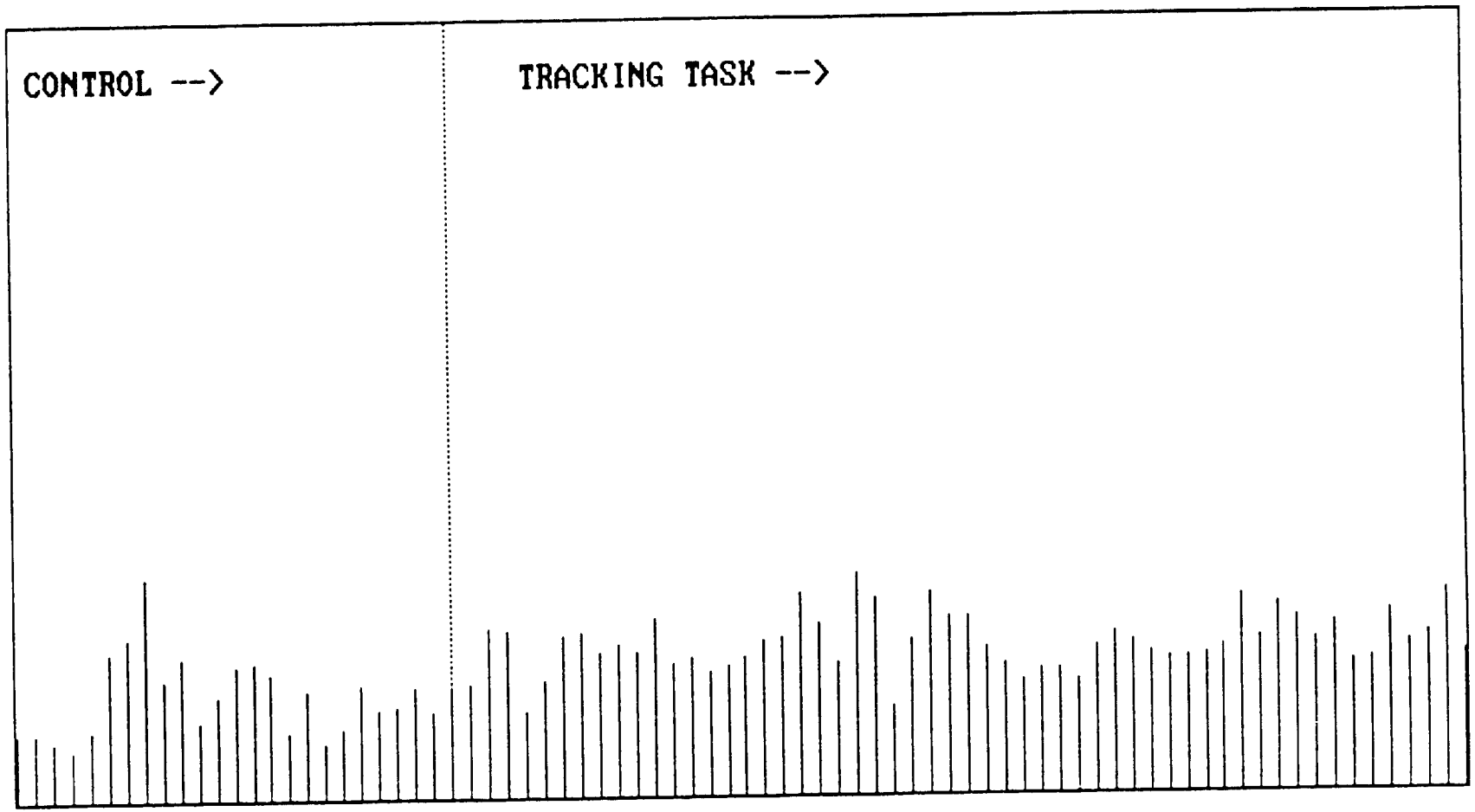

2-SECOND LEFT HEMISPHERE ENERGY INTEGRALS: C:TRAK-07.INT

FIGURE VI.1.-57

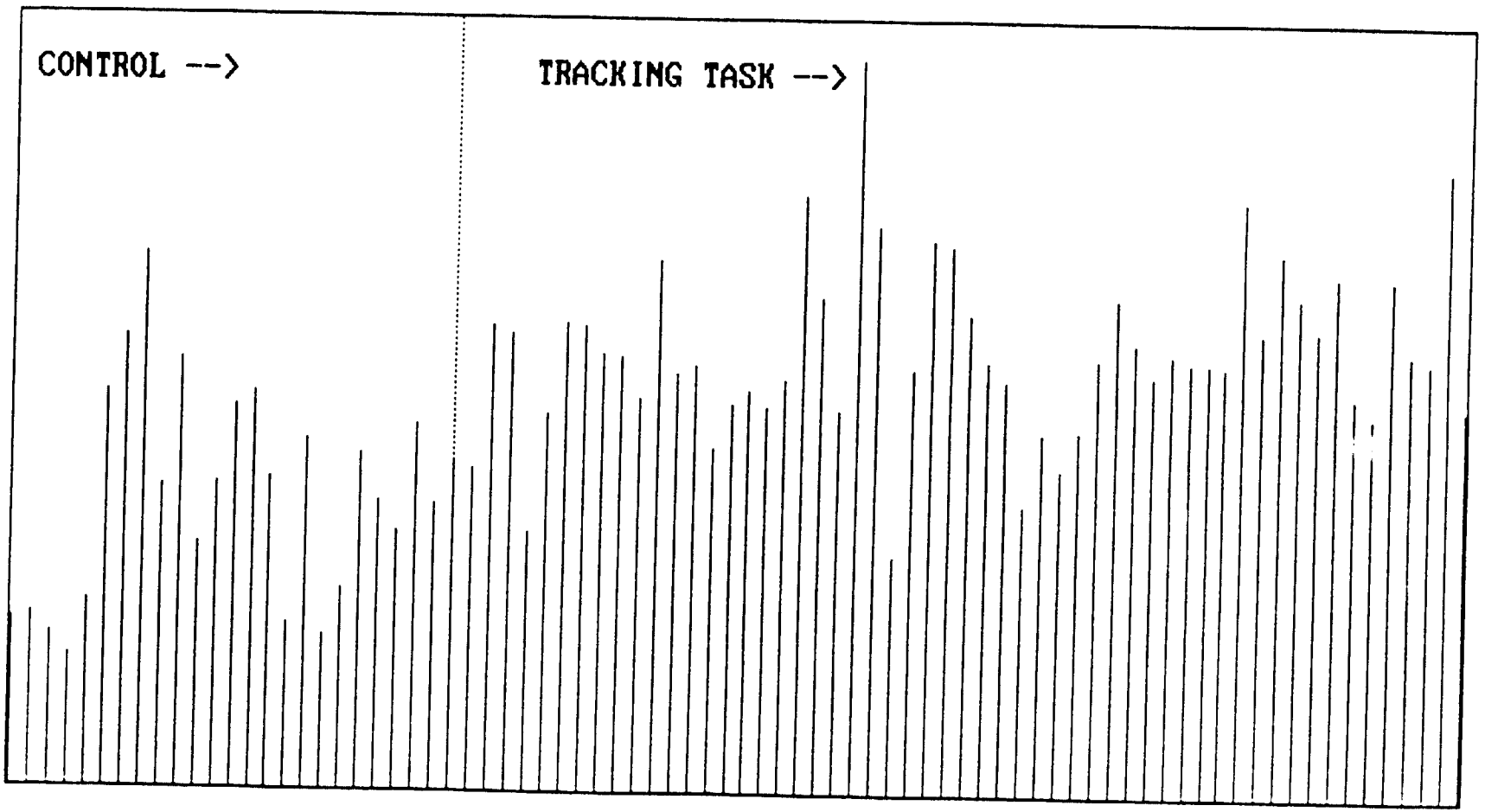

2-SECOND WHOLE HEAD ENERGY INTEGRALS: C:TRAK-07.INT

FIGURE VI.1.-58

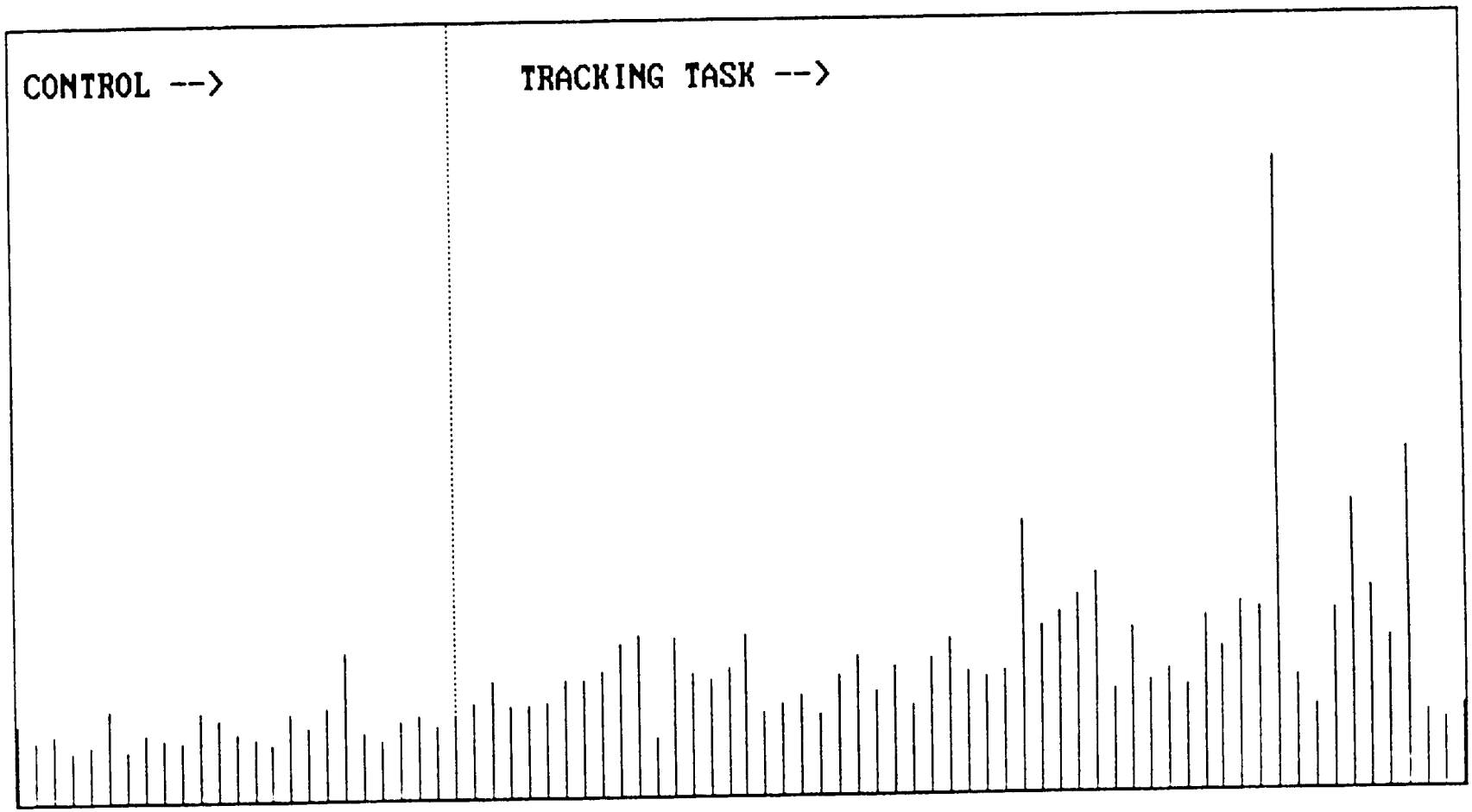

TRACKING TASK -->

2-SECOND RIGHT HEMISPHERE ENERGY INTEGRALS: C:TRAK-08.INT

FIGURE VI.1.-59

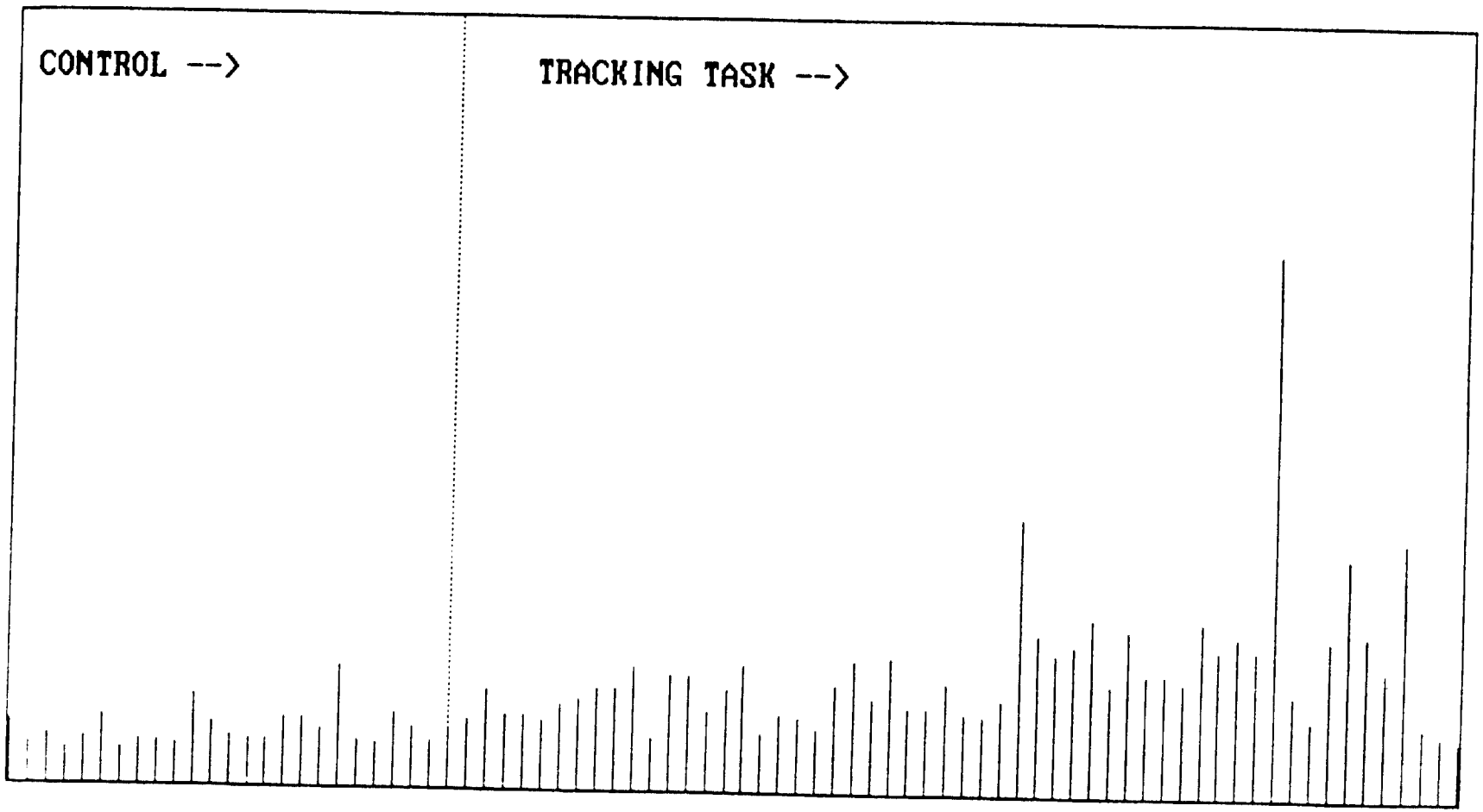

2-SECOND LEFT HEMISPHERE ENERGY INTEGRALS: C:TRAK-08.INT

FIGURE VI.1.-60

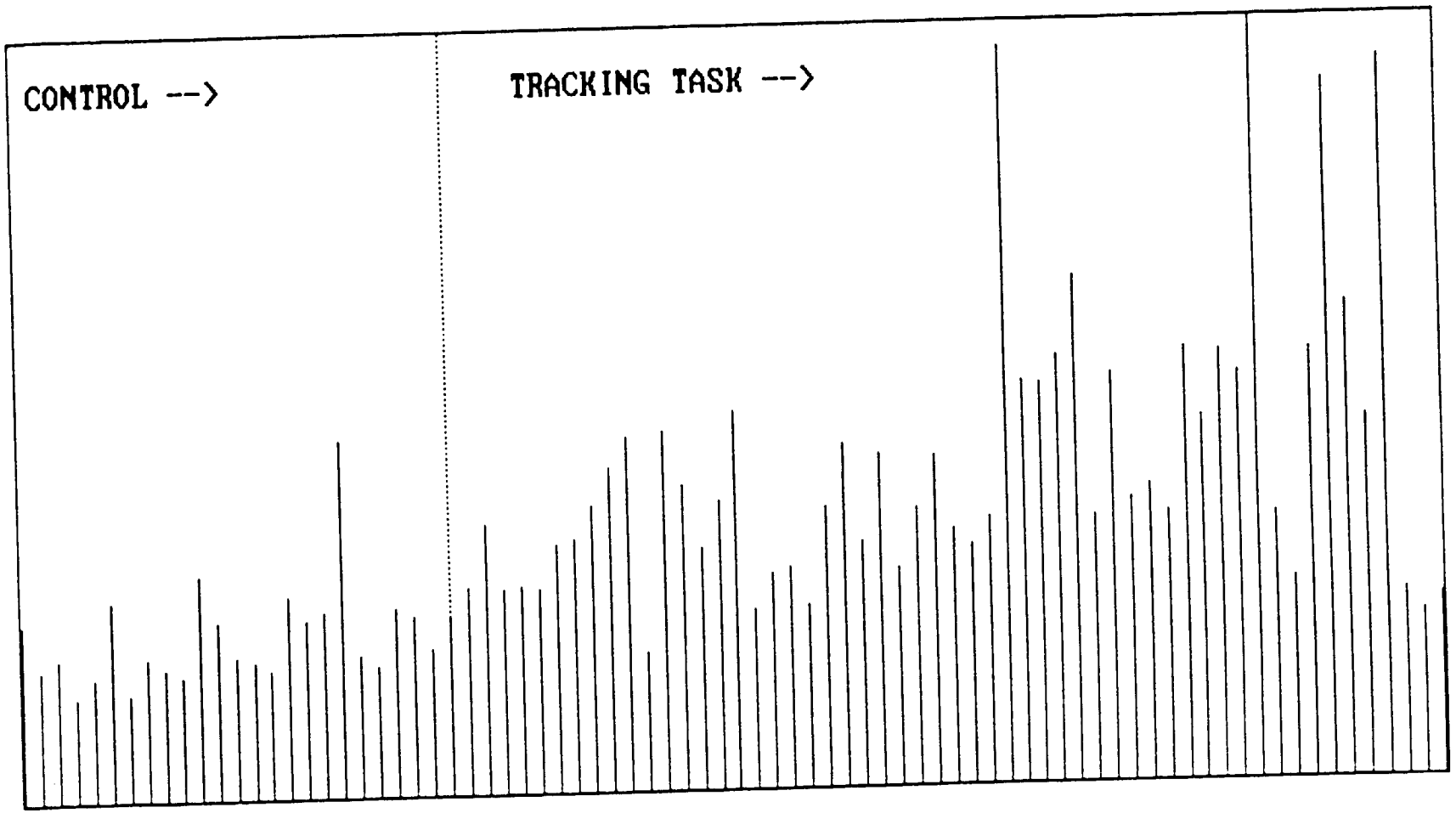

TRACKING TASK -->

2-SECOND WHOLE HEAD ENERGY INTEGRALS: C:TRAK-08.INT

FIGURE VI.1.-61

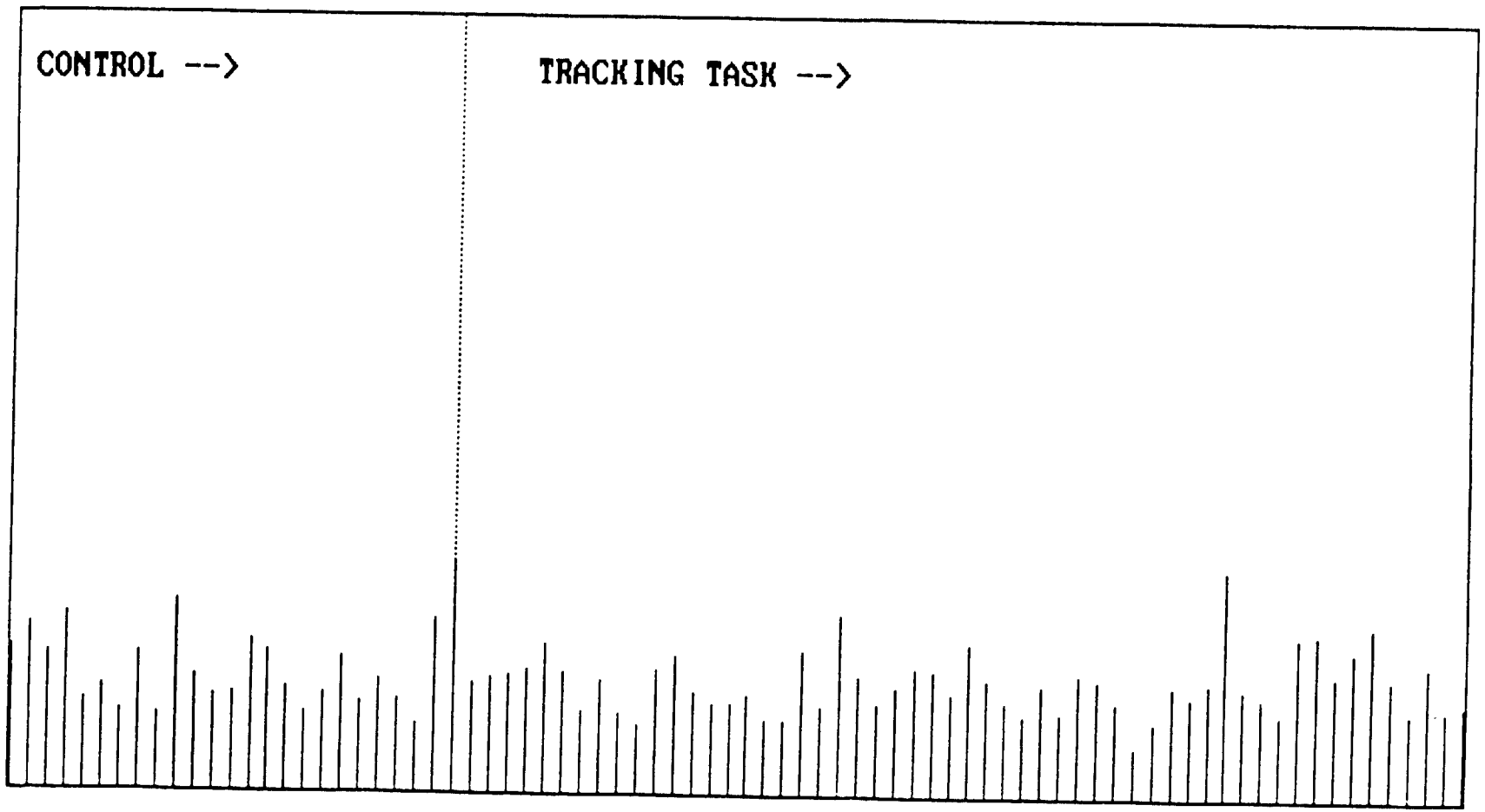

2-SECOND RIGHT HEMISPHERE ENERGY INTEGRALS: C:TRAK-09.INT

FIGURE VI.1.-62

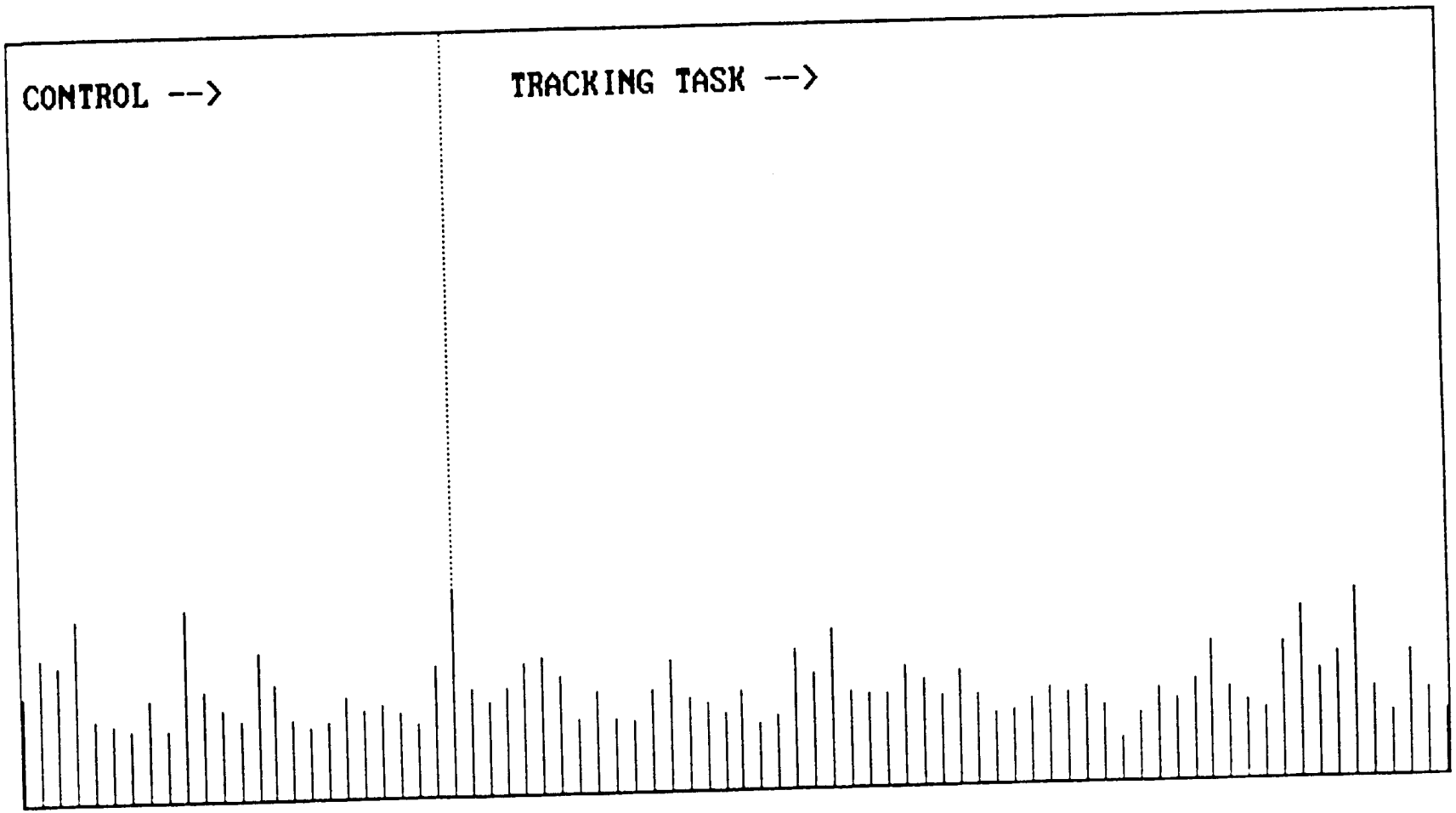

2-SECOND LEFT HEMISPHERE ENERGY INTEGRALS: C:TRAK-09.INT

FIGURE VI.1.-63

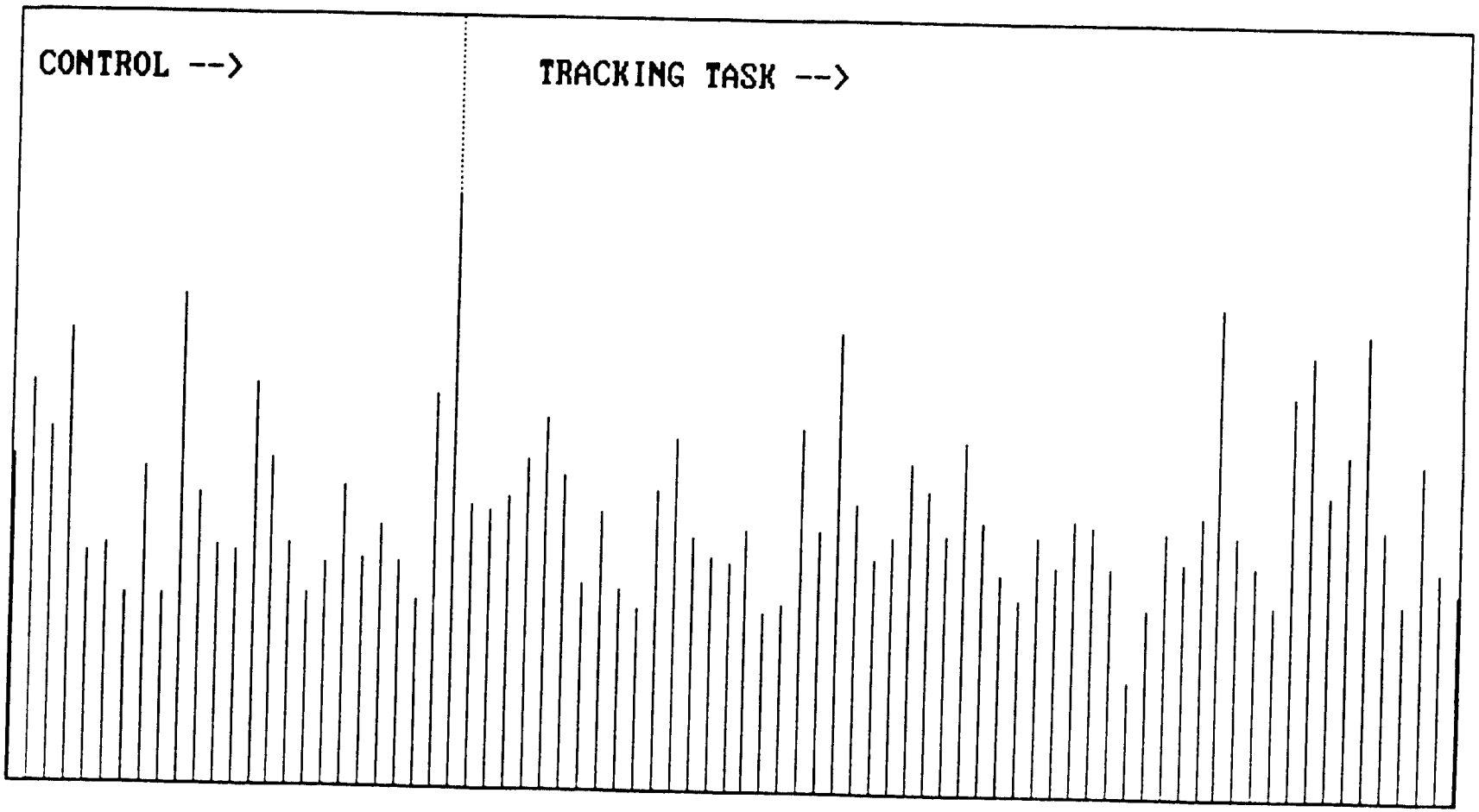

2-SECOND WHOLE HEAD ENERGY INTEGRALS: C:TRAK-09.INT

VI.1.3. Long Term Task. Figures VI.1.-65 through VI.1.-109

The Long Term Task is described in detail in Section III.4. (pages 11-12). Figures 64 to 90 and Tables XI to XIX, show the regression analysis for each task type (MATH, VERB, SPAT), arranged in three sets. Within each set, these data are arranged as follows:

- Tables of regression results (one for each of three subjects across ERPs); within the tables, the results are presented in task type sets of three,

- Example of a good fitting scatterplot (one for each of three subjects),

- Display of R-square variations as a series of surfaces, for each of three subjects,

- Locus diagram of R-square peaks, for each of three subjects.

Although the tables of regression results show many instances of high R-square and high t-value for the slope coefficient, these results are somewhat misleading. Inspection of the scatterplots show that in most cases the subject manifested an extremely small variation in cortical energy density (the independent variable). In such a situation the regression analysis breaks down: in the limiting case, the independent variable is a constant and the data points simply fall on a vertical line above that constant value.

These results show that this approach to cortical localization is not as useful when applied to several data points for the same subject as it is when applied to cross-subject data. These results also confirm the basic findings of this study: 1) that subjects have a robustly stable EEG response (despite experimental variation in task level or task type) and 2) that one subject's stable response may be quite different from another's.

Given that a subject did not manifest a shift in cortical activation pattern over the period (as shown above), then it is reasonable to pool the subjects' six ERPs. This produces in effect, a single ERP for each subject, for each task, based upon (6x48=) 288 individual responses, thus achieving a major increase in statistical power. Locus diagrams of these averaged ERPs, for each subject, are shown in Figures 91 -99. The same averaged ERPs are also presented in the form of TRACES overlays, where, for each subject the three task types are overlayed for comparison. This is done both for voltage (Figures 103-105) and for energy density (Figures 100-102), so that the effect of the energy-density conversion can also be observed (Figures 100-107).

These displays show that there is far more variation between subjects (for any given task type) than between tasks for any given subject. This is the same finding as emphasized above: on the one hand, that implies that even if intertask differences were found for one of the subjects, the intersubject differences are too great to permit statistical generalization. On the other hand, assuming that the null hypothesis is accepted for inter-task differences for a given subject, it is then appropriate to pool the three task type ERPs for each subject, with the result of producing a single ERP based upon (3x288=) 864 individual responses. These are displayed as TRACES diagrams, both for voltage (Figure 107) and for energy density (Figure 106).

Longitudinal energy density ERP comparison.

Since one subject (01) did have performance scores suggesting a trend (learning) for one task (VERB), it was felt that his early ERPs might be distinctly different from those collected at the end of the experiment. Table XX shows the regression results for first 6 ERPs and Table XXI shows the regression results for the last six ERPs on subject 01, VERB task. Figure 108 is the locus diagram for the first 6 ERPs (labeled V1A.COR) and Figure 109 is the locus diagram for the last 6 ERPs (labeled V1B.COR).

The Locus diagram suggests a shift toward greater contingency of performance upon late occipital activation and less contingency upon early frontal activation. This would be consistent with learning and "automatization" of the task, in the sense that less planning (frontal lobe dependent) would be required and performance would depend more upon mere successful encoding of the visual stimulus (occipital lobe dependent). Significantly, for the last six ERPs, where the regression of performance upon energy density is statistically significant for the occipital cortex, the sign of the slope coefficient is negative, implying a lower error rate for higher energy density.

TABLE XI

ERROR INDEX VS. ENERGY DENSITY:
SUBJ 01 -- 6 ARITHMETIC ERPs

ELECTRODE	PERIOD	R-SQUARE	T-VALUE	SLOPE
Fz	8 - 47	0.762	3.581	0.733
F4	8 - 47	0.846	4.684	1.038
C3	8 - 47	0.795	3.934	1.489
Fz	16 - 55	0.811	4.146	0.633
F4	16 - 55	0.790	3.876	0.737
C3	16 - 55	0.874	5.263	0.979
Cz	16 - 55	0.821	4.289	0.654
Fz	24 - 63	0.816	4.216	0.562
C3	24 - 63	0.838	4.553	0.688
Cz	24 - 63	0.816	4.206	0.513
T4	258 - 297	0.791	3.889	1.064
Oz	430 - 469	0.848	-4.716	-0.553
Oz	438 - 477	0.845	-4.664	-0.693

TABLE XII

ERROR INDEX VS. ENERGY DENSITY:
SUBJ 02 -- 6 ARITHMETIC ERPs

ELECTRODE	PERIOD	R-SQUARE	T-VALUE	SLOPE
P3	63 - 102	0.977	13.135	0.897
O1	86 - 126	0.834	4.488	0.385
Oz	86 - 126	0.895	5.854	0.669
T6	110 - 149	0.886	-5.564	-1.071
P3	165 - 204	0.819	4.258	0.877
Cz	297 - 336	0.817	-4.222	-0.596
Cz	305 - 344	0.845	-4.666	-0.584
Fp2	321 - 360	0.901	6.049	0.248
O2	321 - 360	0.896	-5.876	-0.216
Fp2	329 - 368	0.973	11.943	0.246
O2	329 - 368	0.939	-7.858	-0.206
Fp2	336 - 376	0.986	16.556	0.251
P4	336 - 376	0.808	-4.101	-0.232
O2	336 - 376	0.949	-8.617	-0.206
Fp2	344 - 383	0.956	9.353	0.264
O2	344 - 383	0.930	-7.276	-0.212
Fp2	352 - 391	0.889	5.657	0.290
O2	352 - 391	0.885	-5.544	-0.223
O2	360 - 399	0.834	-4.475	-0.237

TABLE XIII

ERROR INDEX VS. ENERGY DENSITY:
SUBJ 04 -- 6 ARITHMETIC ERPS

ELECTRODE	PERIOD	R-SQUARE	T-VALUE	SLOPE
F7	110 - 149	0.920	6.786	0.055
F7	118 - 157	0.948	8.515	0.063
F7	126 - 165	0.976	12.880	0.077
T6	126 - 165	0.901	-6.021	-0.059
F7	133 - 172	0.987	17.179	0.102
T6	133 - 172	0.940	-7.943	-0.068
F7	141 - 180	0.924	6.976	0.136
T6	141 - 180	0.941	-7.968	-0.075
T6	149 - 188	0.936	-7.627	-0.081
T6	157 - 196	0.929	-7.221	-0.085
O2	196 - 235	0.903	-6.113	-0.063
Pz	430 - 469	0.915	6.560	0.055
Pz	438 - 477	0.929	7.221	0.051
P4	438 - 477	0.914	6.523	0.062
Oz	438 - 477	0.901	6.046	0.040
Pz	446 - 485	0.913	6.482	0.048
P4	446 - 485	0.924	6.970	0.060
Oz	446 - 485	0.928	7.159	0.040
P4	454 - 493	0.935	7.558	0.060
Oz	454 - 493	0.915	6.559	0.041
P4	461 - 501	0.951	8.791	0.063

TABLE XIV

ERROR INDEX VS. ENERGY DENSITY:
SUBJ 01 -- 6 WORDPAIR ERPs

ELECTRODE	PERIOD	R-SQUARE	T-VALUE	SLOPE
F4	32 - 71	0.720	3.208	0.227
F4	40 - 79	0.821	4.281	0.257
Fp1	47 - 86	0.878	5.360	0.774
Fpz	47 - 86	0.759	3.549	0.376
F4	47 - 86	0.821	4.286	0.254
F4	55 - 94	0.754	3.505	0.234
O2	55 - 94	0.835	-4.501	-0.197
P4	63 - 102	0.829	-4.399	-0.401
Oz	63 - 102	0.741	-3.379	-0.175
O2	63 - 102	0.943	-8.114	-0.215
P4	71 - 110	0.902	-6.063	-0.479
Oz	71 - 110	0.719	-3.203	-0.165
O2	71 - 110	0.970	-11.420	-0.226
P4	79 - 118	0.794	-3.925	-0.489
O2	79 - 118	0.922	-6.889	-0.237
O2	86 - 126	0.798	-3.974	-0.250
P3	157 - 196	0.712	3.142	0.449
Fp1	165 - 204	0.815	-4.197	-0.553
O1	165 - 204	0.807	4.096	0.494
Fz	172 - 211	0.874	-5.271	-1.387
C3	243 - 282	0.718	3.194	0.859
P3	258 - 297	0.916	6.587	1.224
O1	266 - 305	0.722	3.227	0.847

TABLE XV

ERROR INDEX VS. ENERGY DENSITY:
SUBJ 02 -- 6 WORDPAIR ERPS

ELECTRODE	PERIOD	R-SQUARE	T-VALUE	SLOPE
T6	16 - 55	0.808	4.106	0.189
T6	24 - 63	0.811	4.138	0.162
O2	102 - 141	0.836	4.508	0.112
O2	110 - 149	0.885	5.545	0.118
Oz	118 - 157	0.802	4.021	0.123
O2	118 - 157	0.915	6.581	0.124
Oz	126 - 165	0.881	5.432	0.138
O2	126 - 165	0.918	6.682	0.128
Oz	133 - 172	0.920	6.782	0.155
O2	133 - 172	0.892	5.740	0.133
Oz	141 - 180	0.914	6.514	0.175
O2	141 - 180	0.852	4.795	0.140
Oz	149 - 188	0.861	4.972	0.198
O2	149 - 188	0.814	4.182	0.150
C3	157 - 196	0.863	-5.030	-0.296
C3	165 - 204	0.905	-6.158	-0.297
C3	172 - 211	0.889	-5.653	-0.284
T3	180 - 219	0.823	-4.315	-0.374
C3	180 - 219	0.834	-4.490	-0.265
T3	188 - 227	0.843	-4.628	-0.399

TABLE XVI

ERROR INDEX VS. ENERGY DENSITY:
SUBJ 04 -- 6 WORDPAIR ERPS

ELECTRODE	PERIOD	R-SQUARE	T-VALUE	SLOPE
T6	47 - 86	0.772	-3.678	-0.371
T6	55 - 94	0.843	-4.639	-0.489
T3	63 - 102	0.721	3.214	0.279
C4	126 - 165	0.722	-3.227	-1.083
P3	430 - 469	0.701	-3.063	-0.231
P3	438 - 477	0.754	-3.503	-0.237
Pz	438 - 477	0.754	-3.506	-0.171
O1	438 - 477	0.744	-3.408	-0.138
Oz	438 - 477	0.703	-3.074	-0.091
O2	438 - 477	0.719	-3.200	-0.104
P3	446 - 485	0.796	-3.947	-0.254
Pz	446 - 485	0.826	-4.362	-0.189
O1	446 - 485	0.834	-4.477	-0.147
Oz	446 - 485	0.775	-3.708	-0.097
O2	446 - 485	0.762	-3.575	-0.110
Fp1	454 - 493	0.738	3.358	0.169
P3	454 - 493	0.779	-3.754	-0.266
Pz	454 - 493	0.793	-3.919	-0.196
O1	454 - 493	0.845	-4.676	-0.148
Oz	454 - 493	0.786	-3.829	-0.100
O2	454 - 493	0.736	-3.339	-0.113
Fp1	461 - 501	0.792	3.908	0.186
O1	461 - 501	0.752	-3.482	-0.137
Oz	461 - 501	0.714	-3.158	-0.098

TABLE XVII

ERROR INDEX VS. ENERGY DENSITY:
SUBJ 01 -- 6 SPATIAL ERPS

ELECTRODE	PERIOD	R-SQUARE	T-VALUE	SLOPE
F3	8 - 47	0.853	4.818	0.791
C4	40 - 79	0.820	4.268	0.673
C4	47 - 86	0.914	6.537	0.590
Cz	55 - 94	0.854	4.837	0.548
O1	63 - 102	0.980	13.834	0.319
O1	71 - 110	0.831	4.439	0.243
T6	79 - 118	0.817	4.221	0.339
T6	86 - 126	0.869	5.143	0.339
T6	94 - 133	0.834	4.481	0.340
F7	376 - 415	0.804	-4.047	-0.810
P4	407 - 446	0.847	-4.712	-0.381
Oz	407 - 446	0.832	-4.455	-0.300
Fpz	415 - 454	0.833	4.474	0.604
P4	415 - 454	0.859	-4.936	-0.418
Oz	415 - 454	0.884	-5.512	-0.313
P4	422 - 461	0.829	-4.400	-0.475
Oz	422 - 461	0.878	-5.366	-0.337
Oz	430 - 469	0.819	-4.255	-0.372

TABLE XVIII

ERROR INDEX VS. ENERGY DENSITY:
SUBJ 02 -- 6 SPATIAL ERPs

ELECTRODE	PERIOD	R-SQUARE	T-VALUE	SLOPE
T4	40 - 79	0.898	-5.933	-3.459
T4	47 - 86	0.772	-3.680	-3.051
Fz	172 - 211	0.757	3.526	0.649
Fpz	180 - 219	0.773	3.696	0.332
Fp2	180 - 219	0.753	3.492	0.264
Fz	180 - 219	0.766	3.618	0.592
Fpz	188 - 227	0.776	3.718	0.302
Fp2	188 - 227	0.802	4.030	0.259
Pz	282 - 321	0.767	-3.628	-0.635
F7	290 - 329	0.816	-4.210	-0.778
Pz	290 - 329	0.757	-3.530	-0.527
F7	297 - 336	0.908	-6.287	-1.027
F7	305 - 344	0.858	-4.907	-1.159
T4	344 - 383	0.814	4.188	0.738
T4	352 - 391	0.905	6.186	0.634
T4	360 - 399	0.839	4.559	0.491
Fpz	446 - 485	0.866	5.093	0.568
Fpz	454 - 493	0.952	8.897	0.591
Fpz	461 - 501	0.935	7.612	0.578

TABLE XIX

ERROR INDEX VS. ENERGY DENSITY:
SUBJ 04 -- 6 SPATIAL ERPS

ELECTRODE	PERIOD	R-SQUARE	T-VALUE	SLOPE
P4	102 - 141	0.717	3.185	0.235
Fp2	110 - 149	0.713	-3.156	-0.078
P4	110 - 149	0.808	4.107	0.209
Fp2	118 - 157	0.813	-4.165	-0.098
P4	118 - 157	0.772	3.684	0.172
Fp2	126 - 165	0.856	-4.870	-0.123
P4	126 - 165	0.734	3.325	0.146
Fp2	133 - 172	0.854	-4.829	-0.149
P4	133 - 172	0.736	3.336	0.129
Fp2	141 - 180	0.807	-4.083	-0.161
P4	141 - 180	0.718	3.192	0.109
Fp1	157 - 196	0.714	-3.163	-0.124
Fpz	157 - 196	0.713	-3.155	-0.087
Fp1	165 - 204	0.714	-3.159	-0.114
Fpz	165 - 204	0.775	-3.714	-0.090
Fpz	172 - 211	0.820	-4.269	-0.088
Fpz	180 - 219	0.821	-4.283	-0.081
Fpz	188 - 227	0.778	-3.746	-0.069
F3	454 - 493	0.708	3.115	0.066
Fpz	461 - 501	0.711	3.136	0.027
F3	461 - 501	0.763	3.589	0.071

FIGURE VI.1.-64

CASE	INDEX	ENERGY
Z2	26.42	549.79
Z4	26.61	550.11
Z5	39.84	572.95
Z3	43.57	570.46
Z6	44.62	566.88
Z1	62.77	581.89

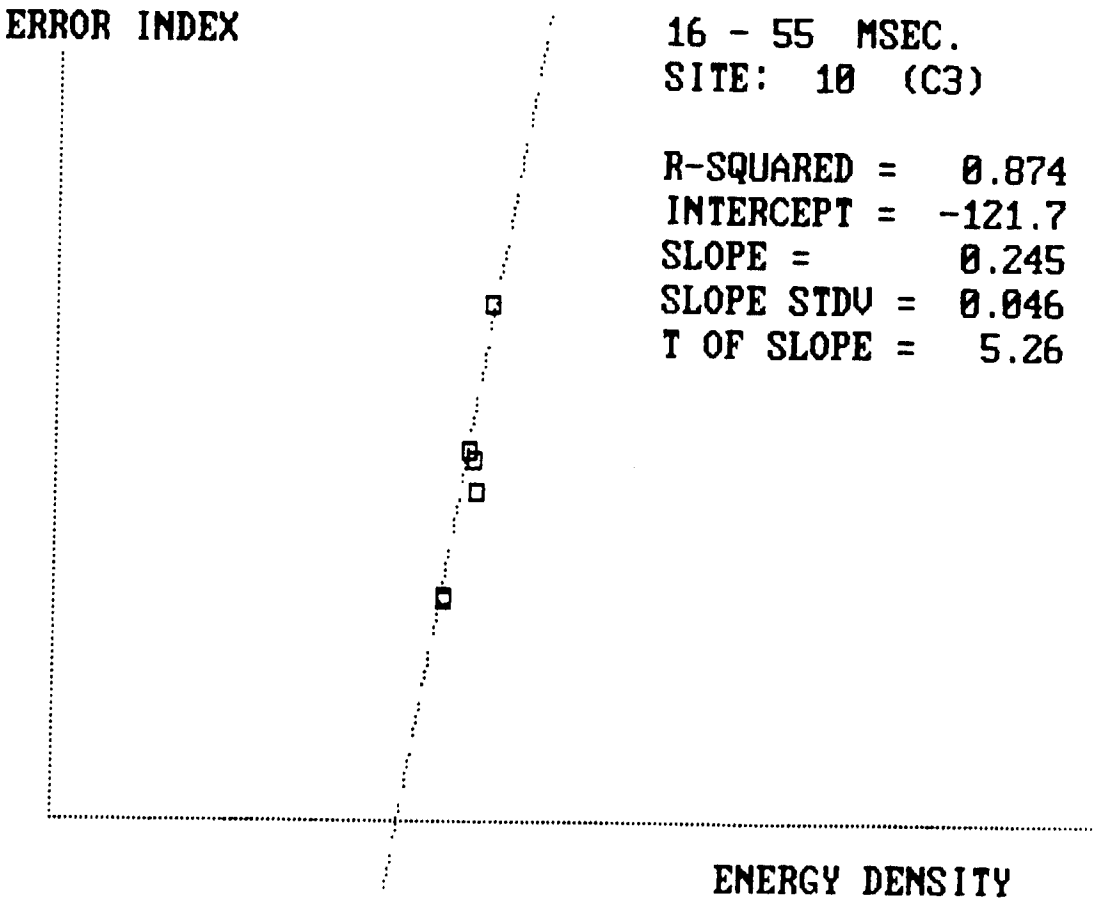

SUBJ 01 (6 ARITHEMTIC ERPs)

FIGURE VI.1.-65

CASE	INDEX	ENERGY
Z6	26.52	584.89
Z5	37.30	595.59
Z4	37.55	596.42
Z2	38.48	600.03
Z1	42.48	601.49
Z3	47.04	607.44

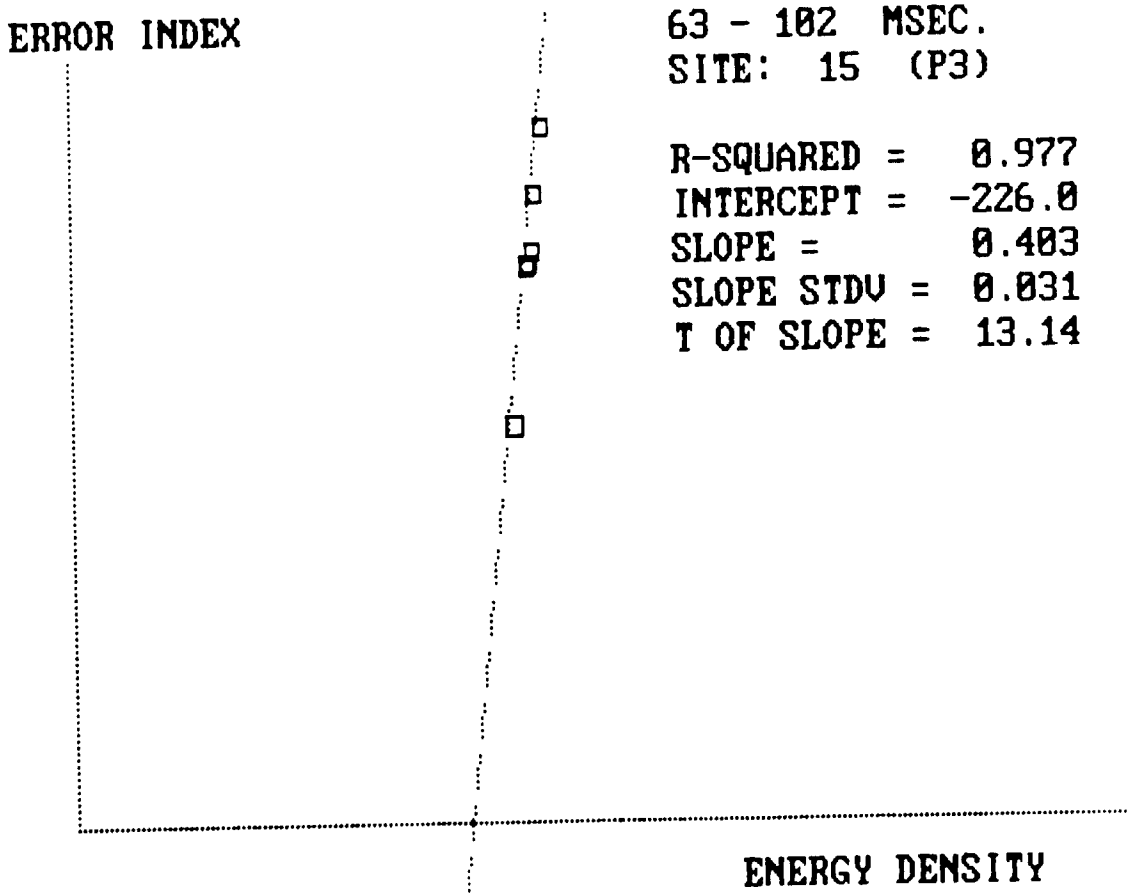

63 - 102 MSEC.
SITE: 15 (P3)

R-SQUARED = 0.977
INTERCEPT = -226.0
SLOPE = 0.403
SLOPE STDV = 0.031
T OF SLOPE = 13.14

SUBJ02 (6 ARITHMETIC ERPs)

FIGURE VI.1.-66

CASE	INDEX	ENERGY
Z4	19.41	523.69
Z2	20.22	540.16
Z3	20.68	542.15
Z6	21.15	547.93
Z1	21.23	546.00
Z5	26.89	600.51

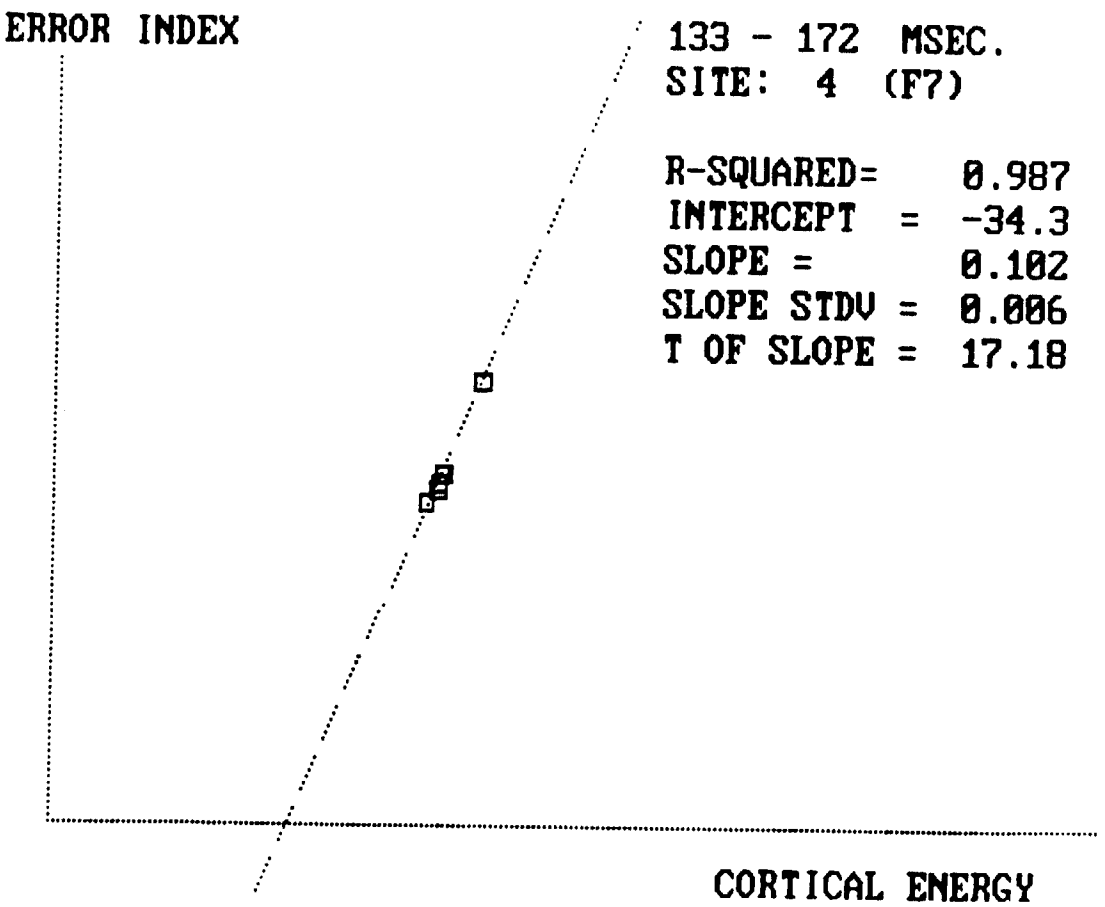

SUBJ04 (6 ARITHMETIC ERPs)

FIGURE VI.1.-67

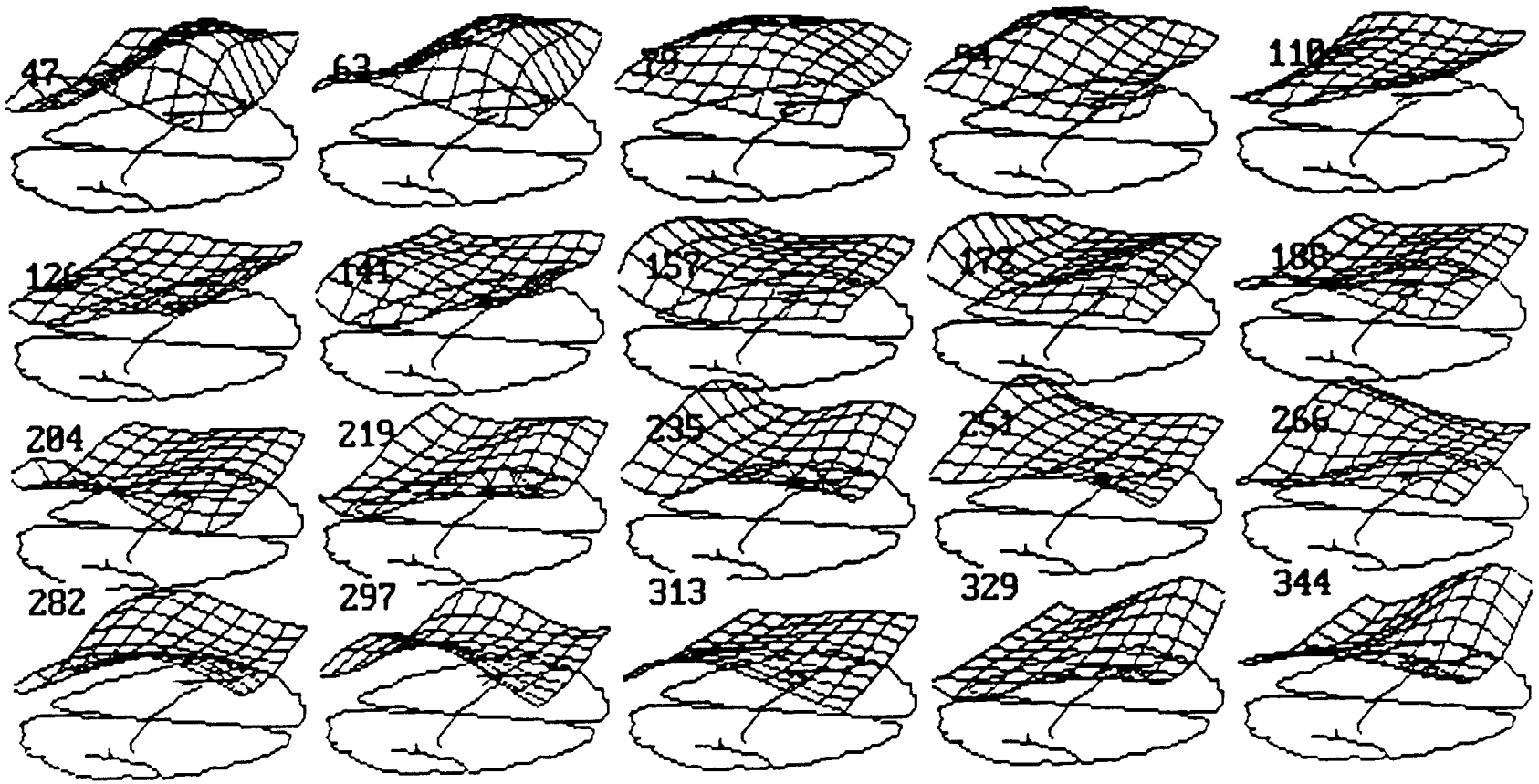

SUBJ 01 -- 6 ARITHEMTIC ERPs
R-SQUARE SURFACES: CORTICAL ENERGY VS TASK PERFORMANCE

FIGURE VI.1.-68

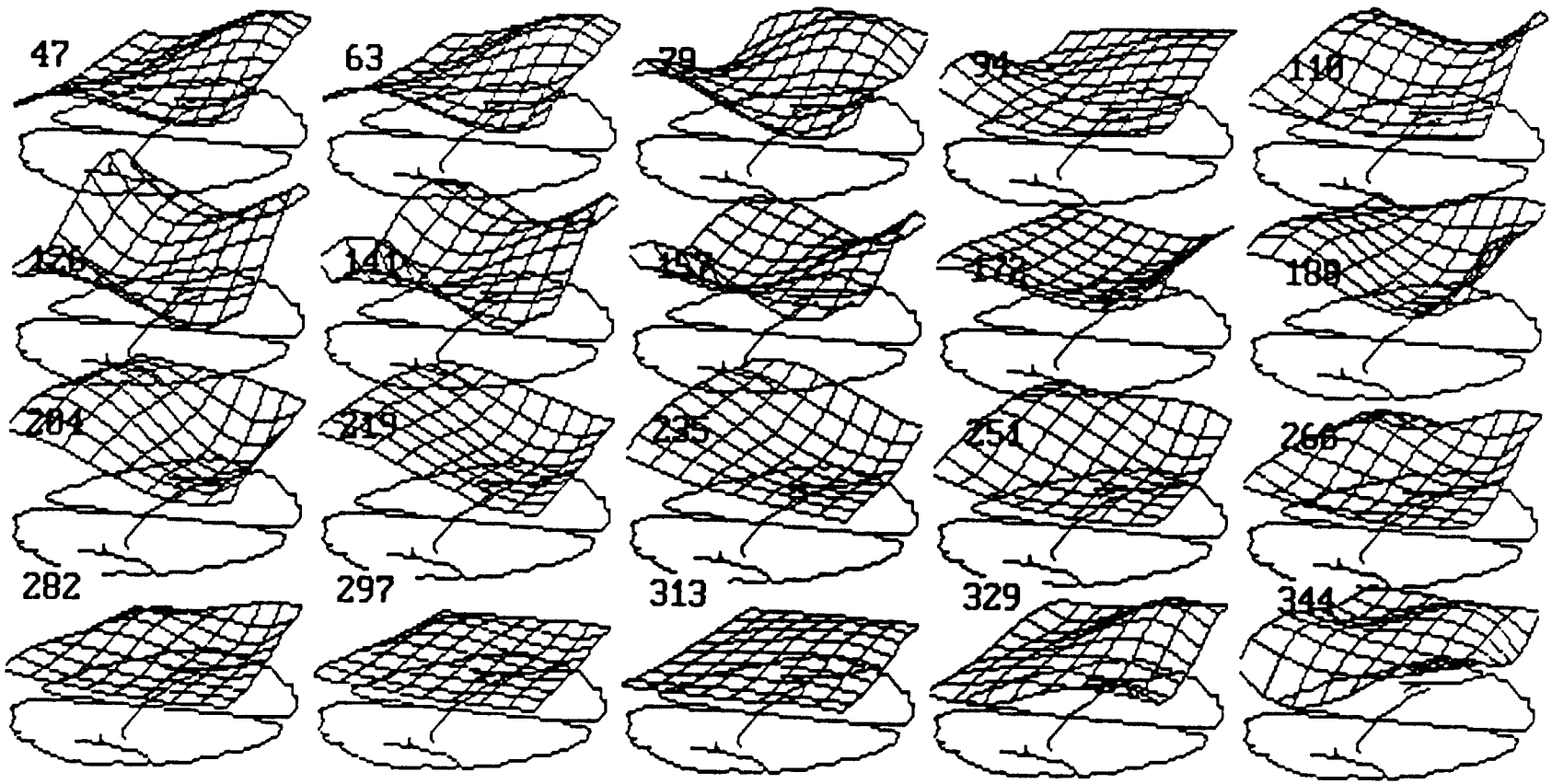

SUBJ 02 -- 6 ARITHMETIC ERPs
R-SQUARE SURFACES: CORTICAL ENERGY VS TASK PERFORMANCE

FIGURE VI.1.-69

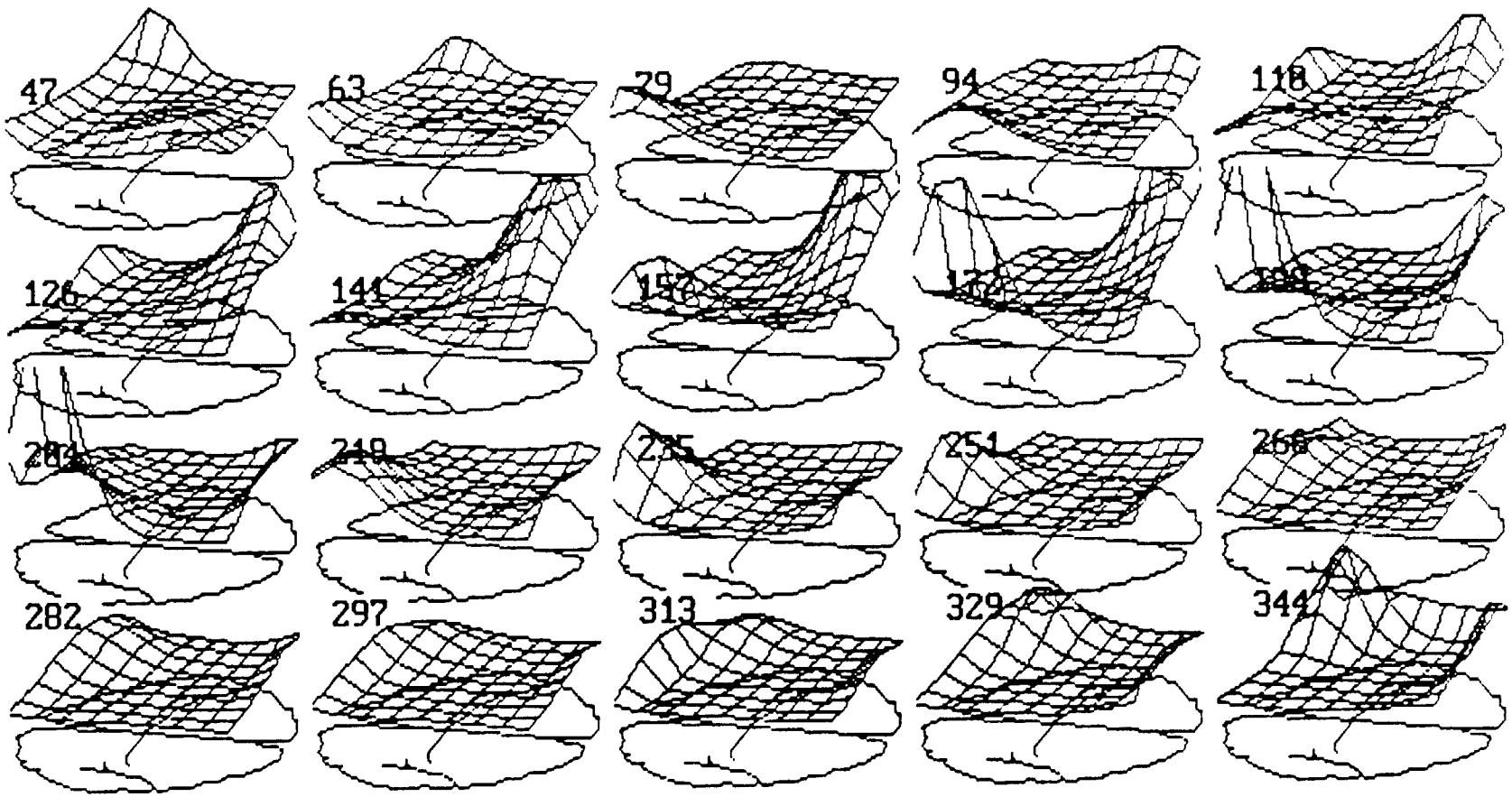

SUBJ 04 -- 6 ARITHMETIC ERPS
R-SQUARE SURFACES: CORTICAL ENERGY VS TASK PERFORMANCE

FIGURE VI.I.-70

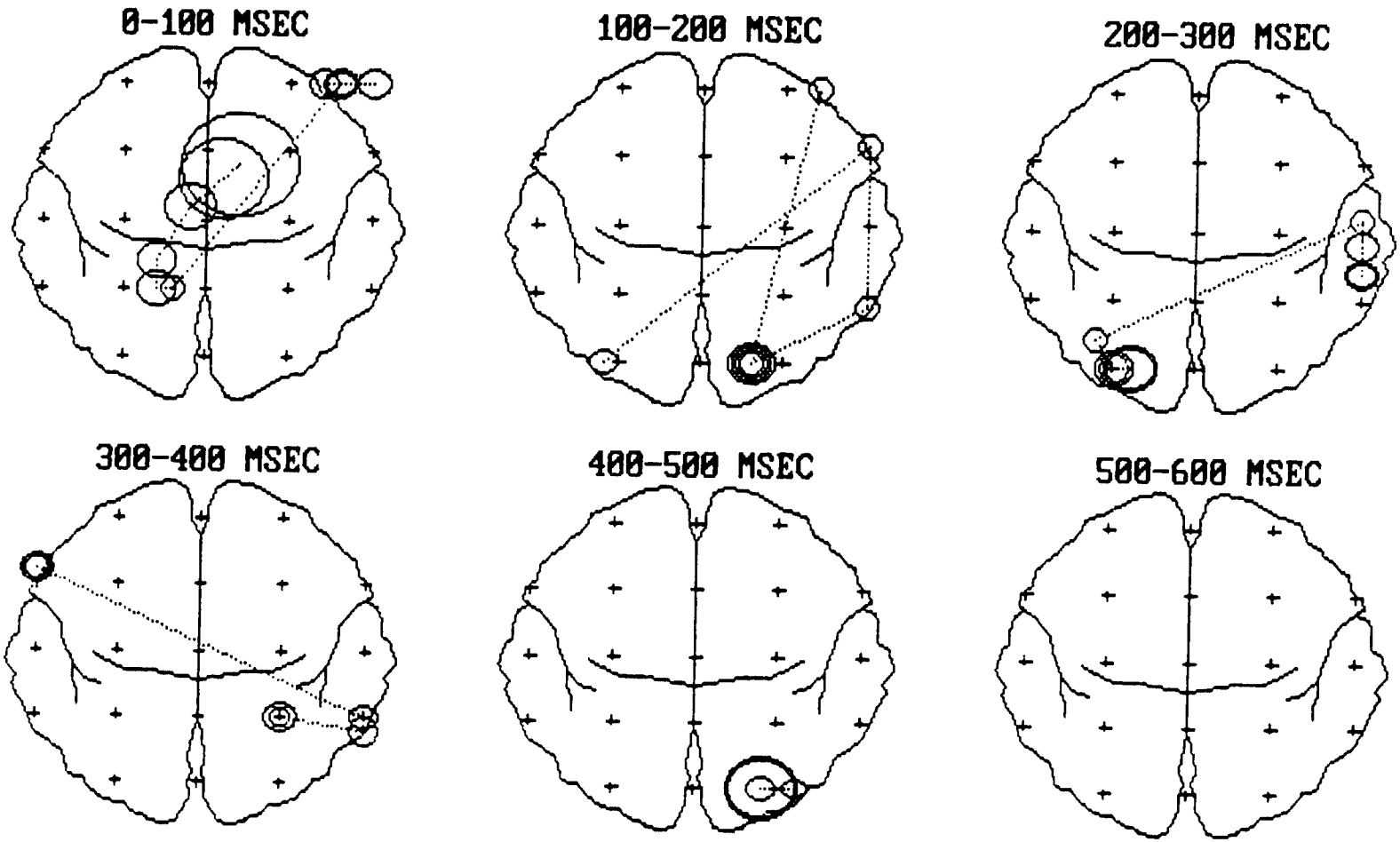

SUBJ 01 -- 6 ARITHMETIC ERPs
CORRELATION OF PERFORMANCE WITH CORTICAL ENERGY

FIGURE VI.1.-71

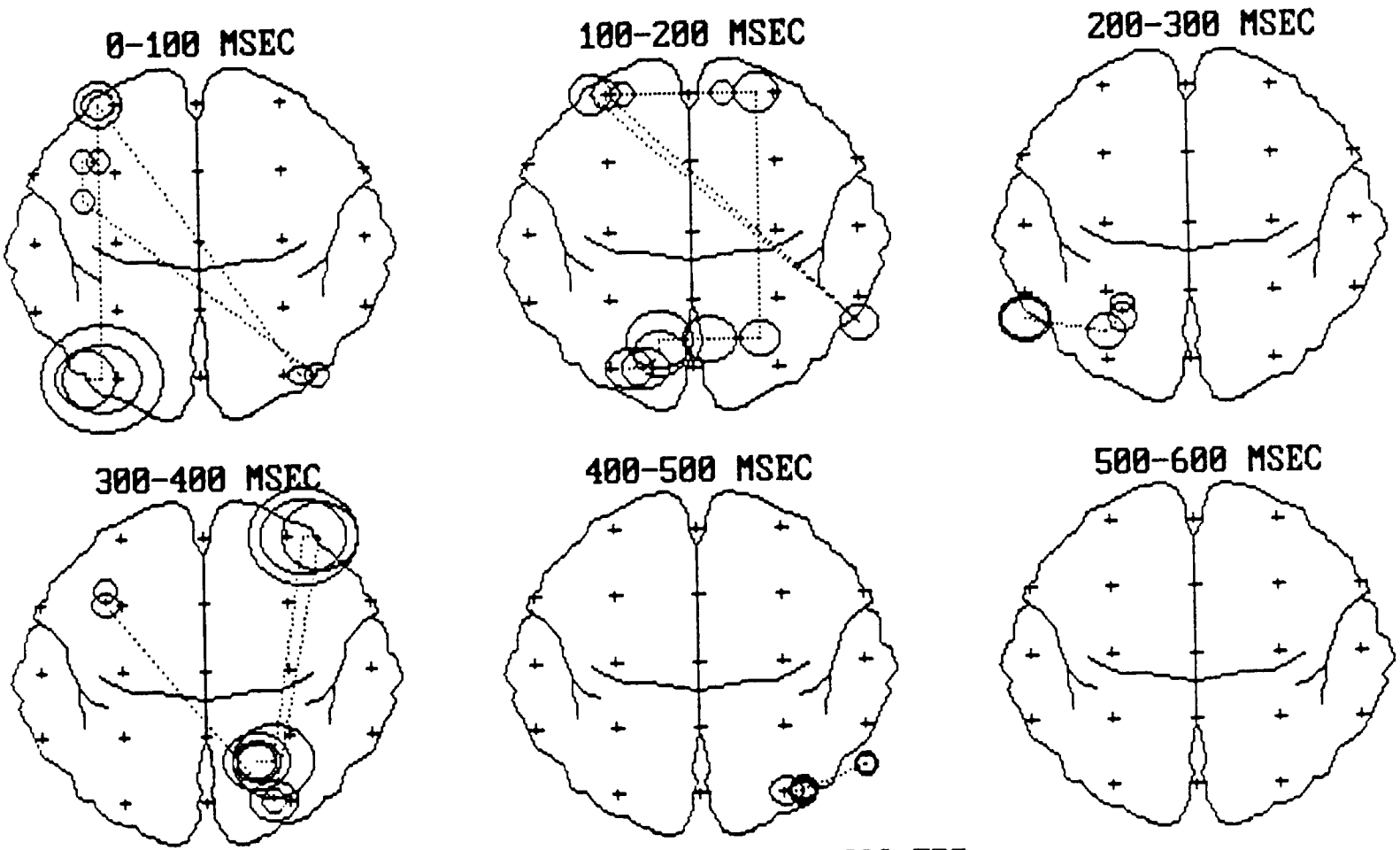

SUBJ 02 -- 6 ARITHMETIC ERPs
CORRELATION OF PERFORMANCE WITH CORTICAL ENERGY

FIGURE VI.1.-72

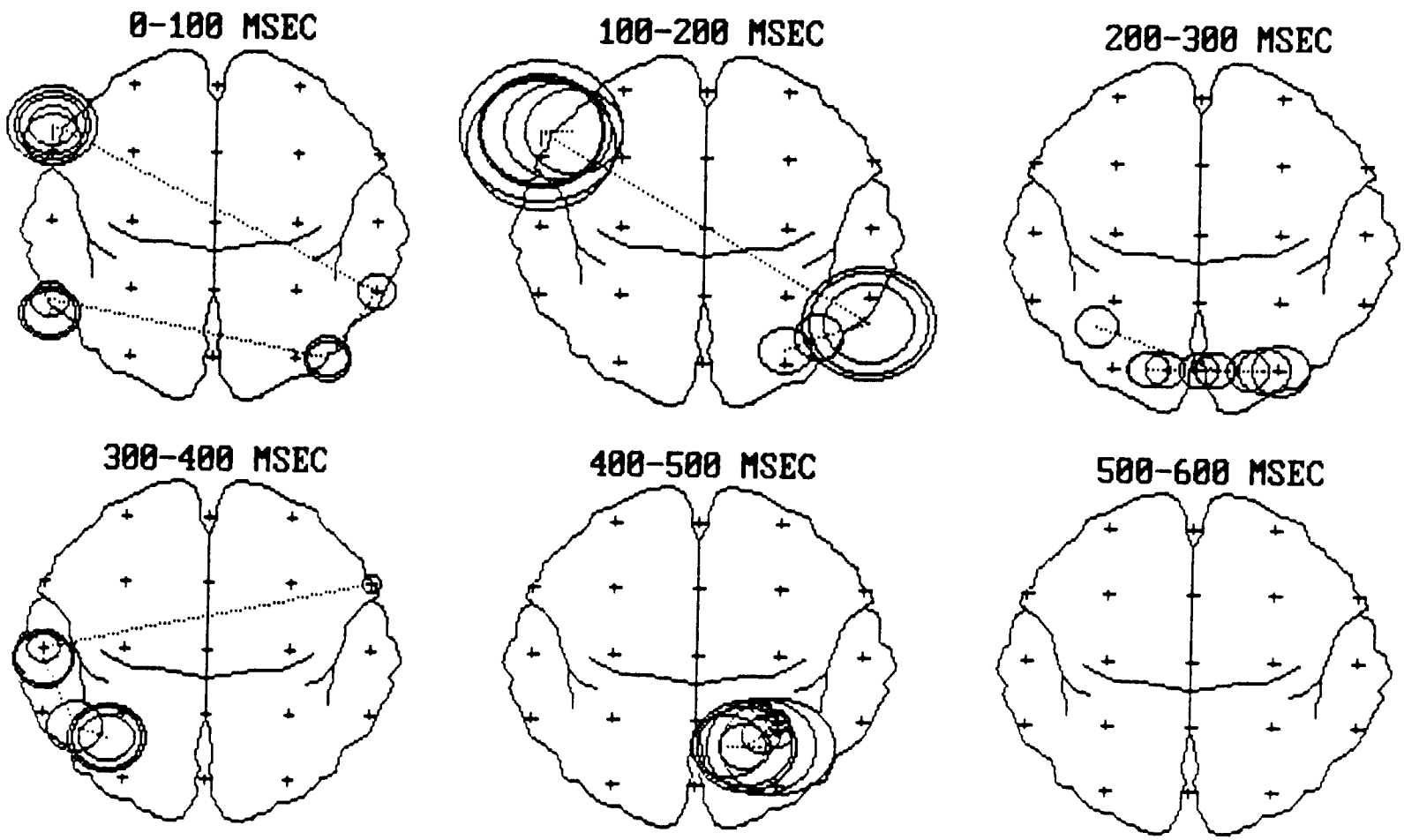

SUBJ 04 -- 6 ARITHMETIC ERPs
CORRELATION OF PERFORMANCE WITH CORTICAL ENERGY

FIGURE VI.1.-73

CASE	INDEX	ENERGY
Z6	7.06	446.61
Z5	10.78	442.14
Z4	11.82	419.69
Z3	15.44	398.62
Z2	16.97	400.90
Z1	36.96	319.67

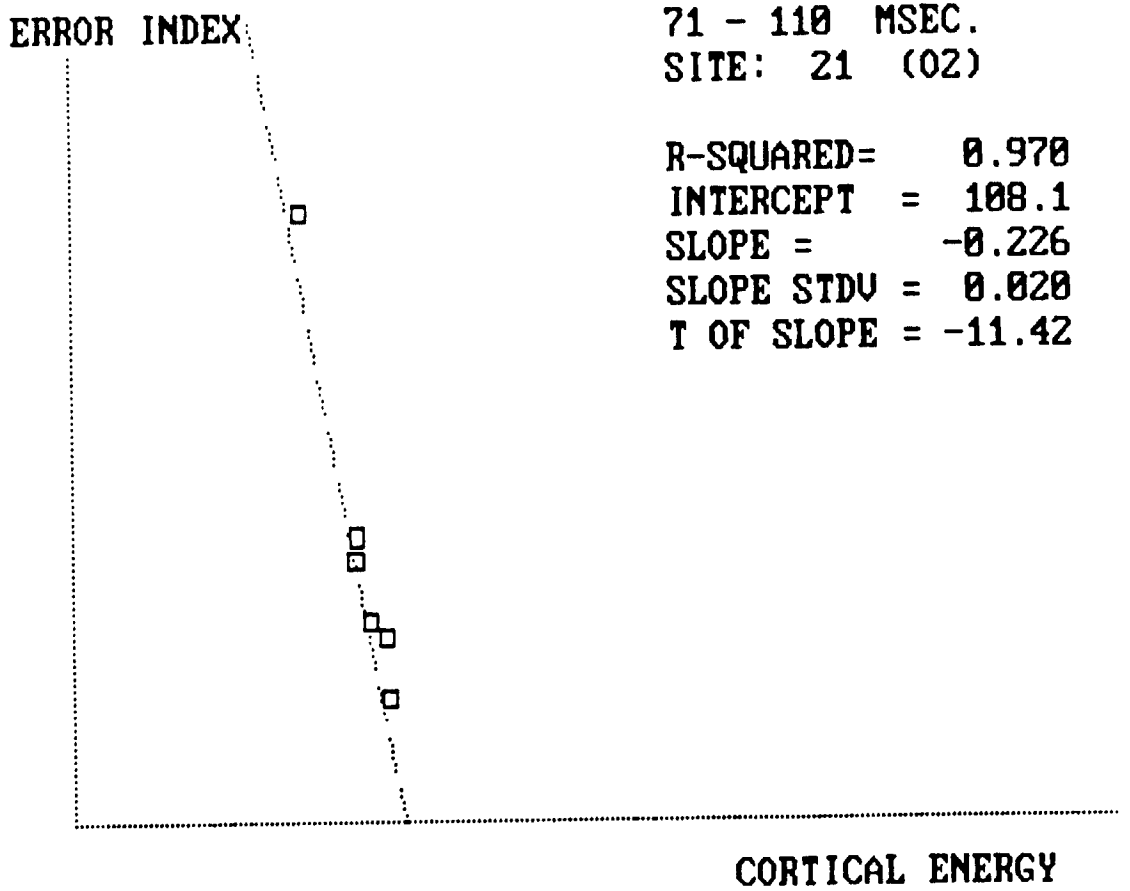

71 - 110 MSEC.
SITE: 21 (02)

R-SQUARED= 0.970
INTERCEPT = 108.1
SLOPE = -0.226
SLOPE STDV = 0.020
T OF SLOPE = -11.42

SUBJECT 01 LONGITUDINAL SERIES (6 WORDPAIR ERPs)

FIGURE VI.1.-74

CASE	INDEX	ENERGY
Z4	12.85	582.45
Z5	16.04	577.15
Z1	19.83	607.85
Z2	22.91	628.07
Z3	25.96	639.76
Z6	27.95	671.75

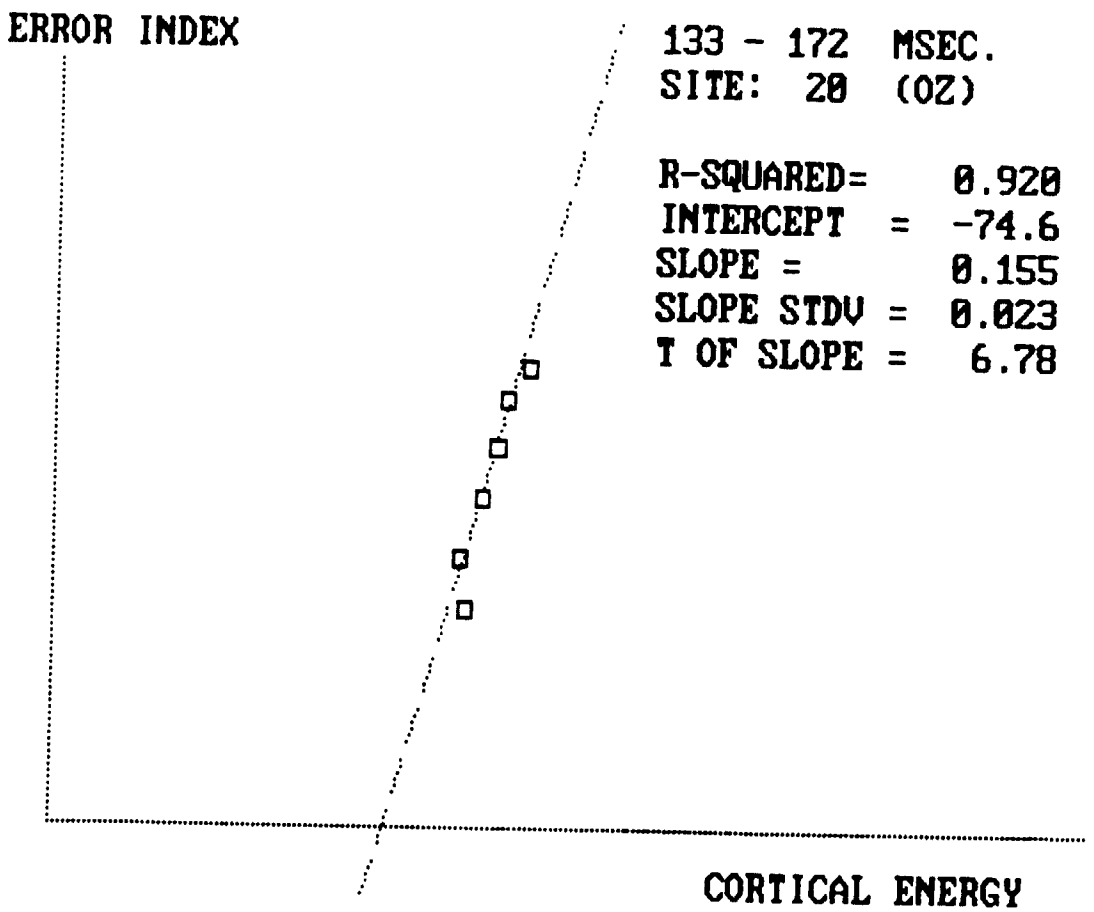

SUBJ02 (6 WORDPAIR ERPs)

FIGURE VI.1.-75

CASE	INDEX	ENERGY
Z5	1.70	522.85
Z2	1.87	494.64
Z4	2.13	513.51
Z3	8.72	477.95
Z6	13.73	424.36
Z1	14.05	457.30

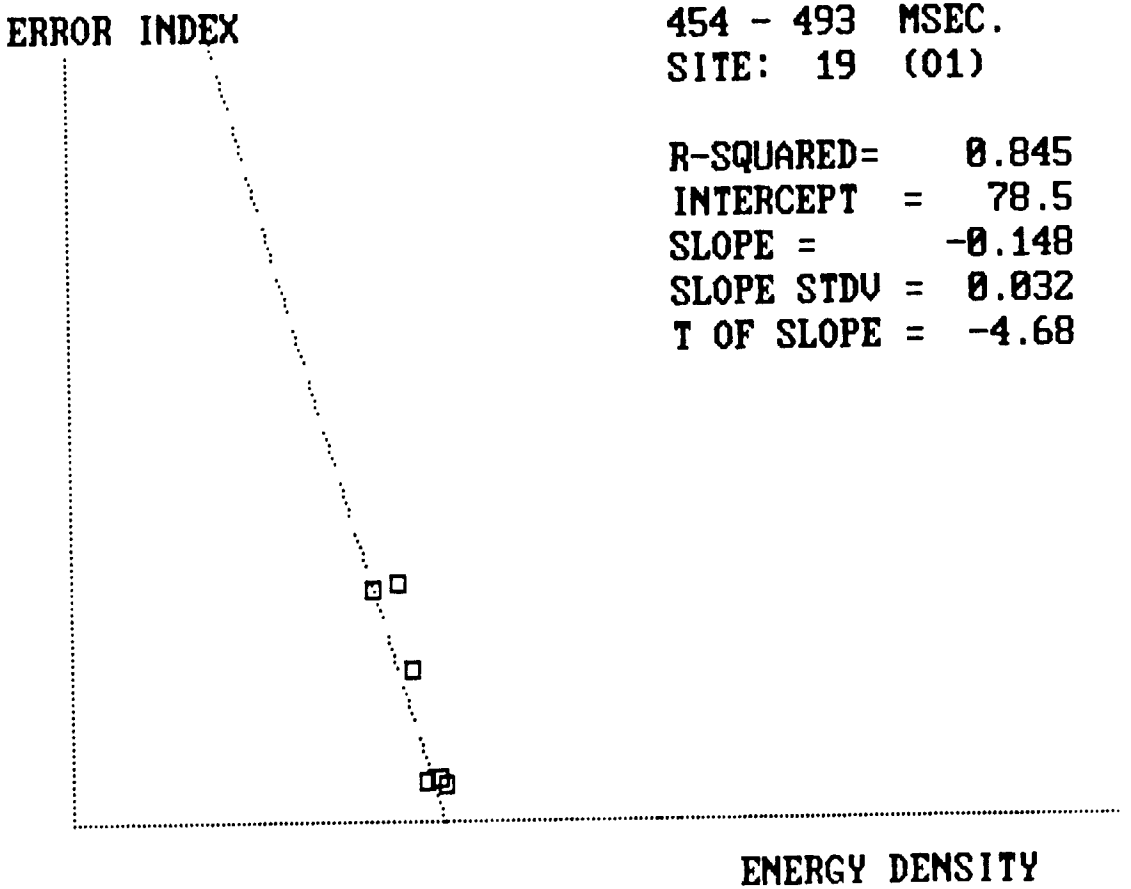

454 - 493 MSEC.
SITE: 19 (01)

R-SQUARED= 0.845
INTERCEPT = 78.5
SLOPE = -0.148
SLOPE STDV = 0.032
T OF SLOPE = -4.68

SUBJ04 (6 WORDPAIR ERPS)

FIGURE VI.1.-76

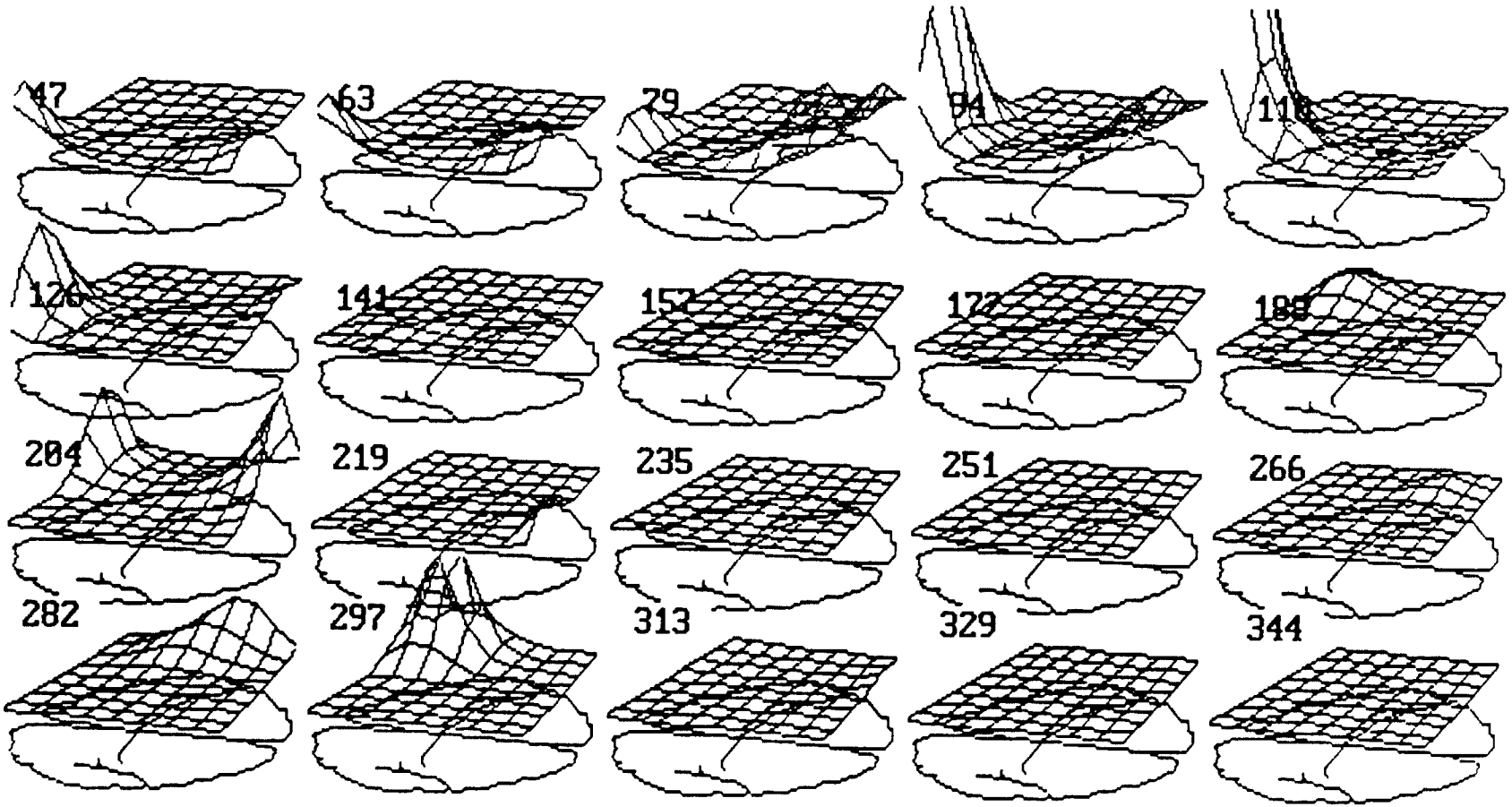

SUBJ 01 -- 6 WORDPAIR ERPS
R-SQUARE SURFACES: CORTICAL ENERGY VS TASK PERFORMANCE

FIGURE VI.1.-77

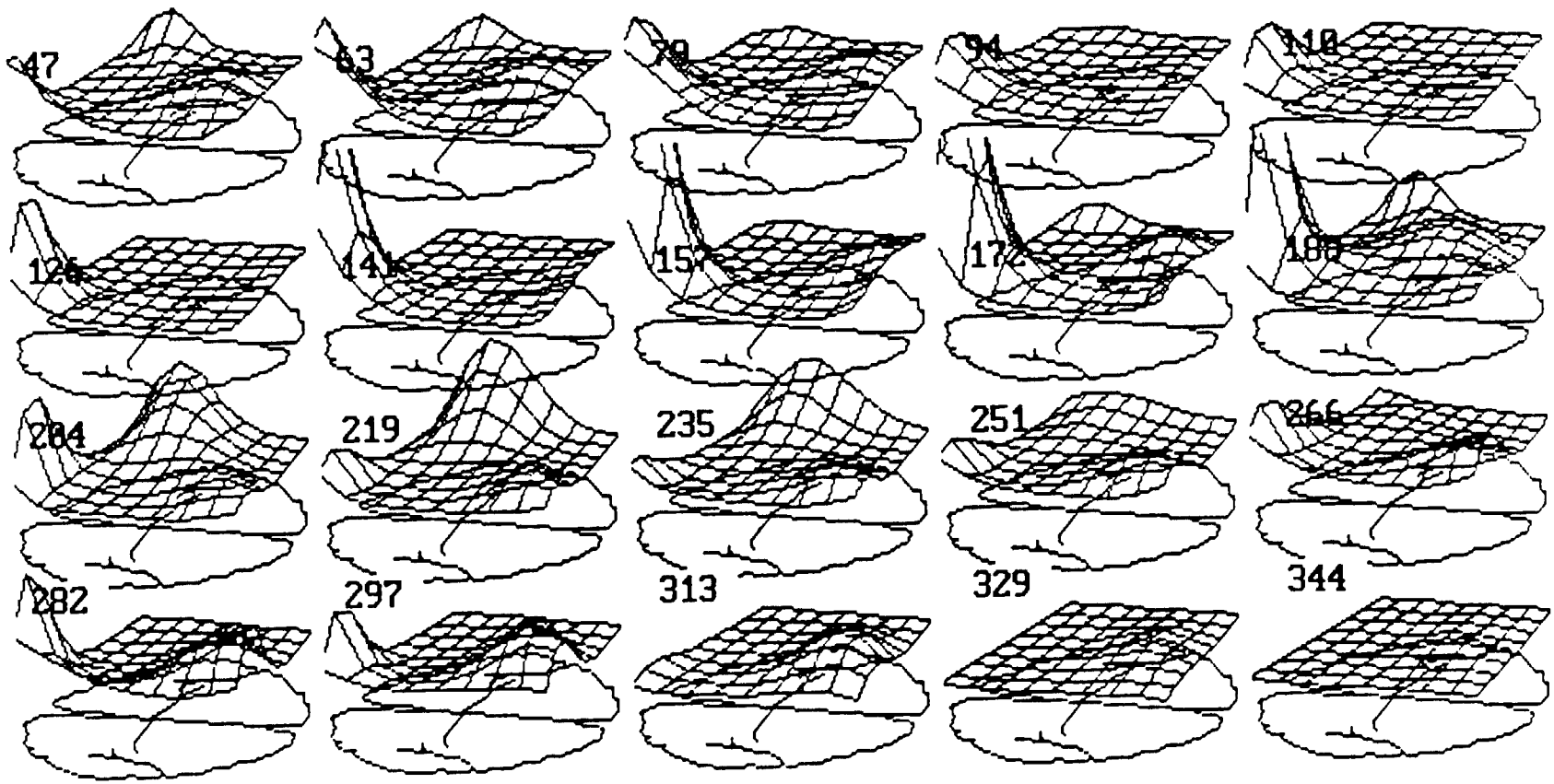

SUBJ 02 -- 6 WORDPAIR ERPS
R-SQUARE SURFACES: CORTICAL ENERGY VS TASK PERFORMANCE

FIGURE VI.1.-78

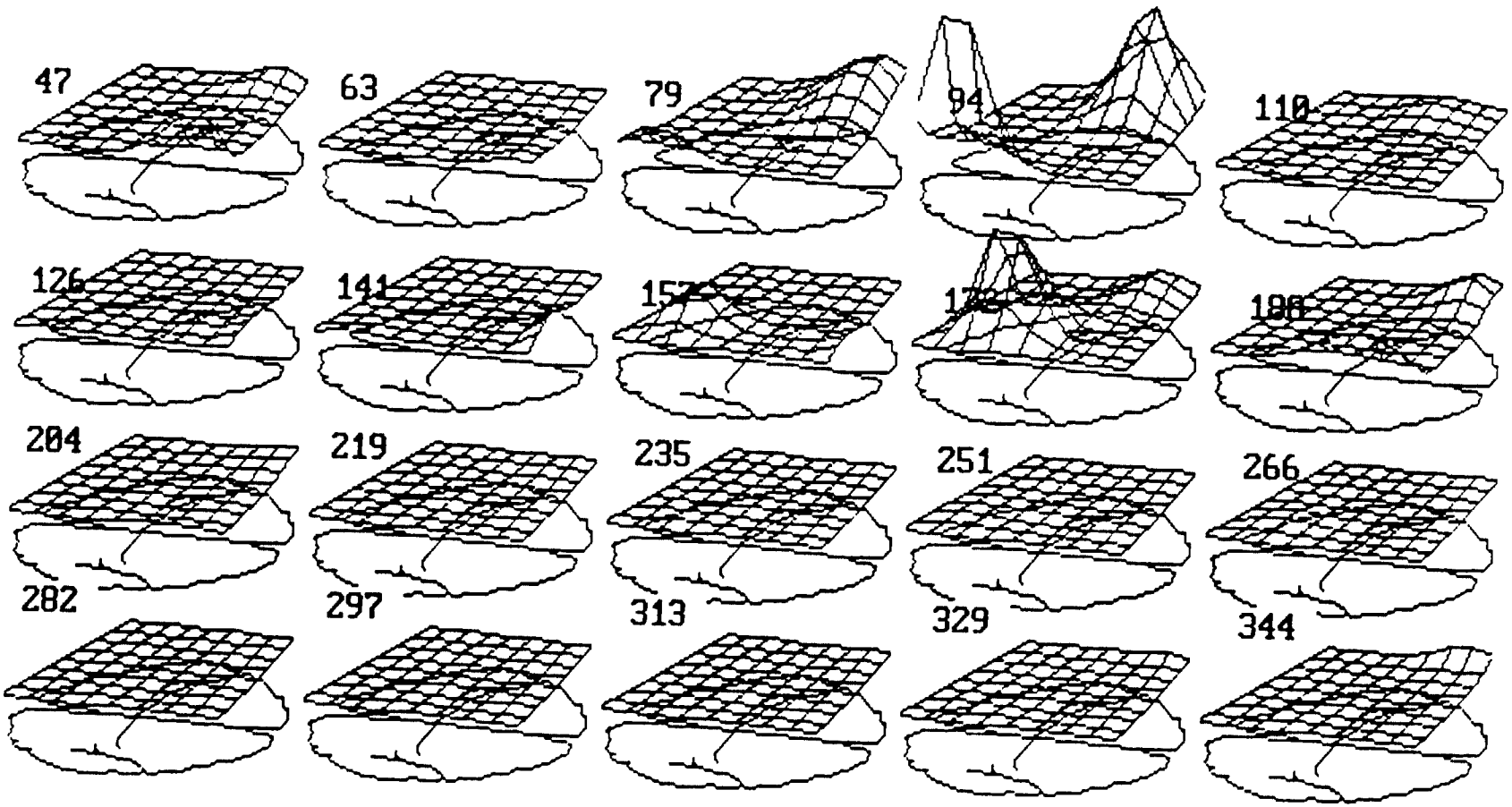

SUBJ 04 -- 6 WORDPAIR ERPS
R-SQUARE SURFACES: CORTICAL ENERGY VS TASK PERFORMANCE

FIGURE VI.1.-79

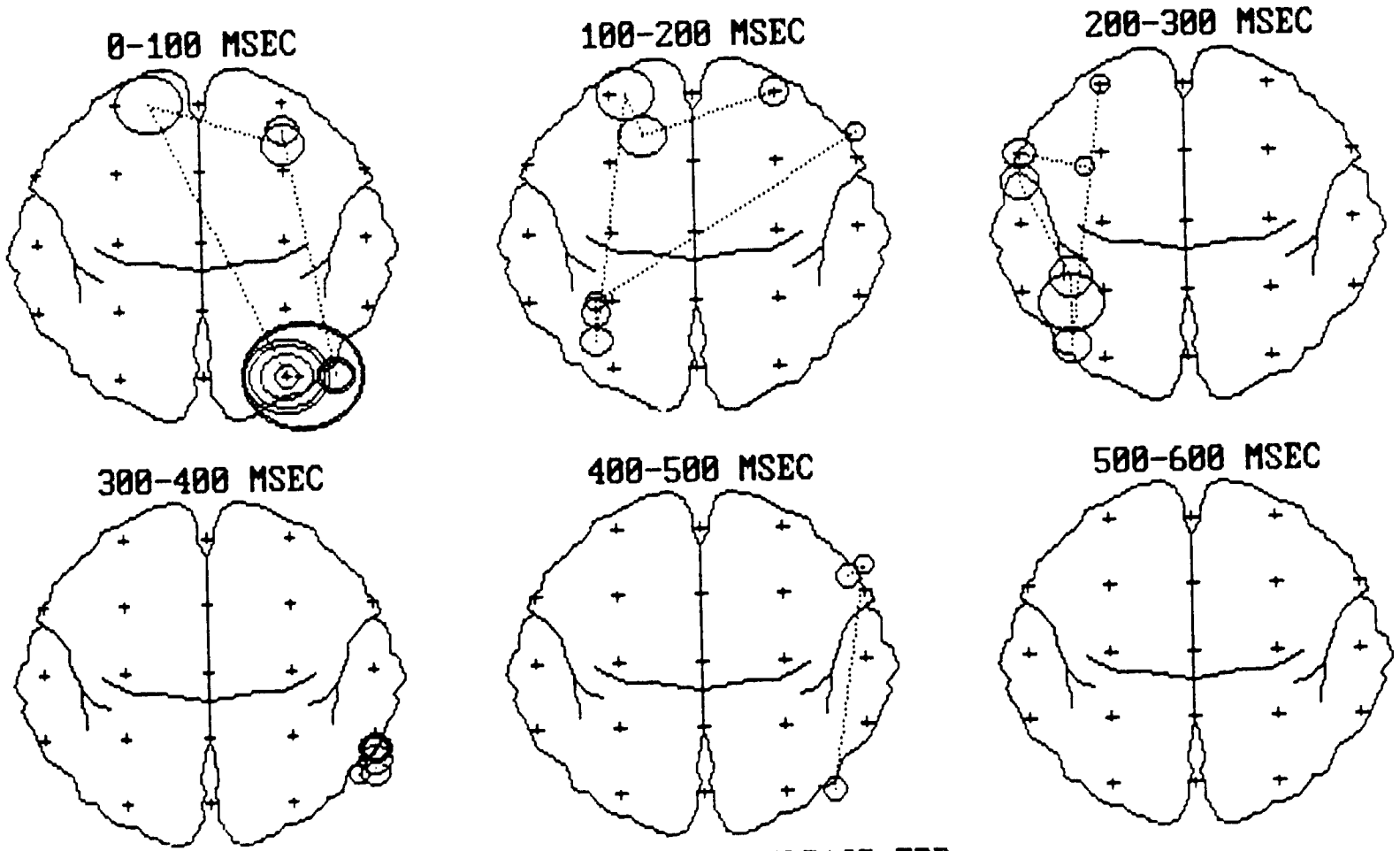

SUBJ 01 -- 6 WORDPAIR ERPs
CORRELATION OF PERFORMANCE WITH CORTICAL ENERGY

FIGURE VI.1.-80

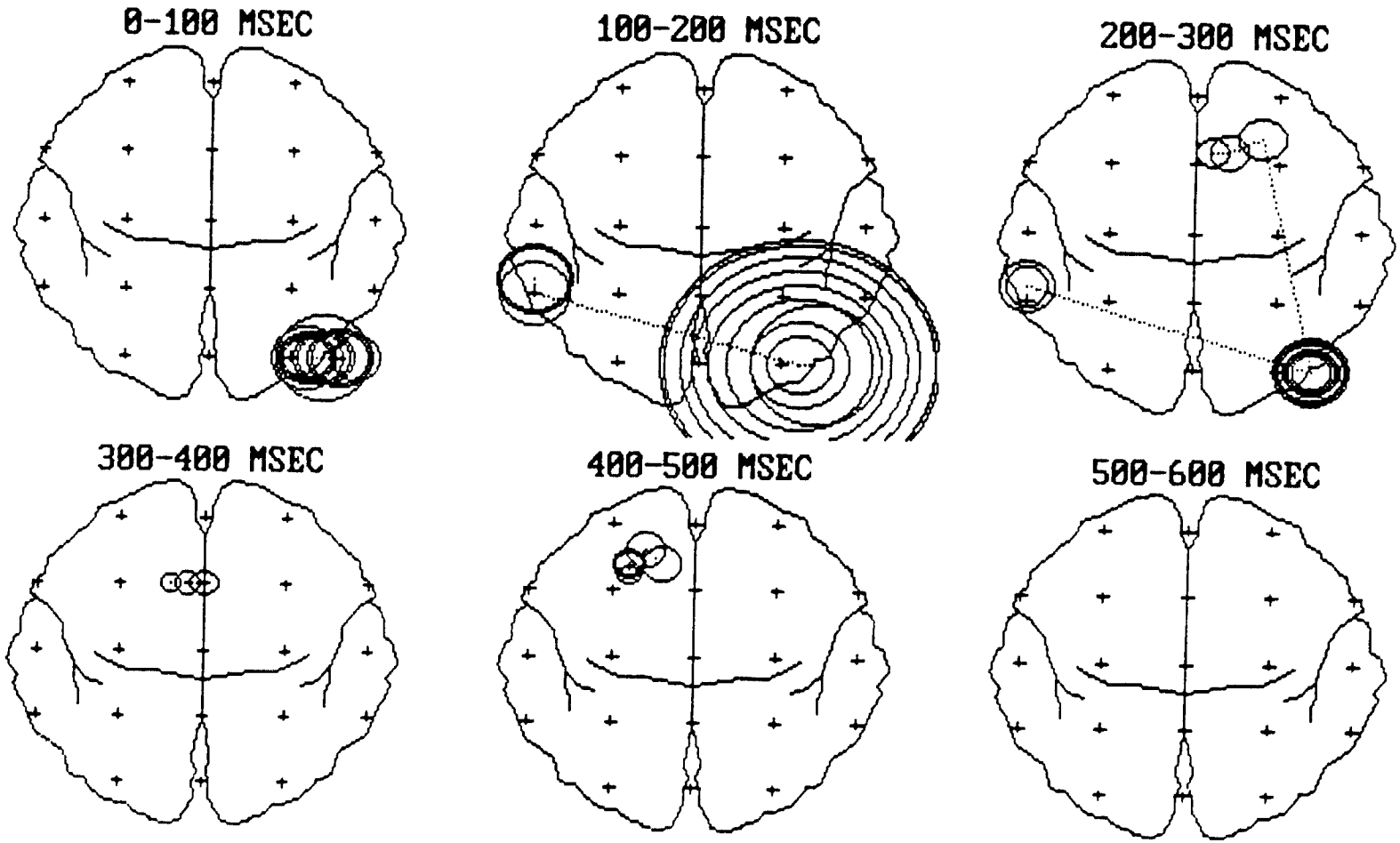

SUBJ 02 -- 6 WORDPAIR ERPs
CORRELATION OF PERFORMANCE WITH CORTICAL ENERGY

FIGURE VI.1.-81

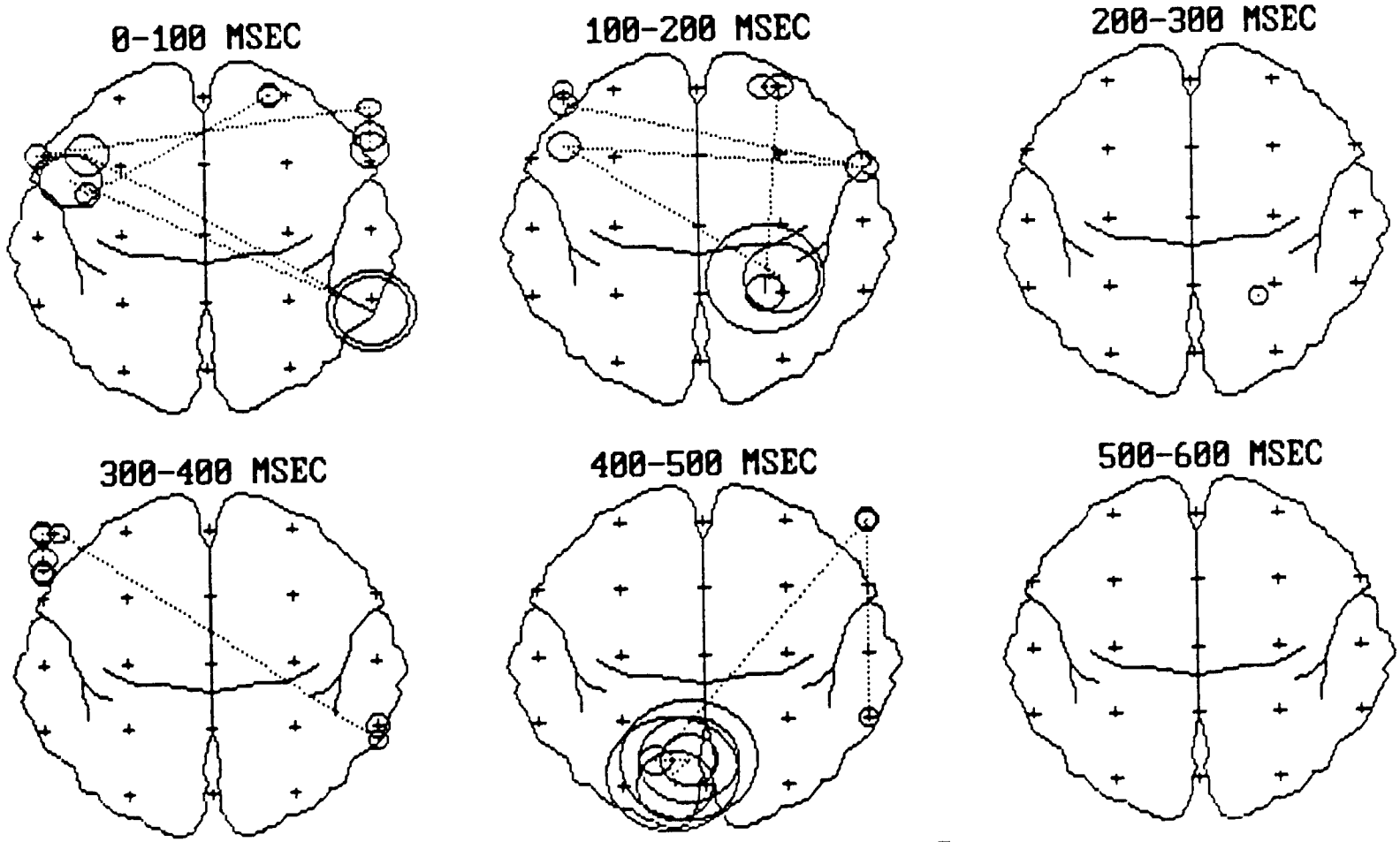

SUBJ 04 -- 6 WORDPAIR ERPs
CORRELATION OF PERFORMANCE WITH CORTICAL ENERGY

FIGURE VI.1.-82

CASE	INDEX	ENERGY
Z6	8.35	405.54
Z1	8.92	403.13
Z2	9.41	414.78
Z4	11.41	405.65
Z5	25.80	458.92
Z3	35.60	487.21

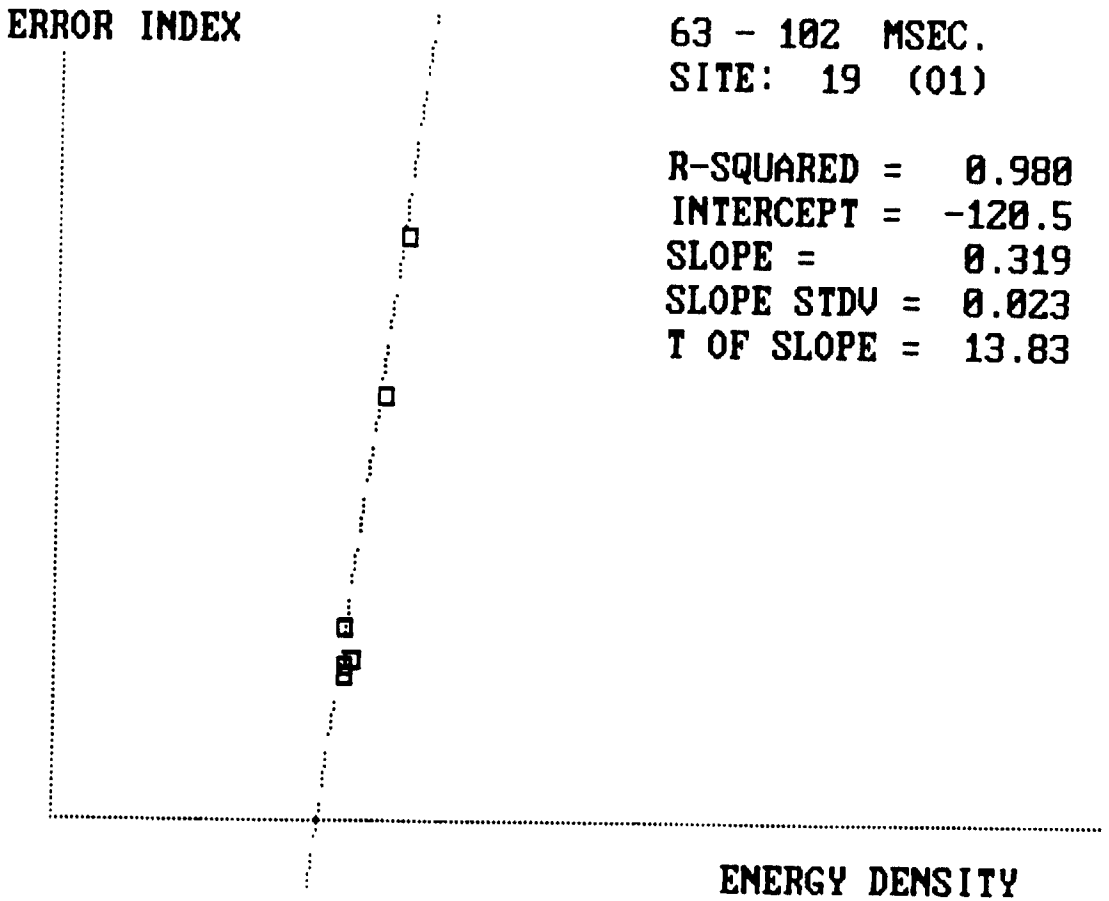

63 - 102 MSEC.
SITE: 19 (01)

R-SQUARED = 0.980
INTERCEPT = -120.5
SLOPE = 0.319
SLOPE STDV = 0.023
T OF SLOPE = 13.83

SUBJECT 01 (6 SPATIAL ERPS)

FIGURE VI.1.-83

CASE	INDEX	ENERGY
Z5	55.61	556.83
Z4	65.96	553.37
Z6	77.47	549.75
Z1	80.70	550.55
Z2	82.05	546.68
Z3	101.70	545.14

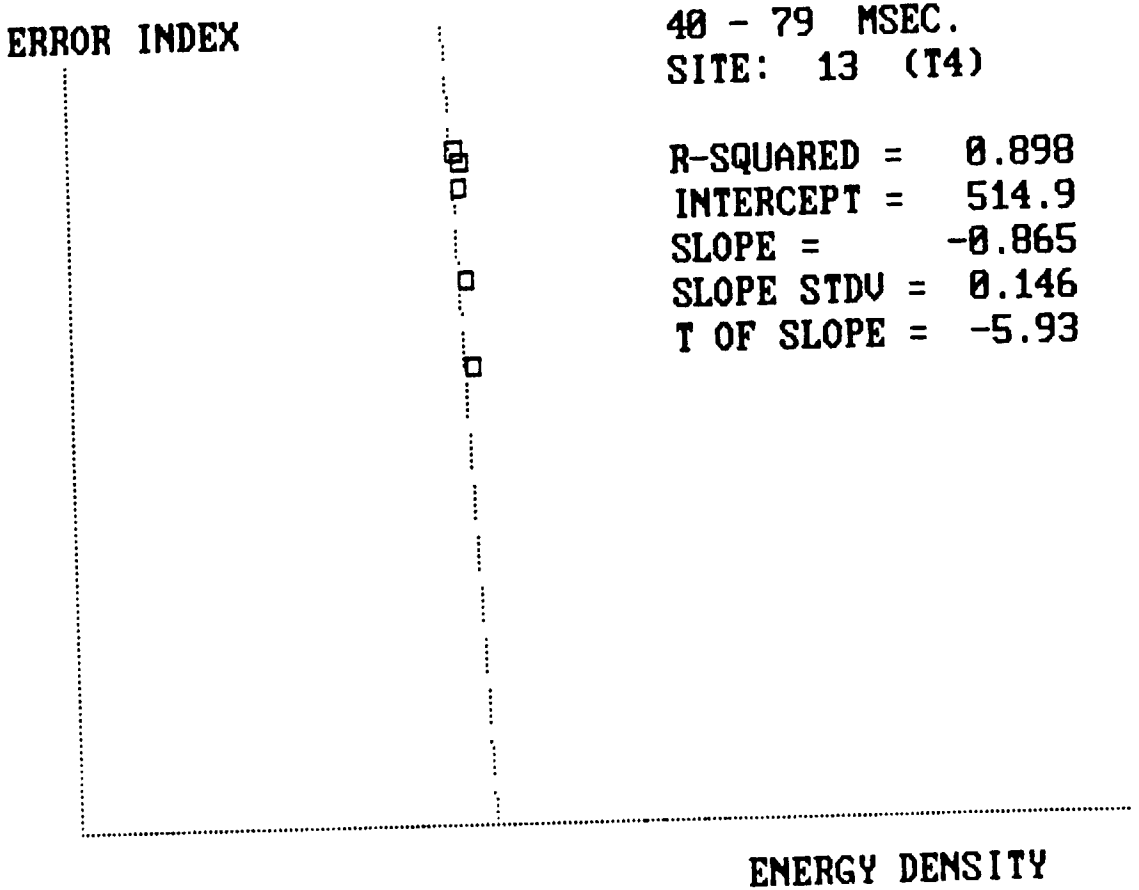

40 - 79 MSEC.
SITE: 13 (T4)

R-SQUARED = 0.898
INTERCEPT = 514.9
SLOPE = -0.865
SLOPE STDV = 0.146
T OF SLOPE = -5.93

SUBJ 02 (6 SPATIAL ERPs)

FIGURE VI.1.-84

CASE	INDEX	ENERGY
Z2	3.97	575.64
Z3	4.08	572.86
Z4	5.38	559.75
Z1	5.77	556.05
Z6	6.53	561.07
Z5	7.37	549.11

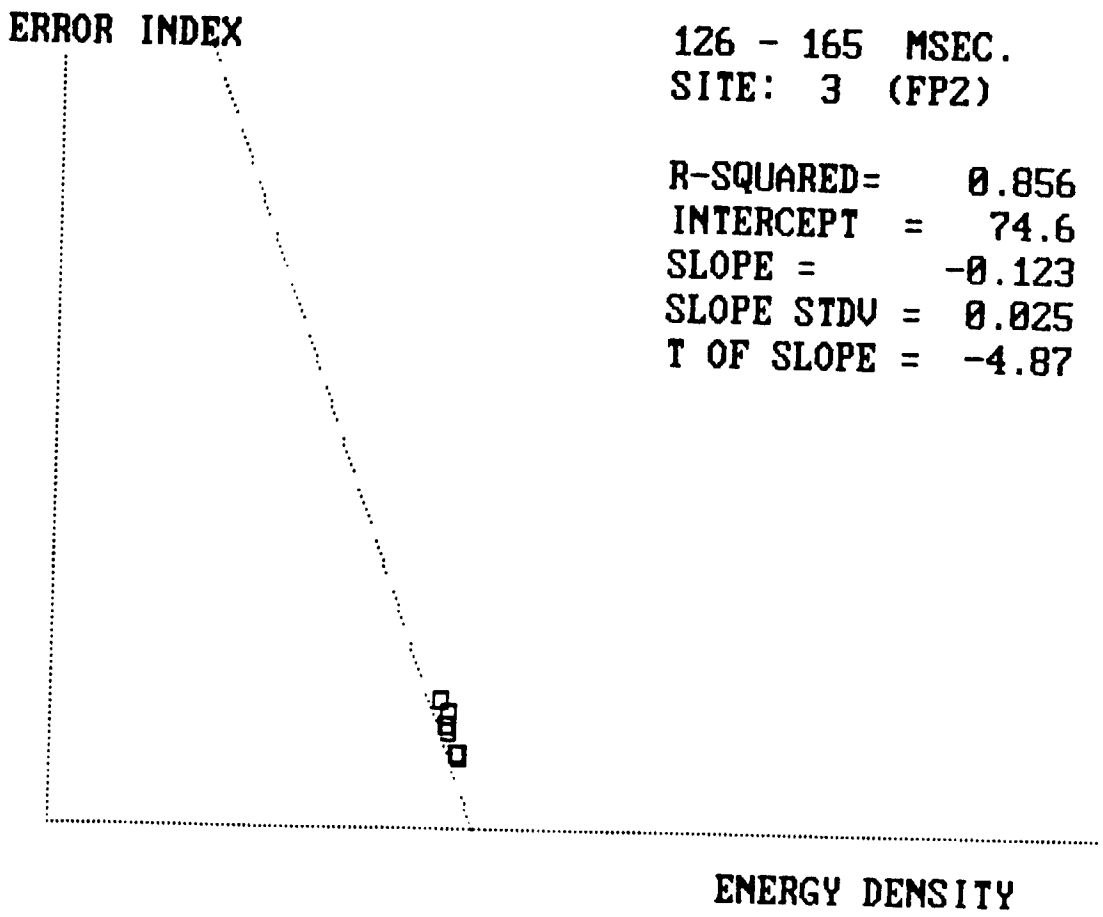

126 - 165 MSEC.
SITE: 3 (FP2)

R-SQUARED= 0.856
INTERCEPT = 74.6
SLOPE = -0.123
SLOPE STDV = 0.025
T OF SLOPE = -4.87

SUBJ04 (6 SPATIAL ERPS)

FIGURE VI.1.-85

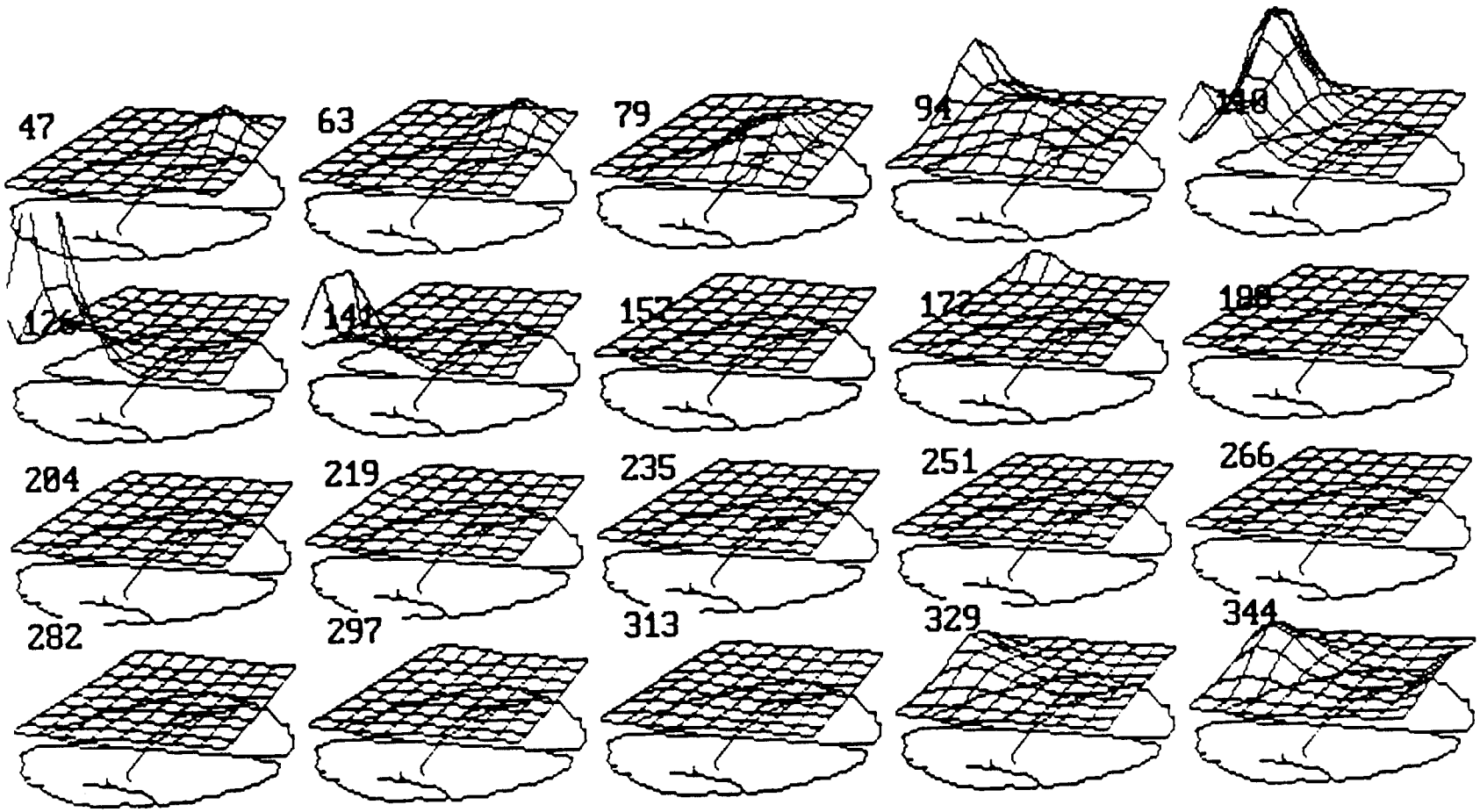

SUBJ 01 -- 6 SPATIAL ERPS
R-SQUARE SURFACES: CORTICAL ENERGY VS TASK PERFORMANCE

FIGURE VI.1.-86

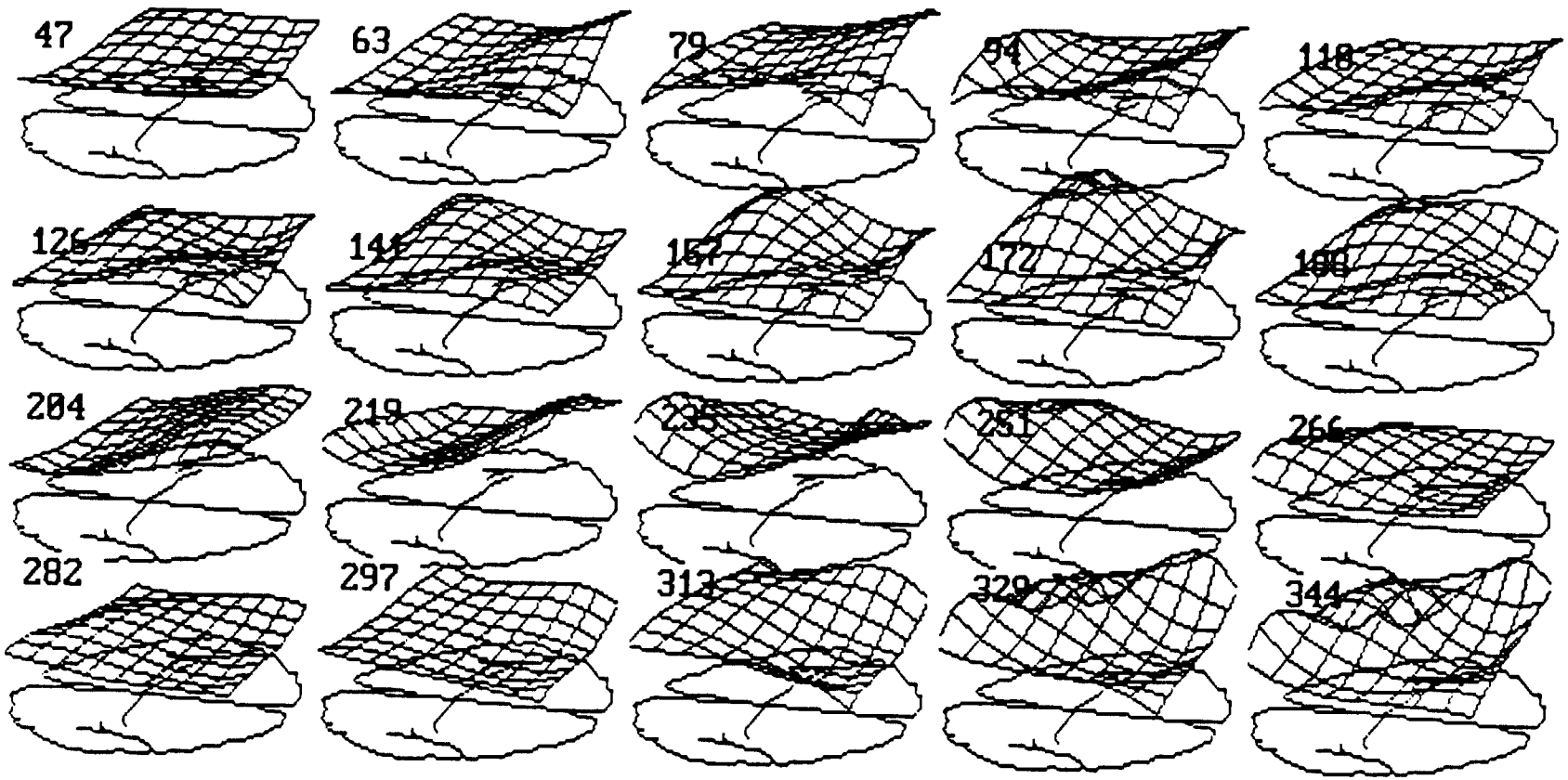

SUBJ 02 -- 6 SPATIAL ERPs
R-SQUARE SURFACES: CORTICAL ENERGY VS TASK PERFORMANCE

FIGURE VI.1.-87

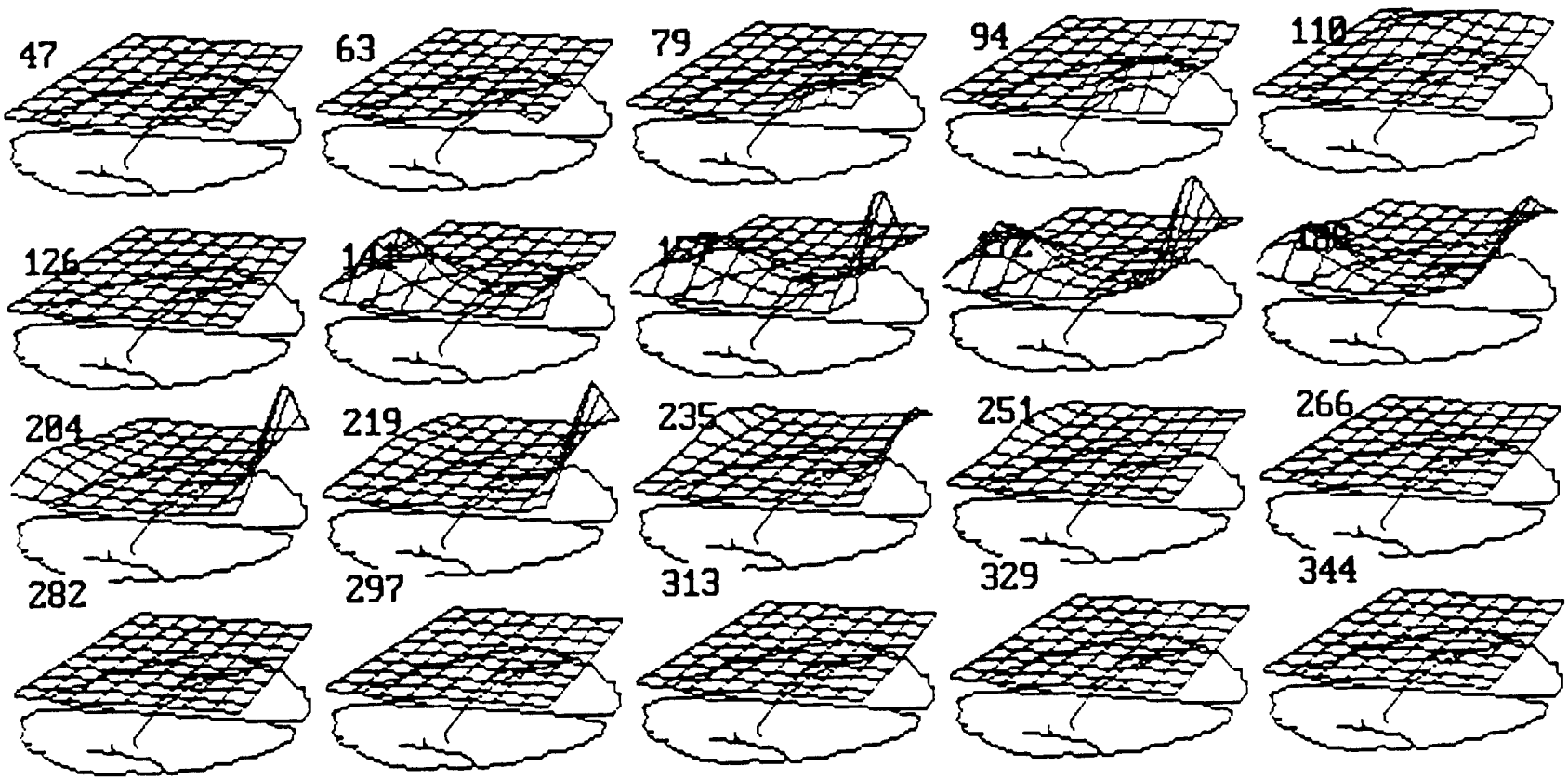

SUBJ 04 -- 6 SPATIAL ERPS
R-SQUARE SURFACES: CORTICAL ENERGY VS TASK PERFORMANCE

FIGURE VI.1.-88

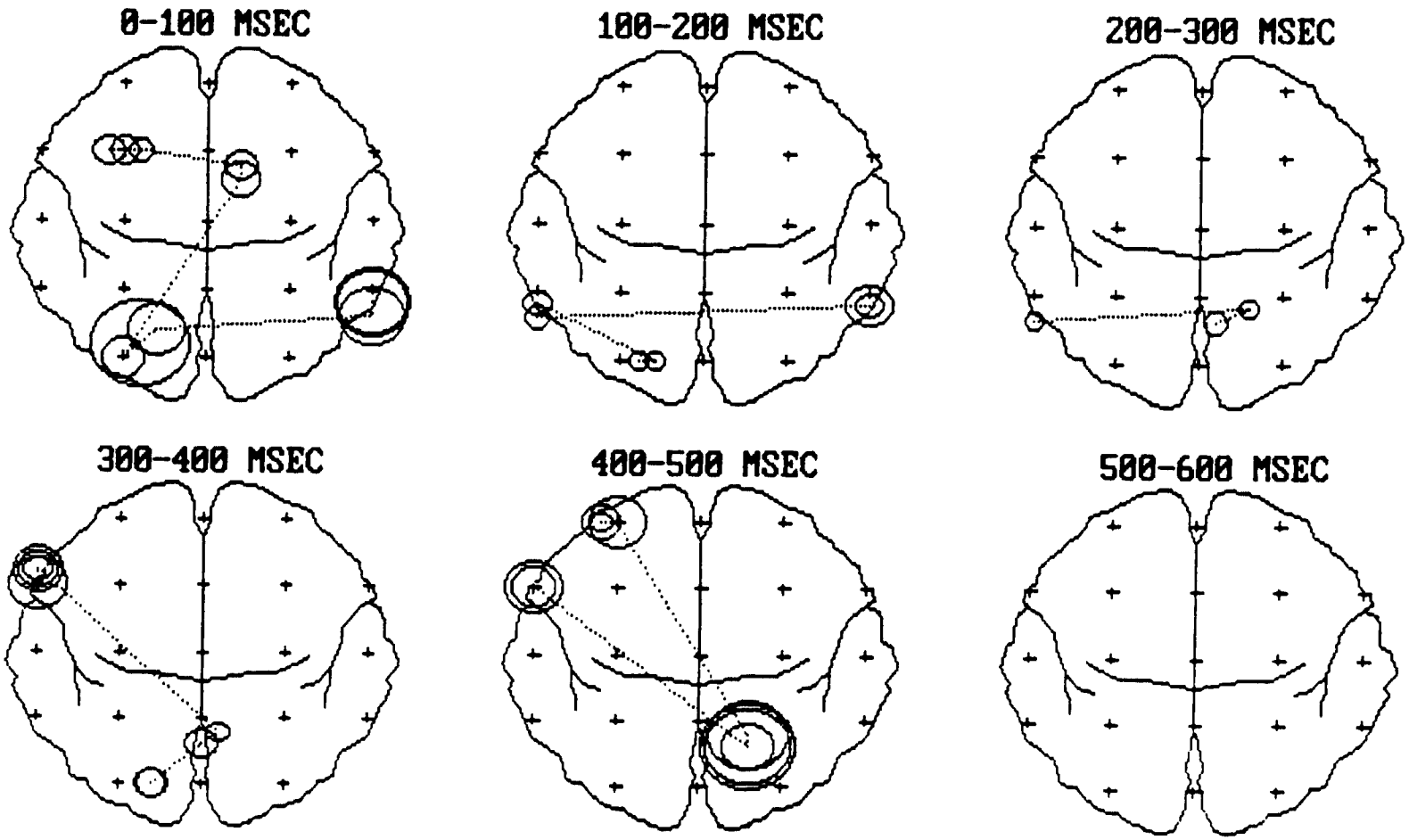

SUBJ 01 — 6 SPATIAL ERPs
CORRELATION OF PERFORMANCE WITH CORTICAL ENERGY

FIGURE VI.1.-89

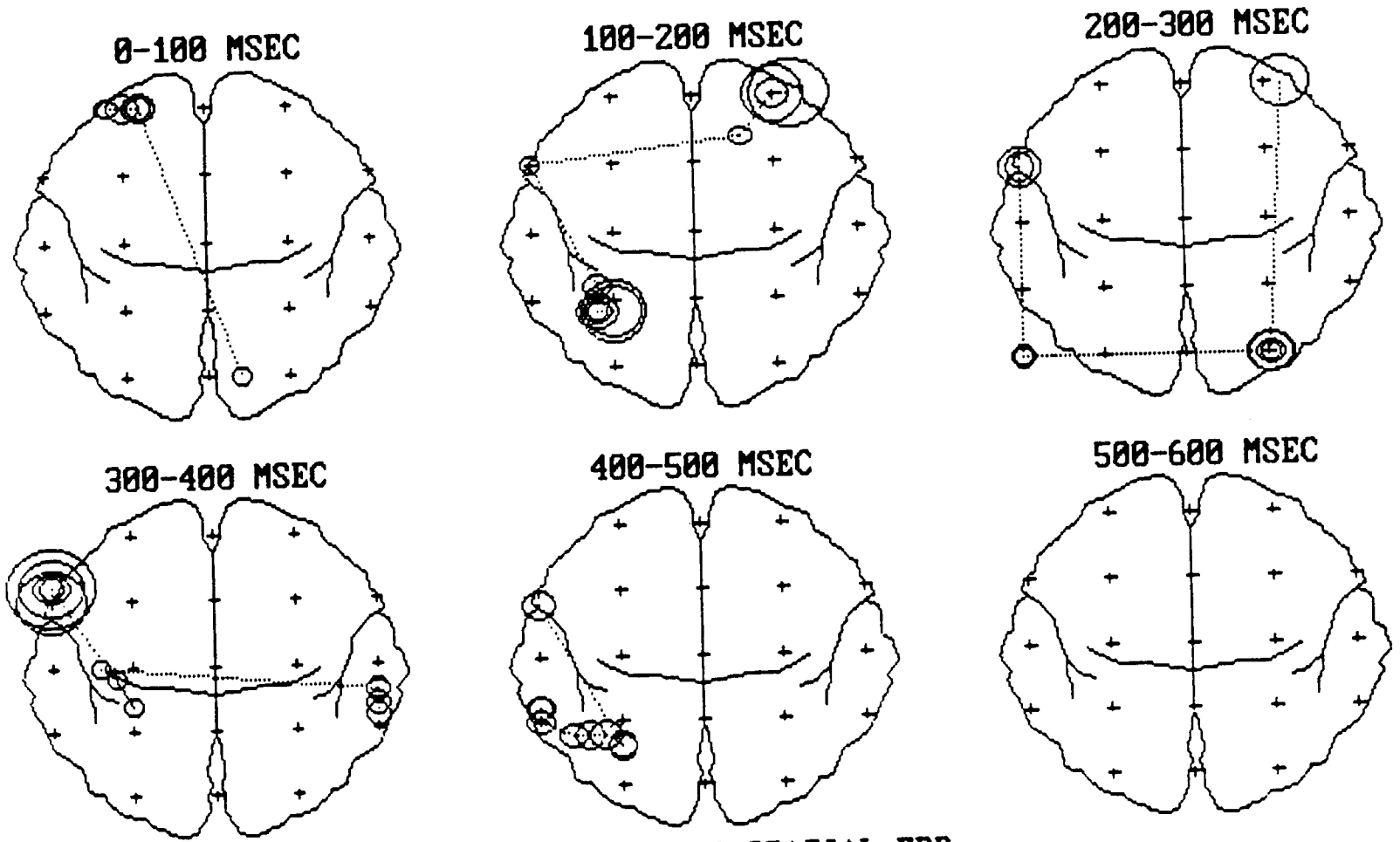

SUBJ 02 -- 6 SPATIAL ERPs
CORRELATION OF PERFORMANCE WITH CORTICAL ENERGY

FIGURE VI.1.-90

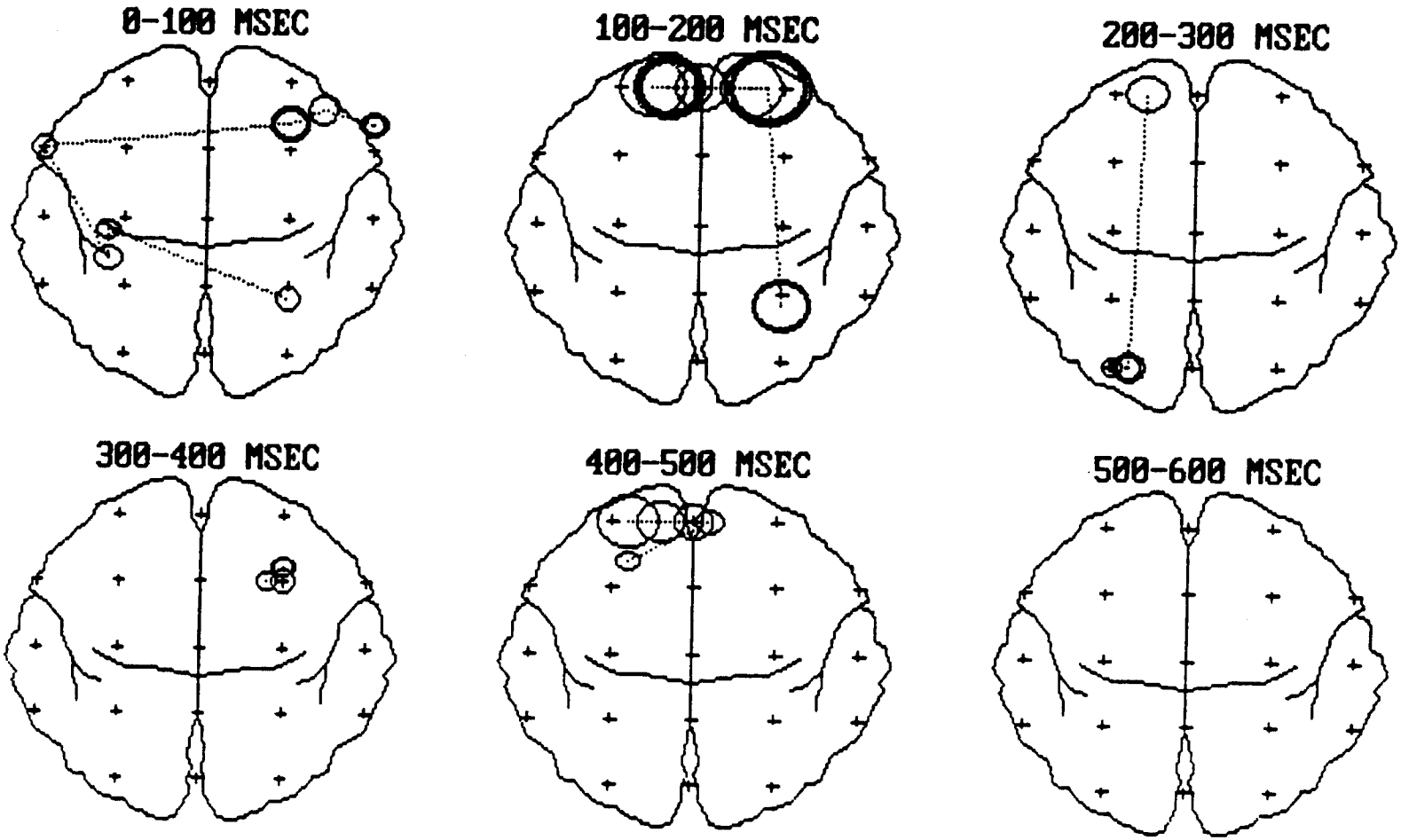

SUBJ 04 — 6 SPATIAL ERPs
CORRELATION OF PERFORMANCE WITH CORTICAL ENERGY

FIGURE VI.1.-91

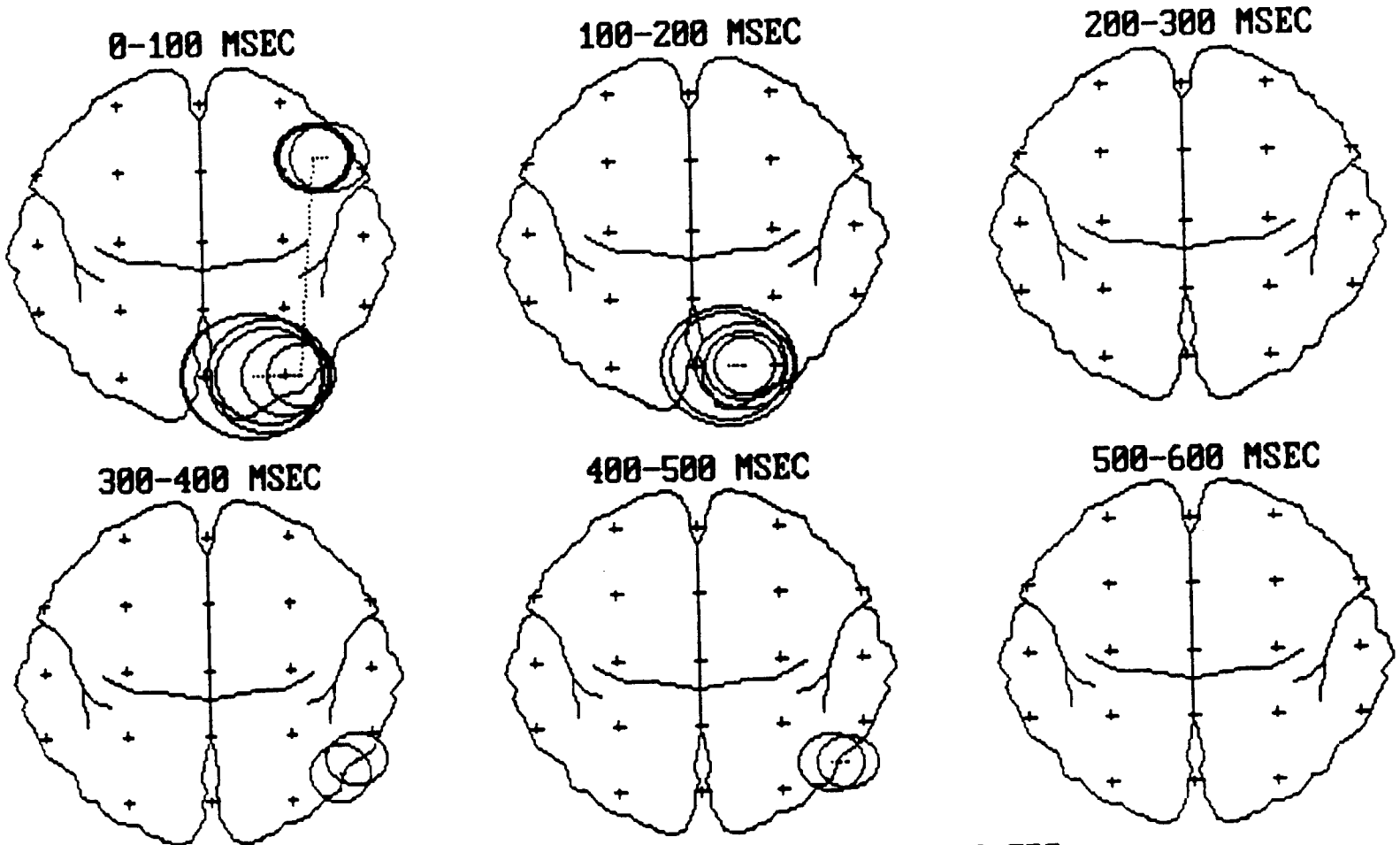

SUBJ 01 — AVERAGE OF 6 ARITHMETIC ERPs
LOCUS OF MAXIMA OF ENERGY DENSITY

FIGURE VI.1.-92

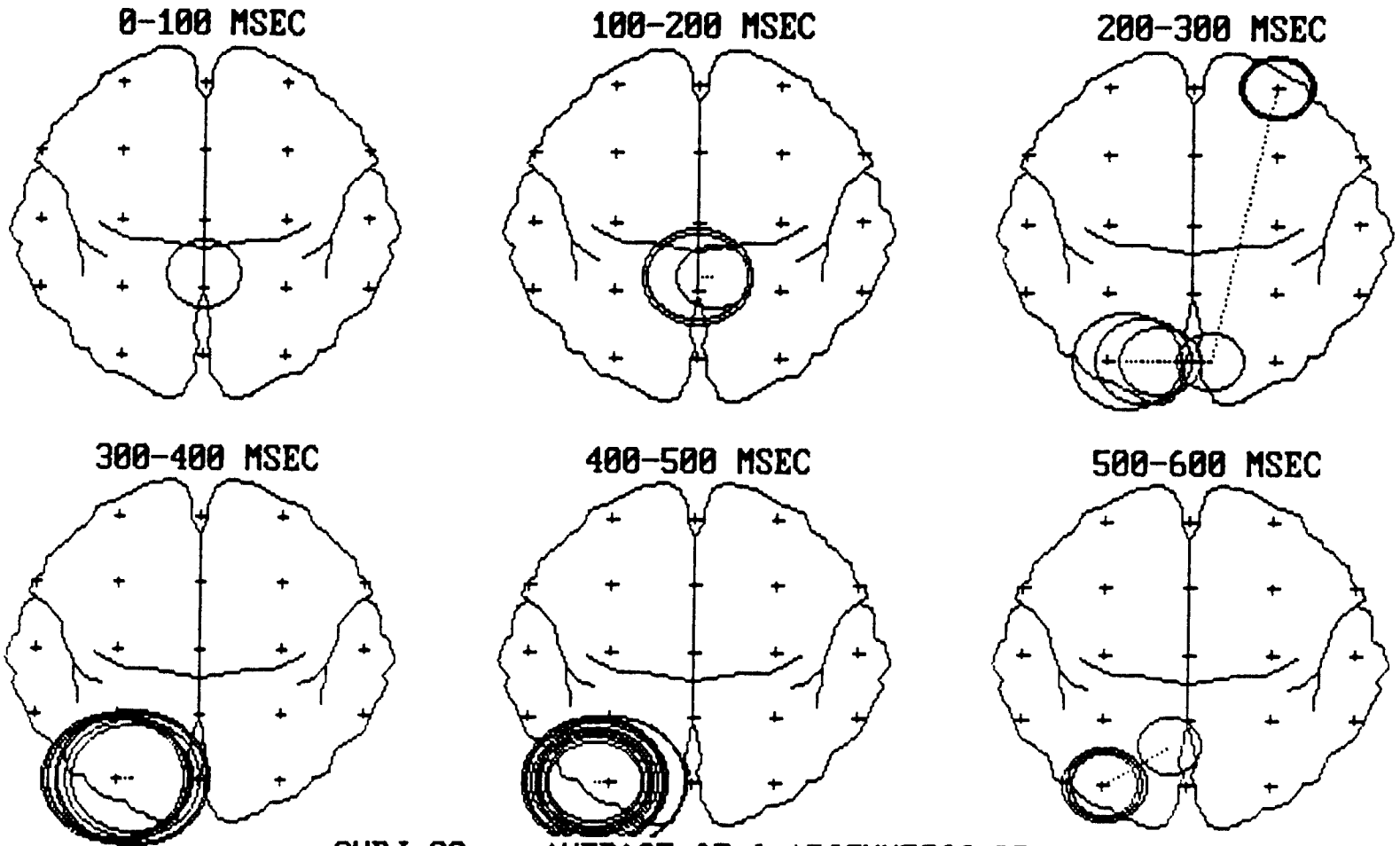

SUBJ 02 -- AVERAGE OF 6 ARITHMETIC ERPs
LOCUS OF MAXIMA OF ENERGY DENSITY

FIGURE VI.1.-93

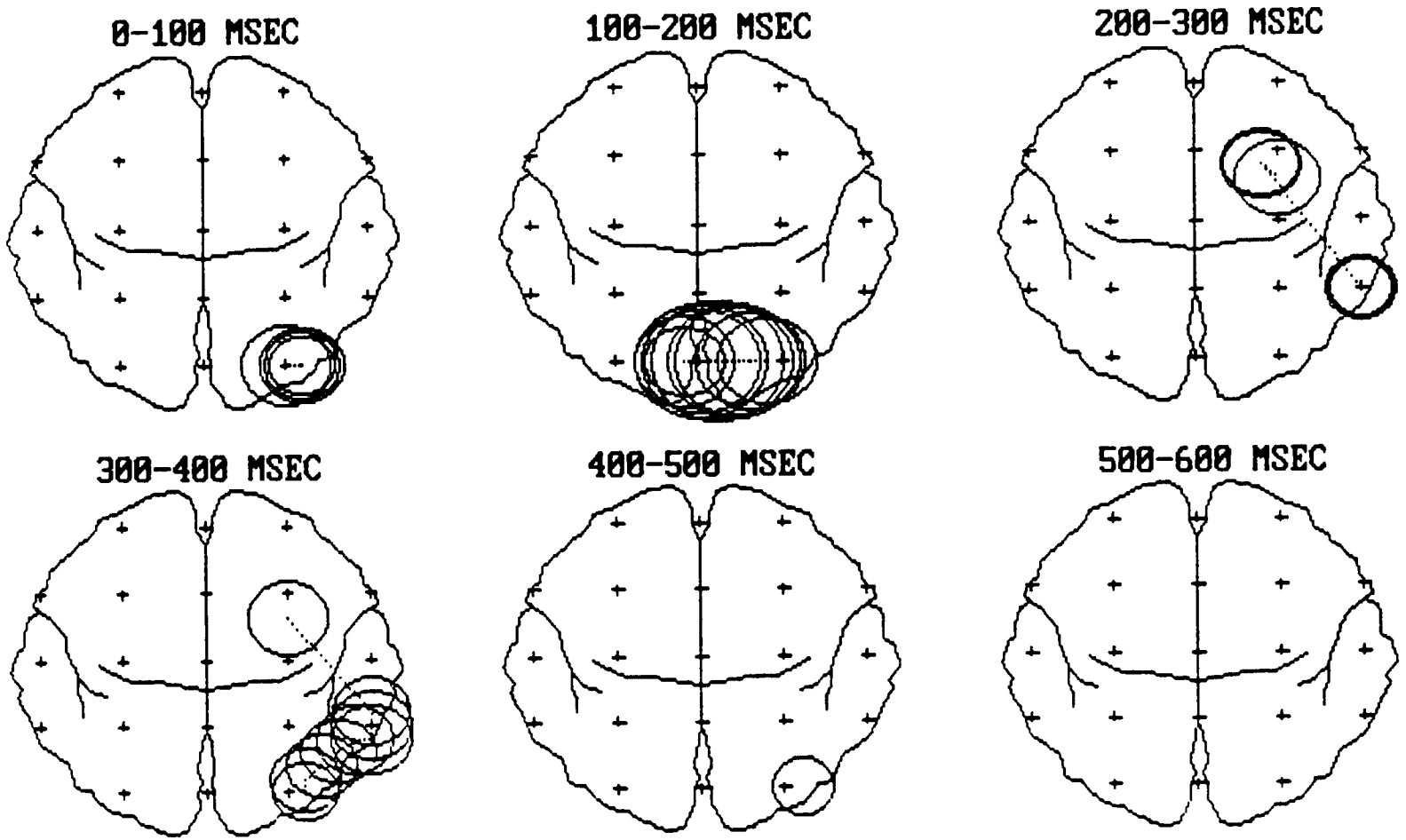

SUBJ 04 -- AVERAGE OF 6 ARITHMETIC ERPs
LOCUS OF MAXIMA OF ENERGY DENSITY

FIGURE VI.1.-94

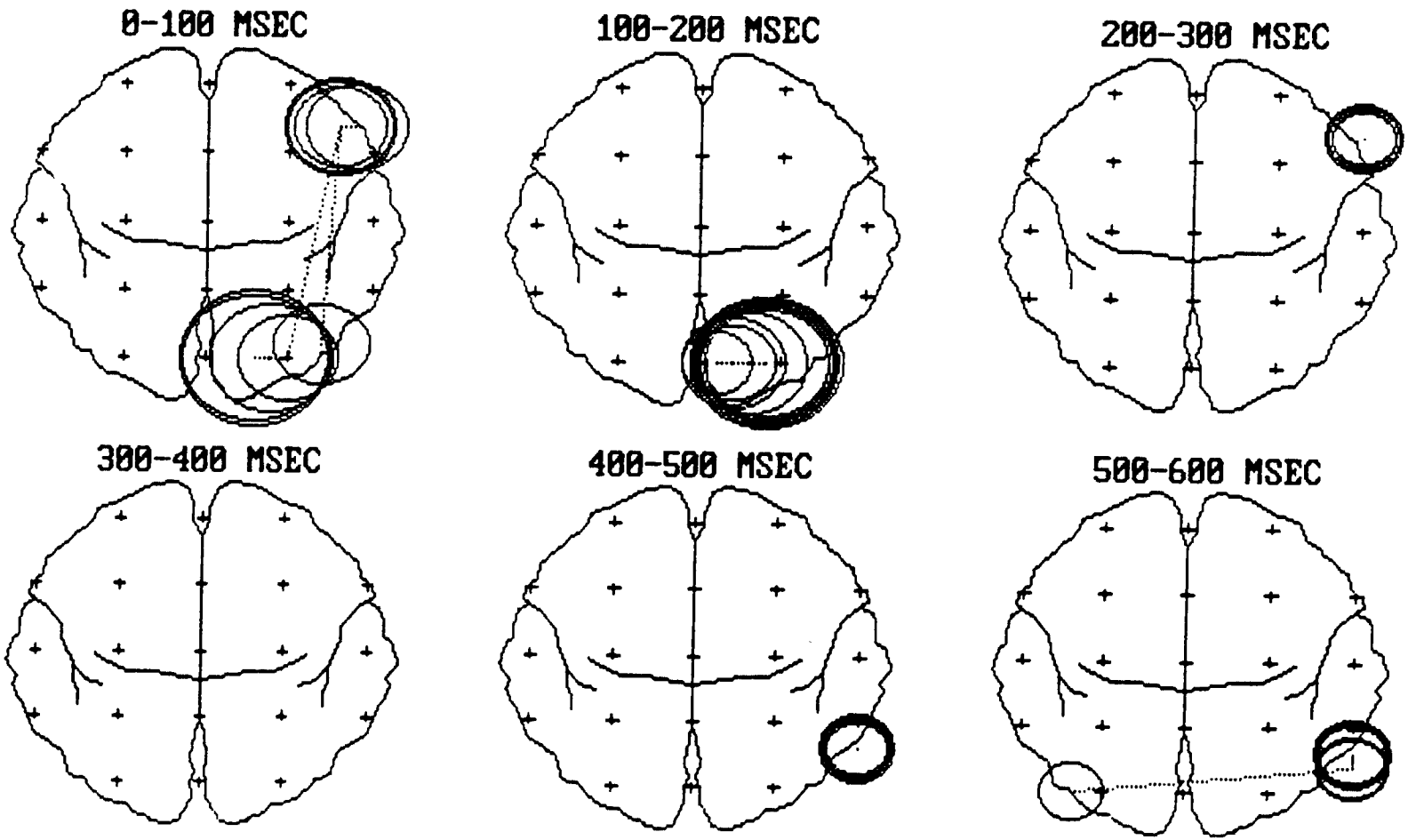

SUBJ 01 -- AVERAGE OF 6 WORDPAIR ERPs
LOCUS OF MAXIMA OF ENERGY DENSITY

FIGURE VI.1.-95

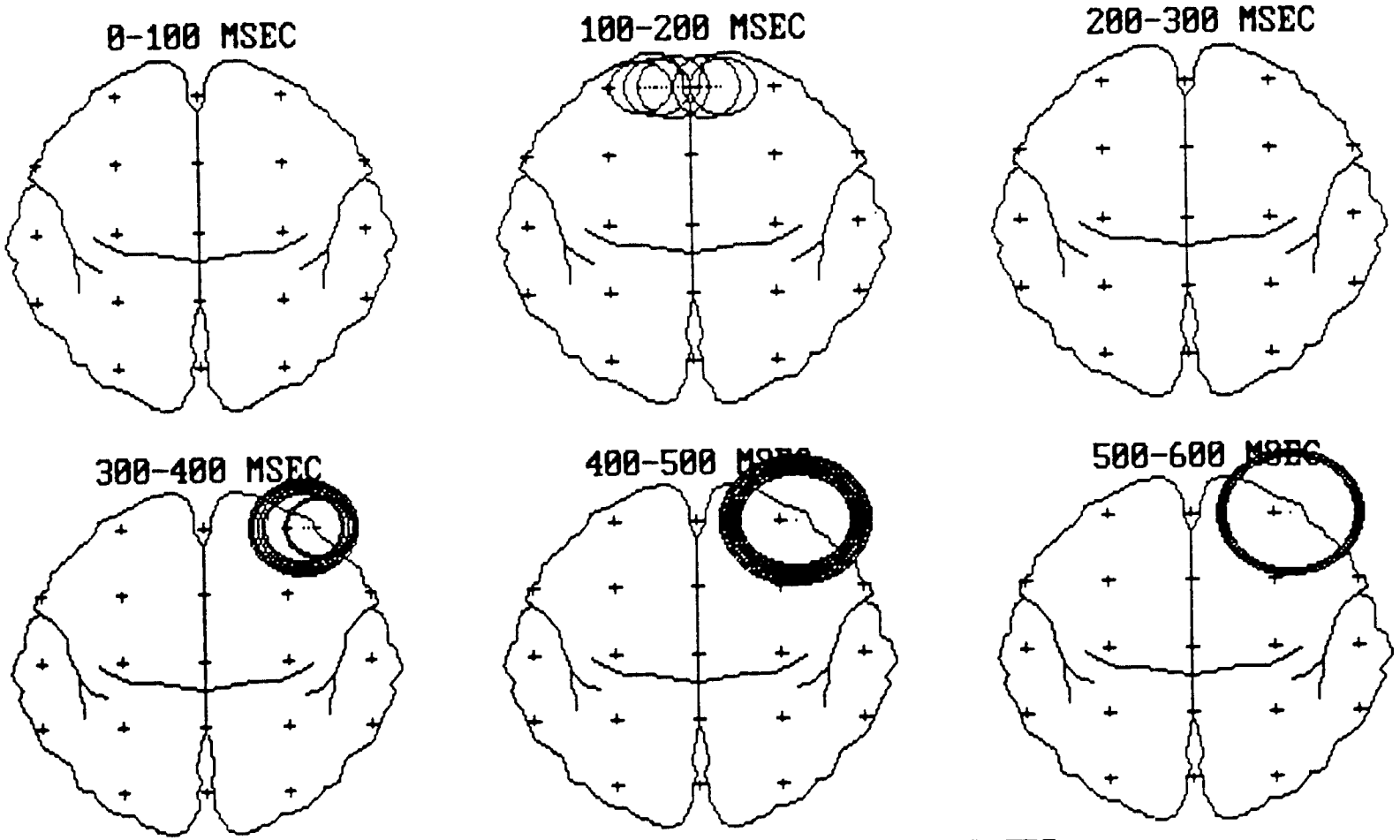

SUBJ 02 -- AVERAGE OF 6 WORDPAIR ERPs
LOCUS OF MAXIMA OF ENERGY DENSITY

FIGURE VI.1.-96

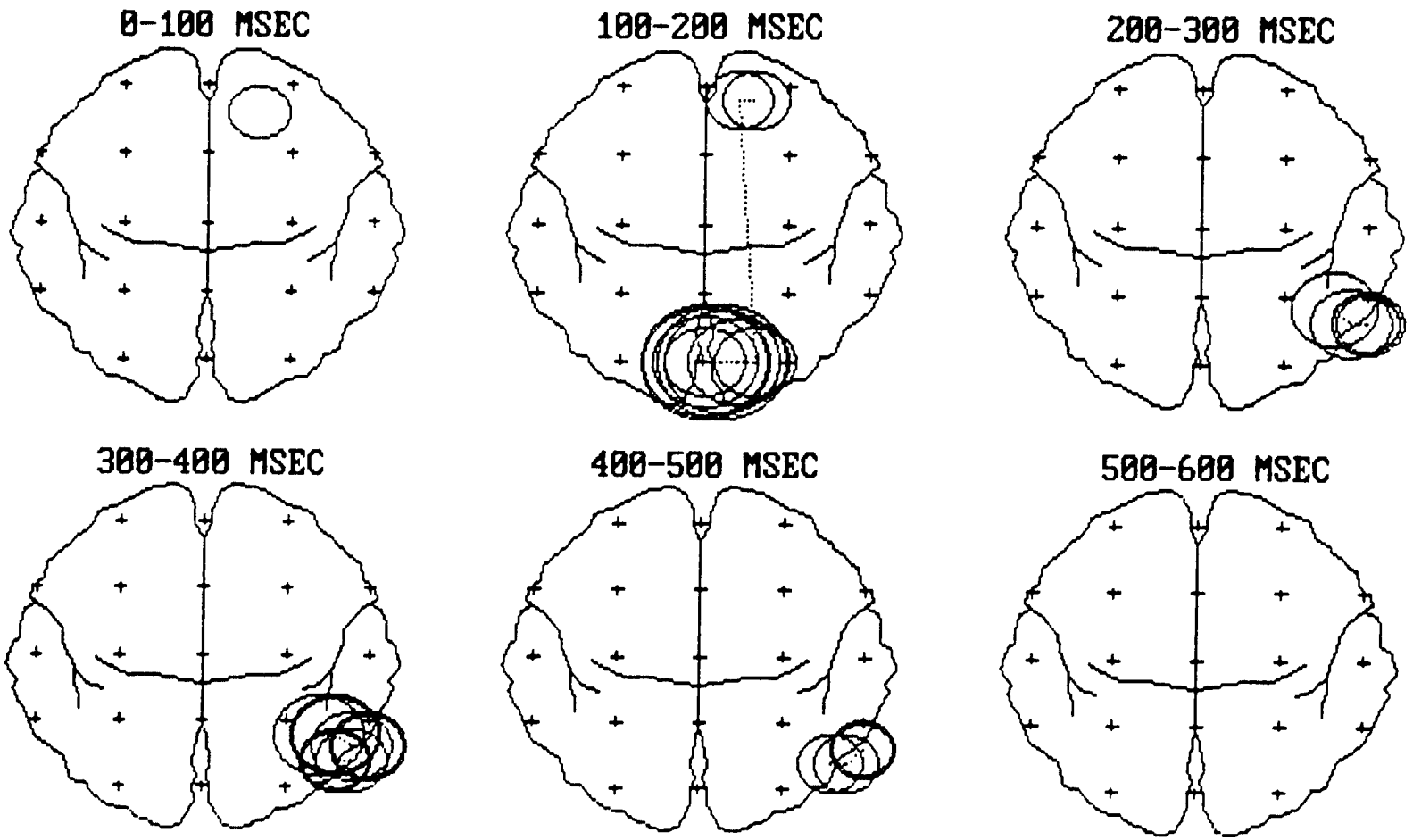

SUBJ 04 -- AVERAGE OF 6 WORDPAIR ERPs
LOCUS OF MAXIMA OF ENERGY DENSITY

FIGURE VI.1.-97

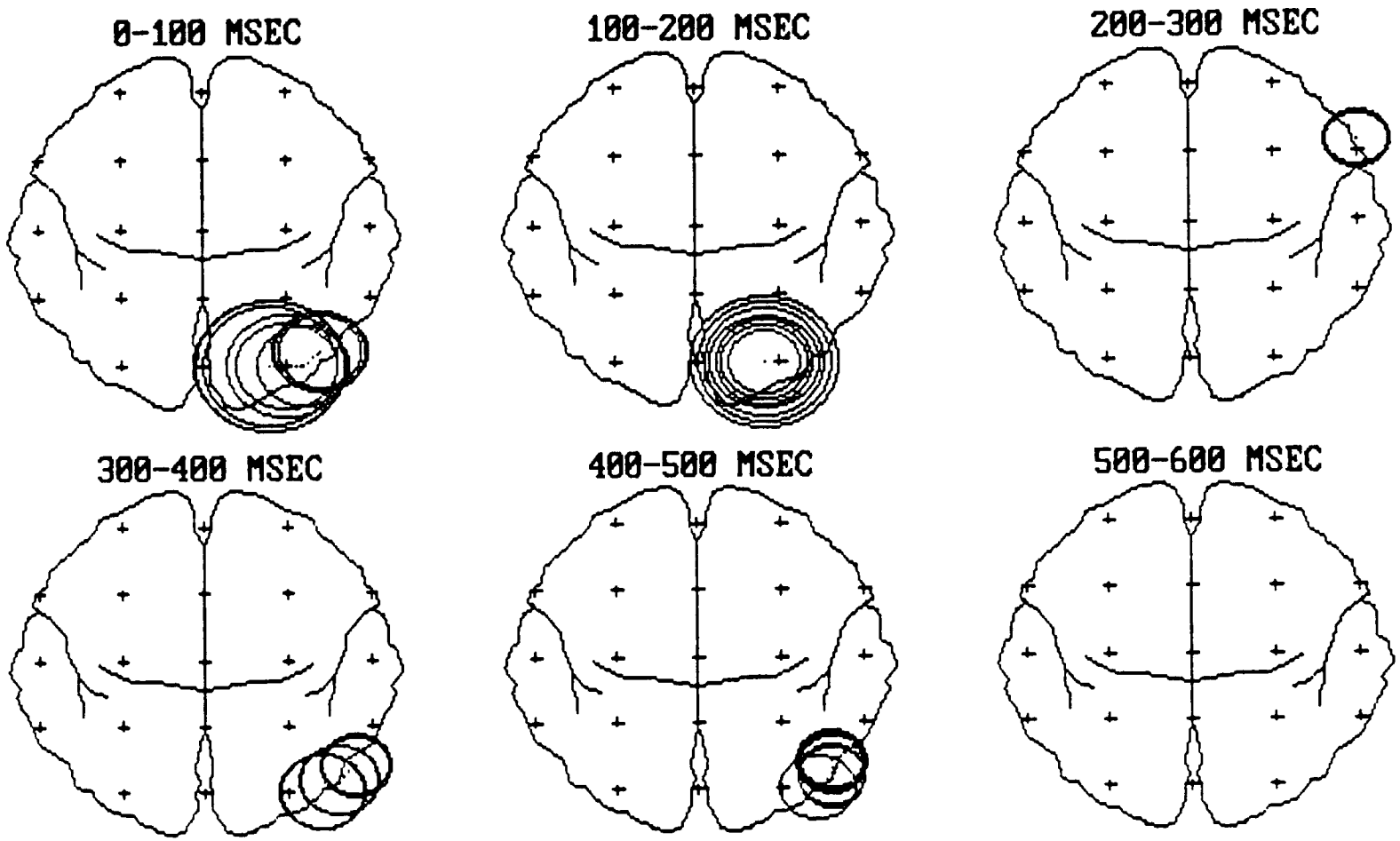

SUBJ 01 -- AVERAGE OF 6 SPATIAL ERPs
LOCUS OF MAXIMA OF ENERGY DENSITY

FIGURE VI.1.-98

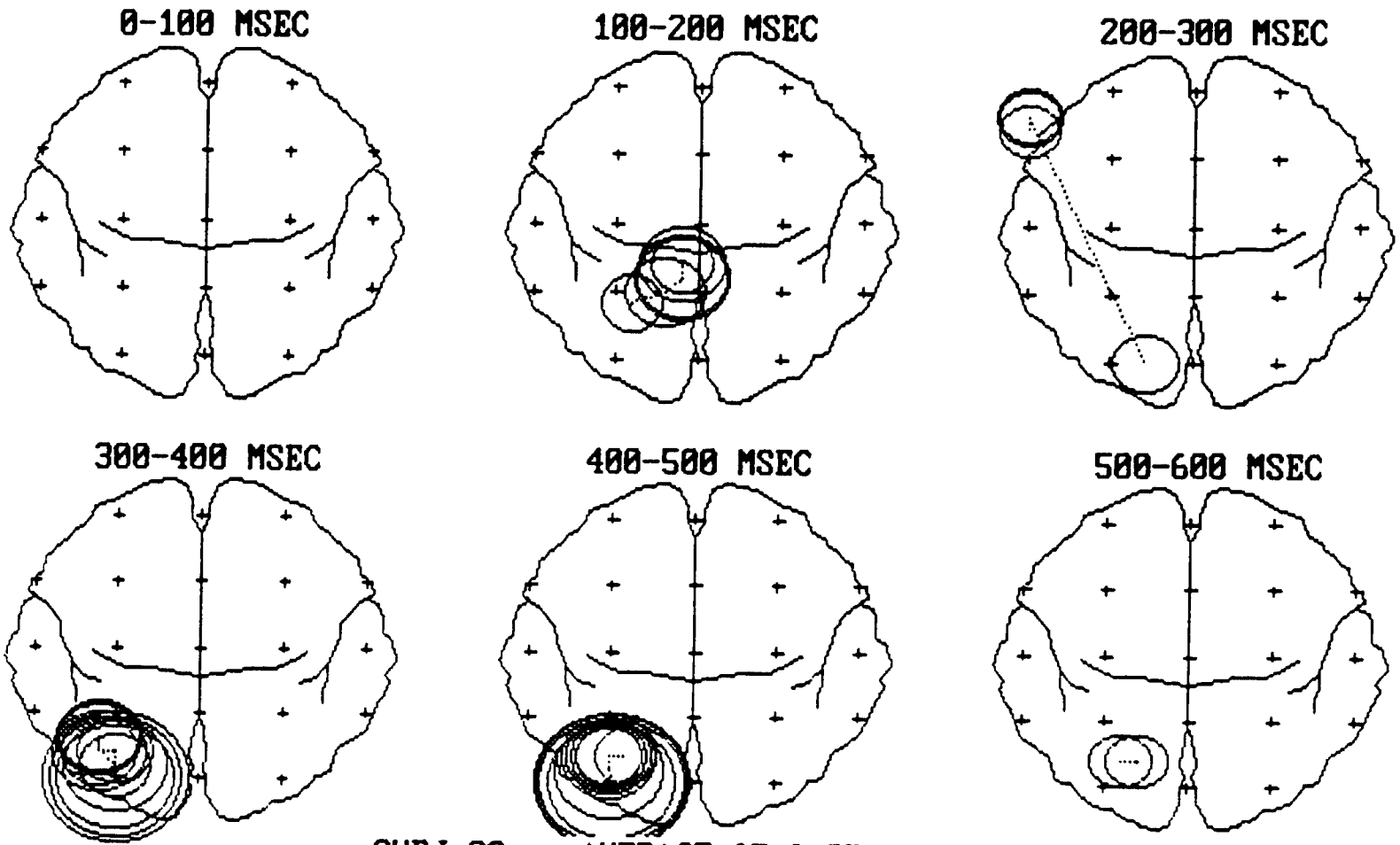

SUBJ 02 -- AVERAGE OF 6 SPATIAL ERPs
LOCUS OF MAXIMA OF ENERGY DENSITY

FIGURE VI.1.-99

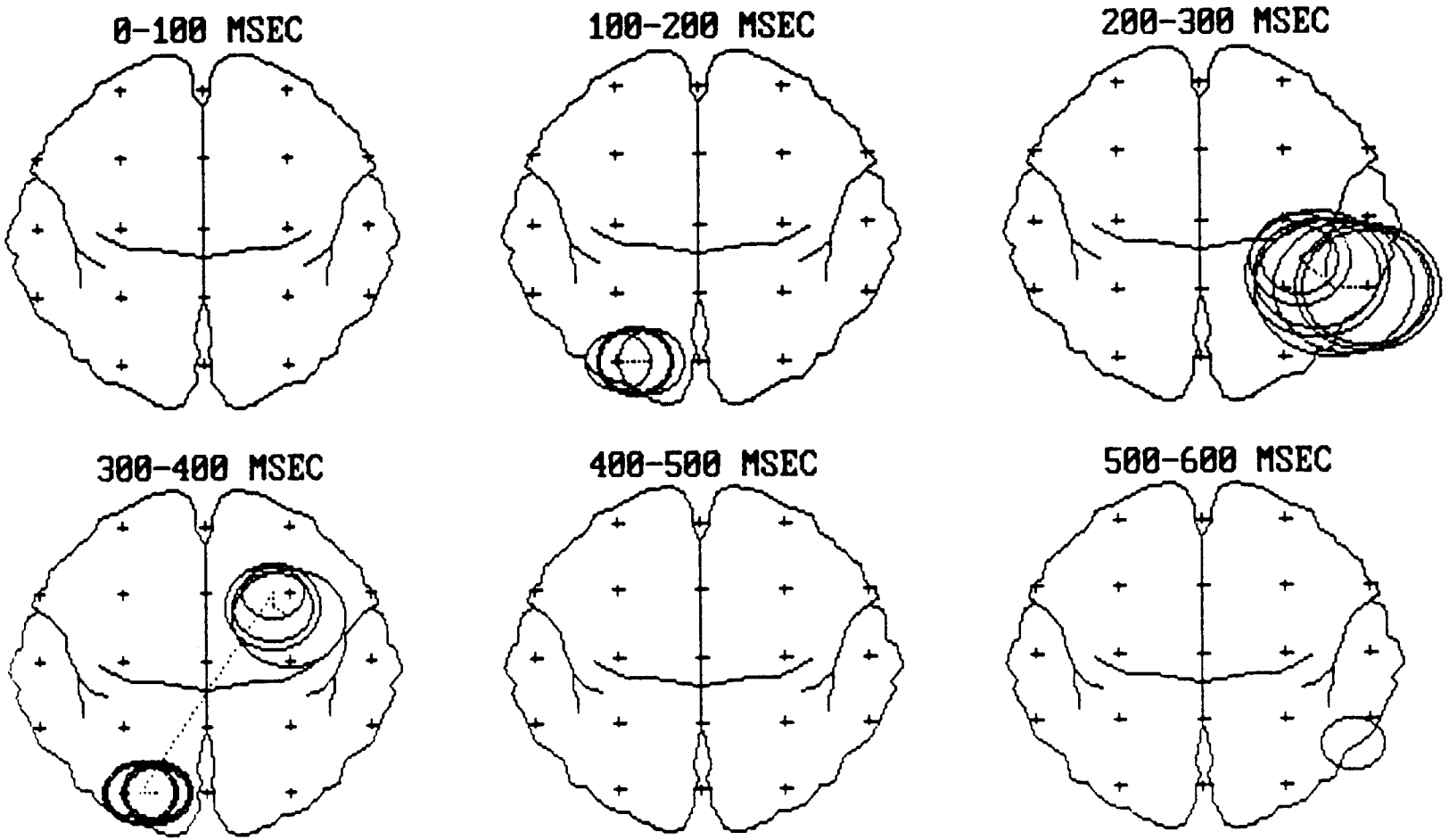

SUBJ 04 -- AVERAGE OF 6 SPATIAL ERPs
LOCUS OF MAXIMA OF ENERGY DENSITY

FIGURE VI.1.-100

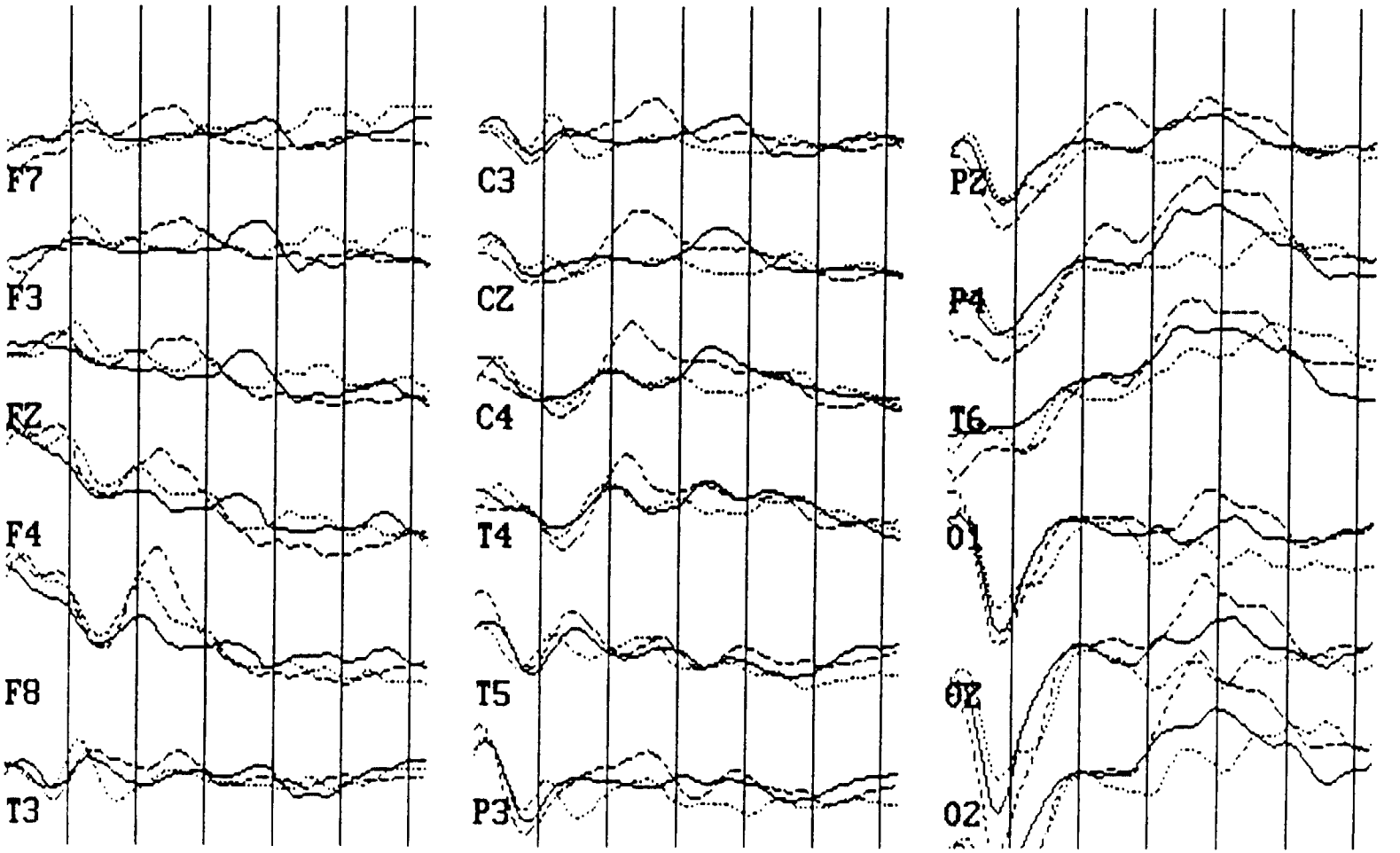

FIGURE VI.1.-101

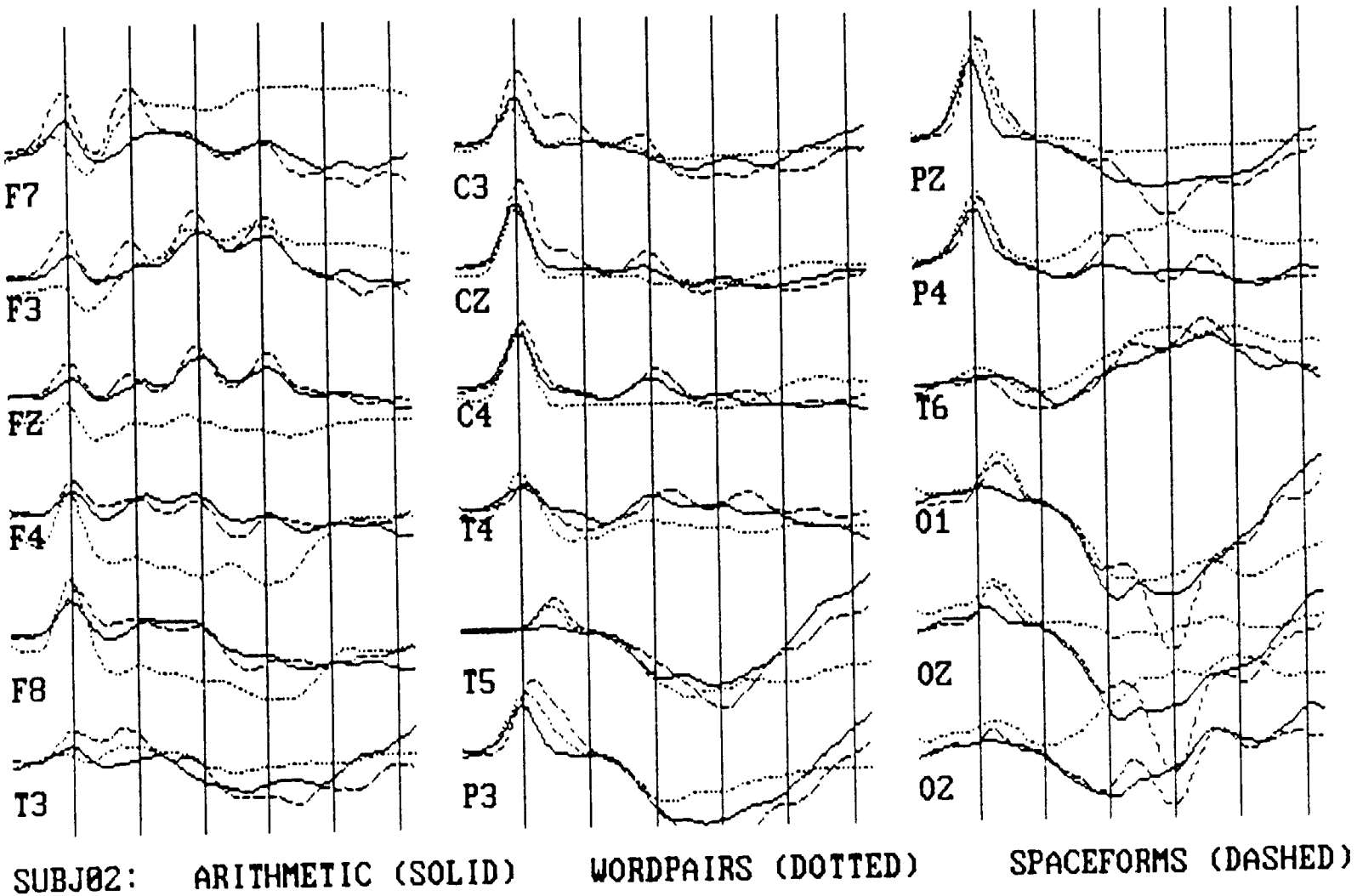

FIGURE VI.1.-102

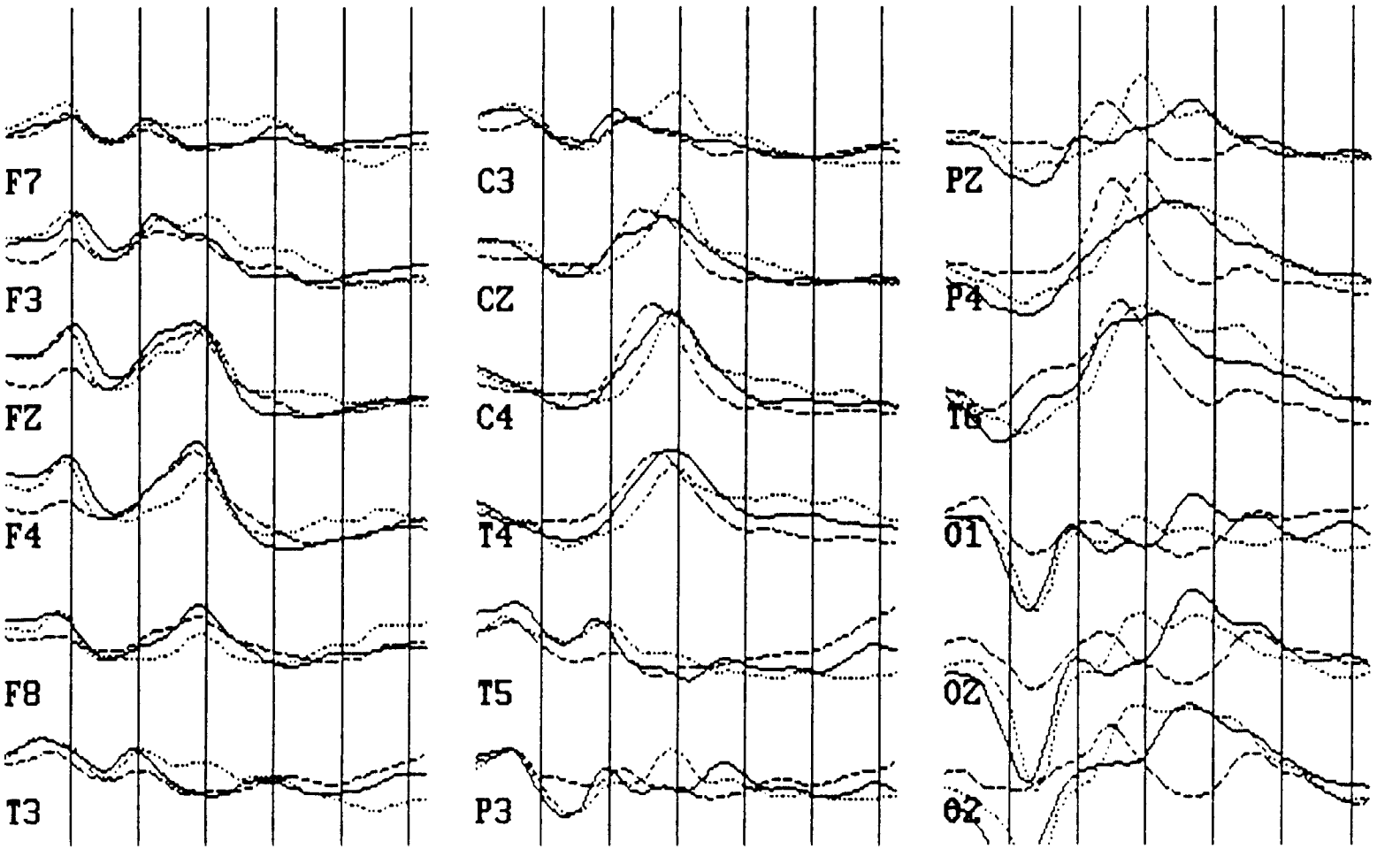

FIGURE VI.1.-103

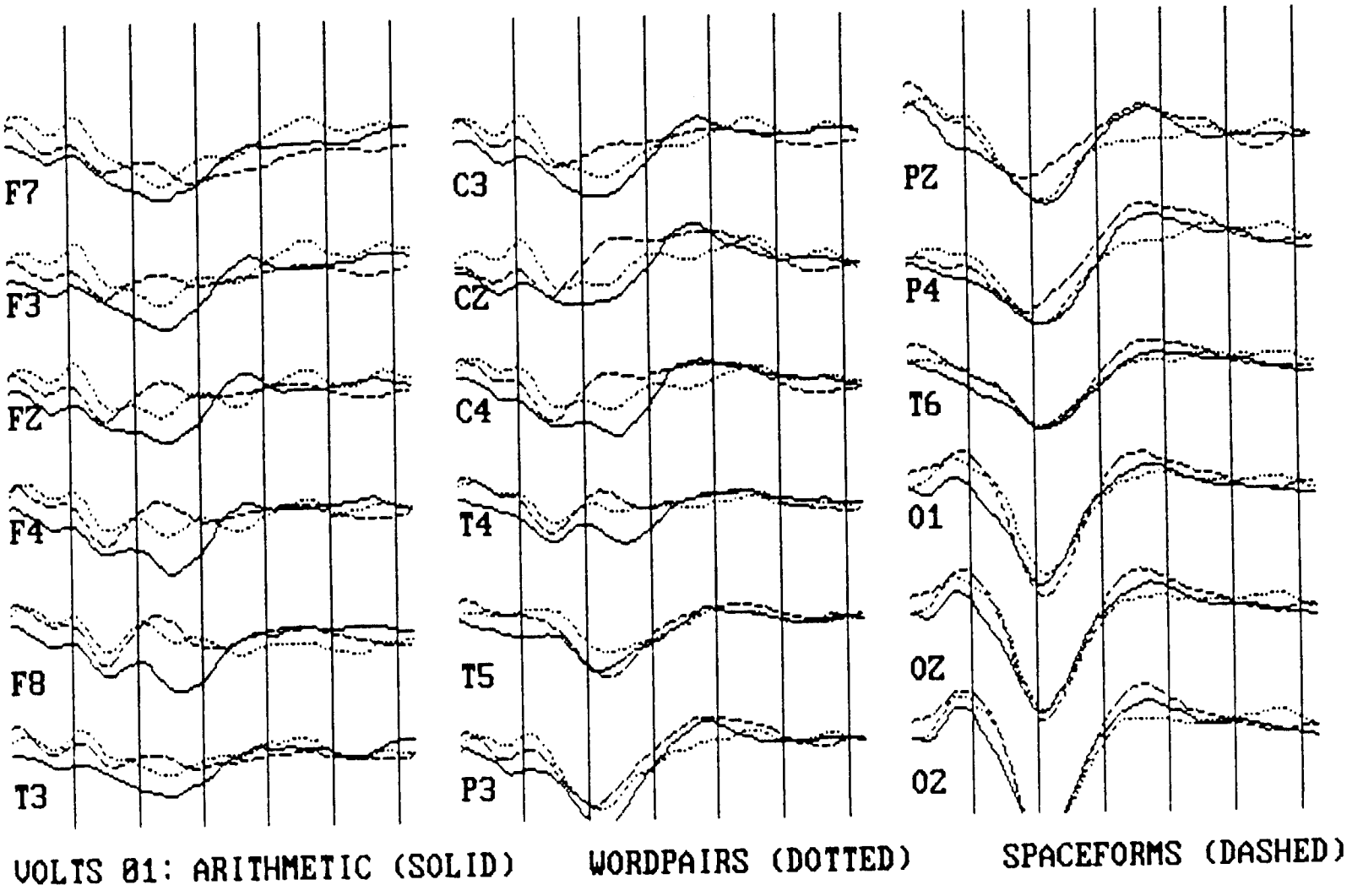

FIGURE VI.1.-104

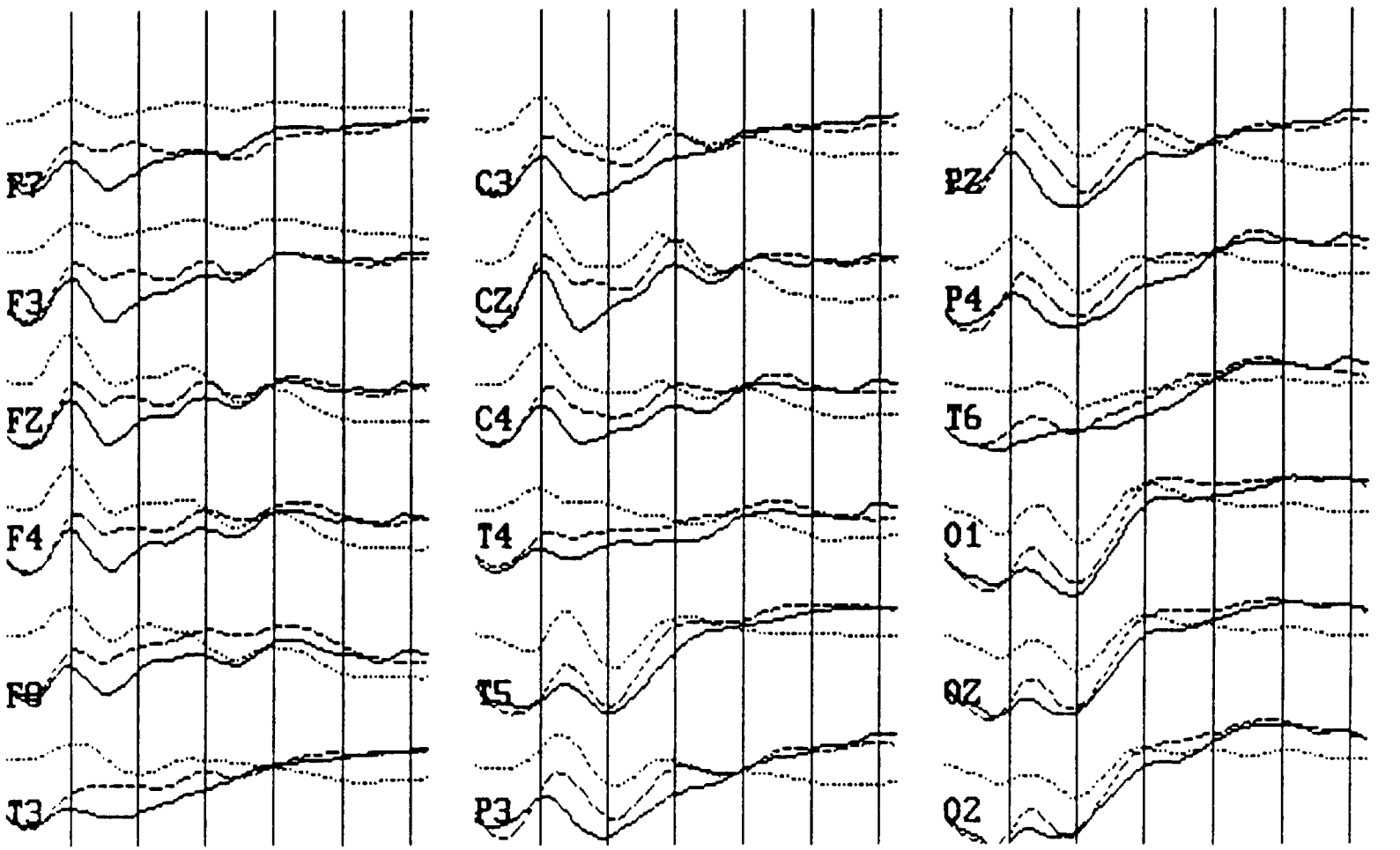

VOLTS 02: ARITHMETIC (SOLID) WORDPAIRS (DOTTED) SPACEFORMS (DASHED)

FIGURE VI.1.-105

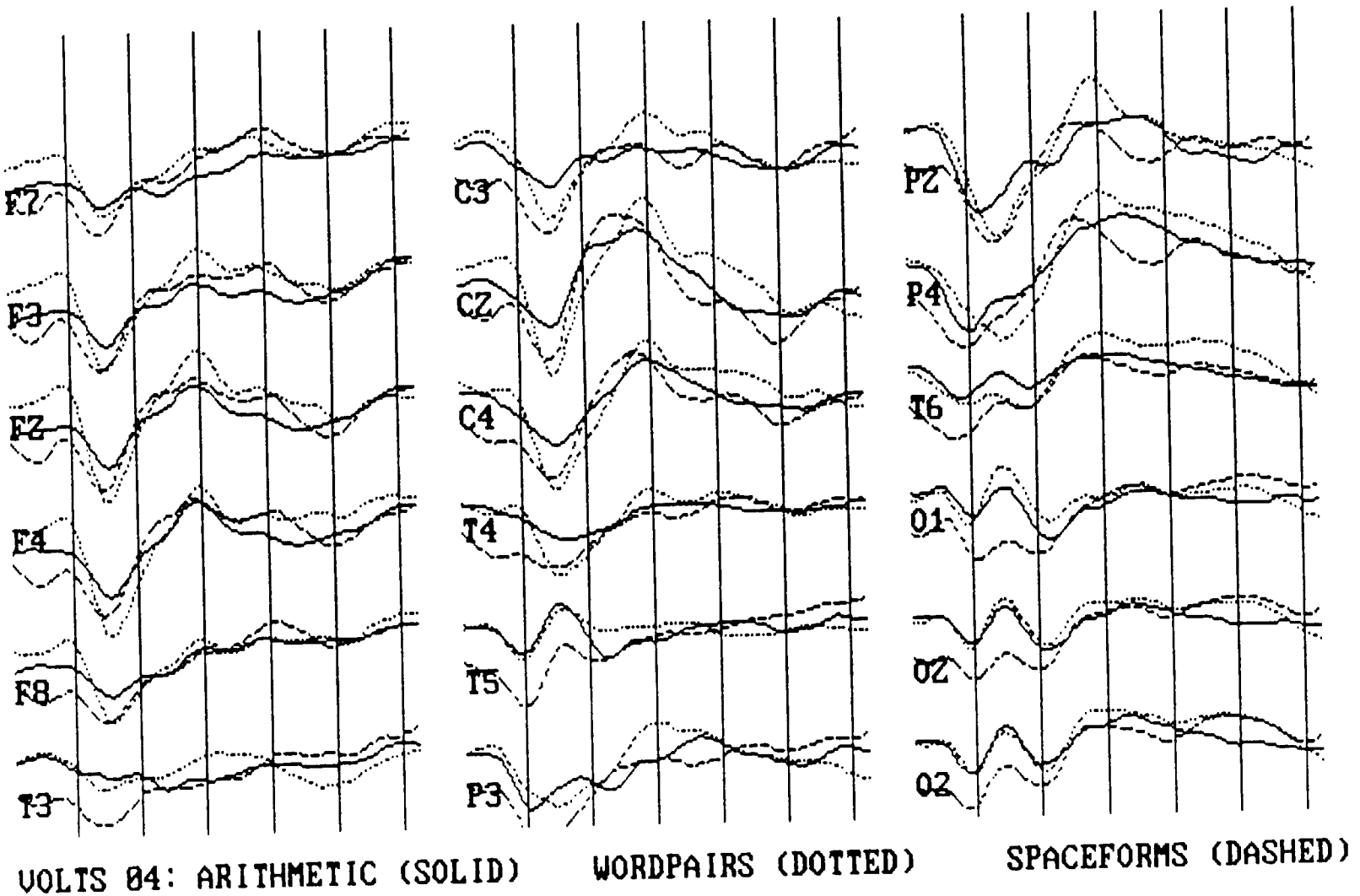

FIGURE VI.1.-106

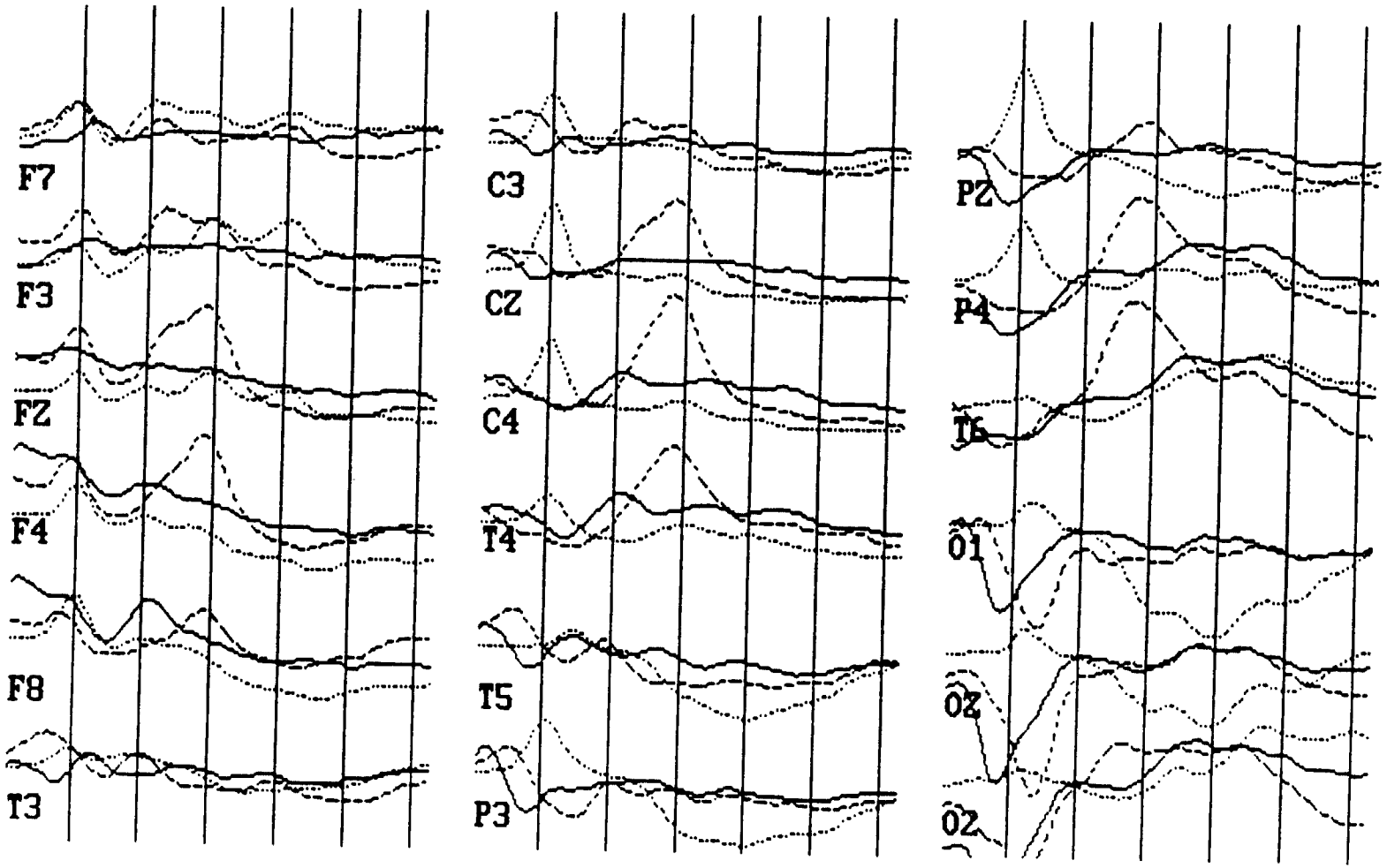

SUBJ01.DNR (SOLID)

SUBJ02.DNR (DOTTED)

SUBJ04.DNR (DASHED)

FIGURE VI.1.-107

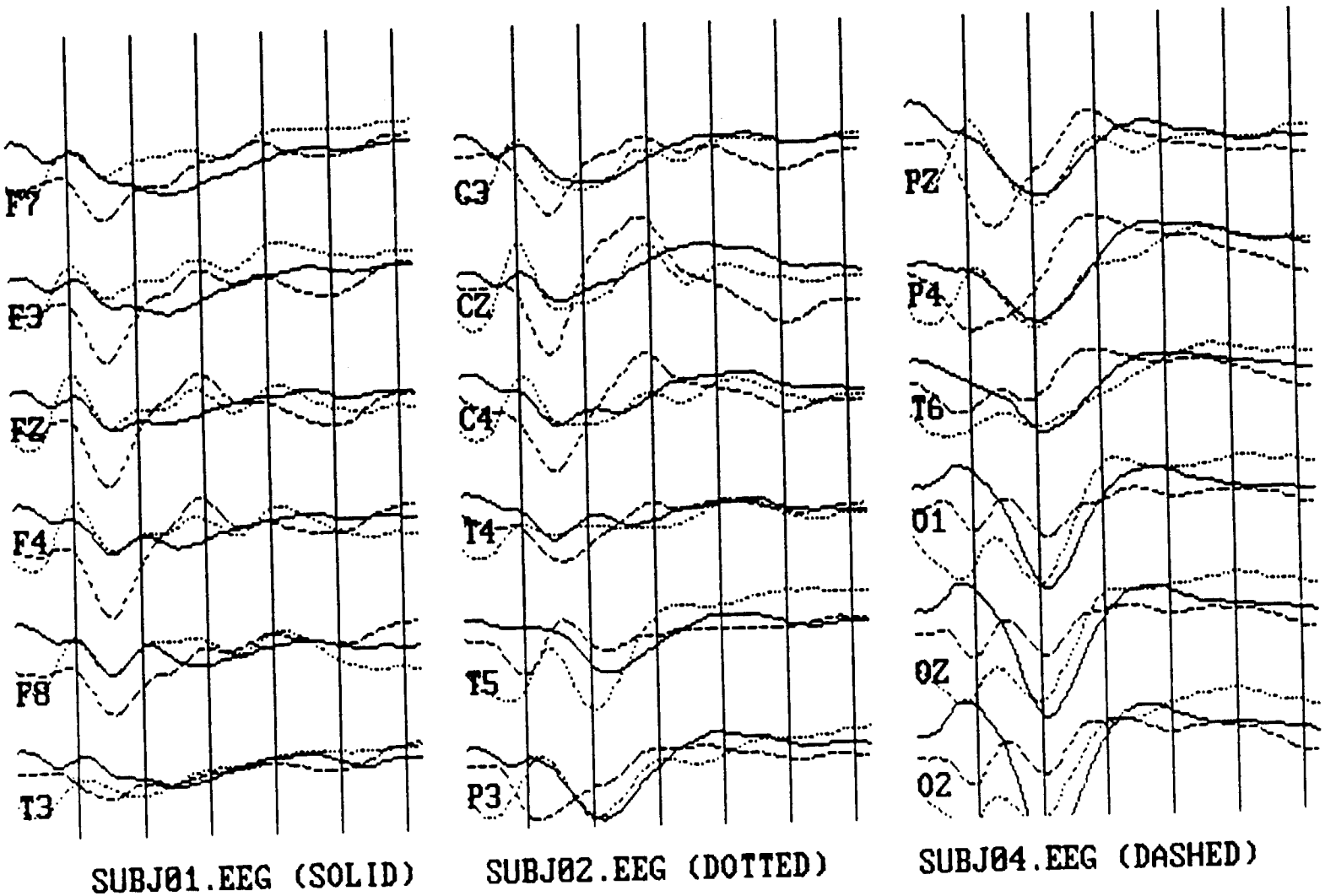

TABLE XX

ERROR INDEX VS. ENERGY DENSITY:
WORDPAIR TASK: SUBJ 01 -- FIRST 6 ERPS

ELECTRODE	PERIOD	R-SQUARE	T-VALUE	SLOPE
O2	32 - 71	0.876	5.317	2.279
P4	40 - 79	0.771	3.675	2.070
F8	47 - 86	0.801	4.018	0.534
F8	55 - 94	0.883	5.501	0.524
F8	63 - 102	0.926	7.066	0.532
F8	71 - 110	0.936	7.658	0.570
F4	79 - 118	0.761	3.564	0.499
F8	79 - 118	0.905	6.166	0.637
Fp2	86 - 126	0.762	3.576	0.563
F8	86 - 126	0.786	3.828	0.711
F4	243 - 282	0.765	-3.612	-1.202
F8	251 - 290	0.778	-3.739	-1.551
F8	258 - 297	0.907	-6.254	-2.308
F8	266 - 305	0.759	-3.550	-3.120
Fp1	383 - 422	0.929	-7.260	-0.964
F3	383 - 422	0.793	-3.910	-0.718
Fp1	391 - 430	0.867	-5.099	-0.778
F3	391 - 430	0.798	-3.971	-0.657
Fz	391 - 430	0.833	-4.468	-0.714
Fz	399 - 438	0.857	-4.892	-0.708
Fz	407 - 446	0.762	-3.577	-0.616
T5	461 - 501	0.885	5.550	1.502

TABLE XXI

ERROR INDEX VS. ENERGY DENSITY:
WORDPAIR TASK: SUBJ 01 -- LAST 6 ERPS

ELECTRODE	PERIOD	R-SQUARE	T-VALUE	SLOPE
O1	157 - 196	0.756	3.519	0.316
Oz	211 - 251	0.789	-3.872	-1.299
T5	376 - 415	0.833	-4.460	-0.452
T5	383 - 422	0.760	-3.564	-0.425
Fz	407 - 446	0.751	-3.477	-0.266
Fz	415 - 454	0.766	-3.615	-0.287
P4	430 - 469	0.751	-3.475	-0.153
Pz	438 - 477	0.841	-4.605	-0.177
P4	438 - 477	0.821	-4.285	-0.150
O1	438 - 477	0.753	-3.489	-0.189
Oz	438 - 477	0.788	-3.851	-0.166
Cz	446 - 485	0.752	-3.481	-0.217
P3	446 - 485	0.830	-4.426	-0.244
Pz	446 - 485	0.970	-11.407	-0.200
P4	446 - 485	0.872	-5.227	-0.158
O1	446 - 485	0.873	-5.234	-0.196
Oz	446 - 485	0.882	-5.467	-0.168
Cz	454 - 493	0.769	-3.645	-0.245
P3	454 - 493	0.792	-3.906	-0.240
Pz	454 - 493	0.985	-16.013	-0.224
P4	454 - 493	0.897	-5.899	-0.180
Cz	461 - 501	0.762	-3.581	-0.284
C4	461 - 501	0.771	-3.669	-0.223
Pz	461 - 501	0.832	-4.451	-0.235
P4	461 - 501	0.800	-4.004	-0.201

FIGURE VI.1.-108

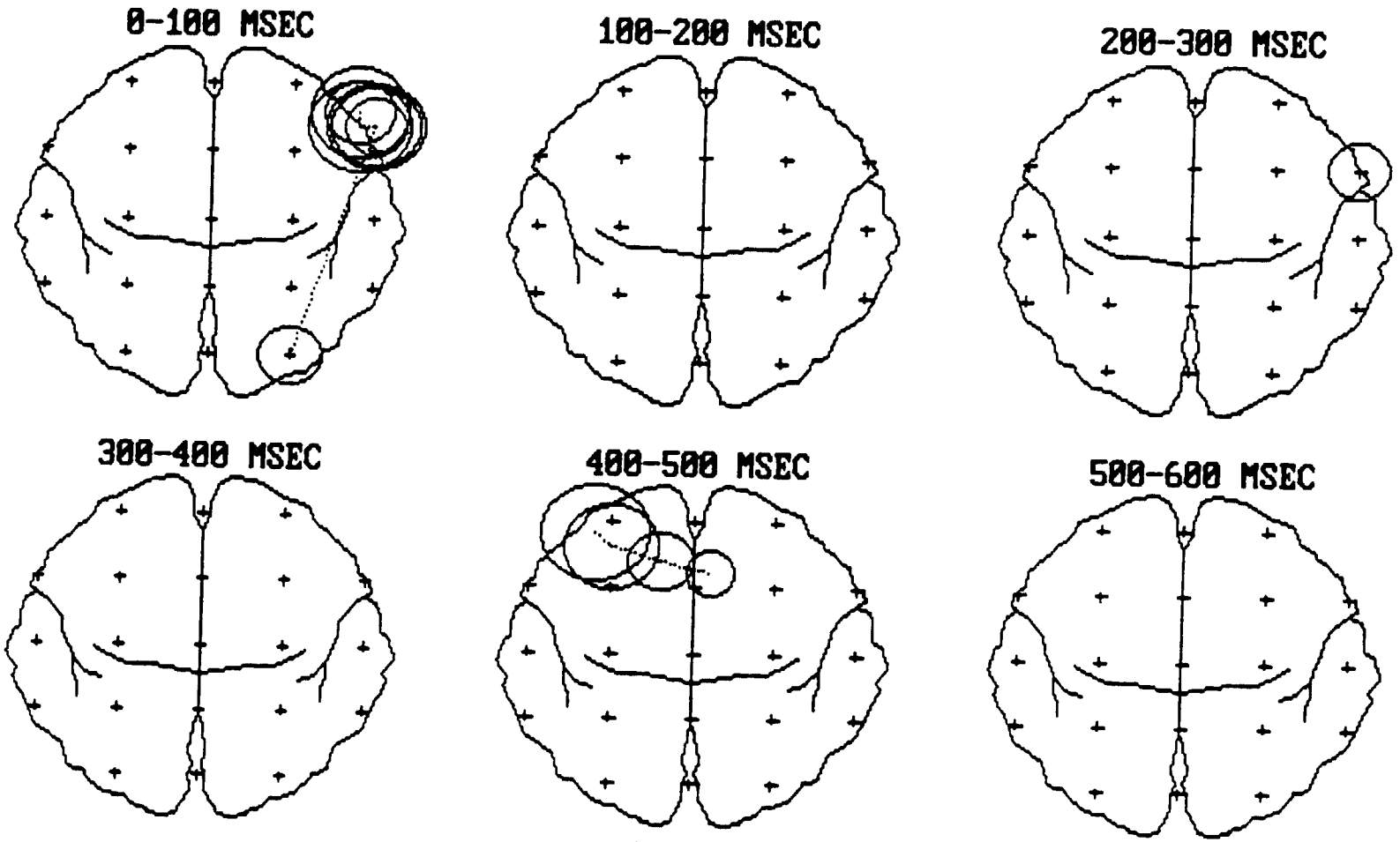

V1A.COR
CORRELATION OF PERFORMANCE WITH CORTICAL ENERGY

FIGURE VI.1.-109

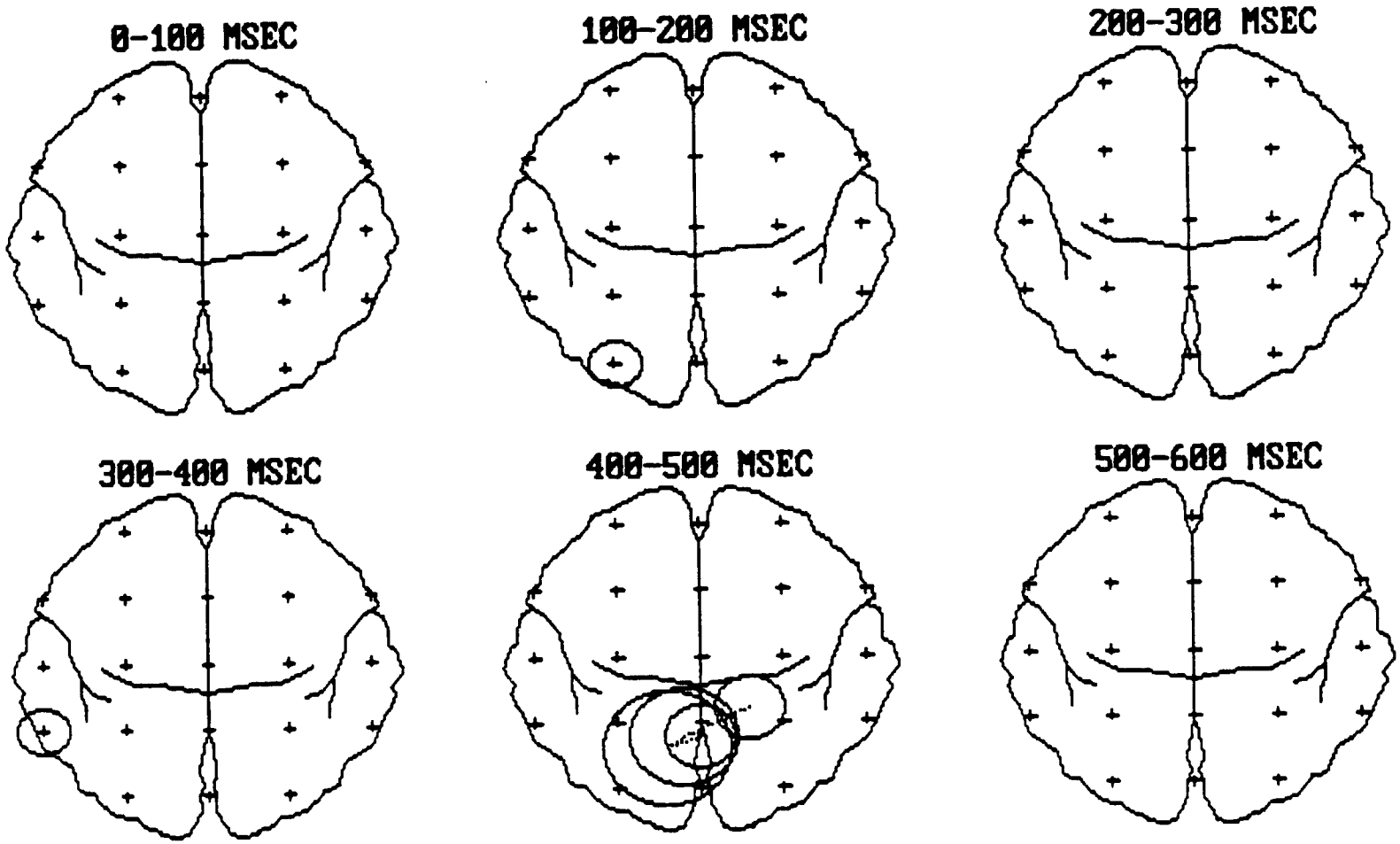

V1B.COR
CORRELATION OF PERFORMANCE WITH CORTICAL ENERGY

VI.2. REG results

VI.2.1. Mixed Task (Figures VI.2.-1 through VI.2.-33)

Observations were made on six adult right handed male volunteers of similar educational background and free of medical, psychiatric or neurological conditions. Cognitive stimulus presentation was synchronized to the cardiac cycle. Right and left hemisphere REG, left forearm IPG and EKG were recorded during each test sequence.

The MATH and VERB tasks produced statistically significant changes in hemodynamic parameters for the right and left hemispheres. Few statistical differences were found between the different difficulty levels of the SPAT task. Figures 1 - 29 illustrate changes in segmental blood flow, contractility, REG pulse rise time, pulse transit time, REG pulse systolic area and the Jacquay F and R indices of vascular hemodynamics A two-tailed paired T test was used to test the differences between the various hemodynamic responses produced by the LOW, MEDium and HIGH levels of each task. Significant differences between LOW and HIGH are shown by a "+", between MED and HIGH are shown by a "*" and between LOW and MED by a "@". Statistical comparisons between the left and right hemisphere hemodynamics to levels of difficulty in each task are shown in the lower left corner of each figure. No comparisons were made between either of the two hemispheres and the forearm.

Figures 1 - 9 show that cerebral blood flow, segmental contractility, pulse rise time, pulse systolic area and the Jacquay F and C indices all increase with increased difficulty of the MATH task. As blood flow and contractility increase, there is a concurrent drop in pulse transit time between the heart and the head (Figure 5), but not in forearm measurements (Figure 2). Heart rate (Figure 9) does not change during the MATH task suggesting that the hemodynamic changes are mediated by local vasomotor reflexes. Figure 10 shows how subject performance correlates with task level, paralleling the hemodynamic changes.

Figures 11 - 19 show similar hemodynamic changes during the SPAT task, although the values do not reach statistical significance. Cerebral blood flow and contractility both decrease slightly while pulse transit time increases with increased task level. Again there is little systemic involvement since neither the heart rate (Figure 19) nor forearm blood flow (Figure 12) change with task level. The hemodynamic changes tend to parallel subject performance as shown by the small decrease in response time during the High SPAT task (Figure 20).

Hemodynamic and performance changes during the VERB task are shown in Figures 21 - 30. The hemodynamic responses to this

task are somewhat different from the other two. Cerebral blood flow, contractility and pulse rise time were essentially the same for the LOW and MED levels and increased significantly only for the HIGH level. These changes are accompanied by a significant decrease in pulse transit time (Figure 25) and in the Jacquay F and R indices of localized vasomotor state (Figures 27 and 28). In addition, both the grouped mean heart rate (Figure 29) and response time (Figure 30) were found to increase (N.S.) with increased verbal task level. Once more, these figures, in general, indicate a cerebral reflex (rather than systemic) since cerebral hemodynamics were significantly altered during the verbal task but forearm blood flow and heart rate did not change significantly with increased task level.

The right hemisphere blood flow is higher than the left in all levels of the three cognitive tasks and significantly higher for the MATH task. However all measures of vasomotor reactivity shown in Figures 1 - 28 tend to be greater on the left hemisphere. This fact suggests a compensatory response to maintain homeostatic equilibrium between both hemispheres.

A "heart rate modulus" (Marble, 1988) (HRM) was calculated for each of the mixed tasks using each subject's beat to beat intervals as follows:

$$HRM = \frac{\text{Max beat interval} - \text{Min beat interval}}{\text{Ave beat interval}}$$

The HRM may be used to assess the balance between sympathetic and parasympathetic influences during any given test sequence. The modulus becomes larger and more varied when the subject is relaxed, less stressed or less attentive. Conversely, the HRM decreases and is less varied as the subject attends to a task and becomes more stressed. As applied to our protocols, the HRM is independent of task difficulty, since it is calculated over an extended period of time. The grouped mean +/- S.E. HRMs for the three tasks are shown in Figures 31 - 33. During the initial time period of each task the HRM is rather varied across subjects (as indicated by the larger error bars). The HRM decreases and becomes less varied (smaller error bars) during the MATH and VERB tasks and remains relatively unchanged during the SPAT task.

These results suggest that the experimental subjects were relaxed and not stressed during the initial periods of all three tasks and that they found the MATH task to be more stressful (or engaging) than the VERB or SPAT tasks. The SPAT task appeared to involve the least amount of thought (or effort) to complete and the VERB task was somewhere in between.

The HRM responses during the Mixed task tend to parallel the hemodynamic responses described above. Cerebral blood flow was graded and varied in a statistically significant manner during the MATH task and was less responsive during the VERB and SPAT tasks.

FIGURE VI.2.-1

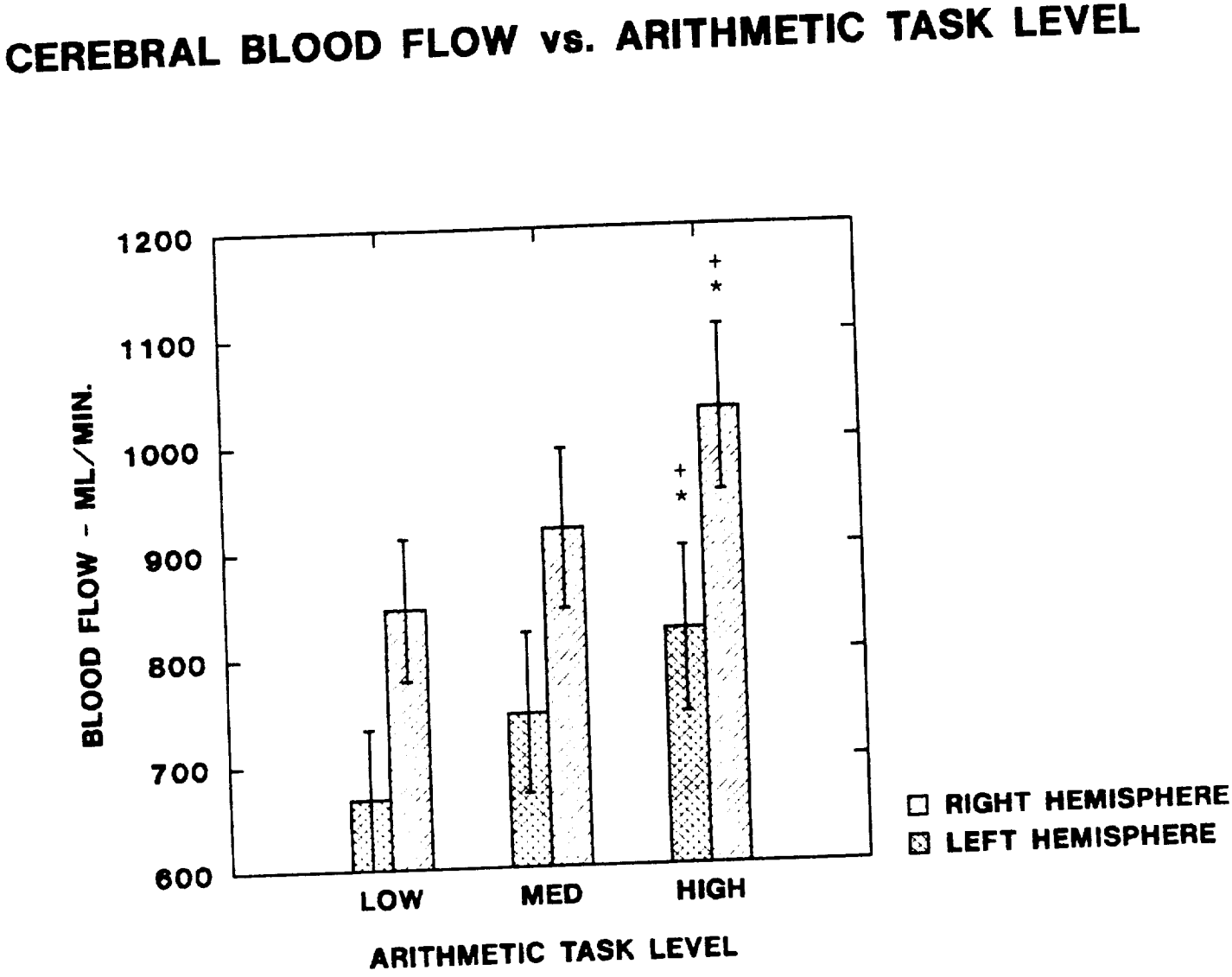

RIGHT > LEFT ($P < 0.01$) FOR ALL TASK LEVELS

FIGURE VI.2.-2

FOREARM BLOOD FLOW vs. ARITHMETIC TASK LEVEL

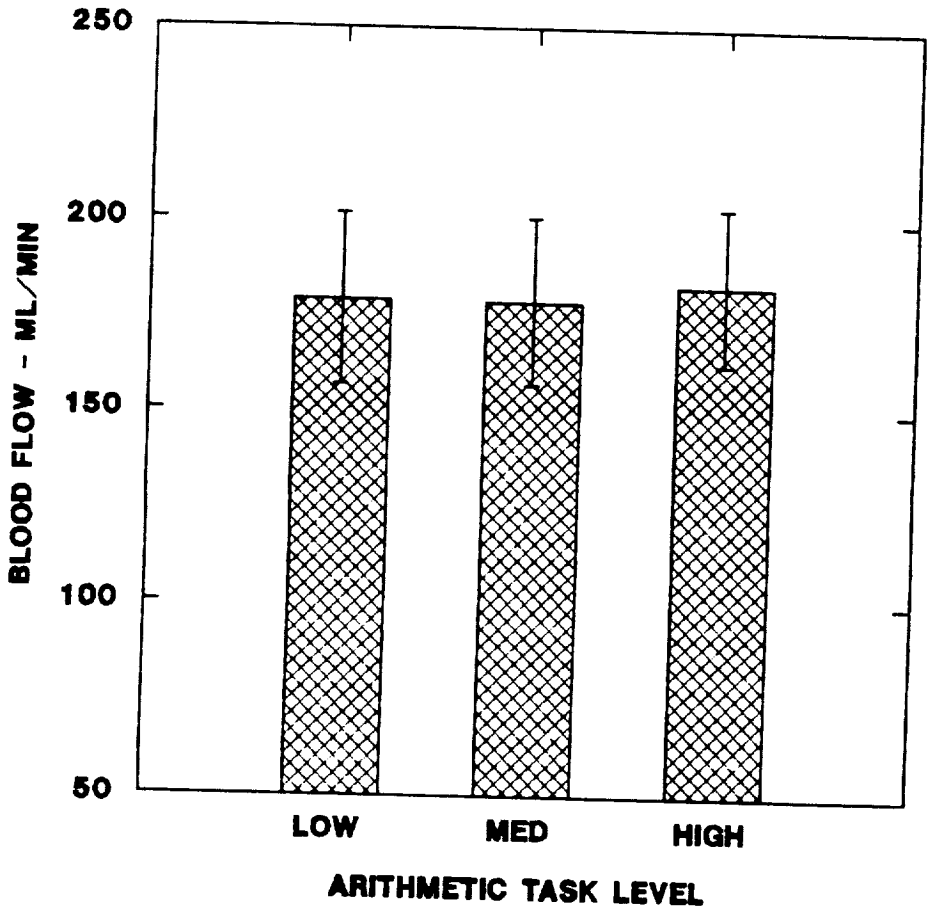

FIGURE VI.2.-3

CONTRACTILITY INDEX vs. ARITHMETIC TASK LEVEL

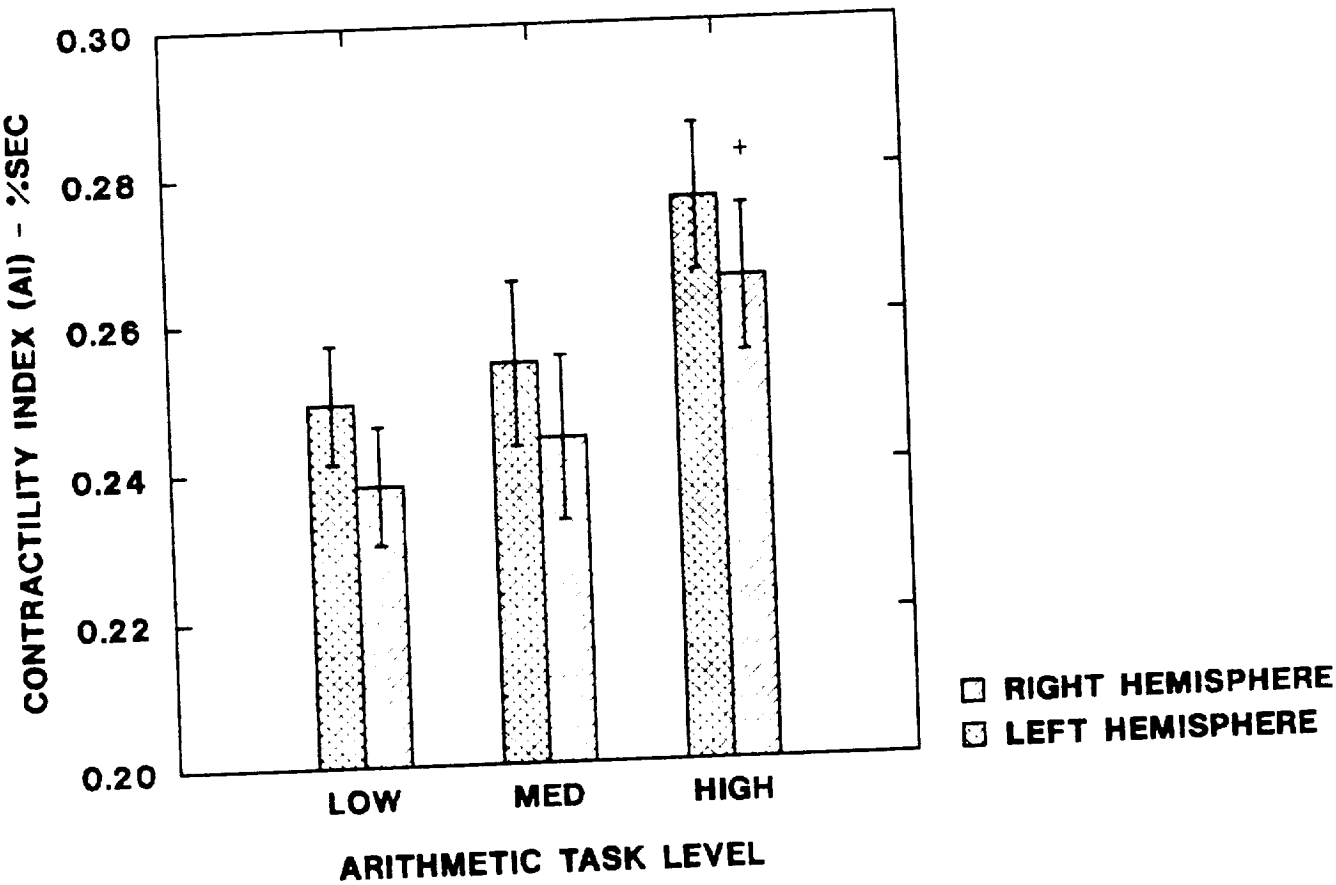

NO SIG. DIFF. RIGHT AND LEFT

FIGURE VI.2.-4

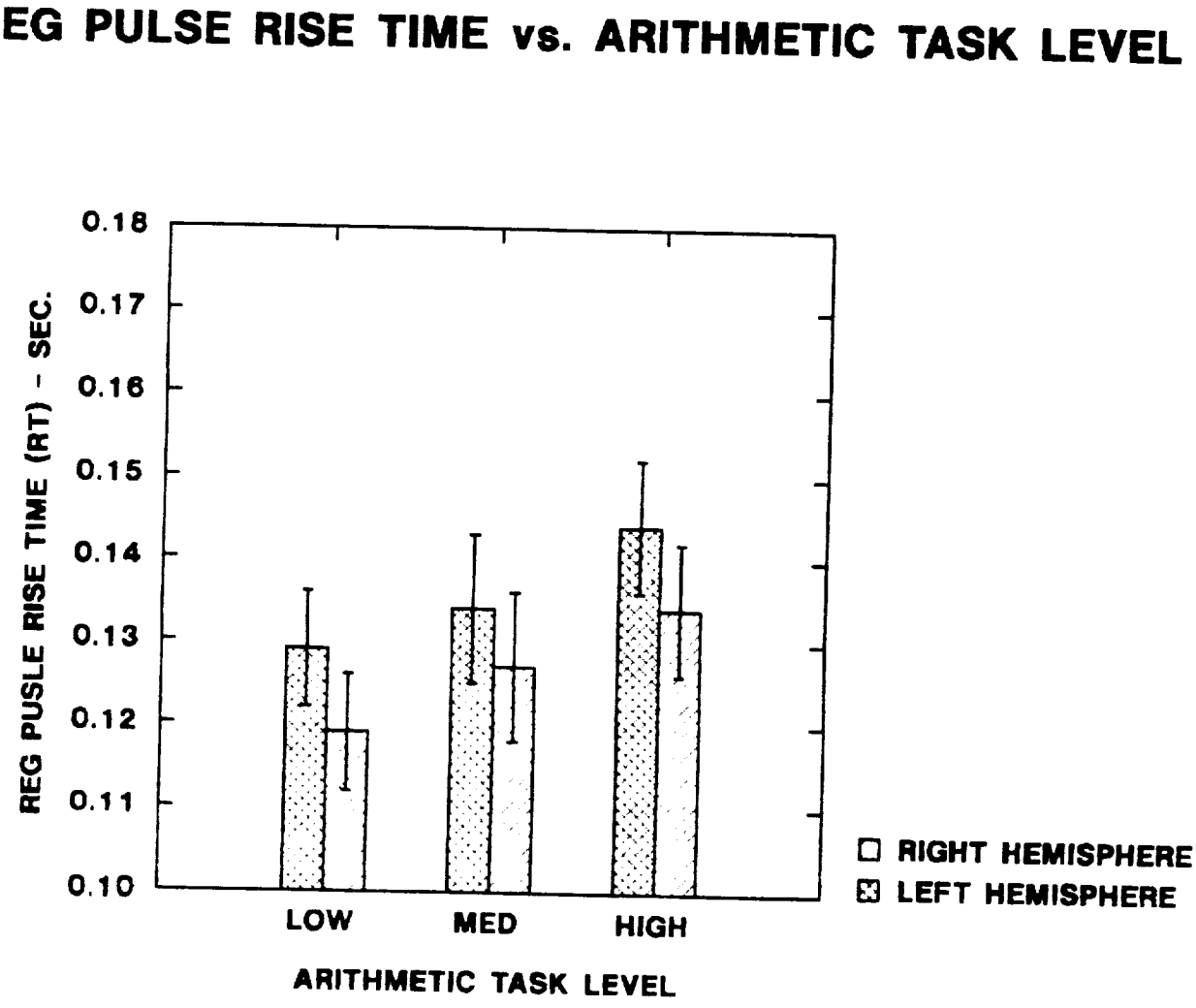

LEFT > RIGHT ($P < 0.01$) FOR ALL TASK LEVELS

FIGURE VI.2.-5

PULSE TRANSIT TIME vs. ARITHMETIC TASK LEVEL

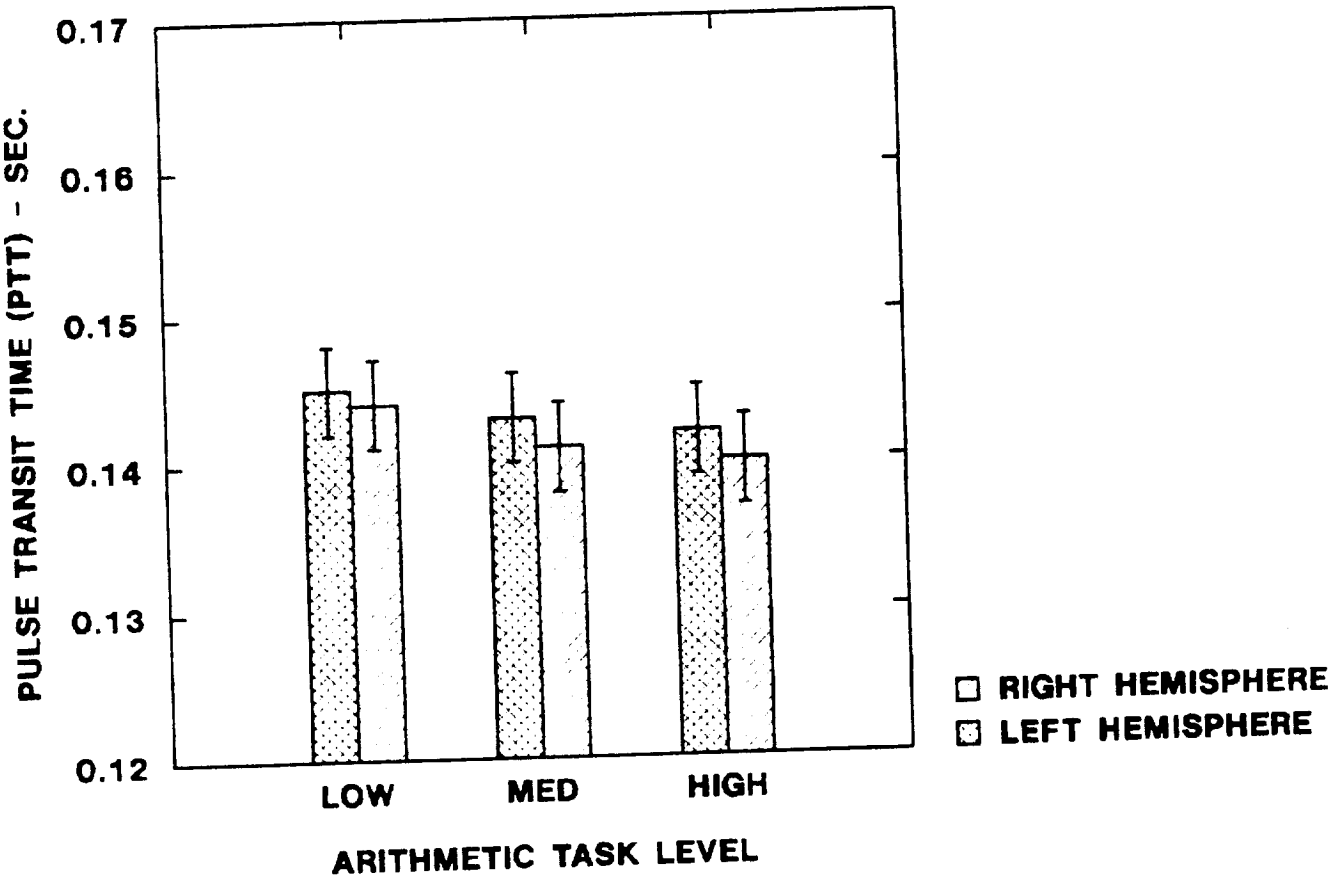

NO SIG. DIFF. RIGHT AND LEFT

FIGURE VI.2.-6

REG PULSE SYSTOLIC AREA vs. ARITHMETIC TASK LEVEL

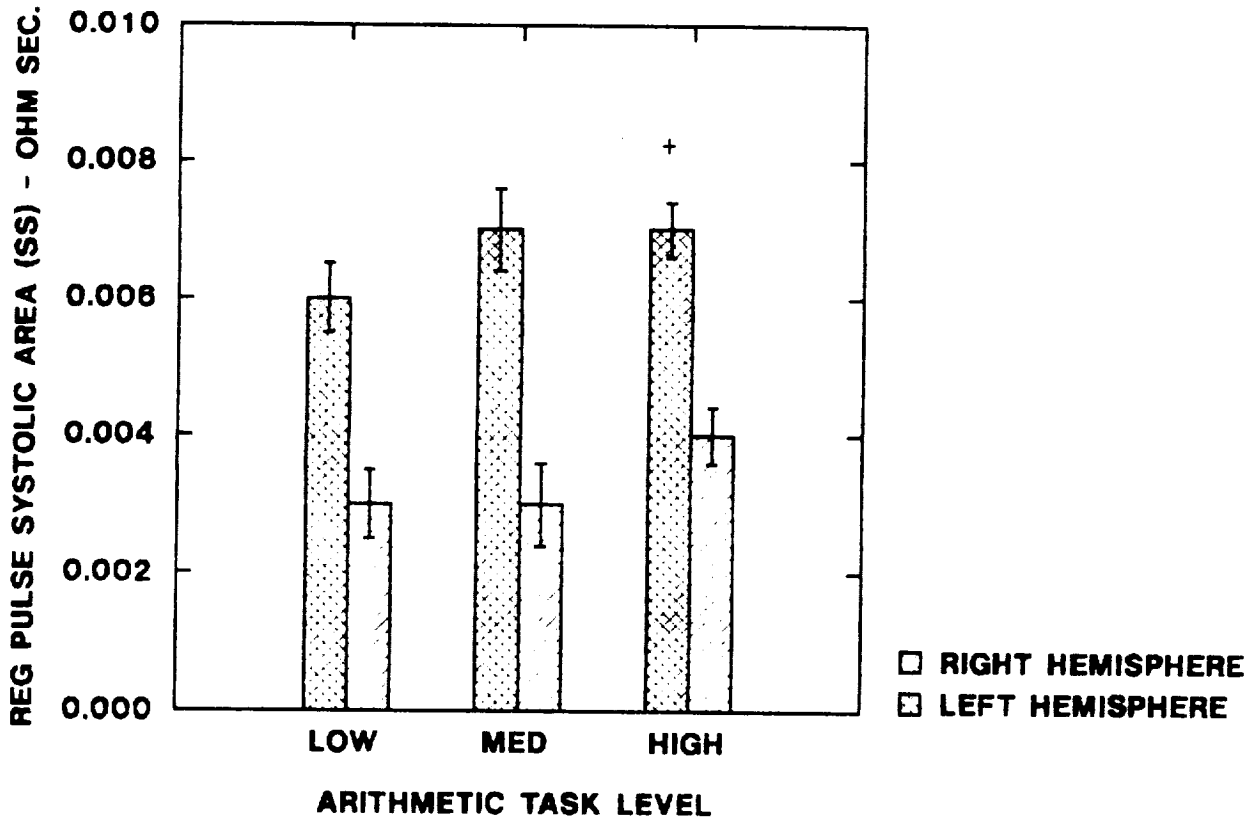

LEFT > RIGHT ($P < 0.05$) FOR ALL TASK LEVELS

FIGURE VI.2.-7

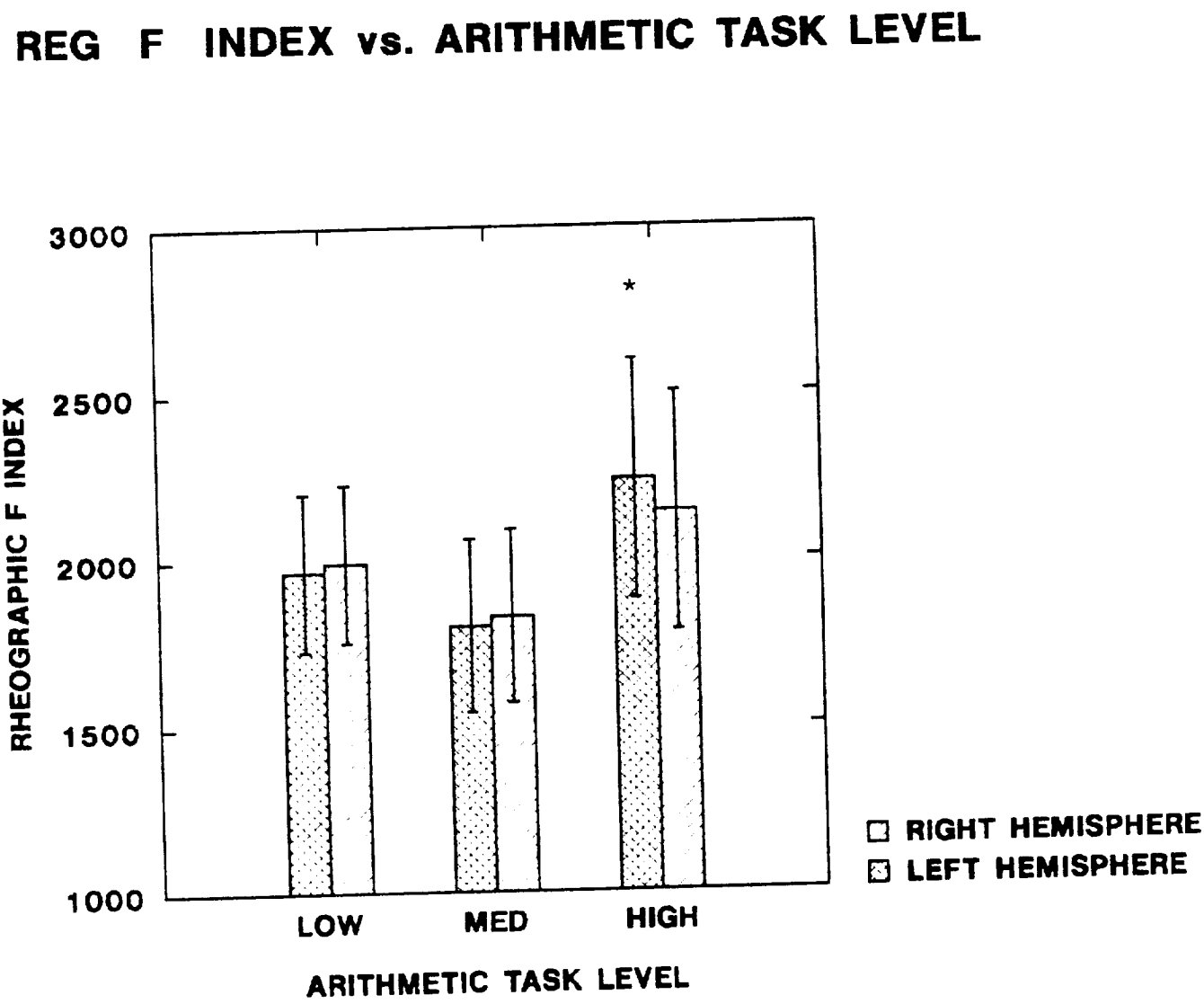

NO SIG. DIFF. RIGHT AND LEFT

FIGURE VI.2.-8

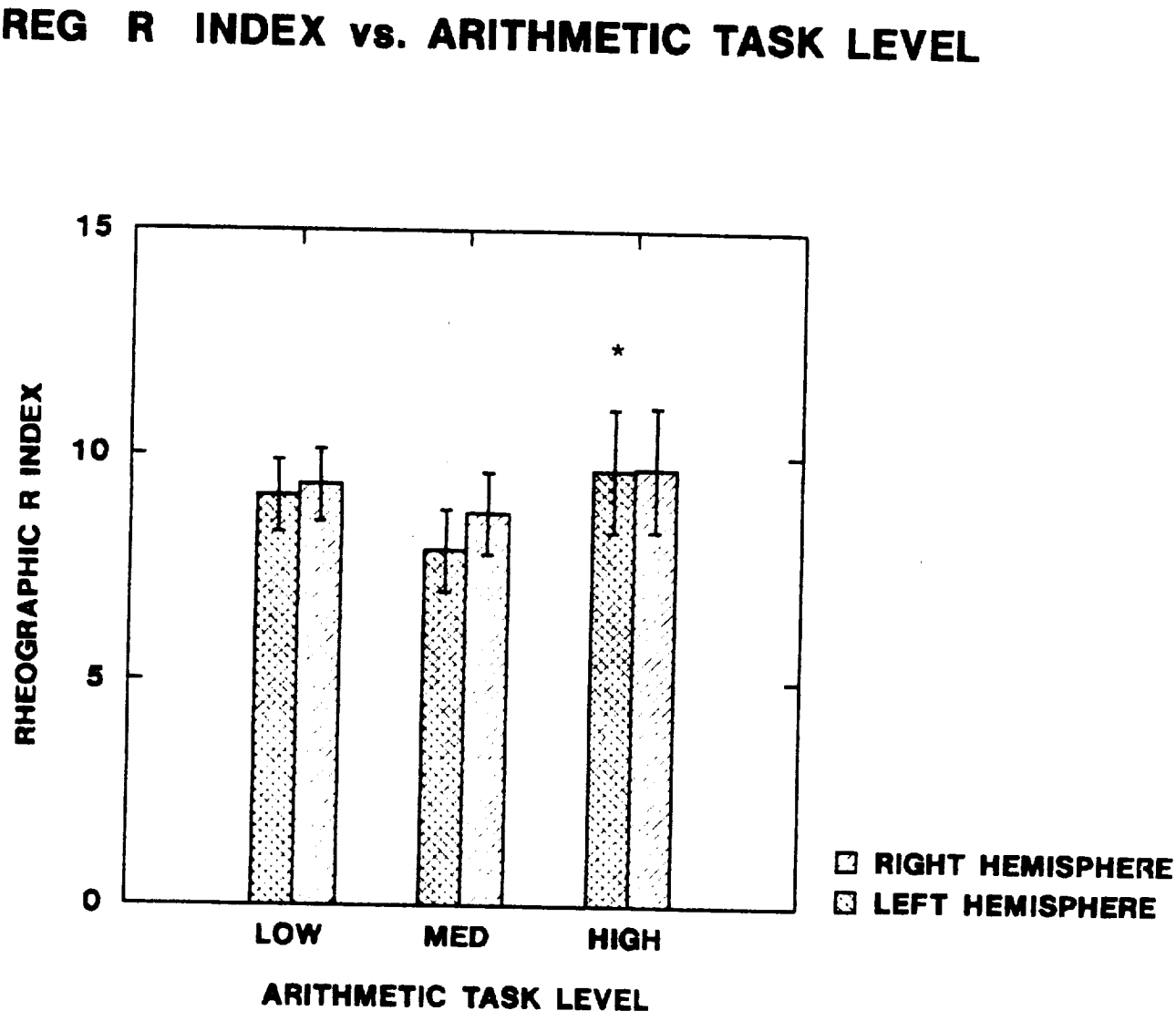

NO SIG. DIFF. RIGHT AND LEFT

FIGURE VI.2.-9

MATH HEART RATE RESPONSE

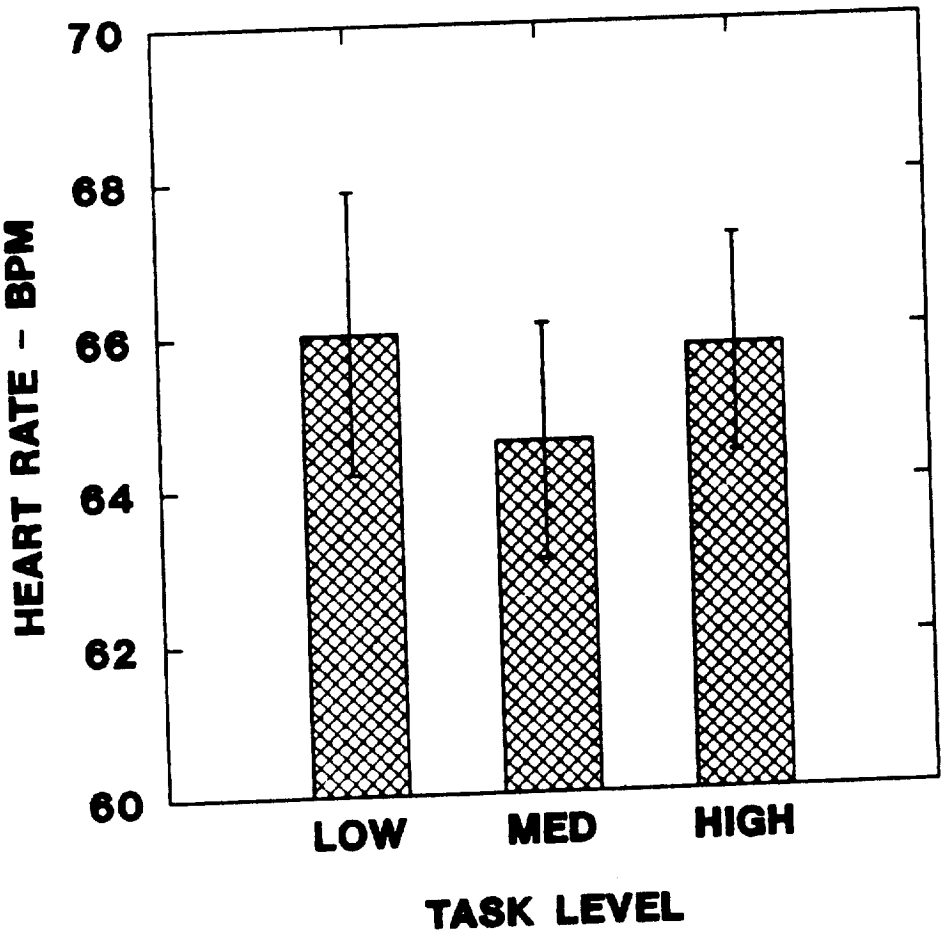

FIGURE VI.2.-10

ARITHMETIC TASK RESPONSE TIME

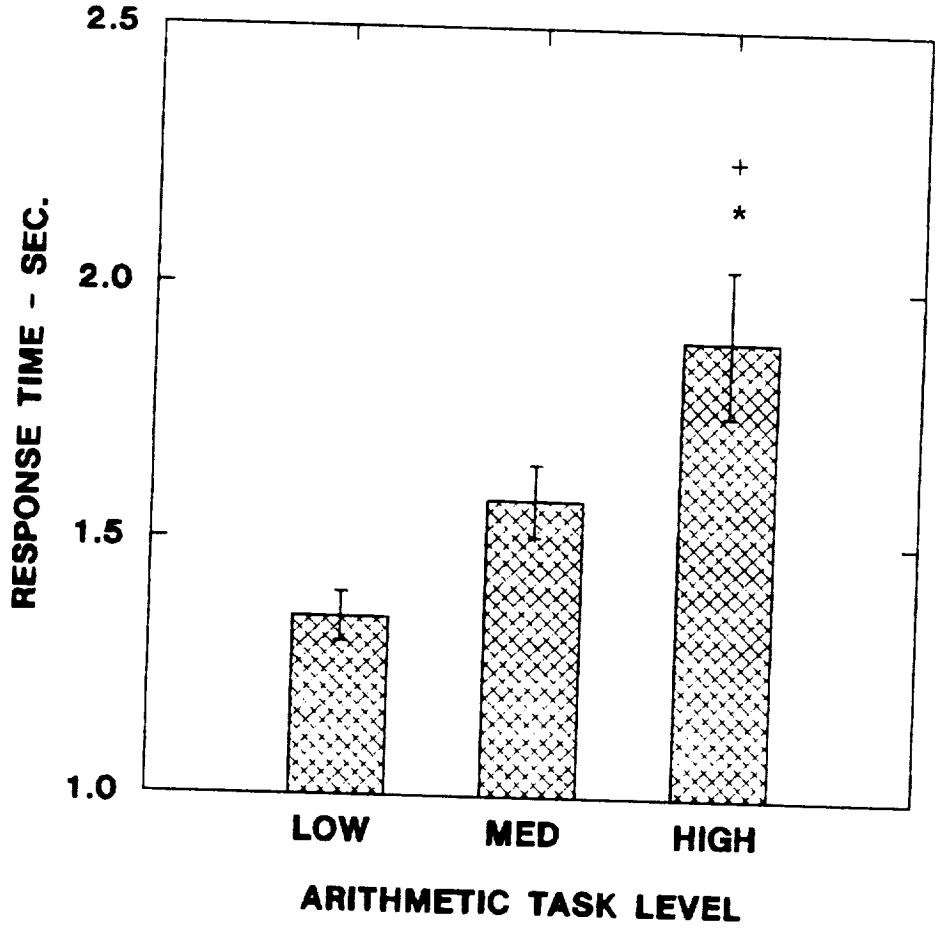

FIGURE VI.2.-11

CEREBRAL BLOOD FLOW vs. SPATIAL TASK

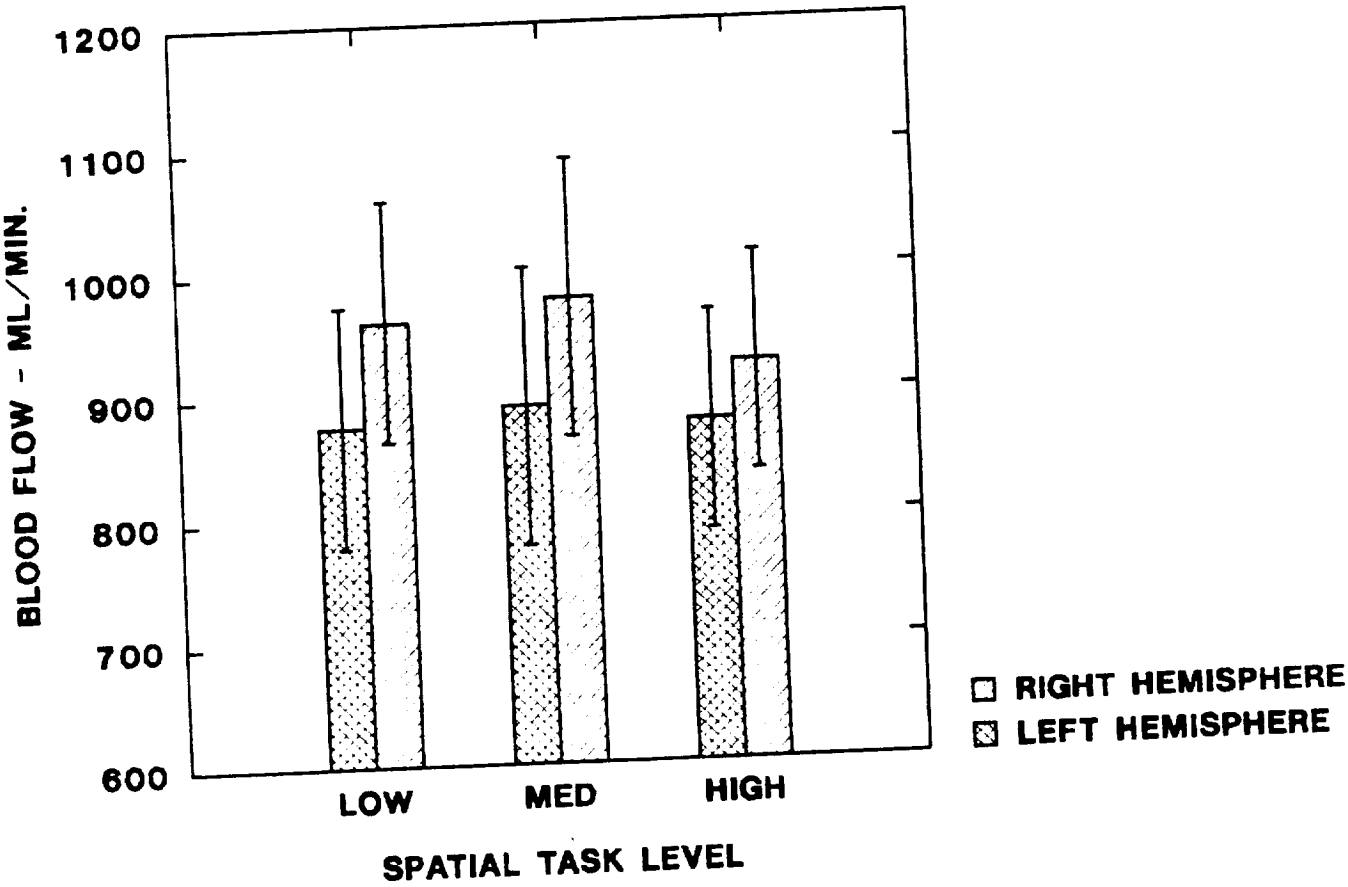

NO SIG. DIFF. RIGHT AND LEFT

FIGURE VI.2.-12

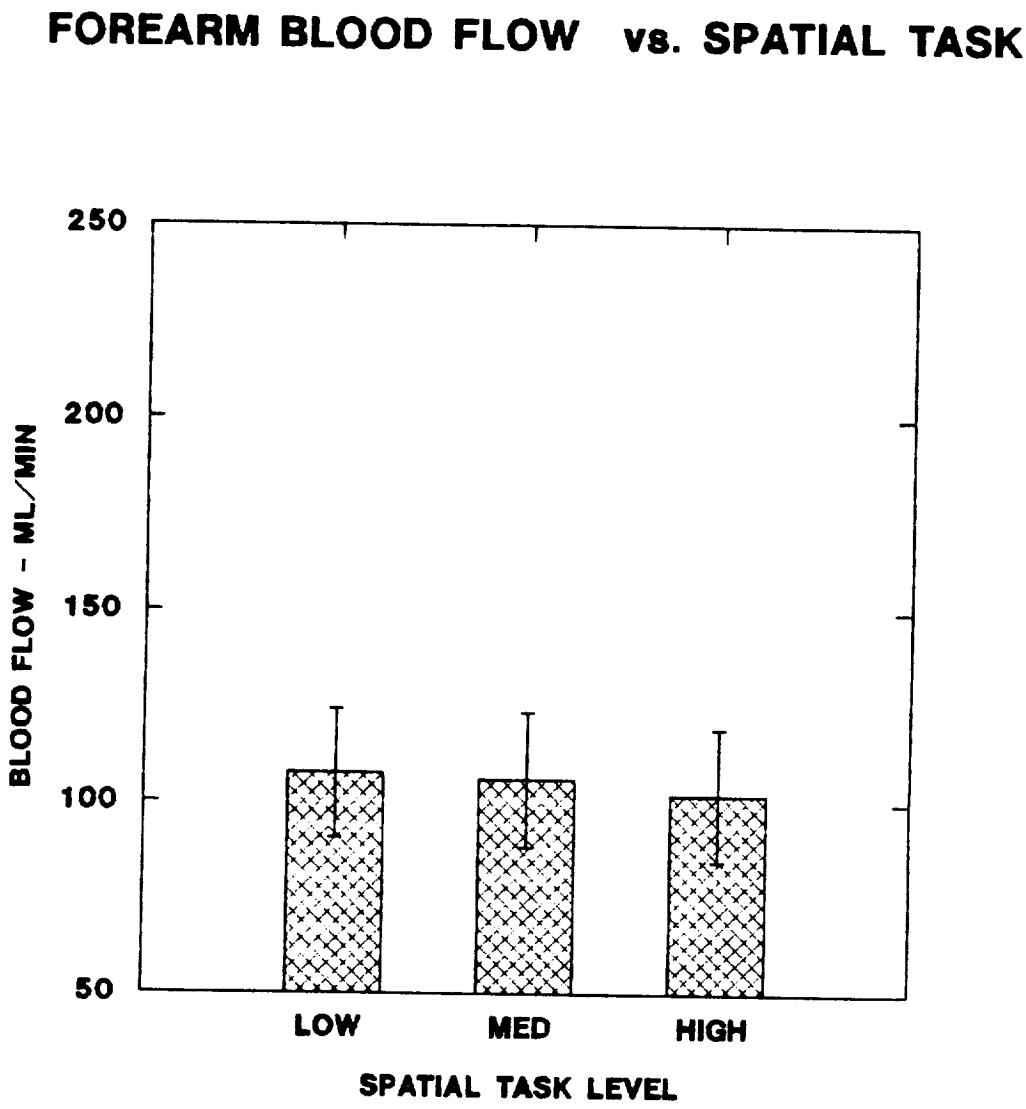

FIGURE VI.2.-13

CONTRACTILITY INDEX vs. SPATIAL TASK

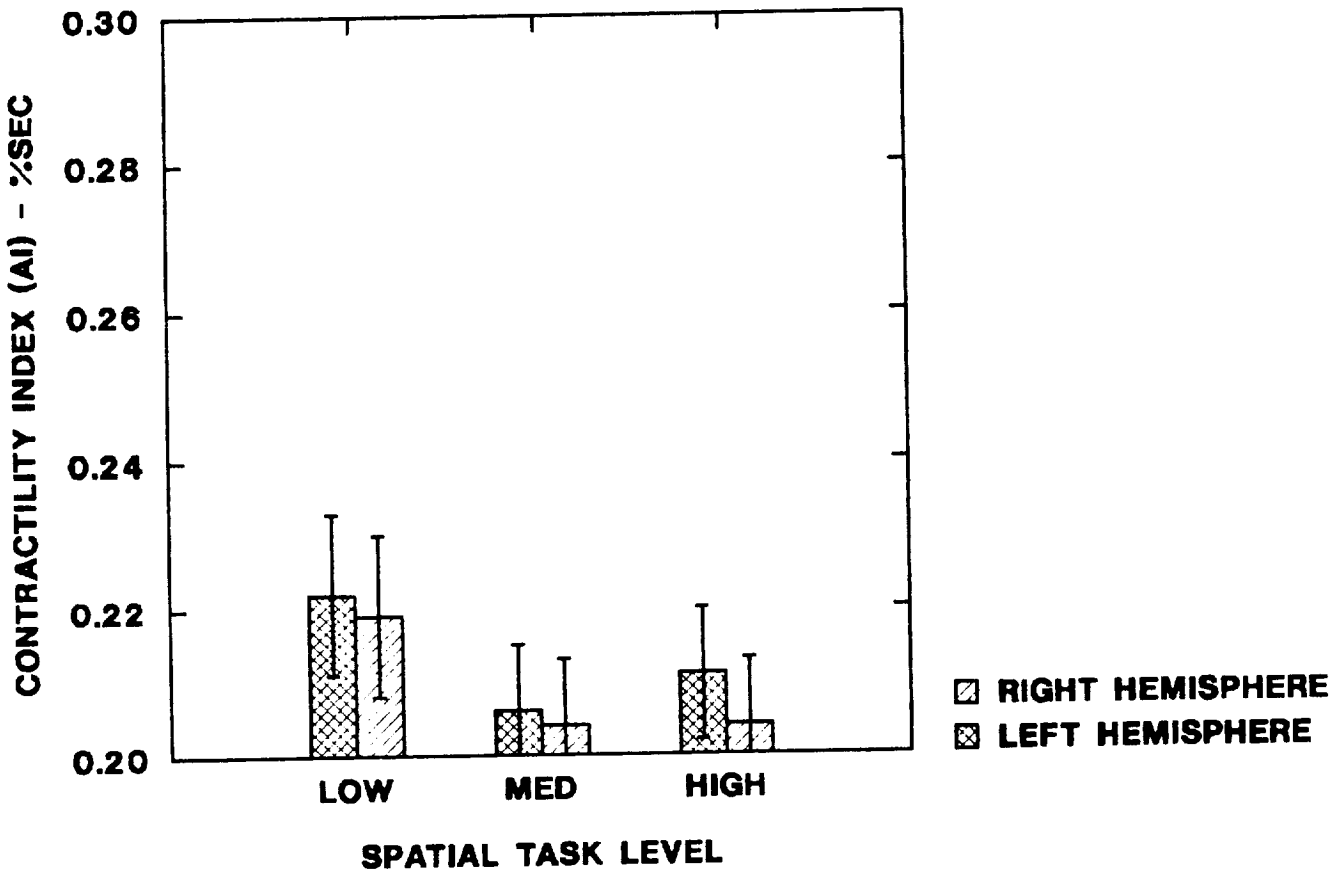

NO SIG. DIFF. RIGHT AND LEFT

FIGURE VI.1.-14

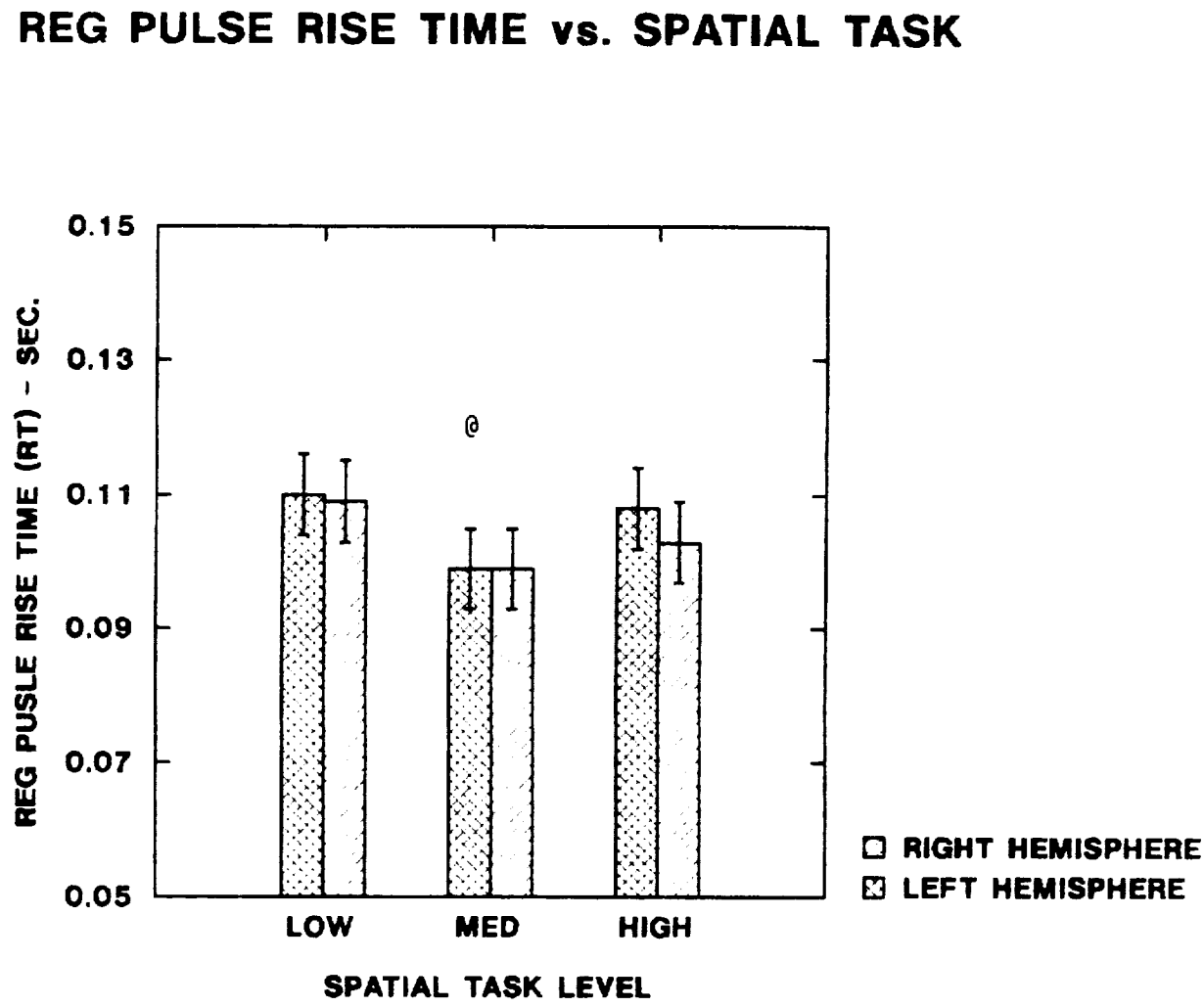

NO SIG. DIFF. RIGHT AND LEFT

FIGURE VI.2.-15

PULSE TRANSIT TIME vs. SPATIAL TASK

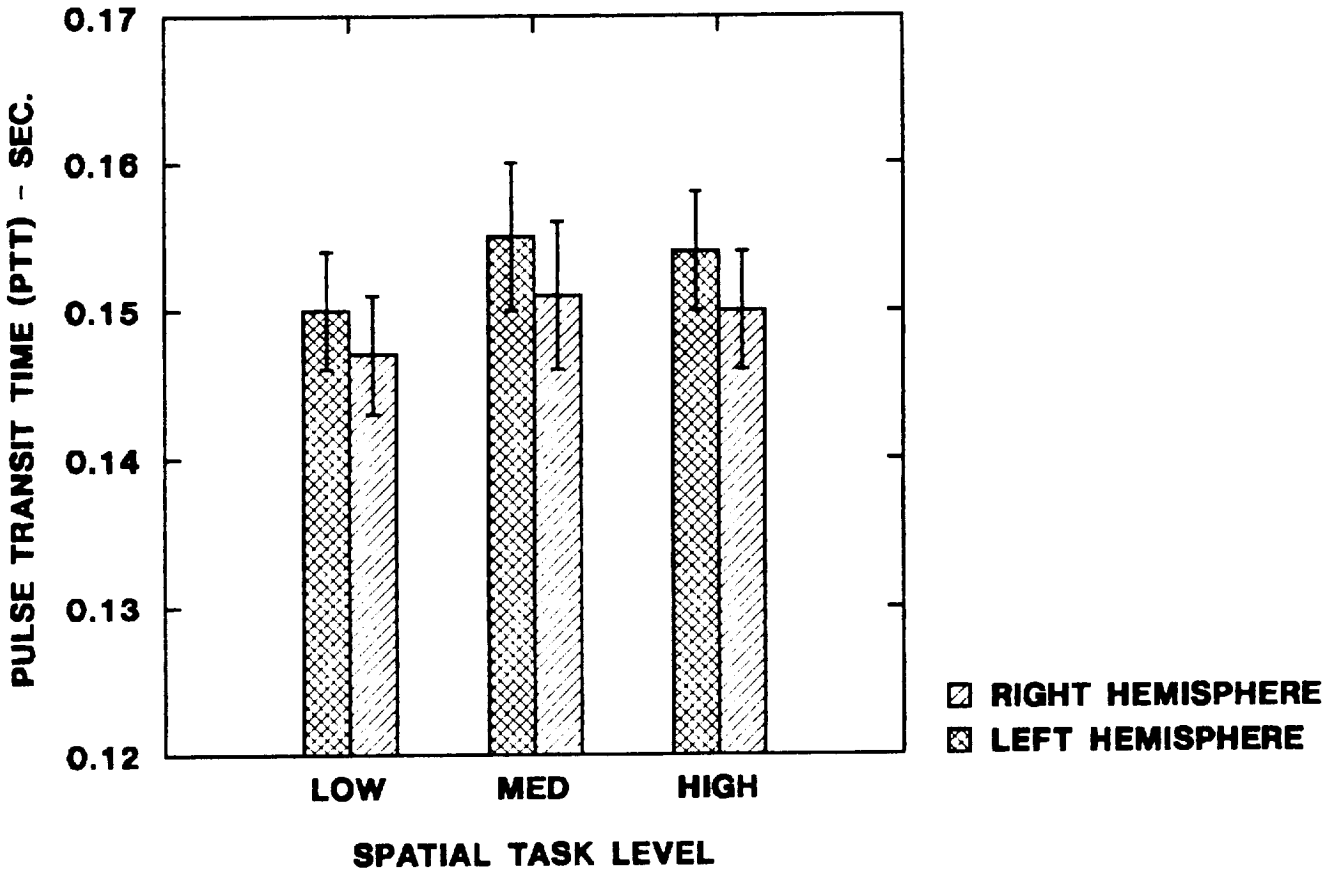

NO SIG. DIFF. RIGHT AND LEFT

FIGURE VI.2.-16

REG PULSE SYSTOLIC AREA vs. SPATIAL TASK

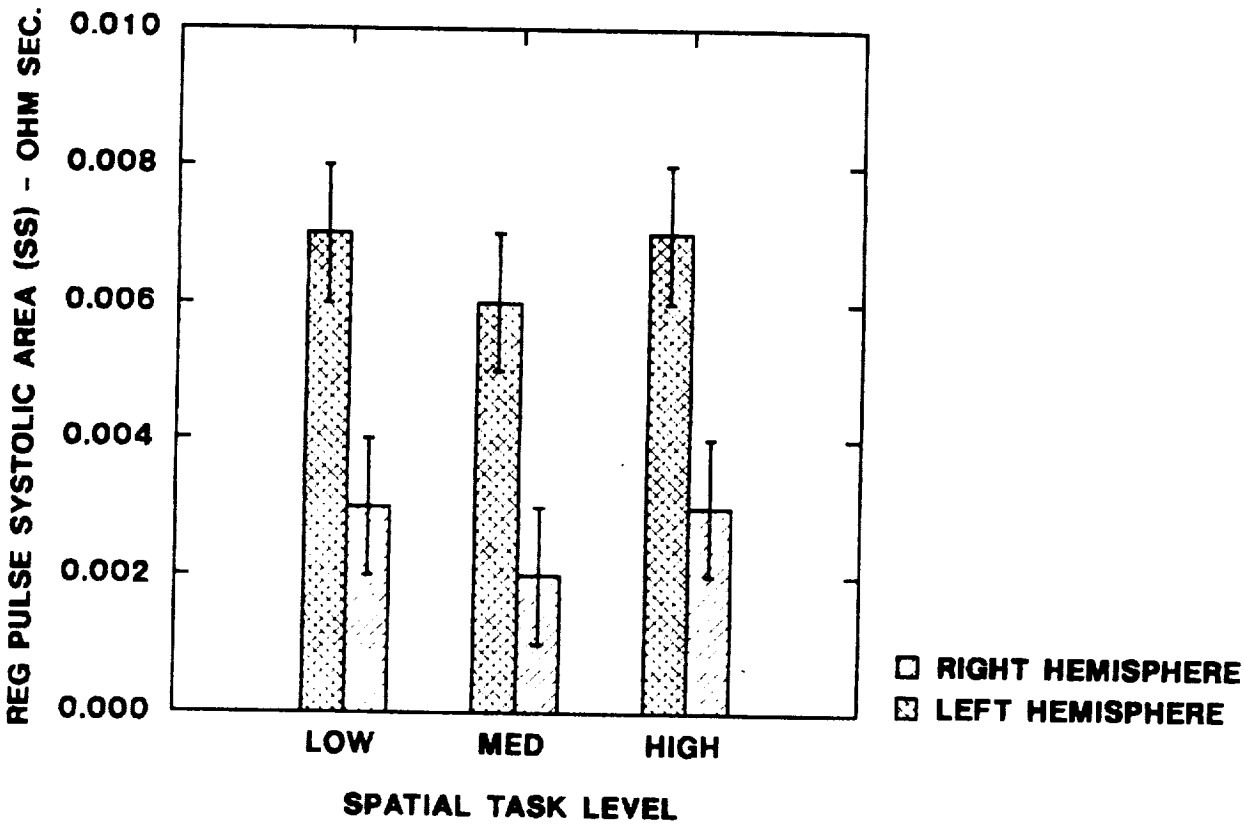

LEFT > RIGHT ($P < 0.01$) FOR ALL TASK LEVELS

FIGURE VI.2.-17

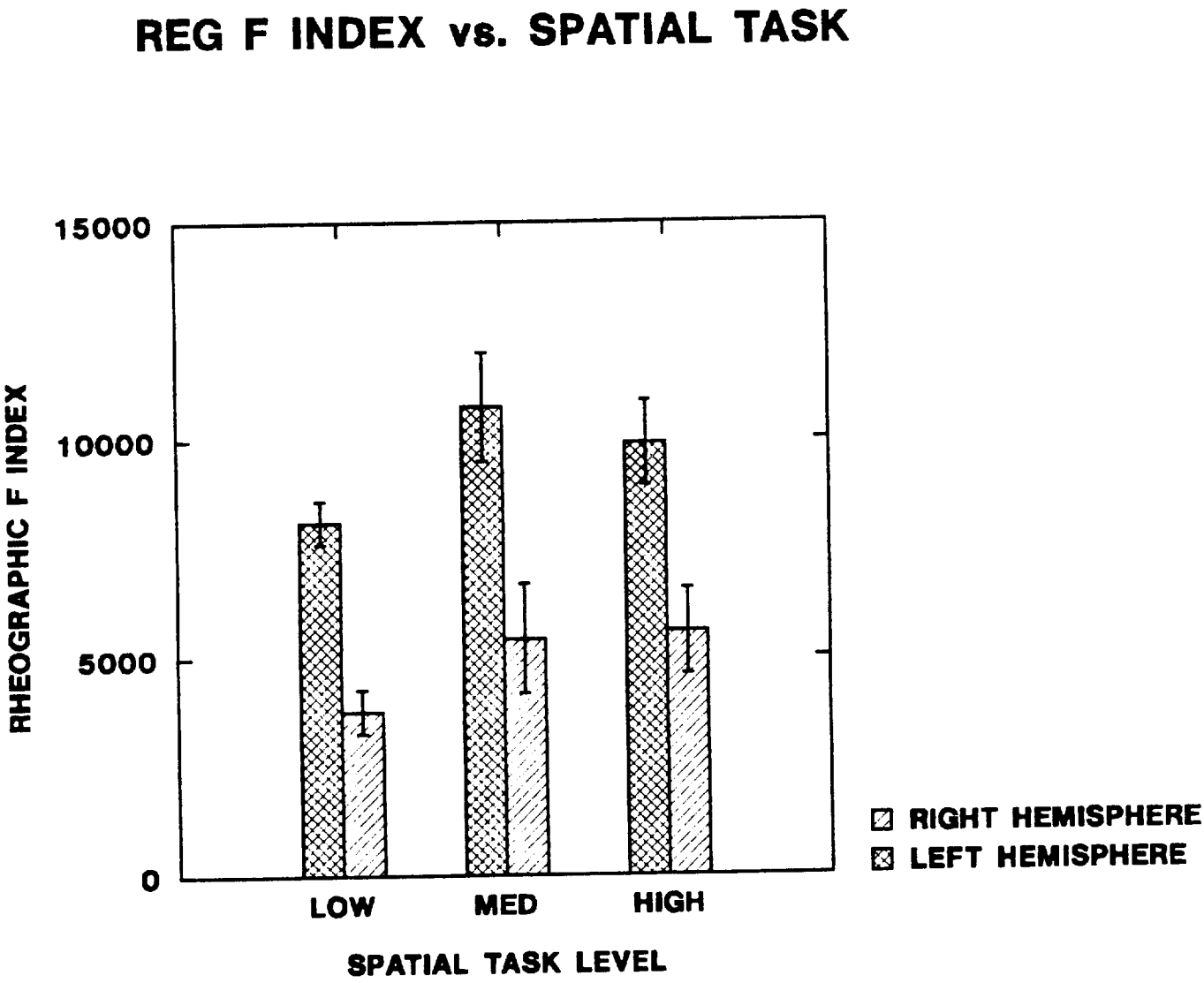

LEFT > RIGHT ($P < 0.01$) FOR ALL TASK LEVELS

FIGURE VI.2.-18

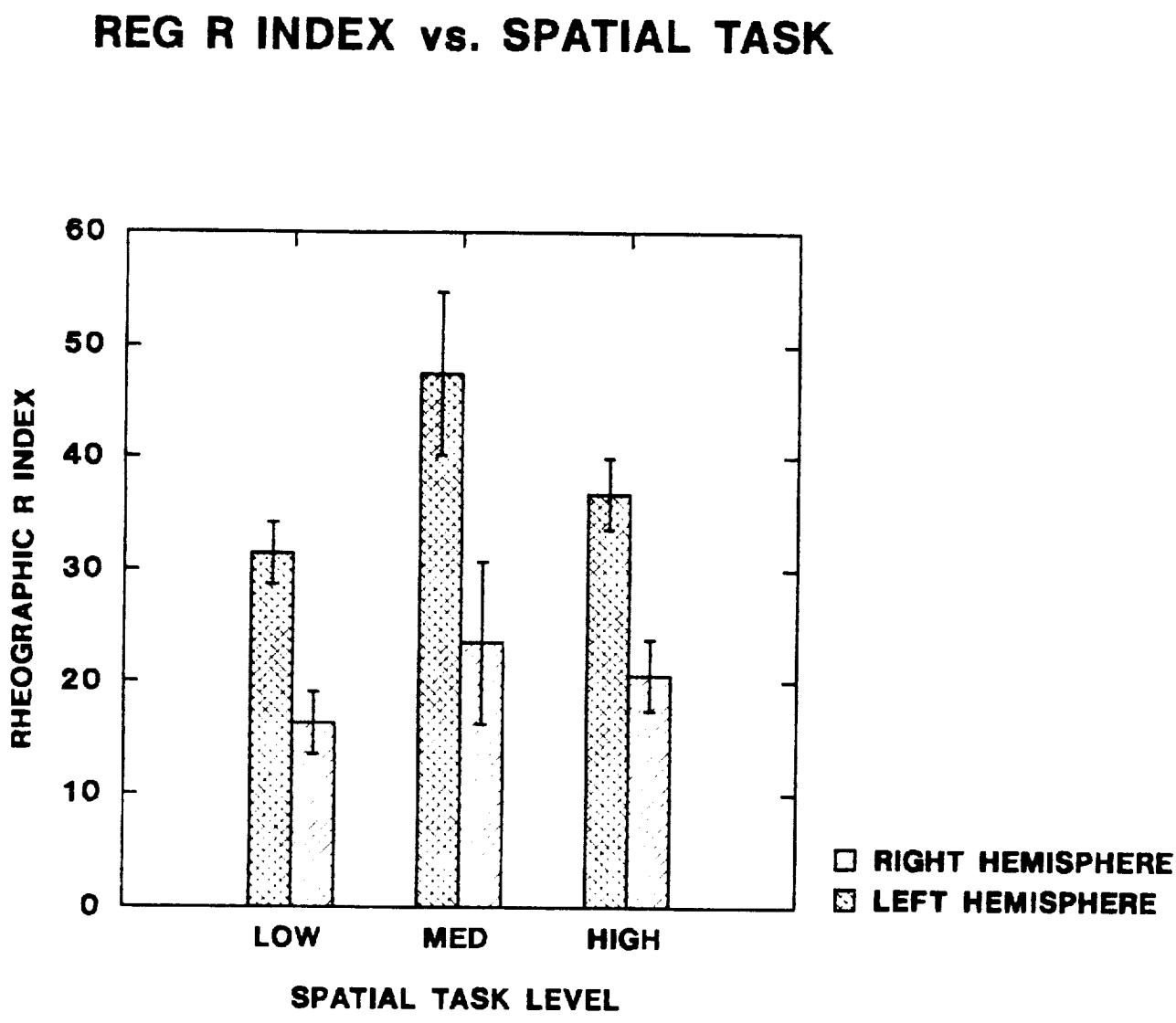

LEFT > RIGHT ($P < 0.01$) FOR ALL TASK LEVELS

FIGURE V.2.-19

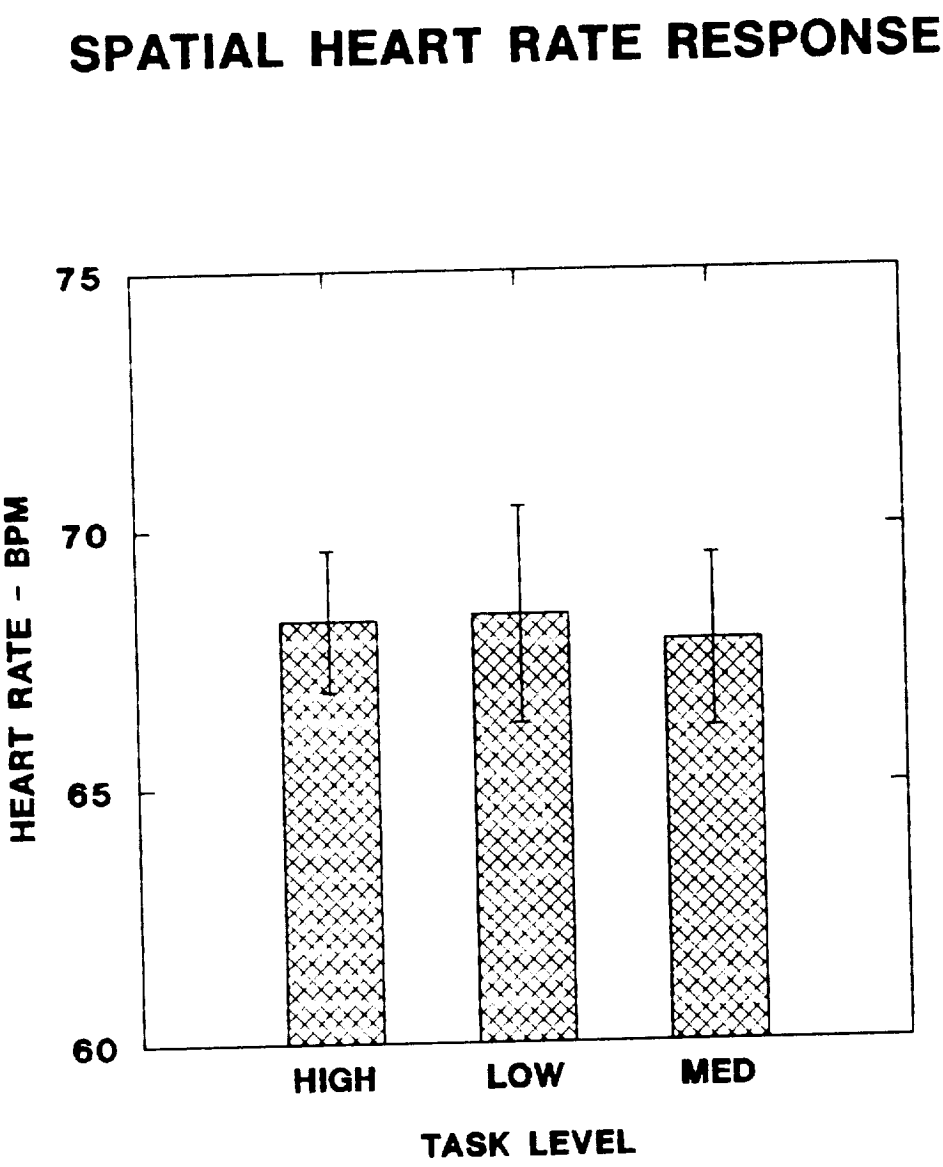
SPATIAL HEART RATE RESPONSE
75
70
65
60
HEART RATE - BPM
HIGH
LOW
MED
TASK LEVEL

FIGURE VI.2.-20

SPATIAL TASK RESPONSE TIME

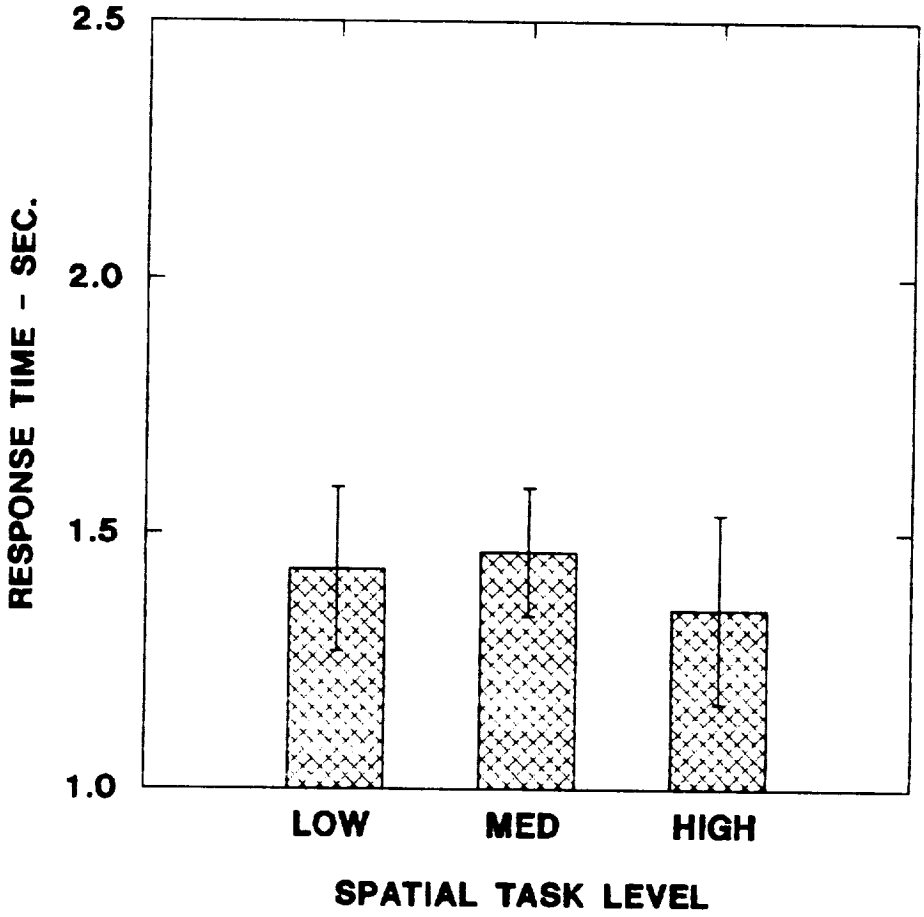

FIGURE VI.2.-21

CEREBRAL BLOOD FLOW vs. VERBAL TASK

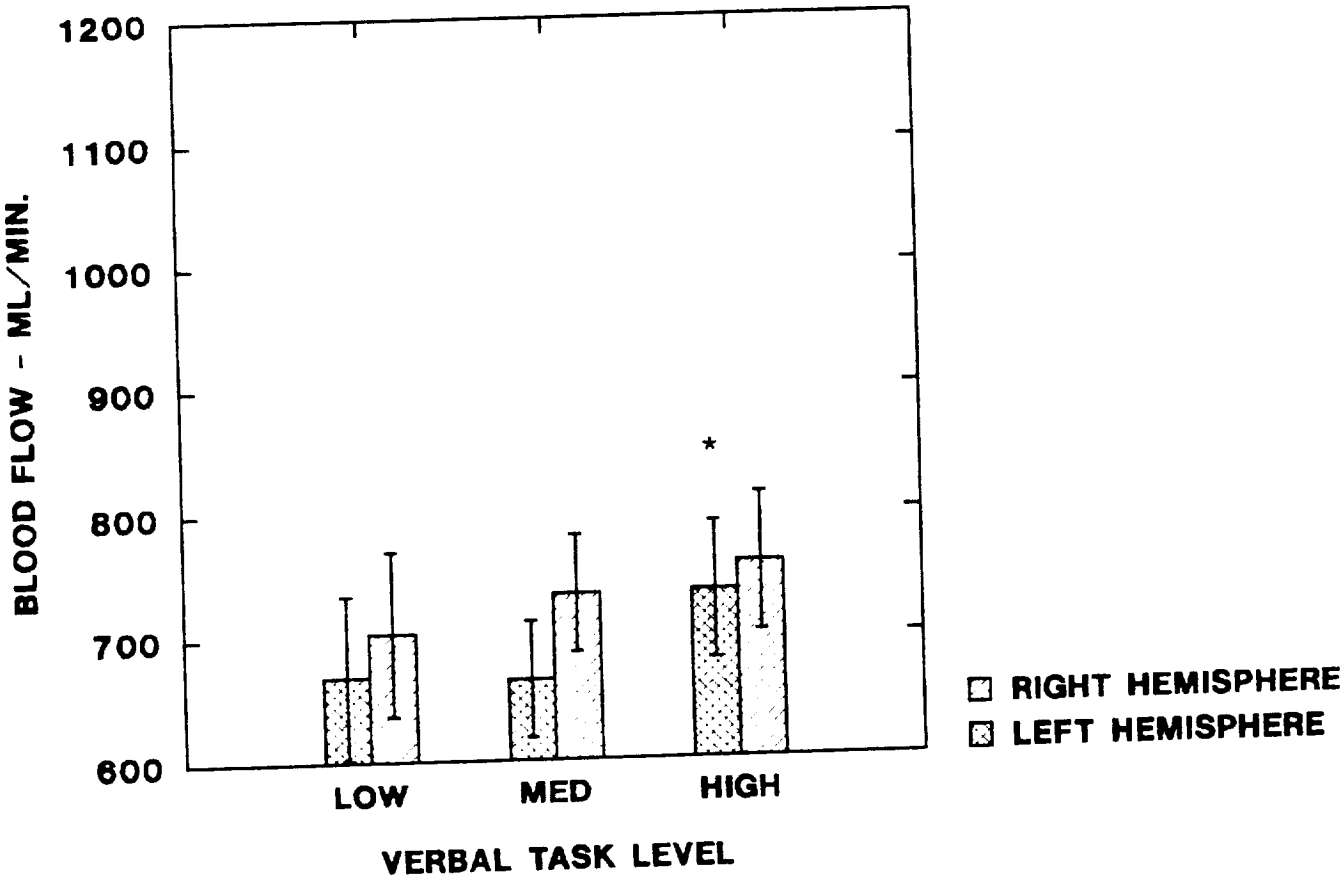

NO SIG. DIFF. RIGHT AND LEFT

FIGURE VI.2.-22

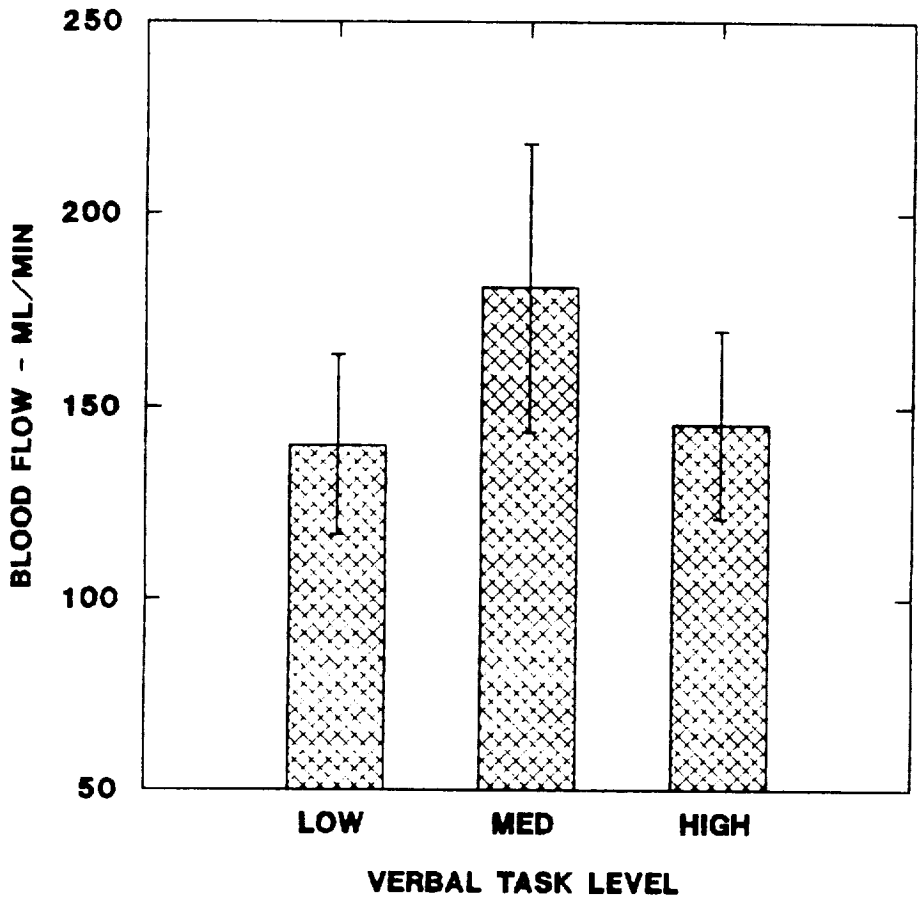

C-3

FIGURE VI.2.-23

CONTRACTILITY INDEX vs. VERBAL TASK

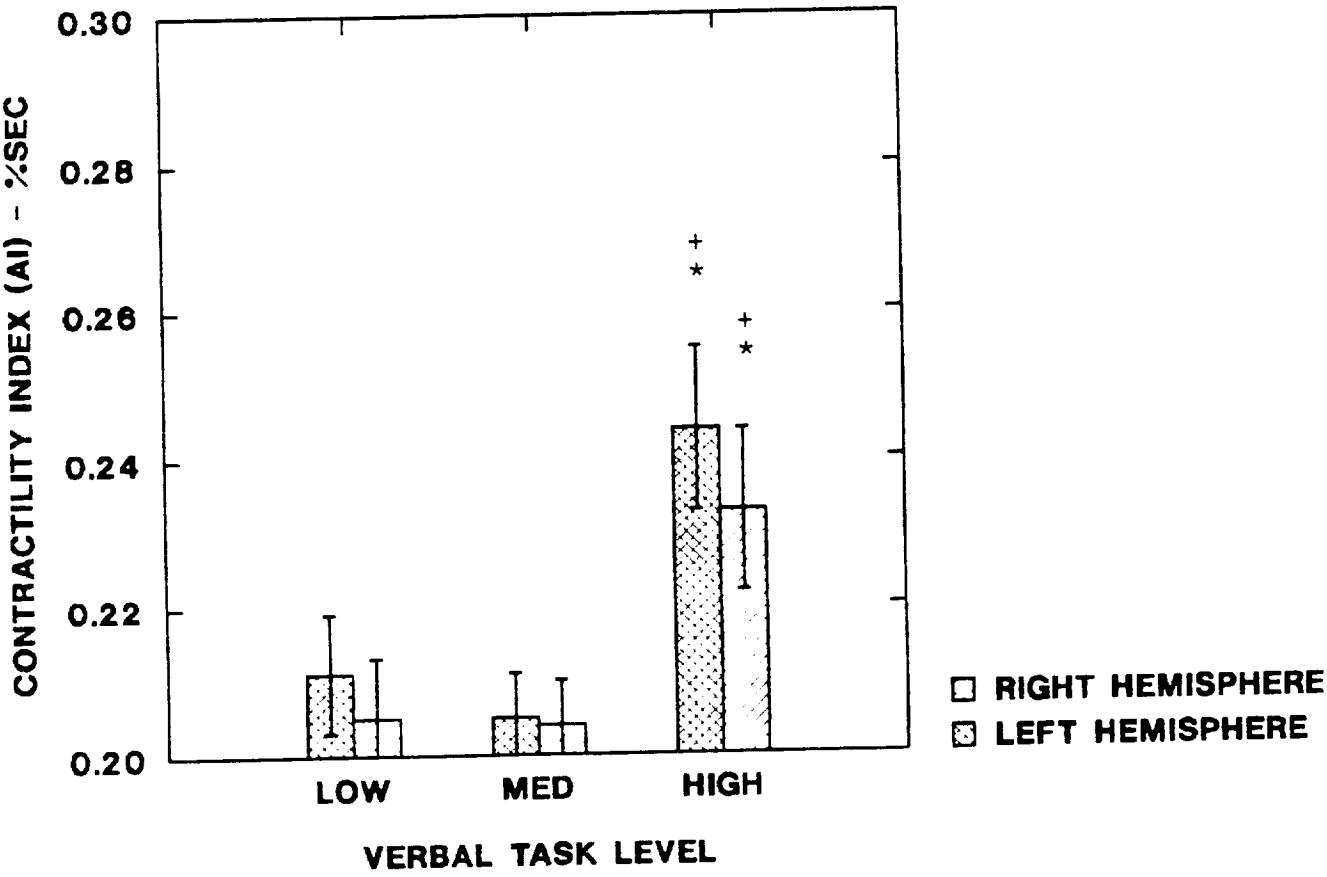

NO SIG. DIFF. RIGHT AND LEFT

FIGURE VI.2.-24

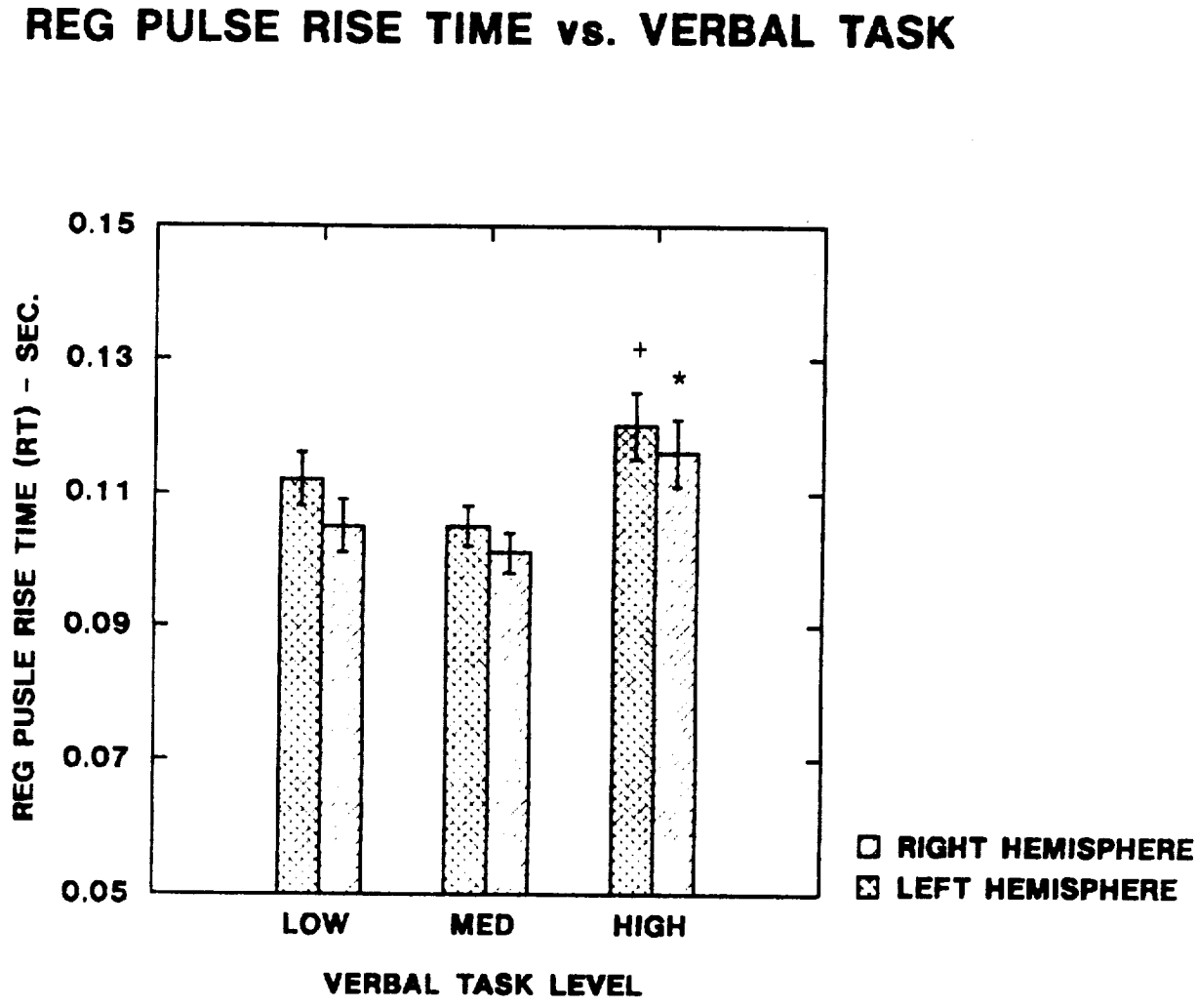

NO SIG. DIFF. RIGHT AND LEFT

FIGURE VI.2.-25

PULSE TRANSIT TIME vs. VERBAL TASK

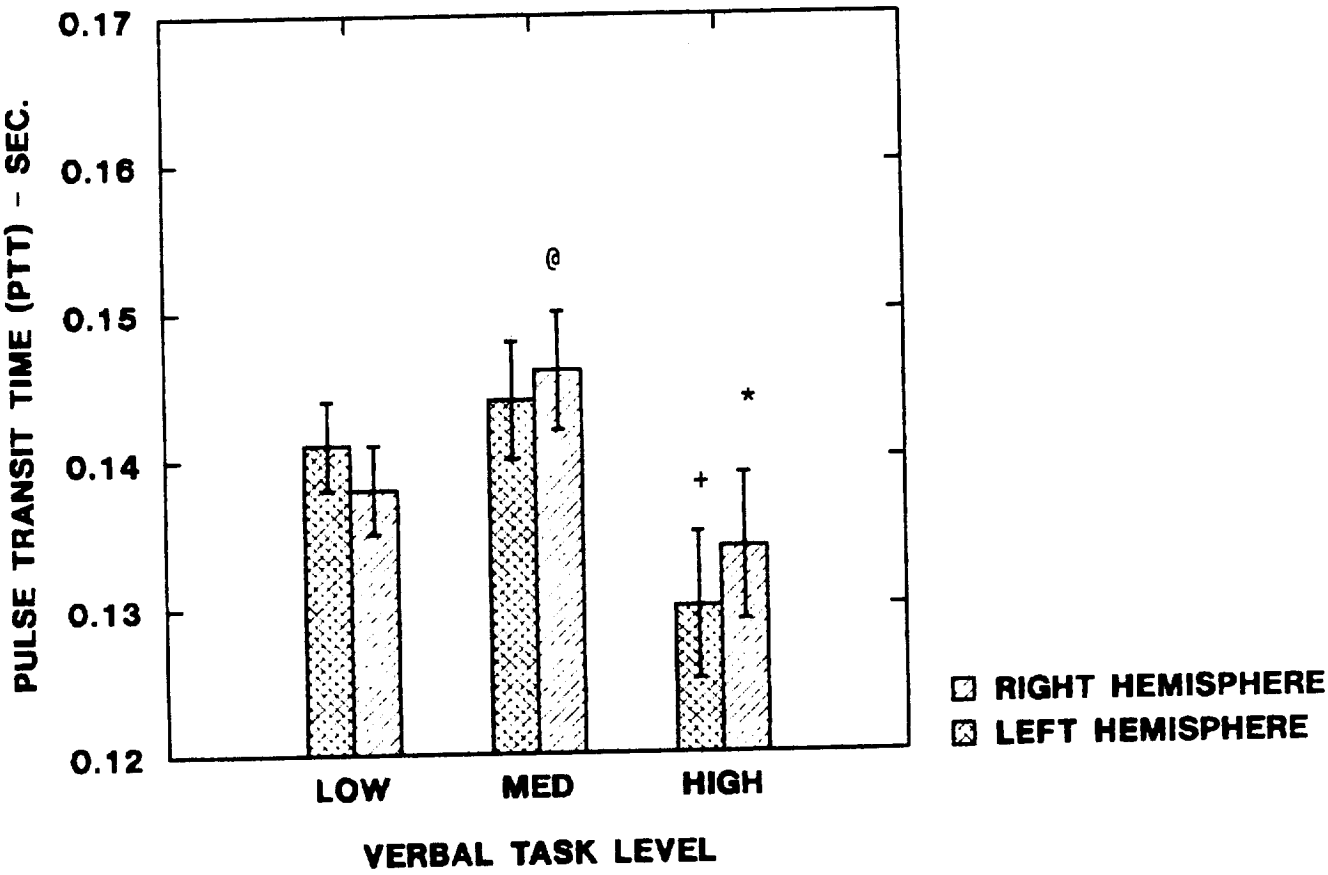

NO SIG. DIFF. RIGHT AND LEFT

FIGURE VI.2.-26

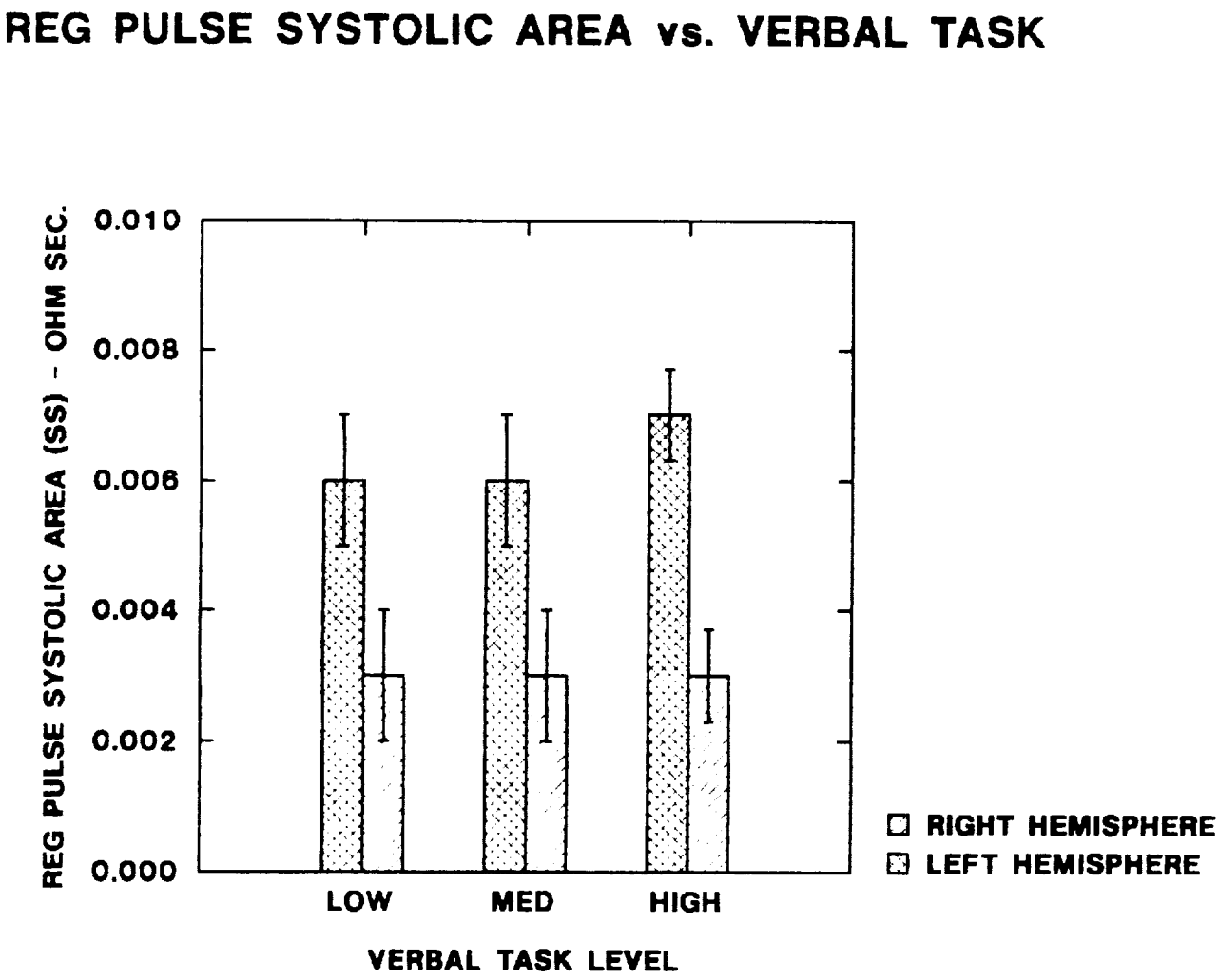

LEFT > RIGHT ($P < 0.01$) FOR ALL TASK LEVELS

FIGURE VI.2.-27

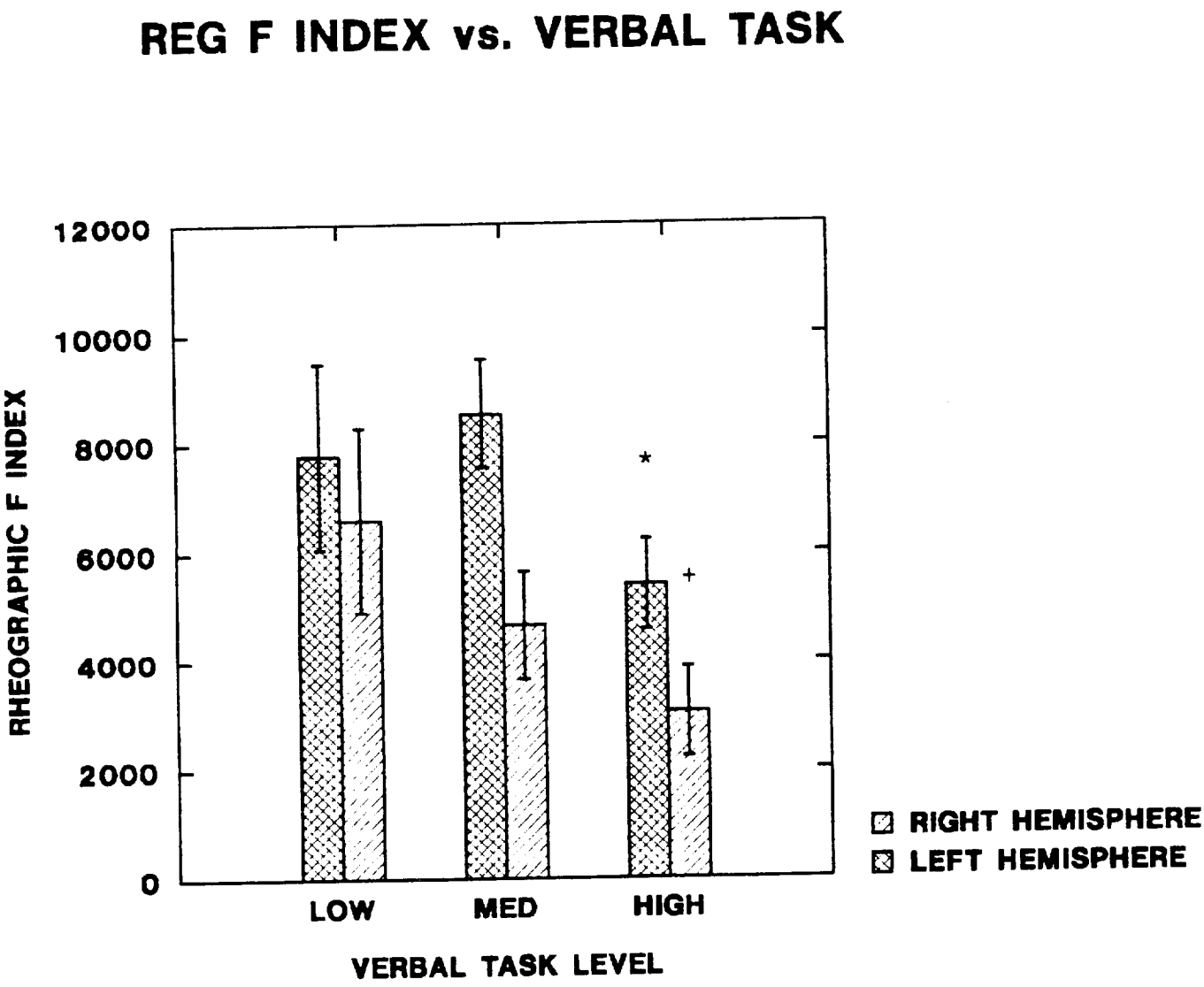

LEFT > RIGHT ($P < 0.01$) FOR MEDIUM AND HIGH TASK LEVELS

FIGURE VI.2.-28

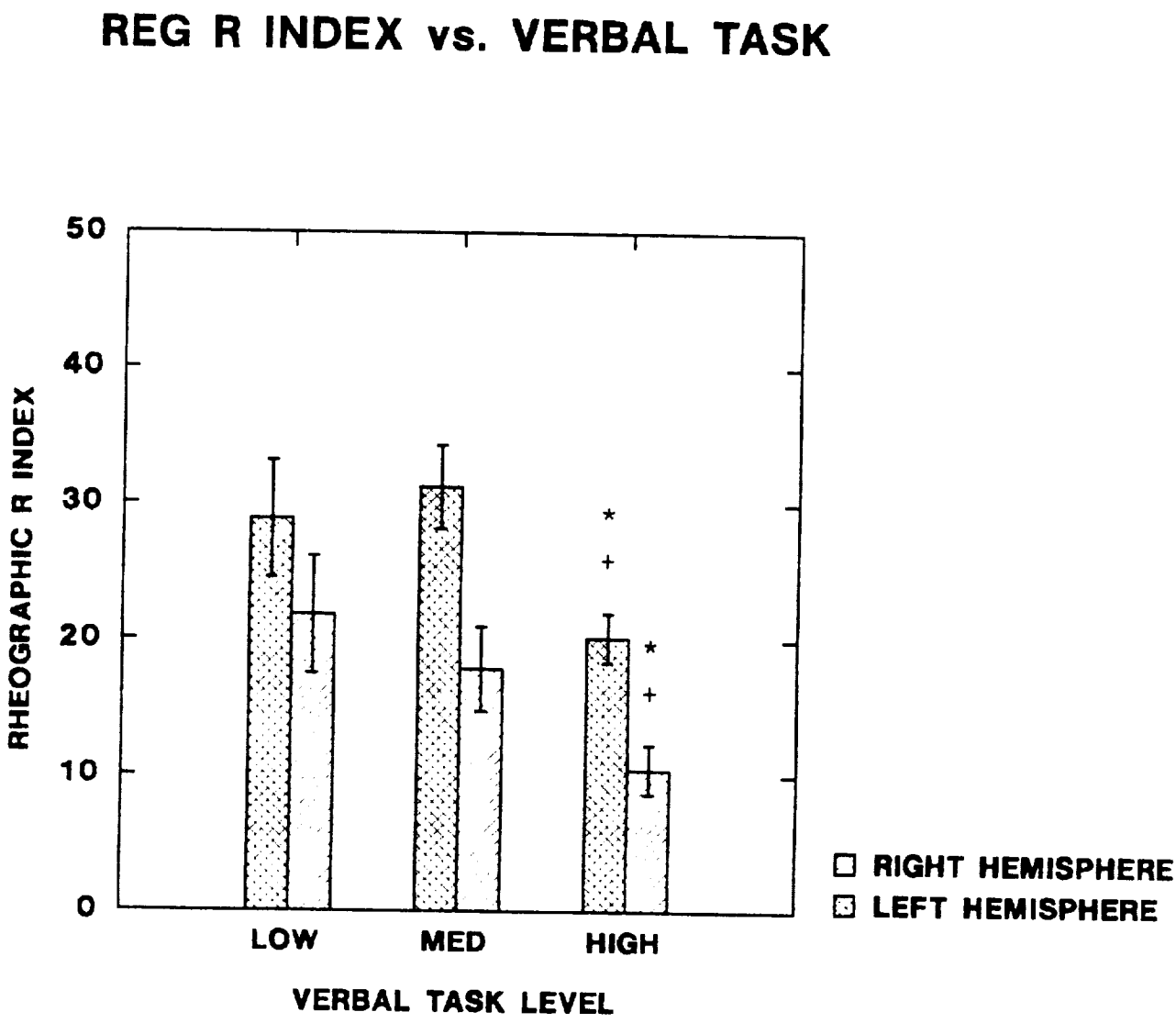

LEFT > RIGHT ($P < 0.01$) FOR MEDIUM AND HIGH TASK LEVELS

FIGURE VI.2.-29

VERBAL HEART RATE RESPONSE

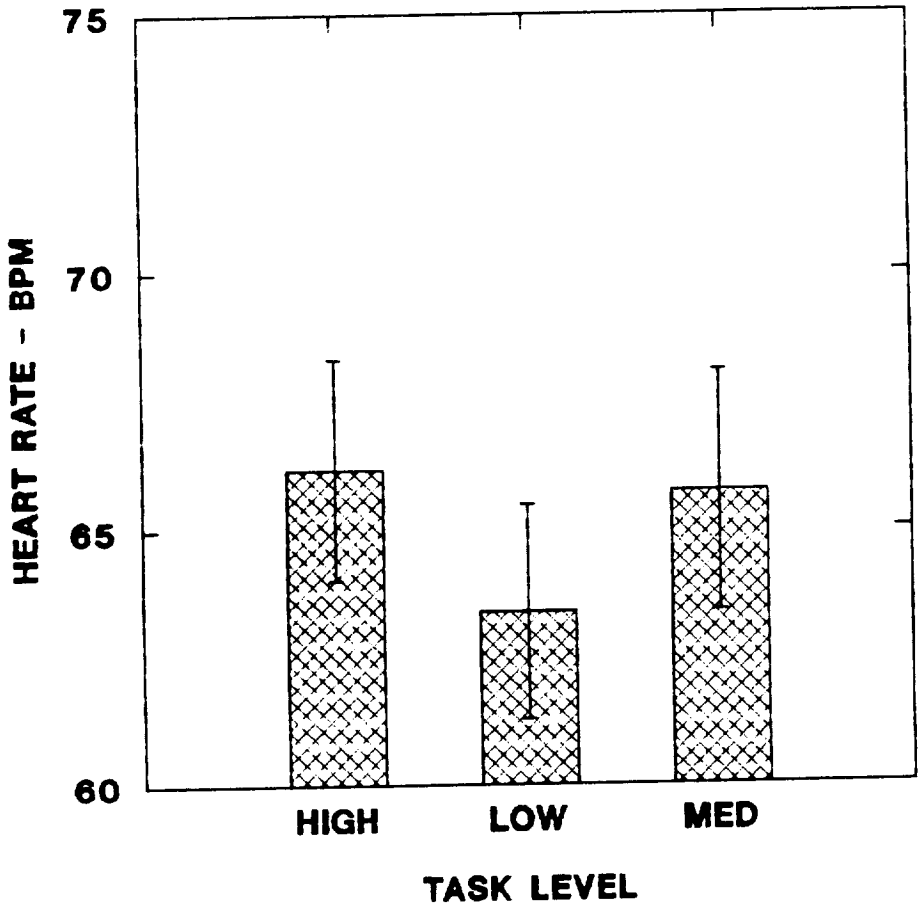

FIGURE VI.2.-30

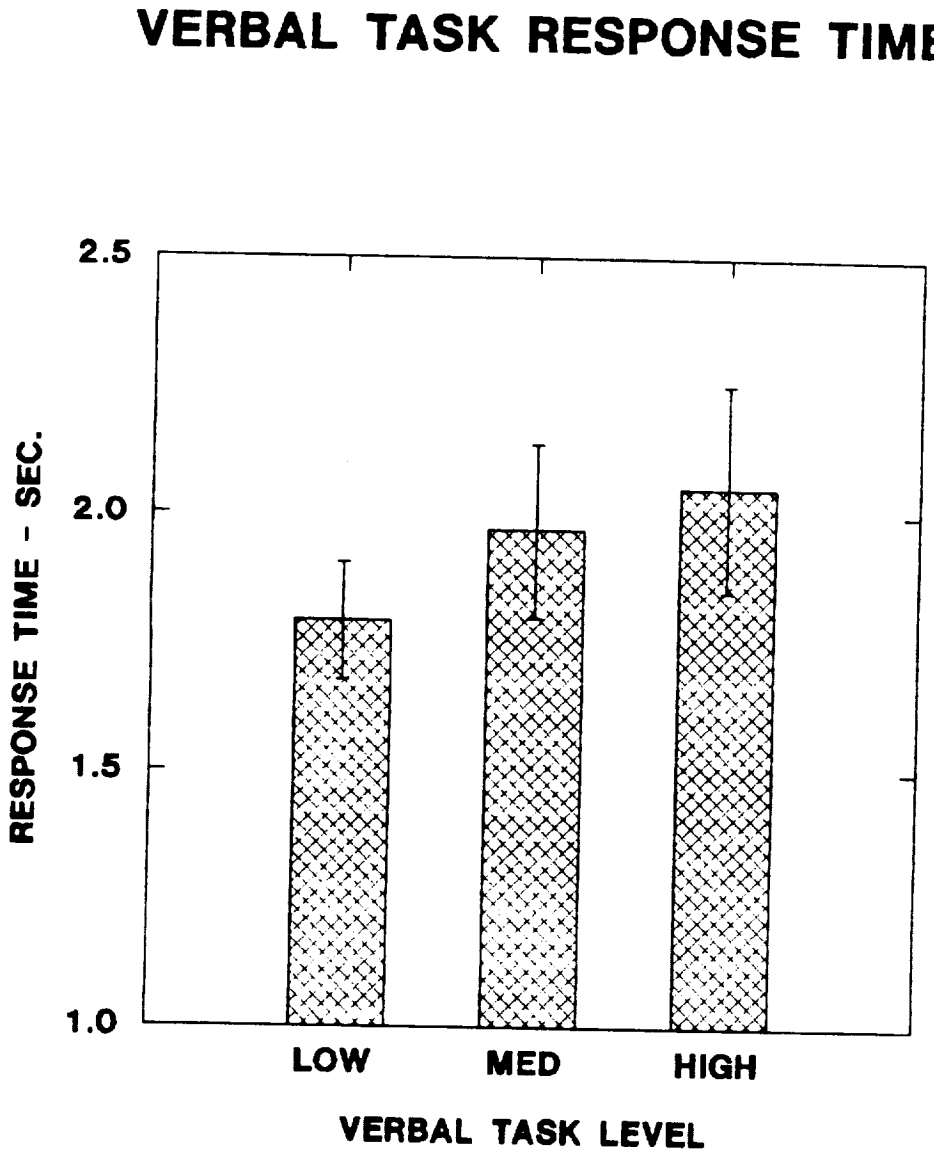

FIGURE VI.2.-31

MATH HEART RATE MODULUS vs. TIME

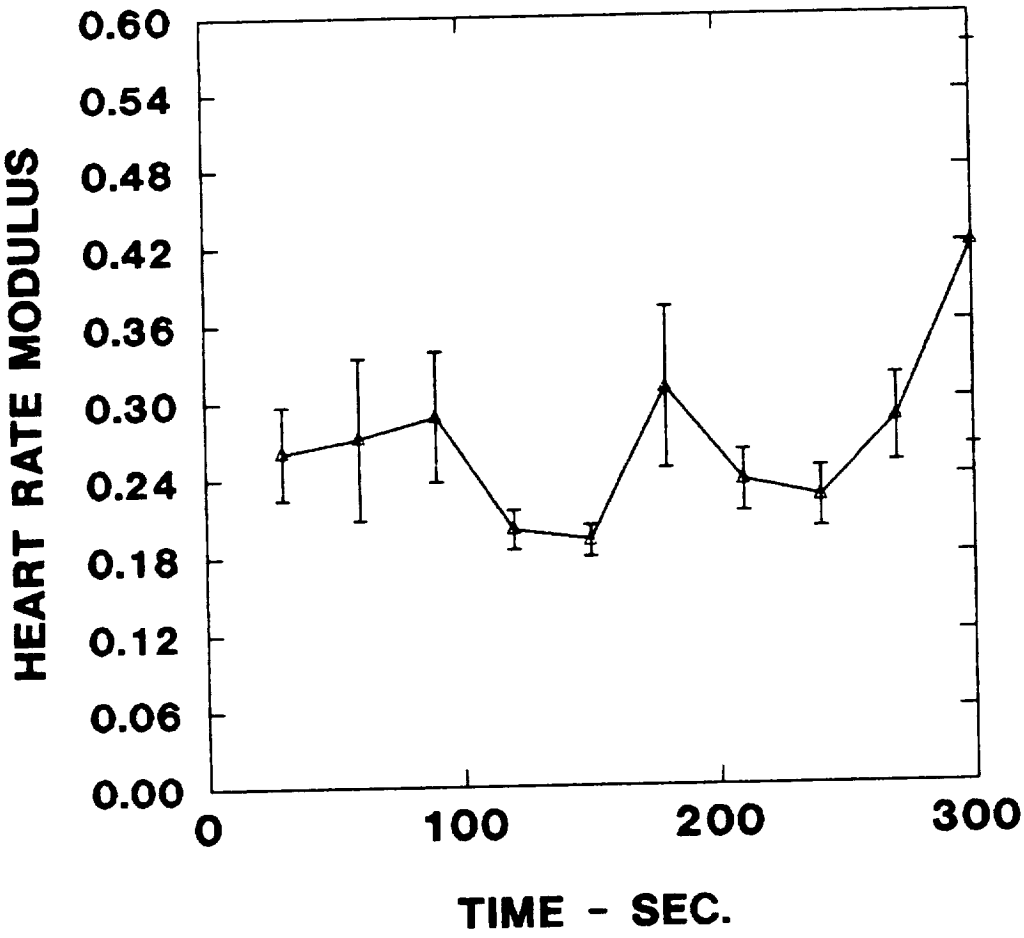

FIGURE VI.2.-32

VERB HEART RATE MODULUS vs. TIME

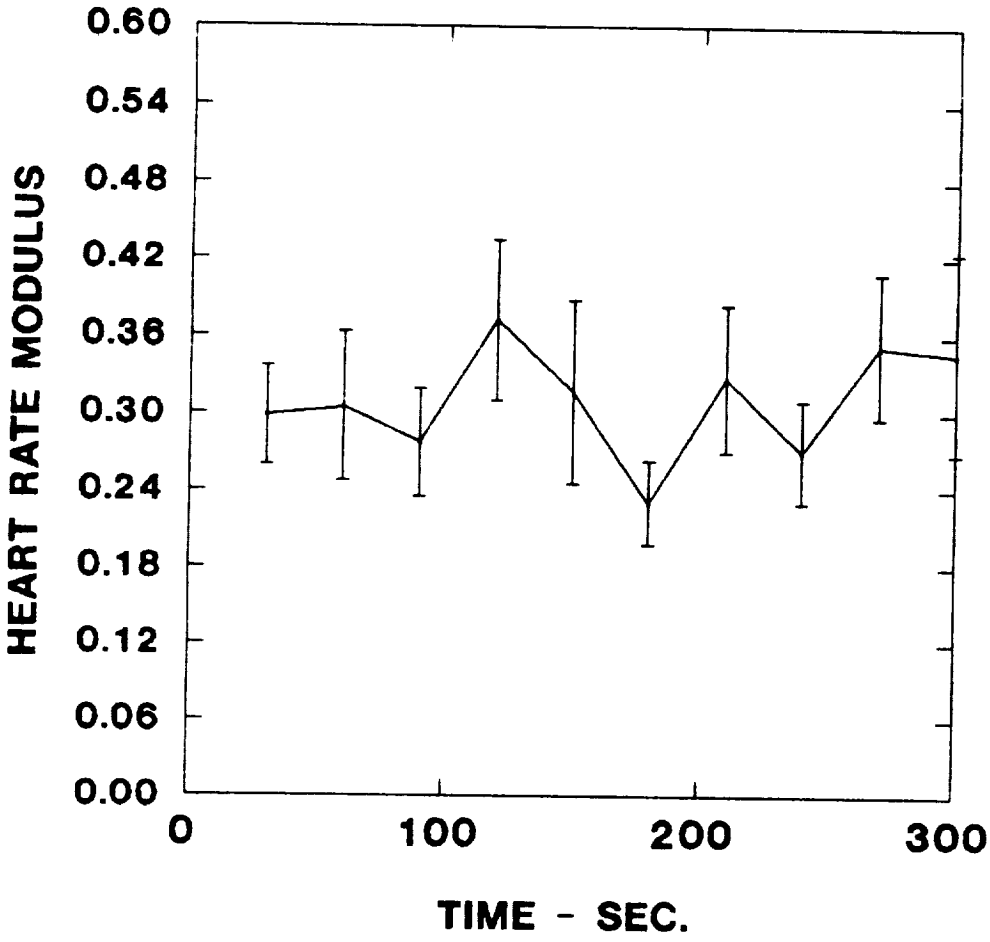

FIGURE VI.2.-33

SPATIAL HEART RATE MODULUS vs. TIME

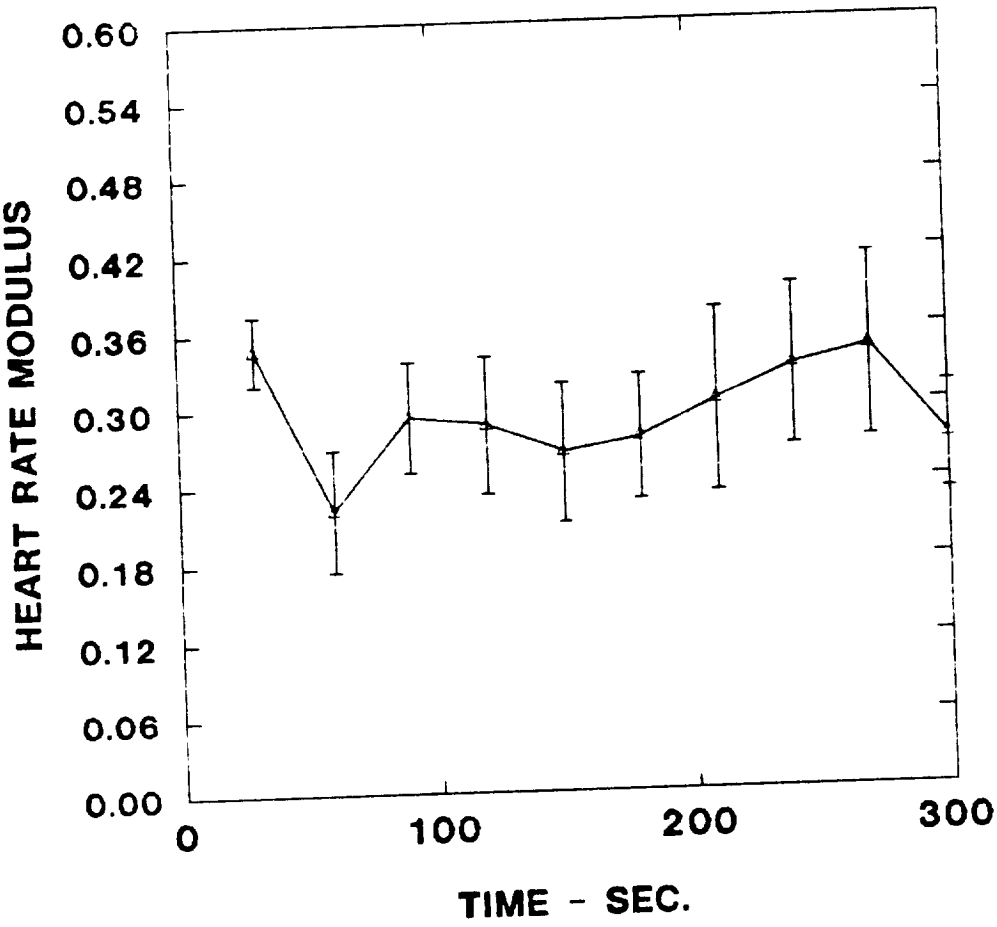

VI.2.2. Tracking Task (Figures VI.2.-34 through VI.2.-45)

The continuous tracking task was conducted to monitor the ongoing REG and peripheral blood flow responses to a continuous task. Instrumentation and procedures for right and left hemisphere REG, forearm IPG and EKG were similar to the ones used for the Mixed Task. Task presentation was independent of EKG cycle and was administered to the same six subjects participating in the Mixed Task. Each test sequence consisted of a five minute control period and a one hour continuous tracking period. Hemodynamic measurements were recorded at times -5, -3, and -1 minutes during the last 5 minutes of the non-tracking control period. The same parameters were recorded at times 3, 1, 36 and 54 minutes during the tracking task.

The results of the REG analysis of the tracking task are presented in Table XXII and Figures 34 through 45. Table XXII lists the grouped mean +/- S.E. blood flow for the right and left hemisphere and forearm. Figures 35 through 43 show the subjects" grouped mean +/- S.E. cerebral and left forearm changes during tracking. Figures 44 and 45 summarize the tracking performance for the six subjects involved. An "*" indicate points that are significantly ($p<0.05$) different from the similar value at 3 minutes. The "+" located between adjacent points in time denote points that are significantly different at $p<0.05$.

Heart rate and right and left hemisphere blood flow increases during the first half of the tracking task and tend to decrease as the task progresses (Figs 34 and 35). Forearm blood flow, in contrast, decreases from the control values and remains depressed for the duration of the task (Fig 36). Similar "balance" between cerebral and systemic circulation is found in the systolic area of the impedance pulsatile waveform (Figs 37 and 38) (a measure of arterial inflow) and in the total pulse height (Figs 39 and 40). Other cerebral hemodynamic adjustments to tracking include a slight increase in arterial tone, decreased pulse transit time and increased vascular contractility (compliance) (Figs 41 to 43).

There was a large intersubject difference in continuous tracking performance between the six subjects. Figure 44 shows the grouped mean +/- S.E. of the tracking index vs. elapsed time of the tracking task. The tracking index increased (longer delay in adjusting to changes in the height of the display bar) during the first 45 minutes of task. In addition, the large standard errors indicate a larger intersubject variance in performance with increased duration of the task. Figure 45 shows the tracking performance values for the points in time corresponding to the REG acquisition times. Left hemisphere venous tone ($r-0.96$, $p<0.04$) was found to be strongly influenced by task performance. In addition, forearm contractility ($r=0.95$, $p<0.05$) and basal resistance

($r=0.95$, $p<0.05$) were also highly correlated to task performance.

TABLE XXII

GROUPED MEAN ± S.E. BLOOD FLOW (ML/MIN.)
RESPONSES TO TRACKING TASK

TIME	LEFT HEMISPHERE	RIGHT HEMISPHERE	FOREARM
-5	882.6 (85.8)	921.4 (96.3)	182.0 (42.2)
-3	914.5 (93.0)	955.9 (91.3)	184.0 (41.3)
-1	829.2 (86.3)	869.8 (104.9)	154.7 (35.4)
3	743.9 (68.9)	842.1 (85.3)	155.3 (35.4)
18	904.1 (141.9)	974.8 (158.8)	152.6 (34.5)
36	893.9 (76.4)	970.9 (92.5)	149.8 (30.7)
54	774.1 (111.9)	834.6 (92.8)	156.9 (31.4)

FIGURE VI.2.-34

HEART RATE vs. TRACKING TASK

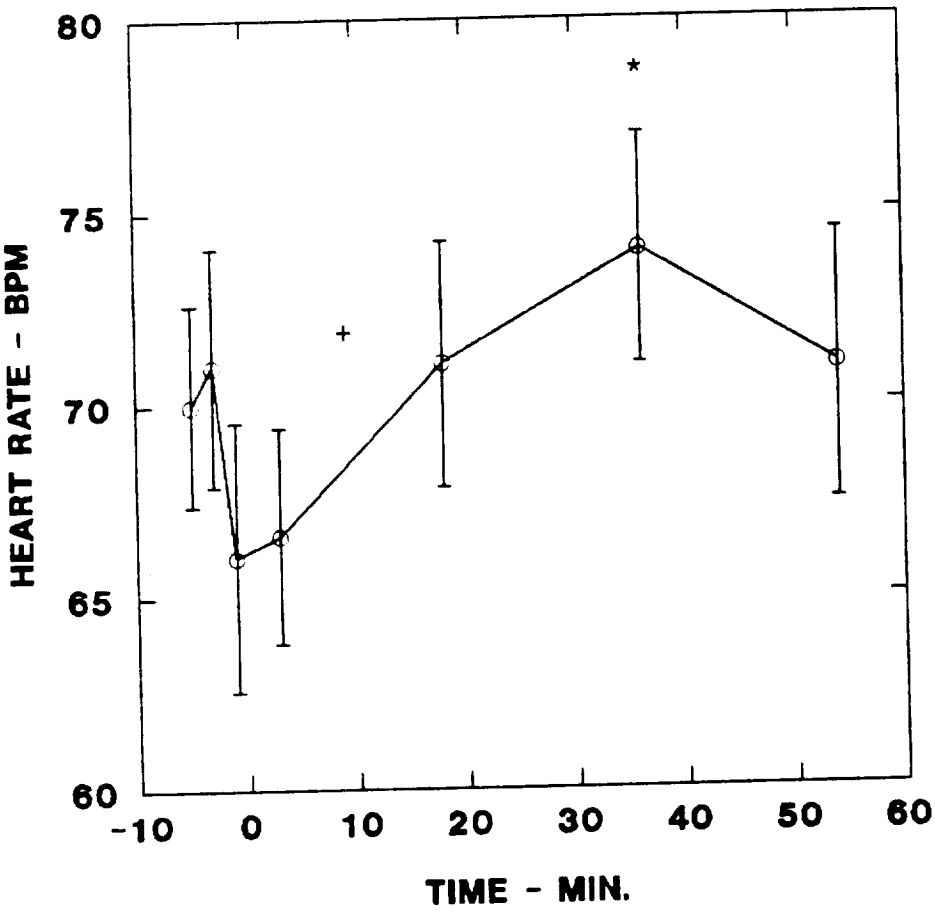

FIGURE VI.2.-35

CEREBRAL BLOOD FLOW vs. TRACKING TASK

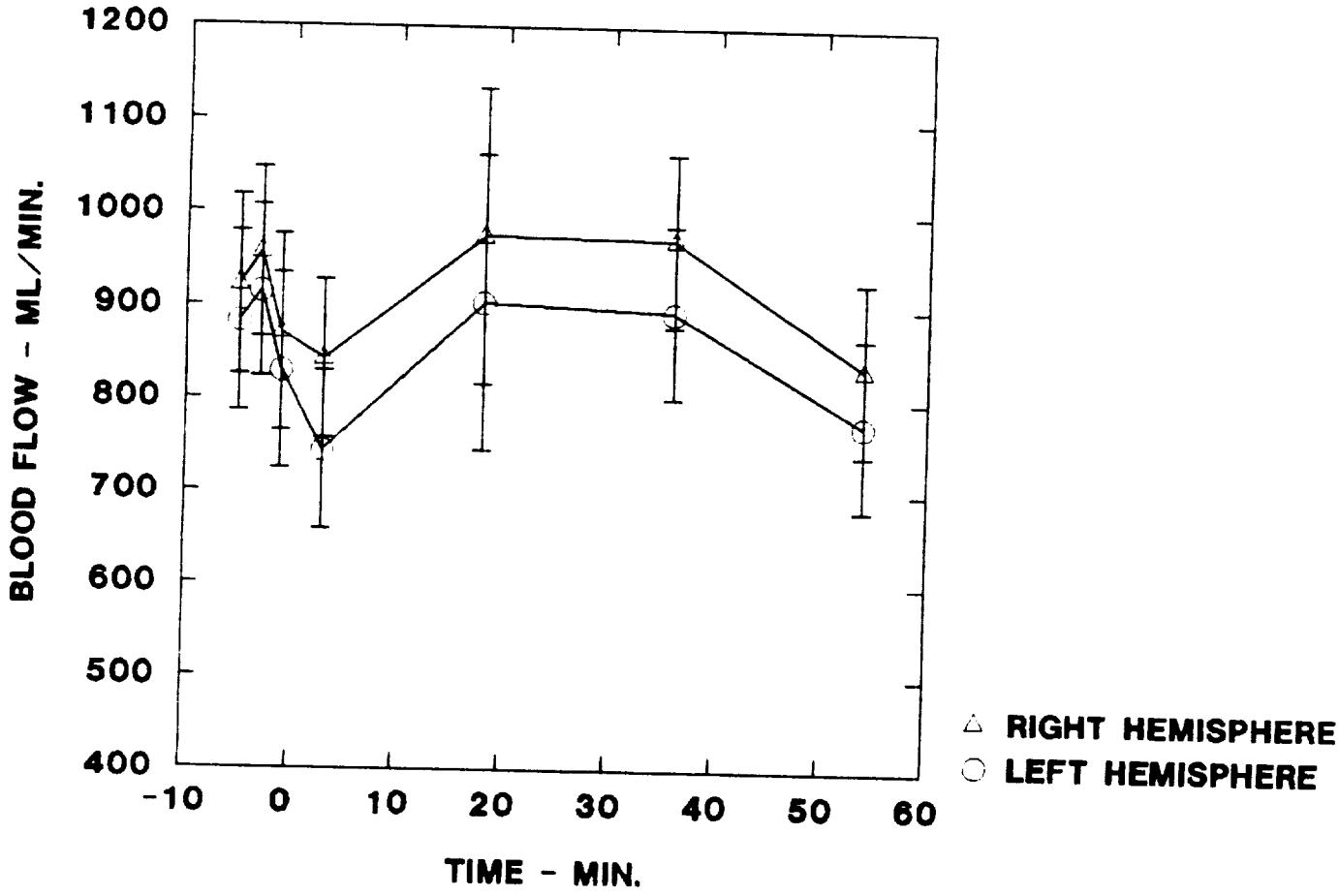

FIGURE VI.2.-36

FOREARM BLOOD FLOW VS. TRACKING TASK

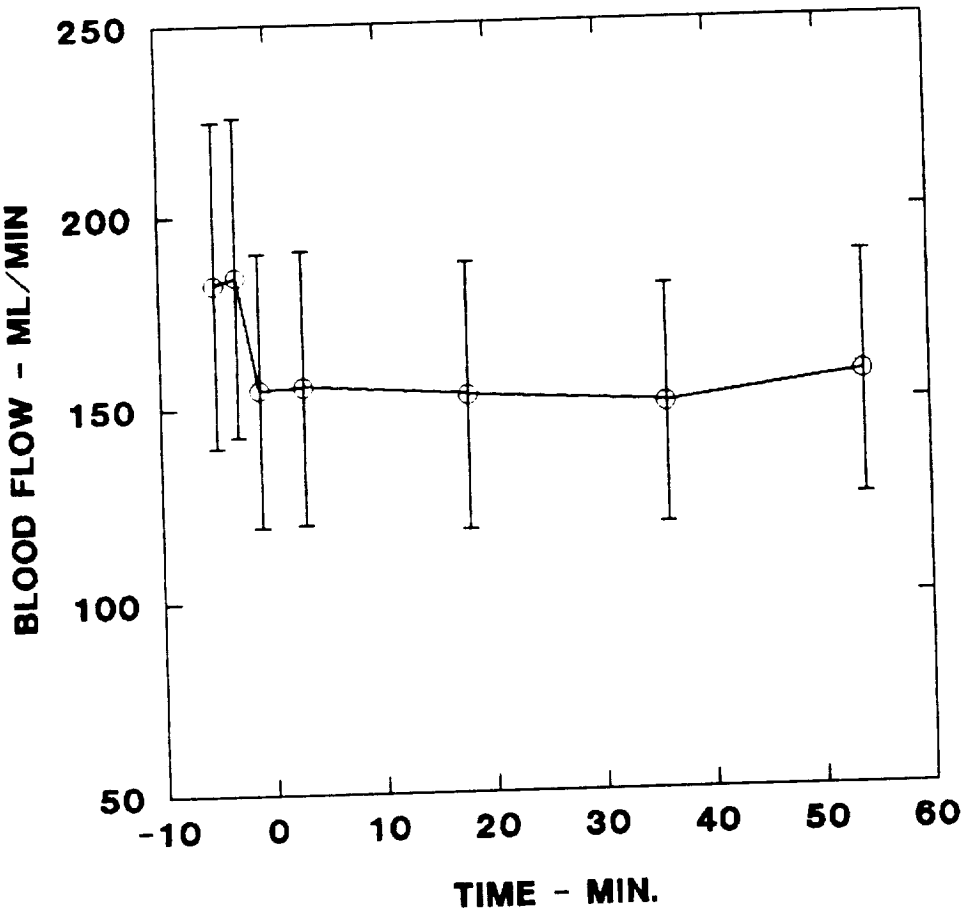

FIGURE VI.2.-37

CEREBRAL SYSTOLIC AREA vs. TRACKING TASK

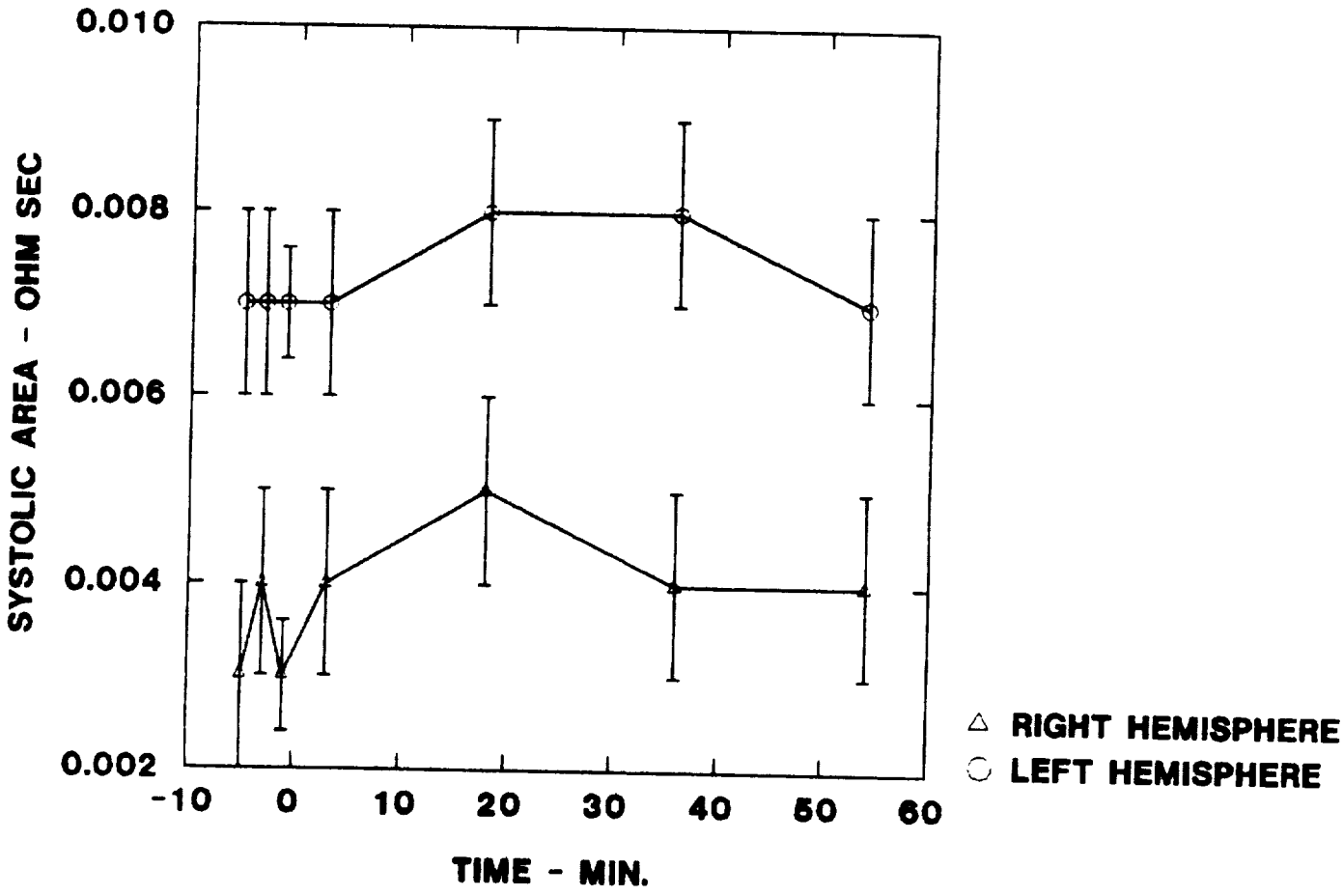

FIGURE VI.2.-38

FOREARM SYSTOLIC AREA vs. TRACKING TASK

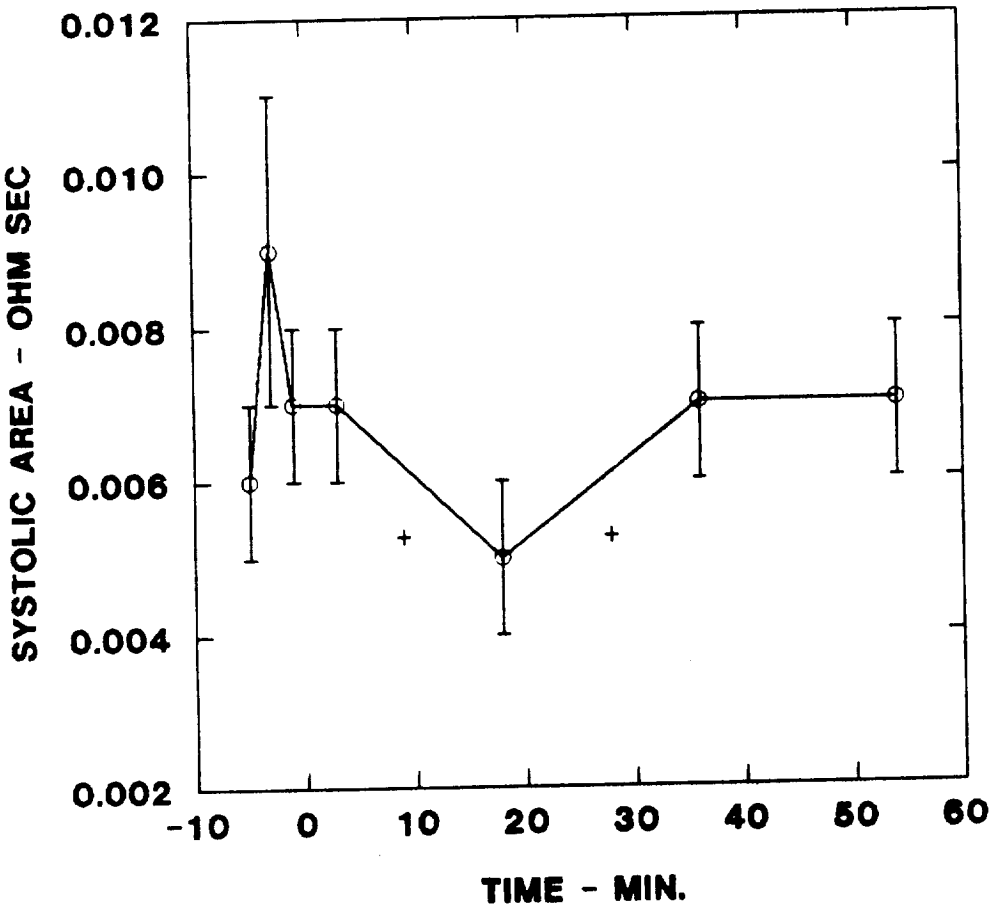

FIGURE VI.2.-39

CEREBRAL PULSE HEIGHT vs. TRACKING TASK

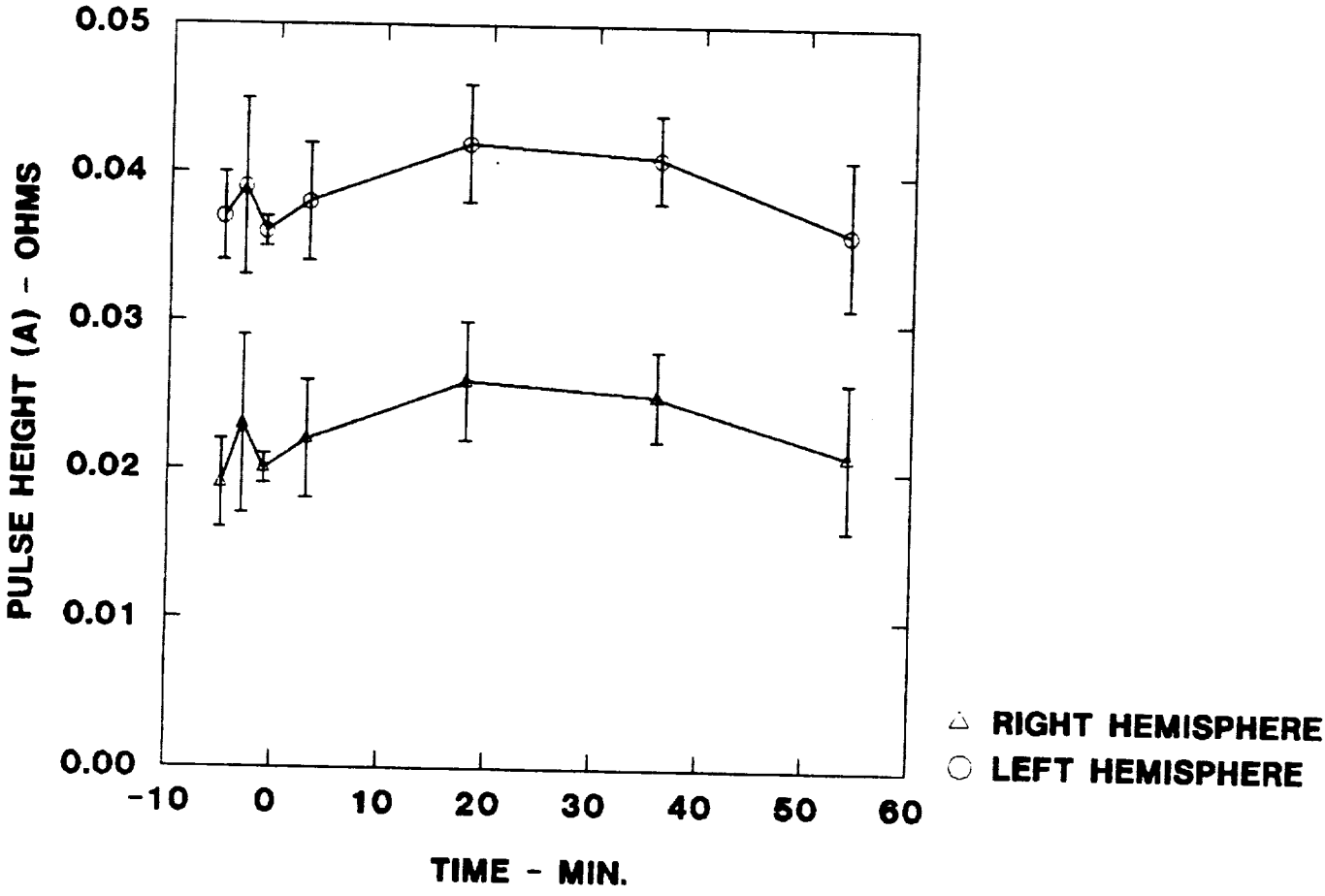

FIGURE VI.2.-40

FOREARM PULSE HEIGHT vs. TRACKING TASK

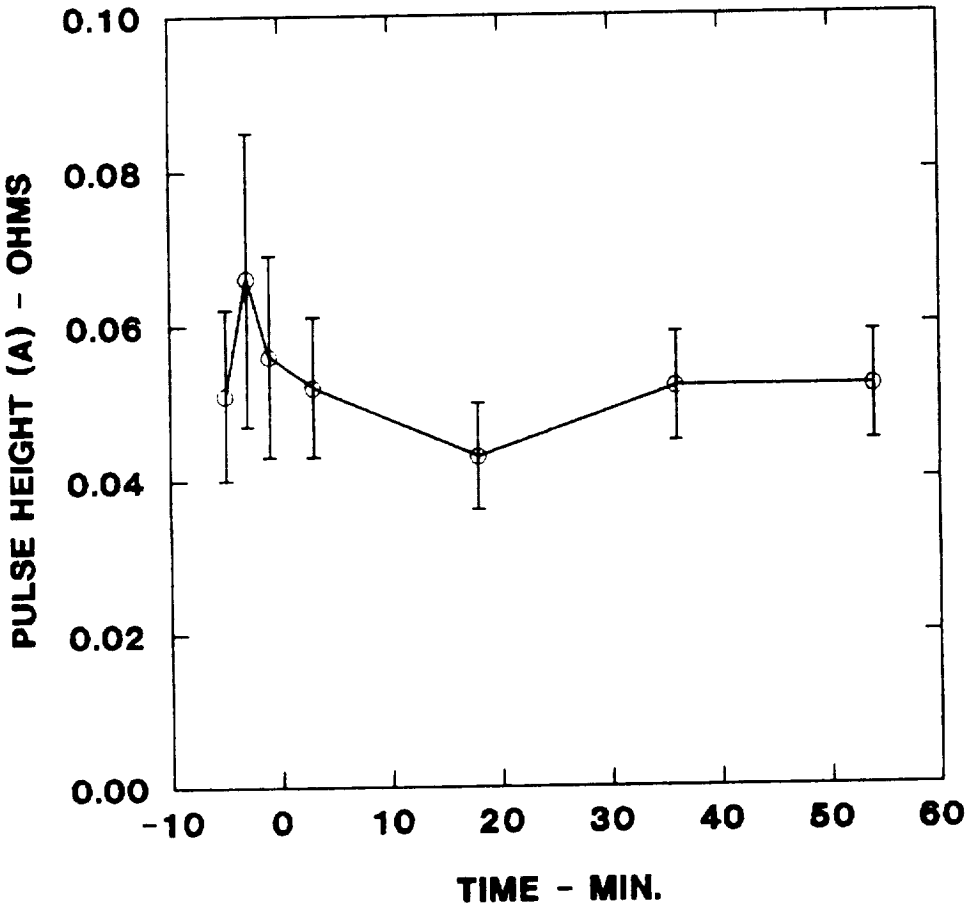

FIGURE VI.2.-41

CEREBRAL ARTERIAL TONE vs. TRACKING TASK

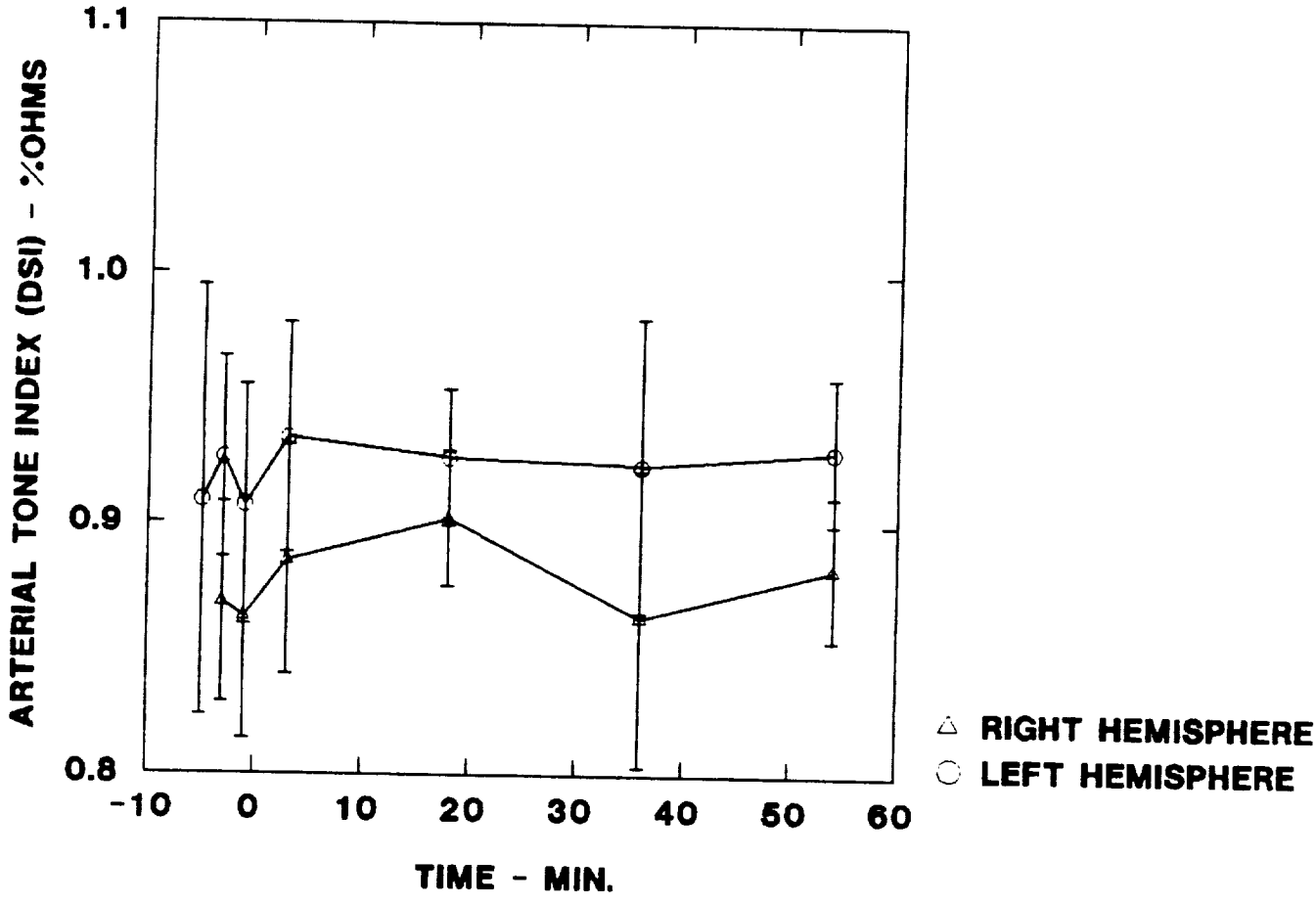

FIGURE VI.2.-42

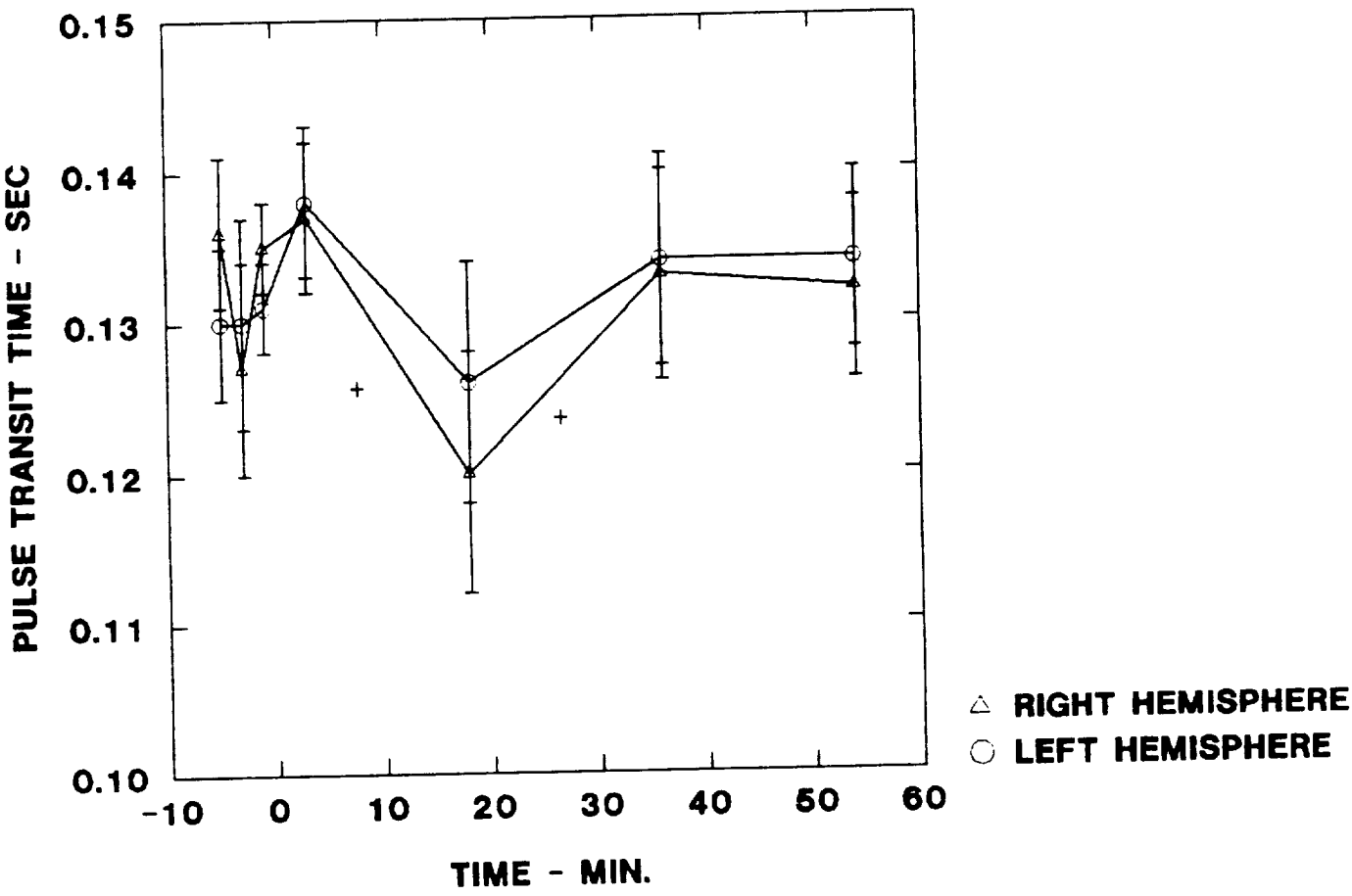

FIGURE VI.2.-43

CEREBRAL CONTRACTILITY vs. TRACKING TASK

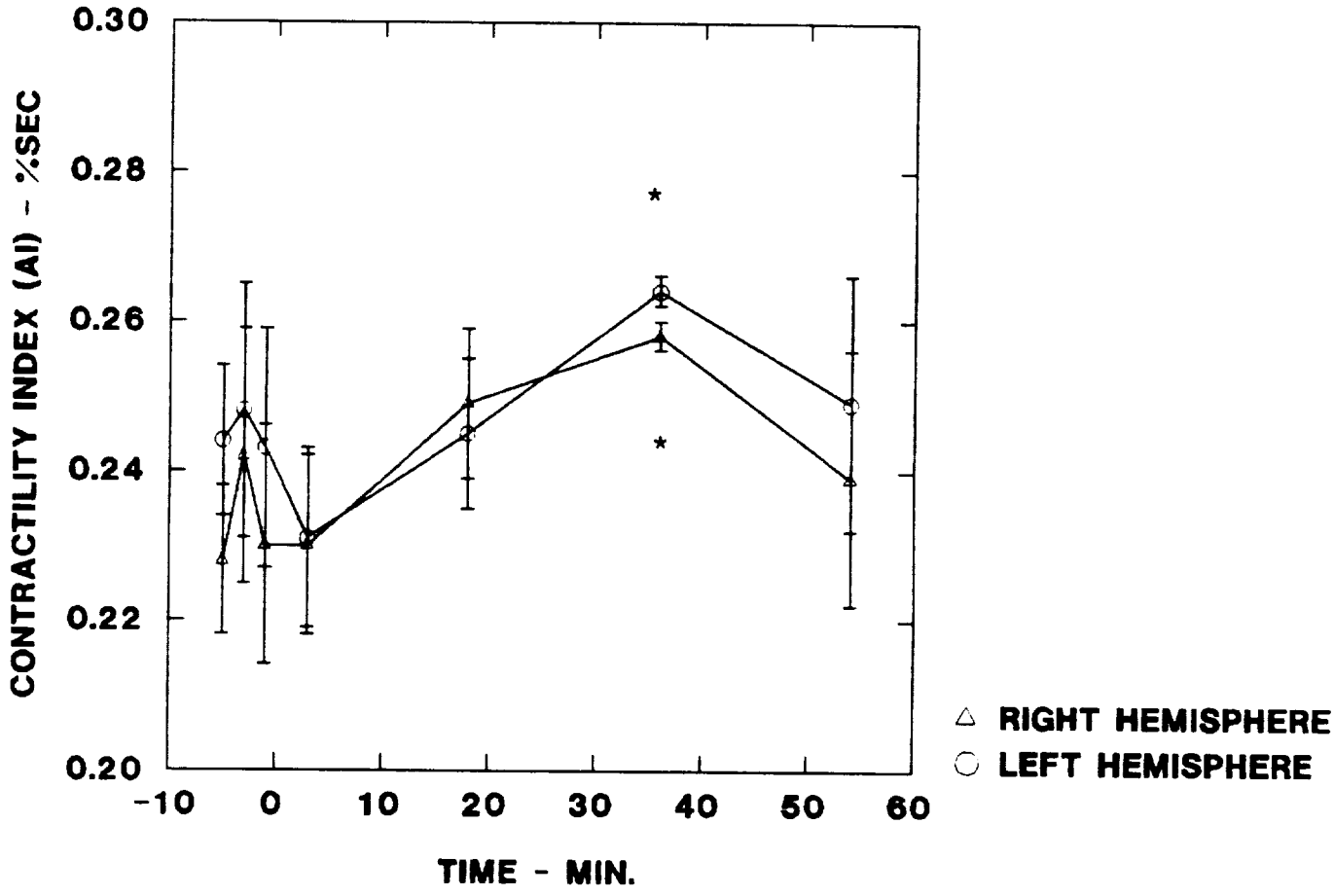

FIGURE VI.2.-44

TRACKING RESPONSE TIME vs. TIME

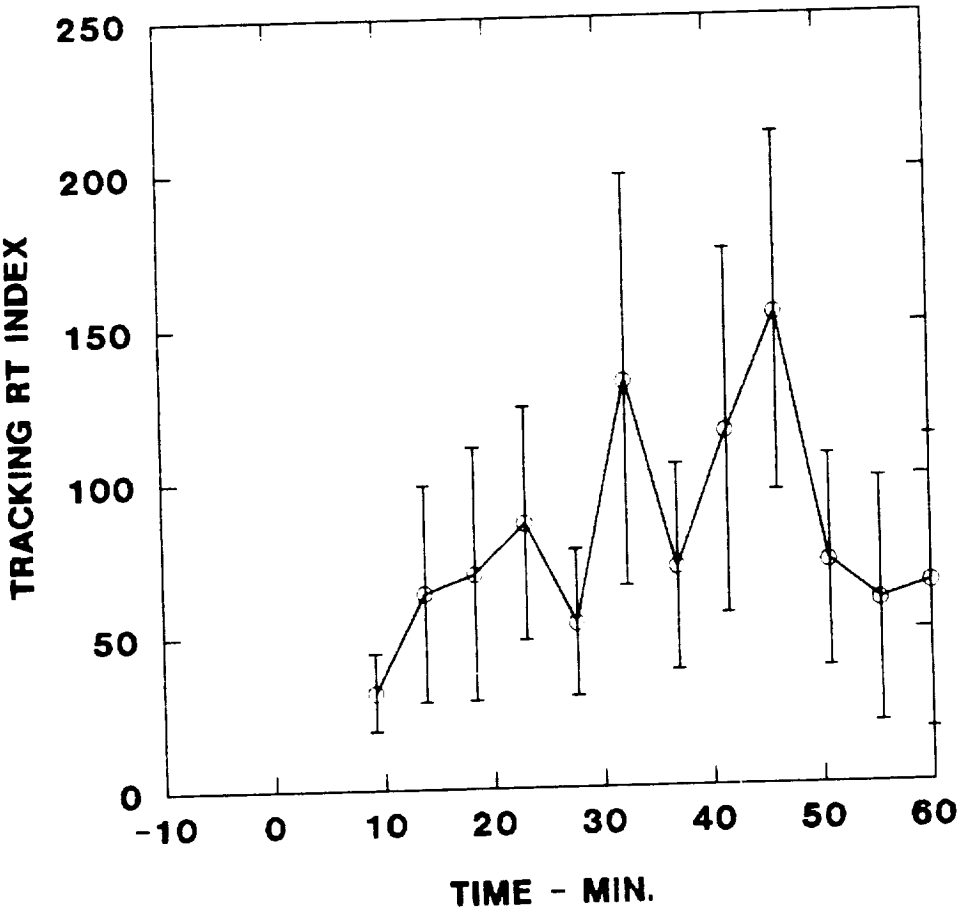

FIGURE VI.2.-45

TRACKING RESPONSE INDEX vs. TIME

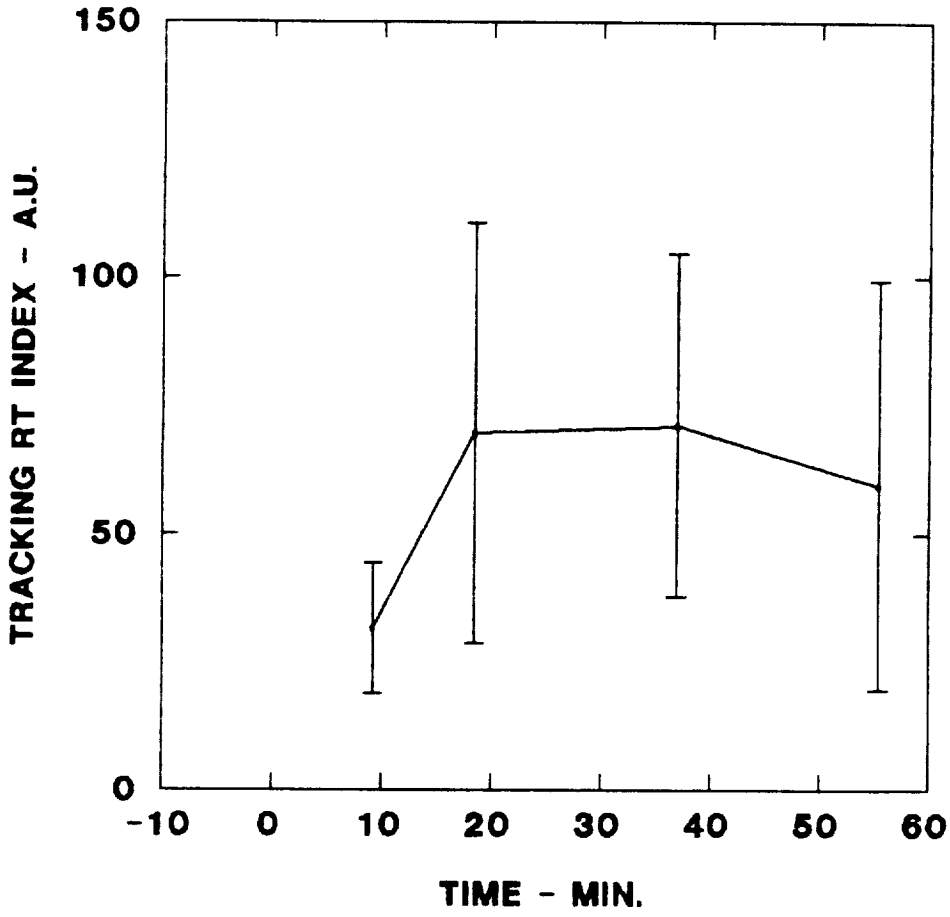

VI.2.3. Long Term Task (Figures VI.2.-46 through VI.2.-62)

(This Task is described in detail in Section III.4., pages 11-12). These results are presented in graphical format to illustrate the time behavior for each measured or derived parameter. Figures 46 and 47 illustrate the cerebral blood flow and heart rate changes for each task. Figure 48 show the total EEG PSD values for the First second (stimulus presentation). Figure 49 shows the same data for the Second second time period, during which no stimulus was presented. Figures 50 through 55 show the percent and total EEG band powers for each cognitive task plotted as function of time. Figure 56 gives the results of the regression analysis comparing the cerebral blood flow and EEG changes during the Long task. The remaining figures (Figures 57 through 62) are provided to demonstrate how the various REG indices can be used to gain some insight into the intracranial vasomotor responses during each test.

Each figure consists of three panels, arranged according to Low, Medium and High task levels. The top panel shows the results for the SPAT task, the middle panel shows the results of the MATH task and the lower panel those of the VERB task. In all these figures, LT= left, RT= right, FT= front, RR= rear. The reader is urged to inspect these figures from the top panel to the bottom panel to see how each response becomes more fully developed as a function of task type.

Due to the small sample size, grouped mean responses are presented without standard error bars. No attempt was made to test the statistical significance of the various physiologic changes over time or of the observed differences between the three cognitive task types. However, multiple regression tests were made to compare the cerebral blood flow and frequency domain EEG responses of each quadrant for each test sequence.

As shown in Figure 46, grouped mean blood flow remains relatively constant or decreases in all quadrants during the first 90 minutes of the Long task. After this time the blood flow continues to decrease in the posterior quadrants but tends to increase in the frontal or anterior quadrants. The degree of frontal increase in blood flow is graded between the three tasks. Thus, regional cerebral blood flow changes are related both to time on task and task type. The decrease in blood flow during the first 90 minutes of each task can be partially accounted for by the general decrease in the grouped mean heart rate as shown in Figure 47. The changes seen during the remainder of the continuous task cannot be explained by this mechanism, but seem to depend on central vasomotor changes.

An attempt was made to determine the extent to which these blood flow changes may be related to neural activity. As

illustrated in Figures 48 and 49, the EEG PSD magnitudes also remained relatively constant during the first half of each task and generally increased in the front quadrants of the head during the last half of each task. By comparing the ordinate values in Figures 48 and 49 (note ordinate scales), it can also be seen that the total EEG PSD power in all segments of the head was larger during stimulus presentation than during the one second period immediately following stimuli presentation. The increased total EEG PSD power was found to be larger during both time periods for the MATH and VERB tasks than for the corresponding SPAT task time periods. In addition, the frontal EEG PSD magnitudes remained elevated during the total last half of the VERB task which is in contrast to the rise and fall found during the last half of the SPAT and MATH tasks. These results suggest that neural activity during the time period of task presentation may be strongly related to regional cerebral blood flow. They also show that this relationship may be a function of both task content and time on task.

The relative percent band powers during the First Sec. time period are illustrated for the SPAT, MATH, AND VERB tasks as function of time in Figures 50, 51, and 52, respectively. The band widths for each frequency band are given from the top panel to the bottom panel in each figure as follows:

Band1	0 - 4 Hz
Band2	4 - 8 Hz
Band3	8 - 13 Hz
Band4	13 - 23 Hz
Band5	23 - 32 Hz.

Once again, the relative stability of the measured variables is evident during the first half of each task, particularly during the verbal task. The percent band powers of the SPAT task do not show a marked difference between the various quadrants of the head. Panels 2 and 4 (Figure 51) show that a slight shift in neural activity occurs in the frontal quadrants during the MATH task. The 4 - 8 Hz percent band power increases while the 13 - 23 Hz percent band power decreases after 90 min. elapsed time. This tendency to increased low frequency and decreased high frequency activity in the frontal segments at later than 90 minutes becomes more evident for the VERB task in Figure 52. The differentiation between the anterior and posterior quadrants also becomes more pronounced during the VERB task.

When the total, rather than the percent, band powers are examined as shown by the ordinate values in Figures 53, 54, and 55 the influence of task content and time on task upon frontal neural activity becomes even more obvious. The low frequency band powers (0 - 4 Hz and 4 - 8 Hz) are higher in the frontal segments of the head and higher for the MATH and VERB tasks than for the SPAT task (note ordinate scale). The

total band powers for Bands 3 through 5 respond similarly to increased task duration in all three of the cognitive tasks, being rather stable during the first half of the task and increasing in power between 100 and 180 min. elapsed time.

By comparing blood flow and total band powers for each task and quadrant a strong statistically significant relation was found between these parameters for BAND3 (8 - 13 Hz) in the frontal quadrants during the VERB task. Figure 56 illustrates the results of this regression analysis. As can be seen from the top panels of Figure 56, a positive relation exists between cerebral blood flow and total BAND3 PSD power for the frontal quadrants:

Right Anterior Blood Flow = 906.3 BAND3 Pwr - 39.6

$r = 0.93$
$T = 4.925$
$P < 0.008$

Left Anterior Blood Flow = 1218.5 BAND3 Pwr - 5.6

$r = 0.89$
$T = 3.683$
$P < 0.02$

A weak negative relation was found between these two variables for the posterior quadrants of the head during the VERB task:

Right Posterior Blood Flow = -1076.2 BAND3 Pwr + 351.6

$r = 0.77$
$T = -2.380$
$P < 0.07$

Left Posterior Blood Flow = -474.7 BAND3 Pwr + 257.3

$r = 0.42$
$T = -0.92$
$P < 0.41$

Figures 57 through 62 illustrate how local cerebral vasomotor responses react in a coordinated manner to provide the increased blood flow in the frontal segments of the head. Figure 57 shows that the basal resistance increases in the posterior quadrants and decreases in the anterior quadrants during all three of the cognitive tasks. This is another indication that conductive tissue (blood) is being redistributed from the back of the head to the front during the latter phases of each task. This is accomplished by a constriction in the posterior vascular bed and increased delivery of blood to the anterior quadrants.

Rheoencephalographic evidence of posterior vasoconstriction includes 1.) a decreased posterior pulse volume (REG Pulse Systolic Area - Figure 58) and 2.) increased posterior venous outflow (Figure 59) during each task. The increased REG systolic rise time (longer period of arterial inflow) shown in Figure 60 and increased vascular compliance or elasticity in the anterior quadrants (Figure 61) are evidence of increased blood delivery to the frontal portions of the head during each task.

These changes in regional vascular activity, obtained from the REG waveform analysis, are corroborated by the maximum amplitude pulse transit time (MAPTT) values shown in Figure 62 that were calculated independently of the REG technique. As the vascular bed constricts, the MAPTT decreases. Similarly, vasodilation or increased vascular volume is accompanied by an increase in MAPTT.

MAPTT remains relatively constant in all four quadrants during the first half of all three tasks. This means that the state of the vascular bed in all quadrants remains fairly static during the first 90 minutes of each test sequence. MAPTT increases in the anterior quadrants after approximately 100 min. of task duration. As explained above, these changes indicate that the frontal vascular beds are more dilated with an increased volume of blood.

The regional and temporal changes in blood flow, EEG percent and total band powers, and REG vasomotor indices found during prolonged cognitive testing can be interpreted in the following manner: as a subject initiates and attends to a task he becomes relaxed or more confident during the first hour. As the task continues he becomes aware of his possible deterioration of performance. To maintain his performance he becomes more aroused (or less relaxed) and has to mobilize his neural resources, particularly in the frontal segments of the head. The increased neural activity in the frontal segments during the midtask test sequences require a larger inflow of blood which is accomplished by increased heart rate and regionally active vasomotor reflexes.

The results shown in Figures 46 through 62 suggest that a close relationship exists between the neural activity and brain blood flow that may be task as well as time dependent. The regression analysis of blood flow and EEG activity showed that these variables are highly correlated.

FIGURE VI.2.-46

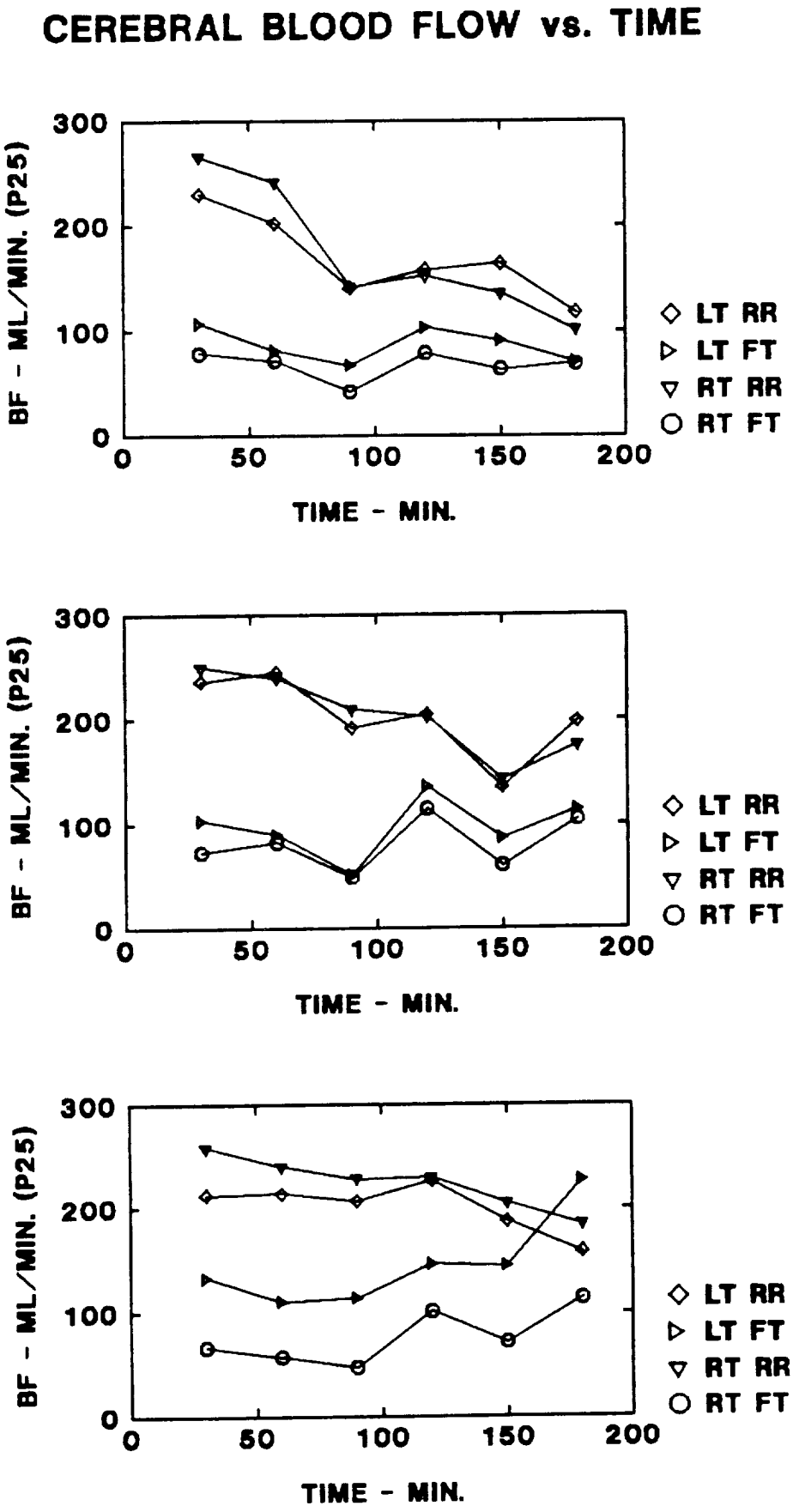

FIGURE VI.2.-47

HEART RATE vs. TIME

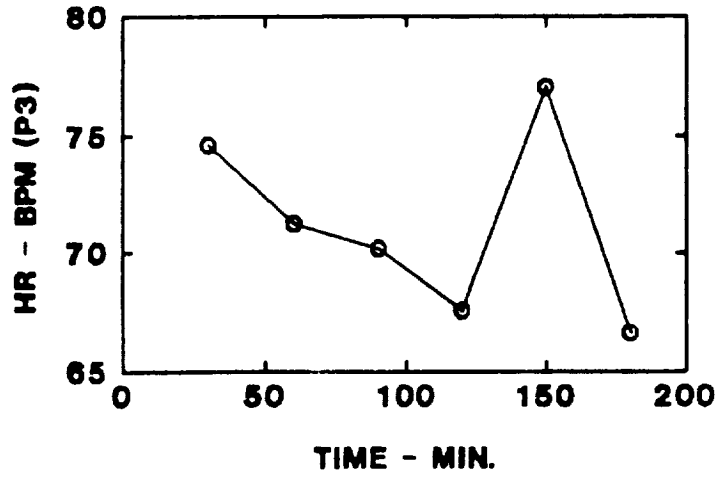

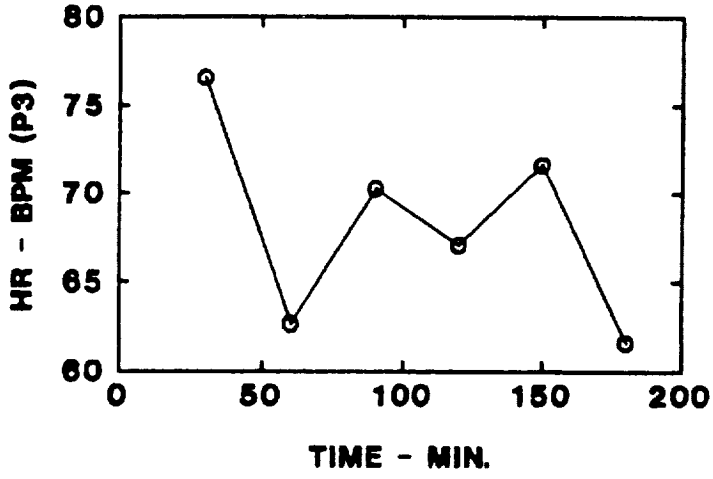

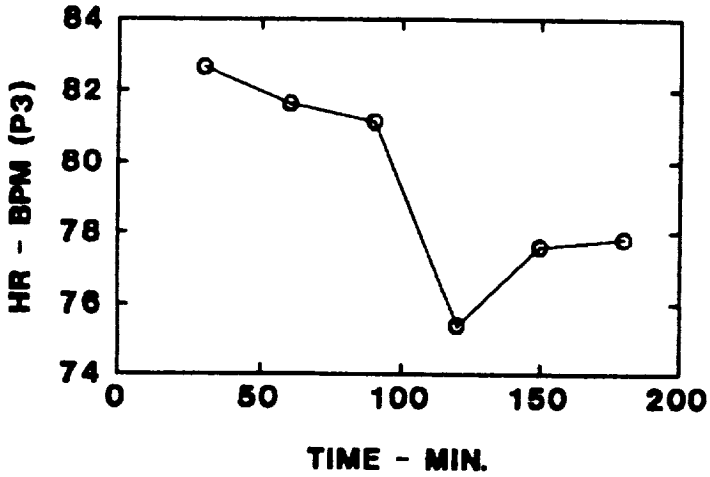

FIGURE VI.2.-48

TASK/MAT EEG FIRST SEC. PSD

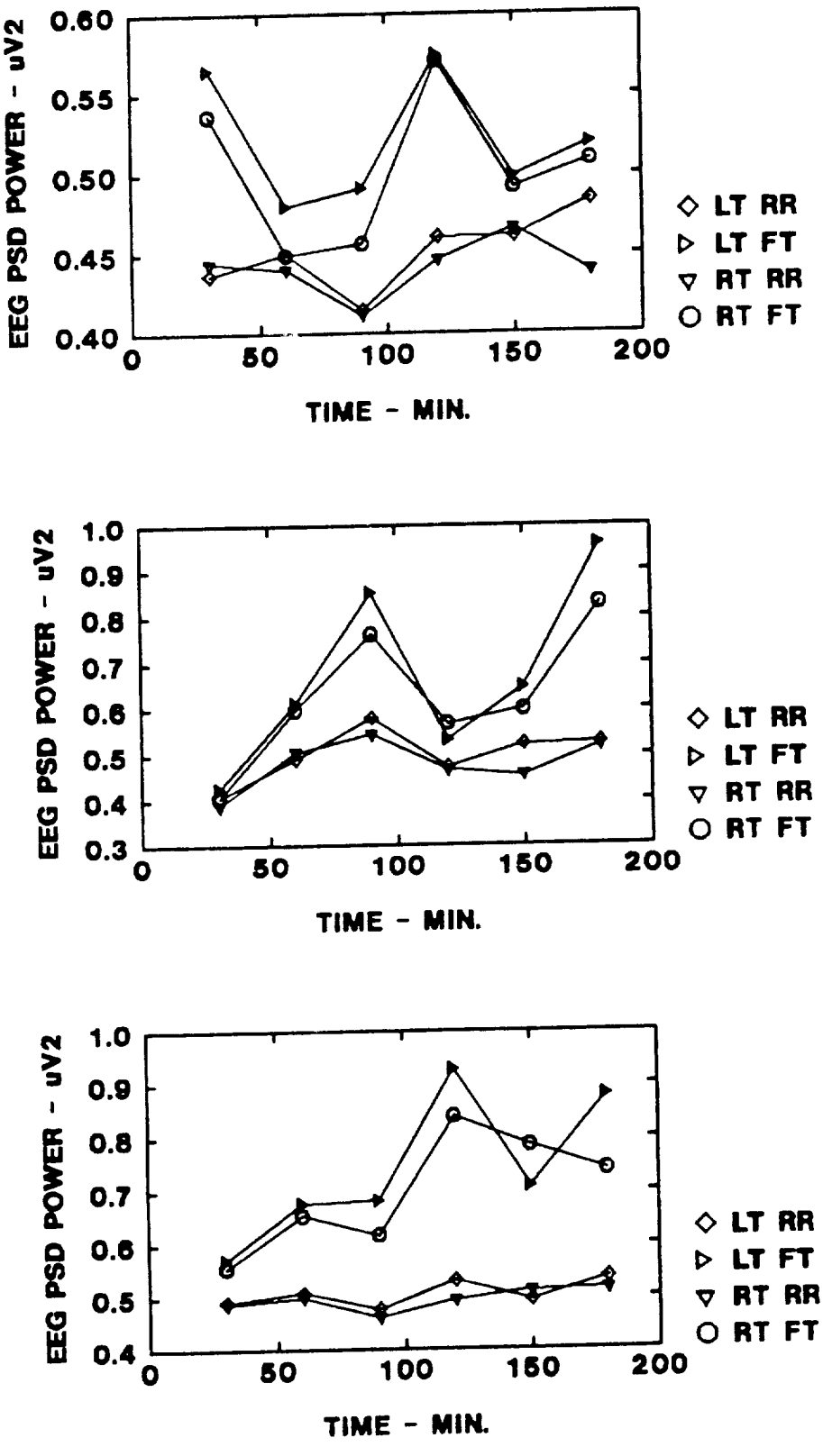

FIGURE VI.2.-49

TASK/MAT EEG SECOND SEC. PSD

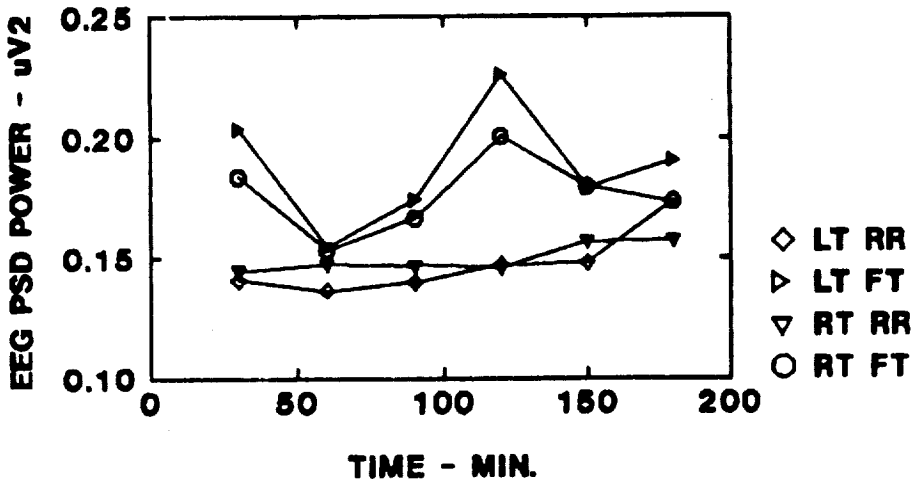

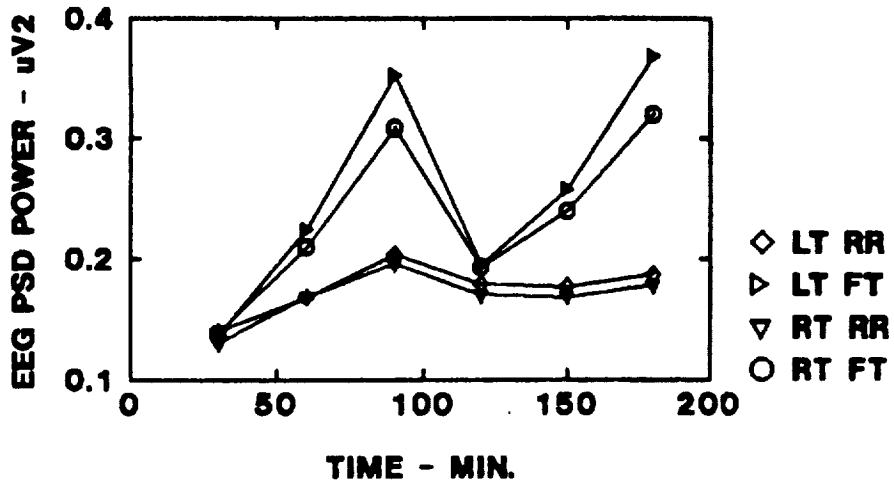

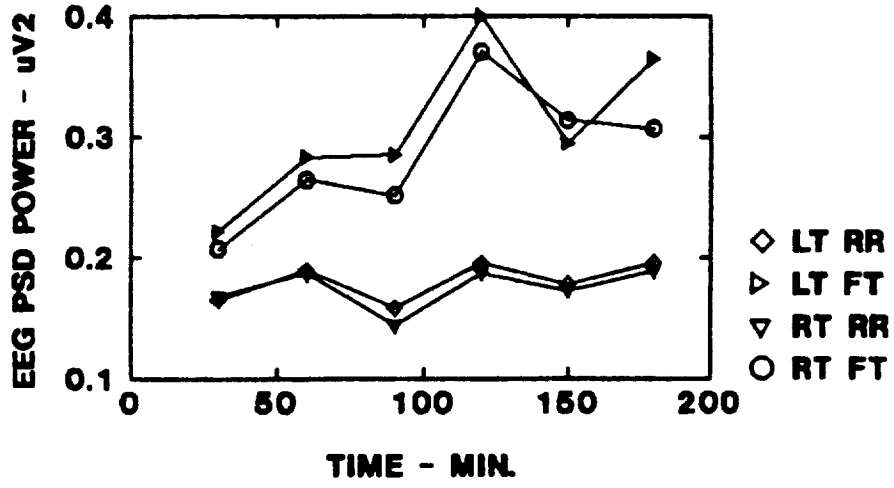

FIGURE VI.2.-50

SPATIAL/MAT EEG % BAND POWER vs. TIME

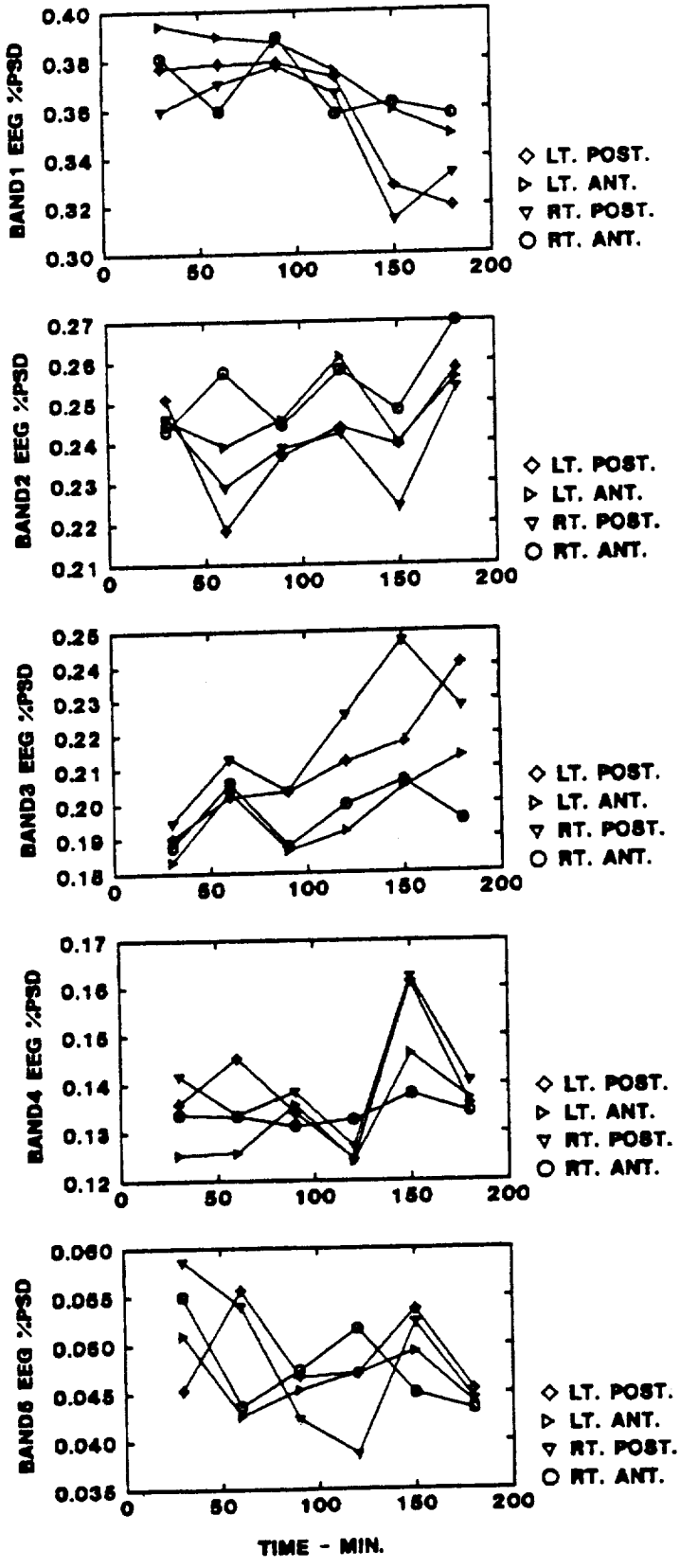

FIGURE VI.2.-51

MATH/MAT EEG % BAND POWER vs. TIME

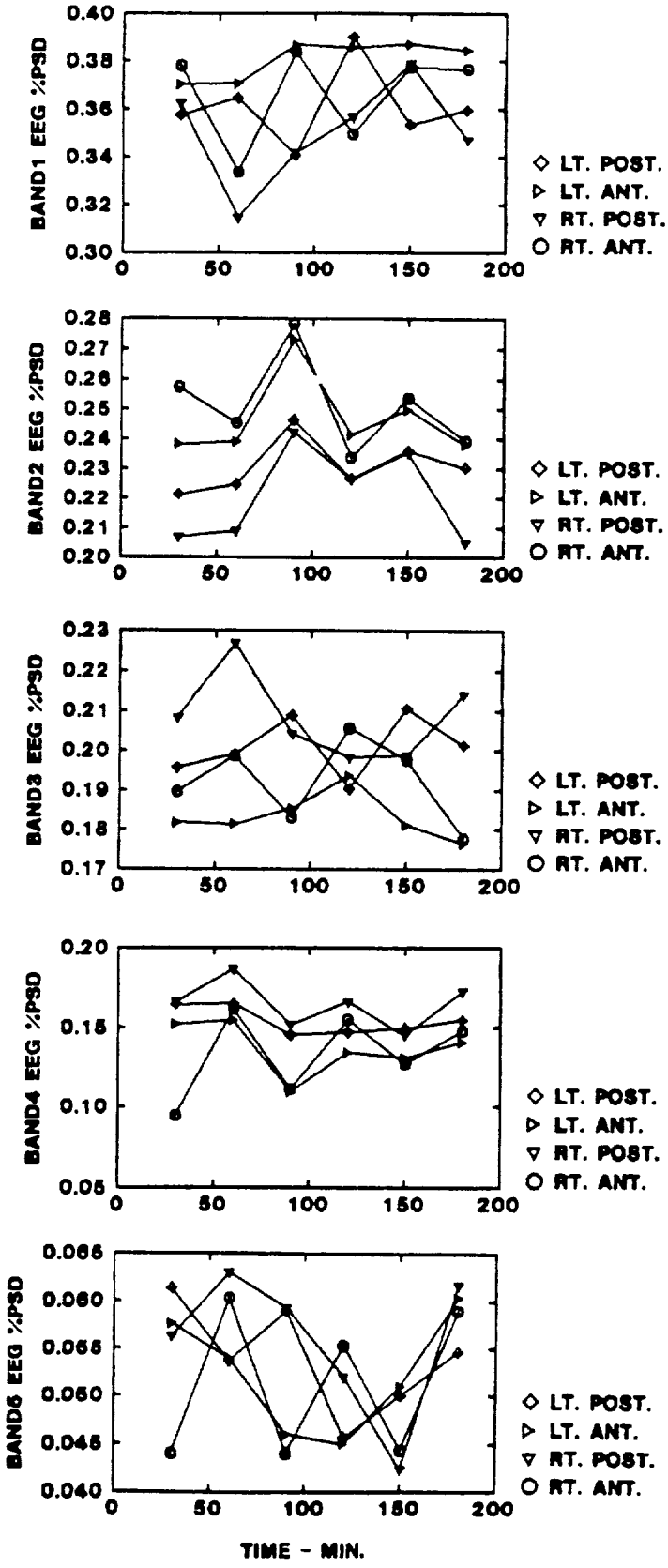

FIGURE VI.2.-52

VERBAL/MAT EEG % BAND POWER vs. TIME

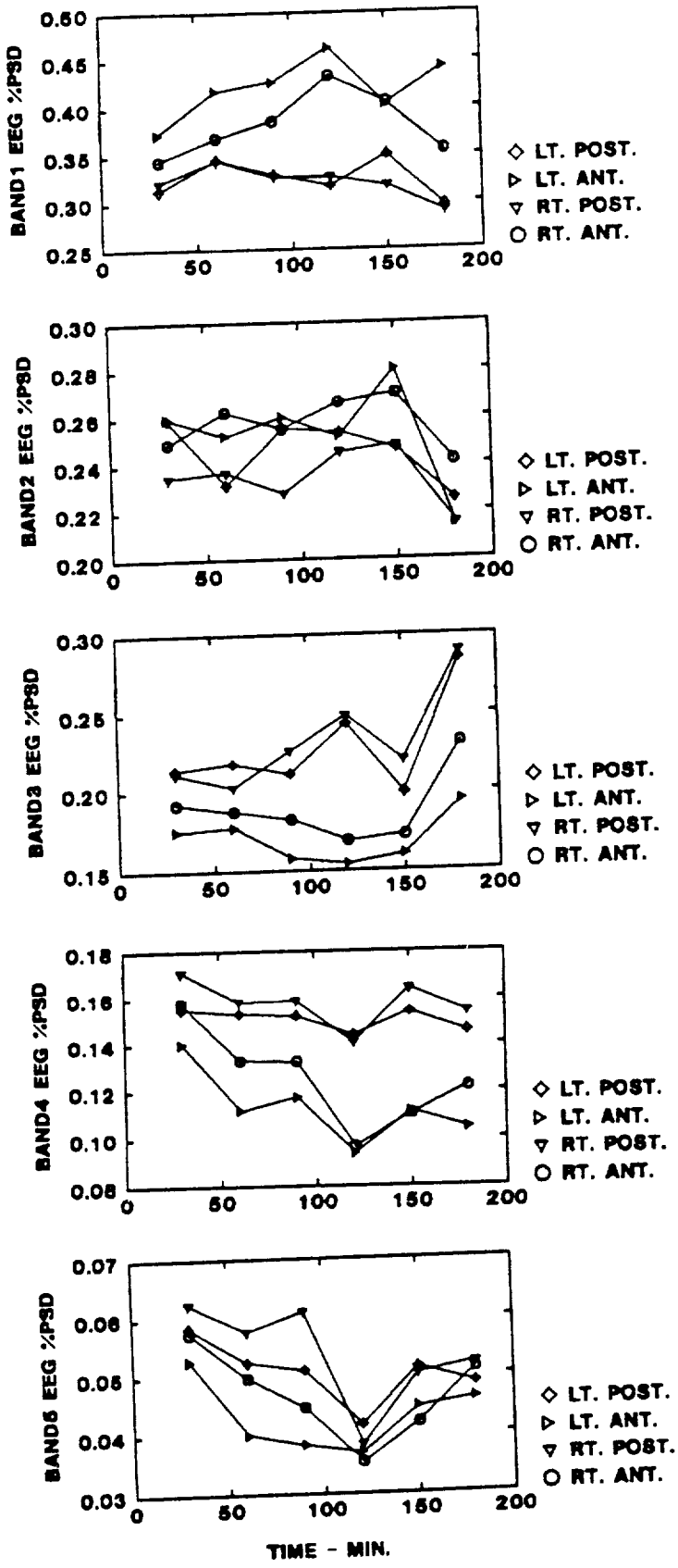

FIGURE VI.2.-53

SPATIAL/MAT EEG TOTAL BAND POWER vs. TIME

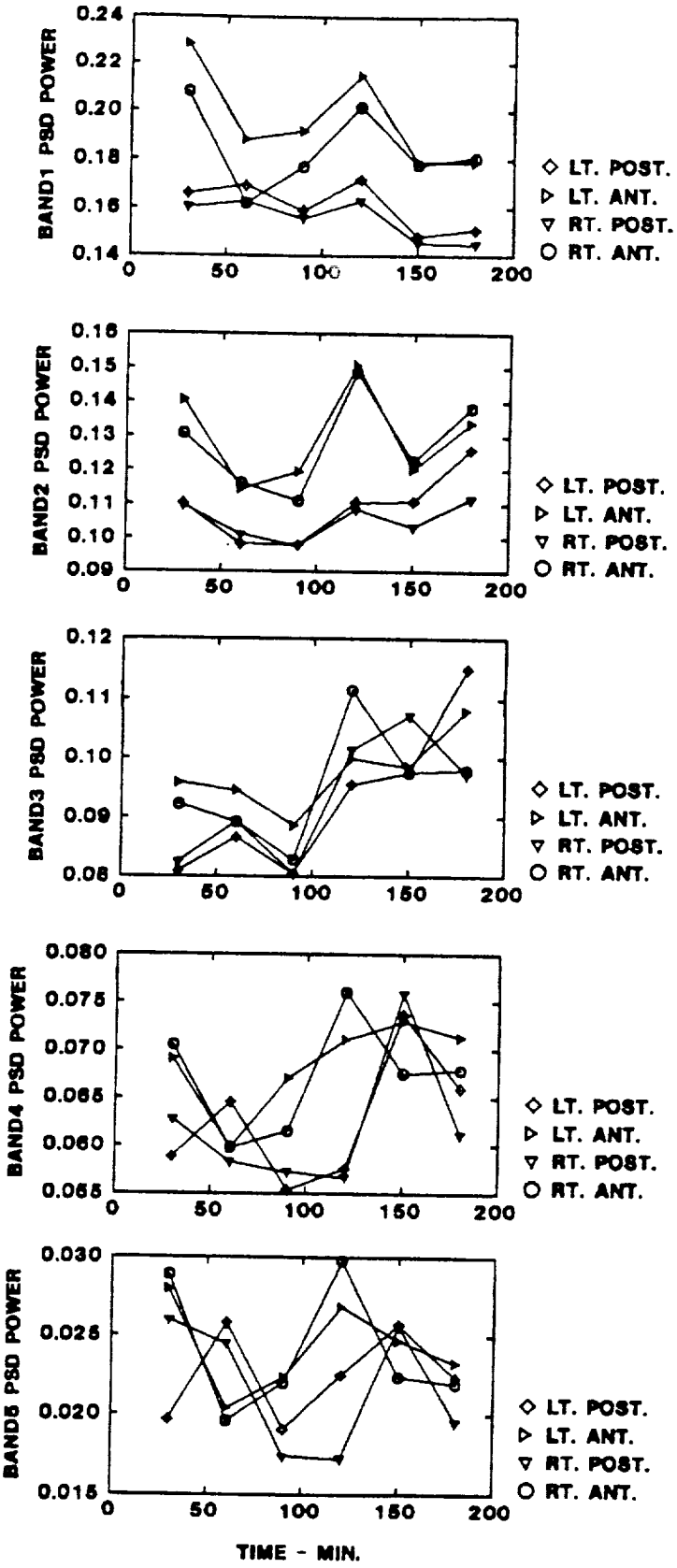

FIGURE VI.2.-54

MATH/MAT EEG TOTAL BAND POWER vs. TIME

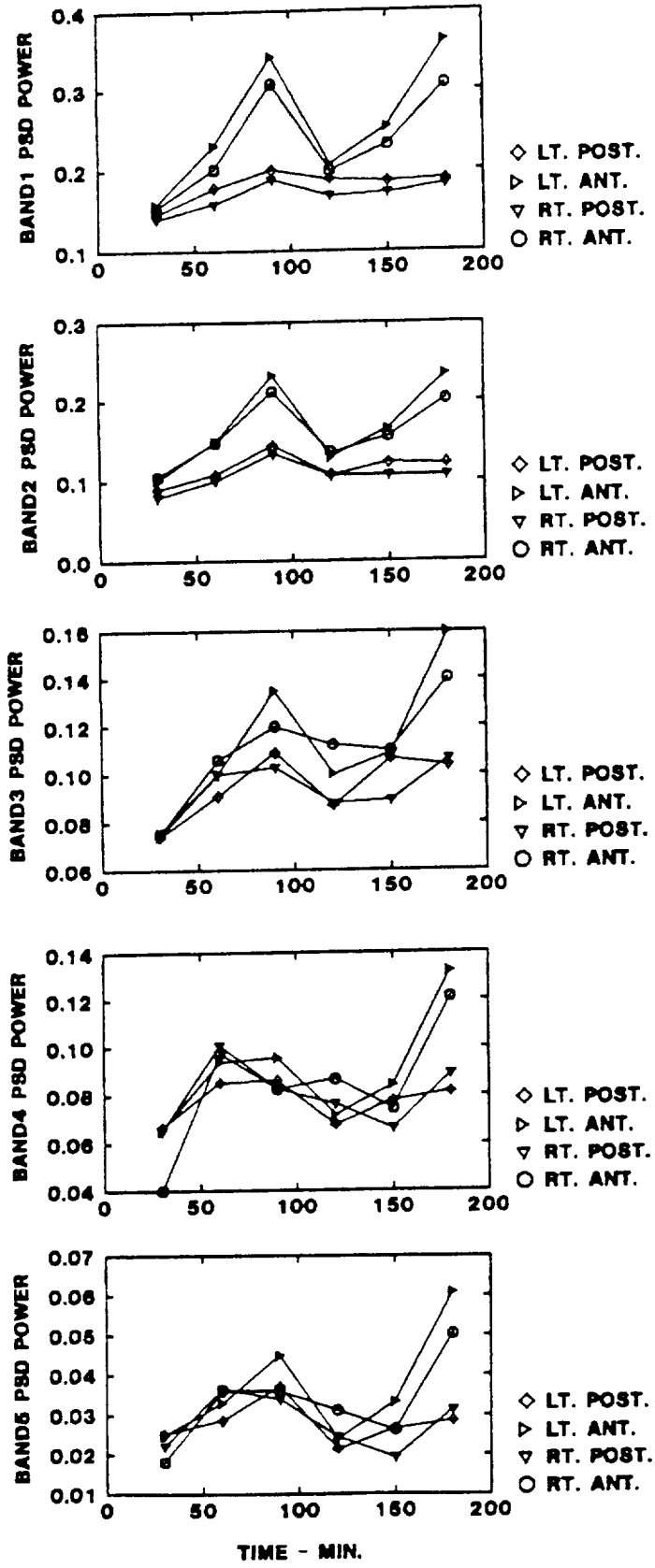

FIGURE VI.2.-55

VERBAL/MAT EEG TOTAL BAND POWER vs. TIME

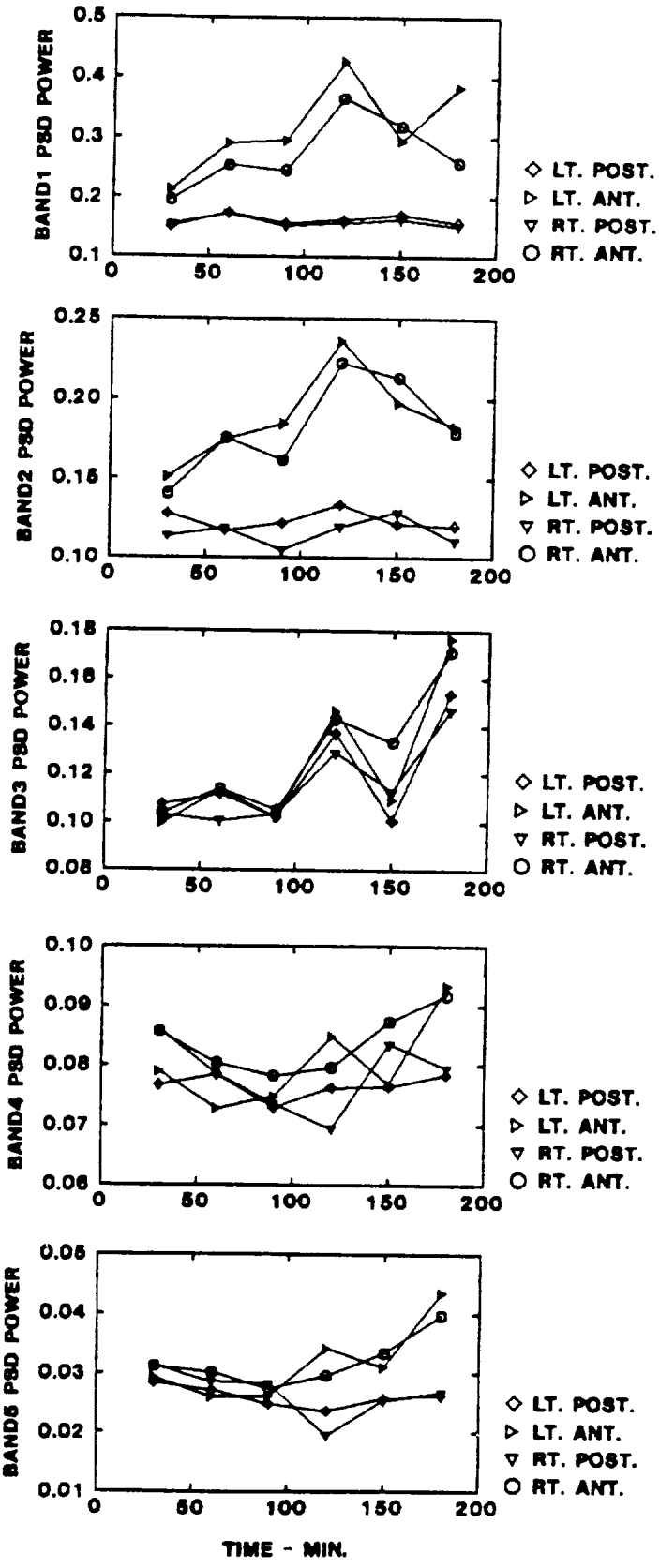

FIGURE VI.2.-56

VERBAL/MAT BLOOD FLOW vs. BAND3 EEG PSD

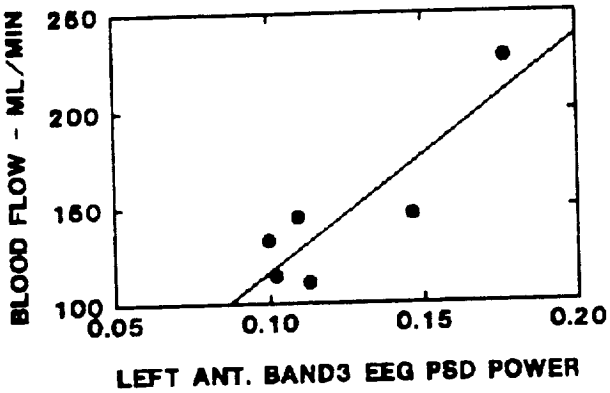

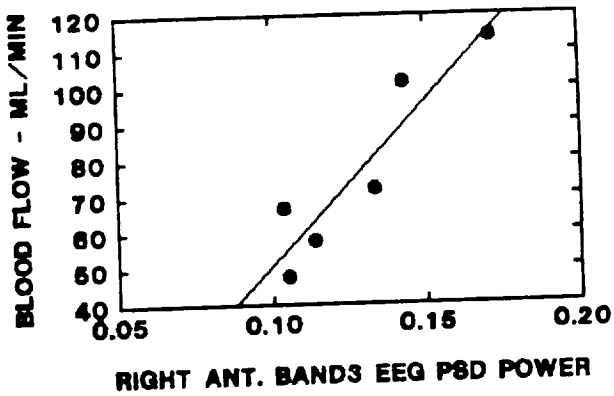

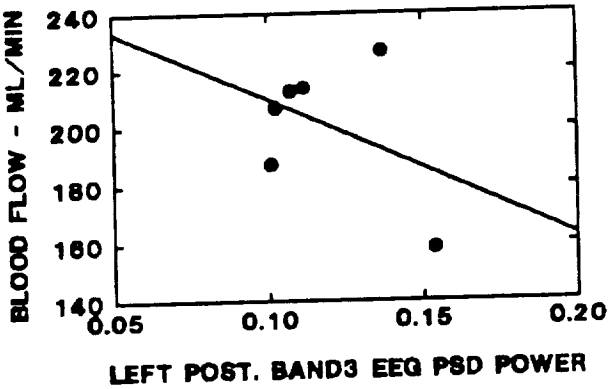

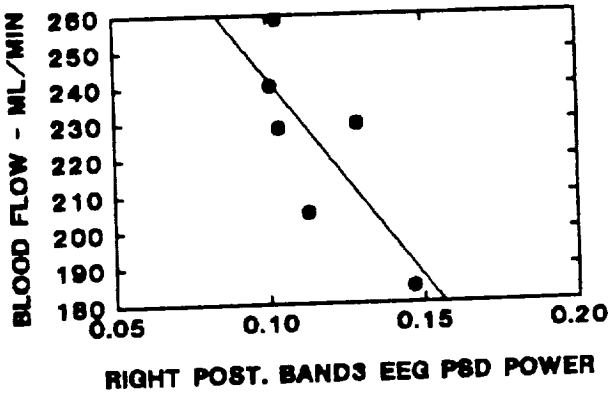

FIGURE VI.2.-57

SEGMENTAL BASE RESISTANCE vs. TIME

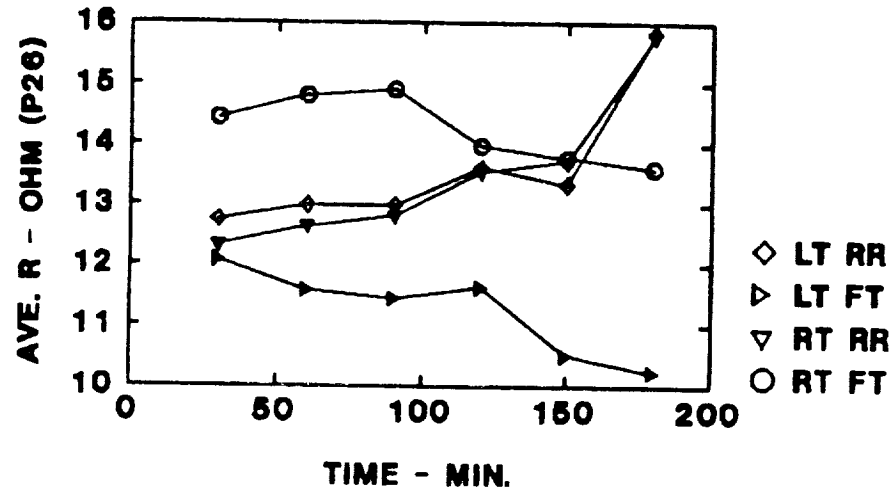

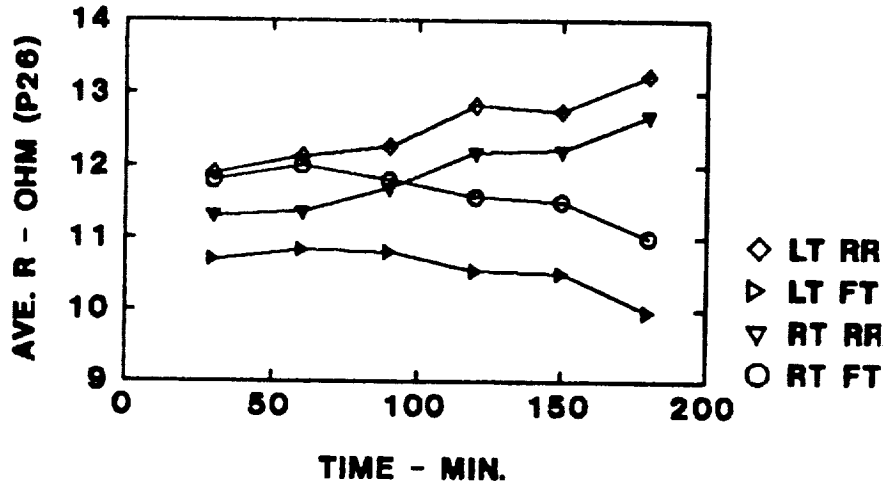

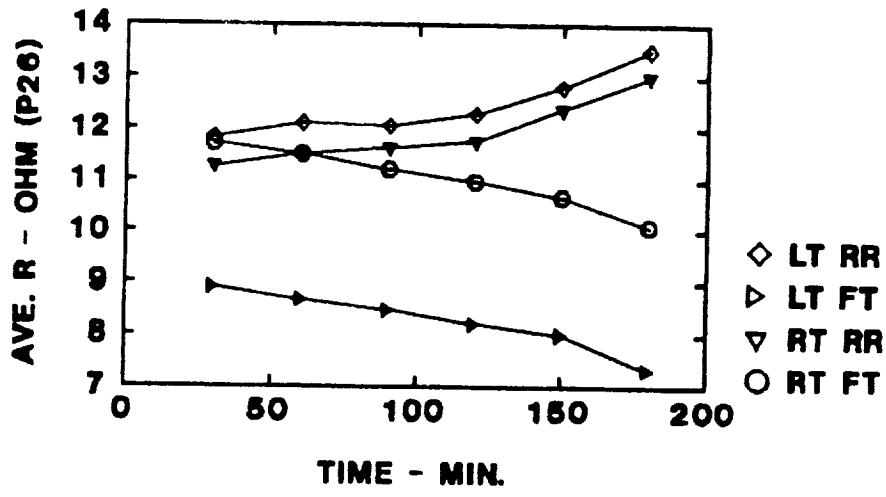

FIGURE VI.2.-58

REG PULSE SYSTOLIC AREA vs. TIME

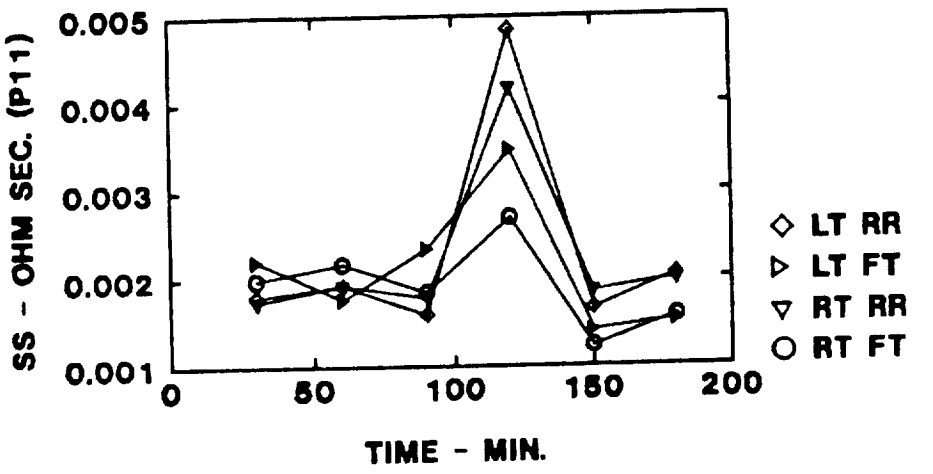

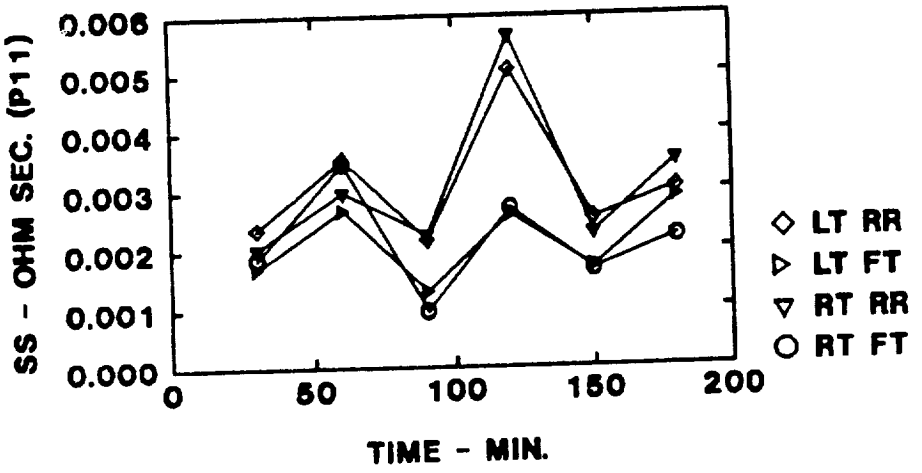

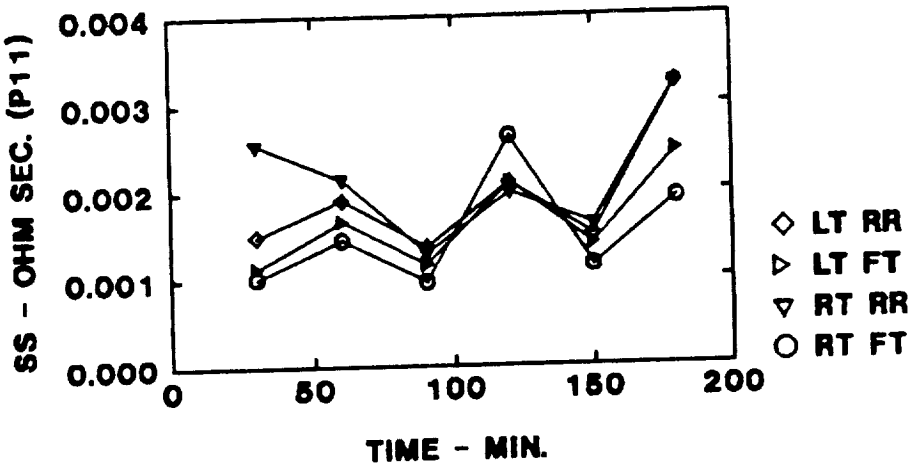

FIGURE VI.2.-59

INDEX OF VENOUS OUTFLOW vs. TIME

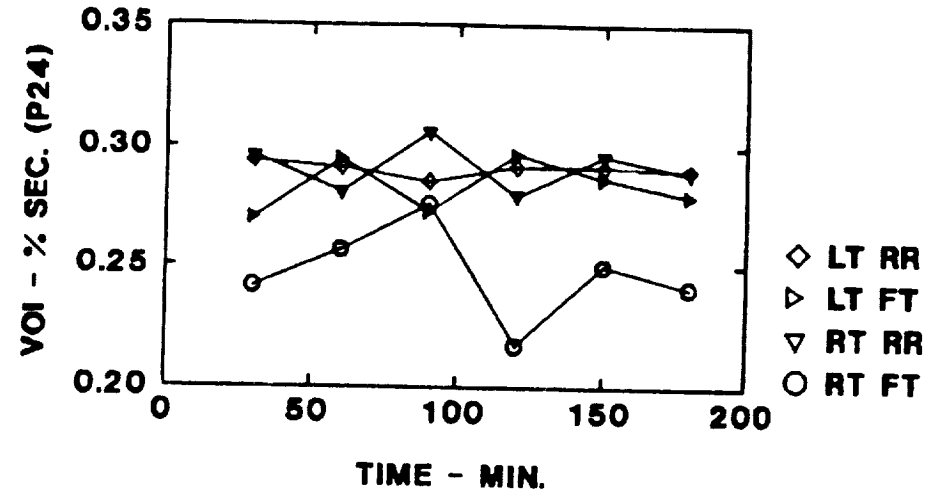

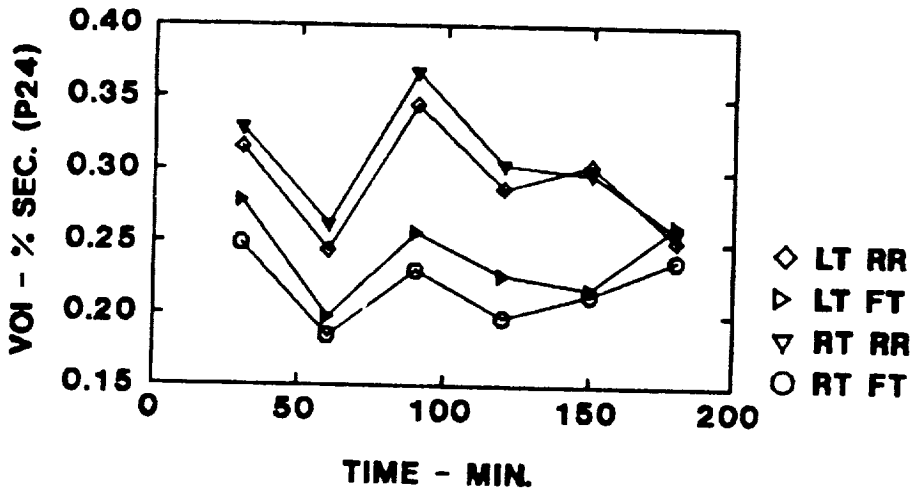

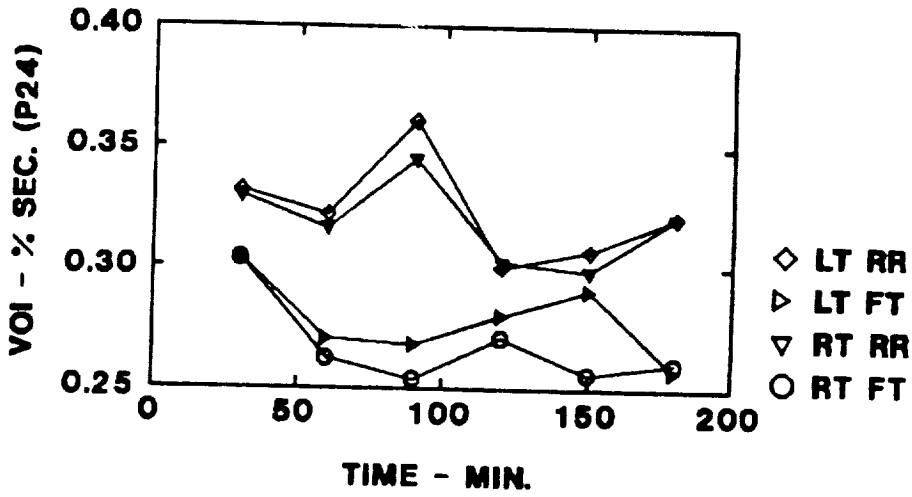

FIGURE VI.2.-60

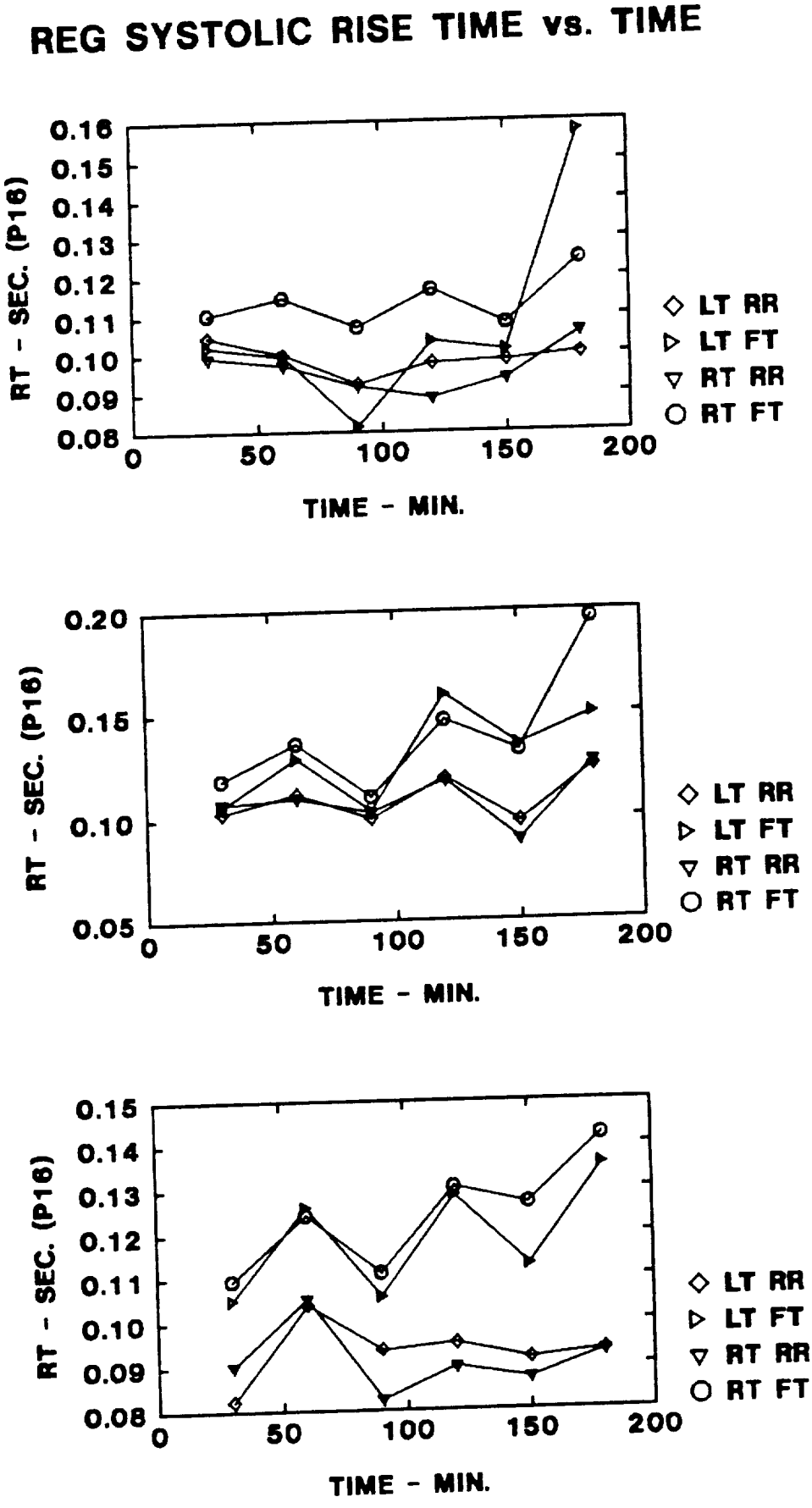

FIGURE VI.2.-61

INDEX OF VASCULAR COMPLIANCE vs. TIME

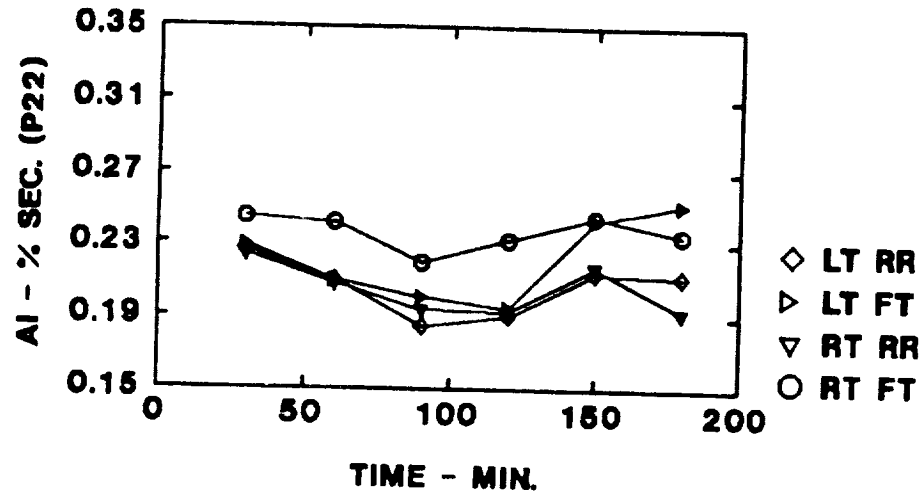

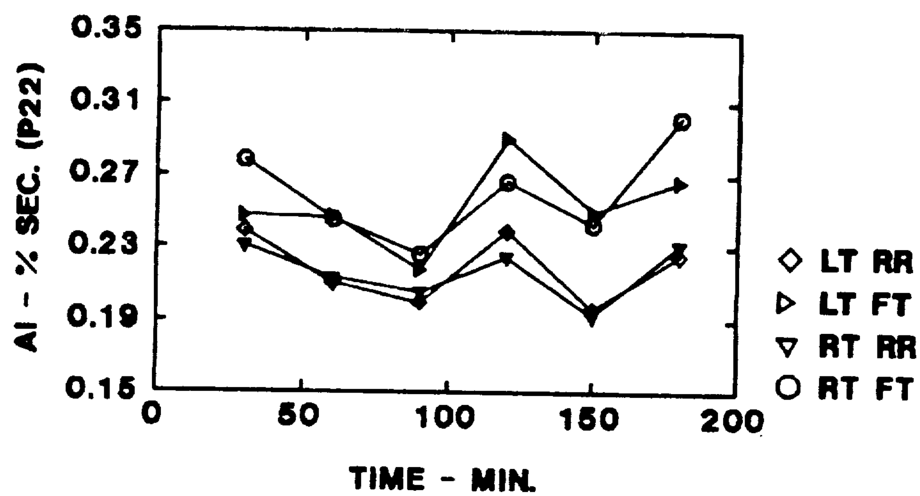

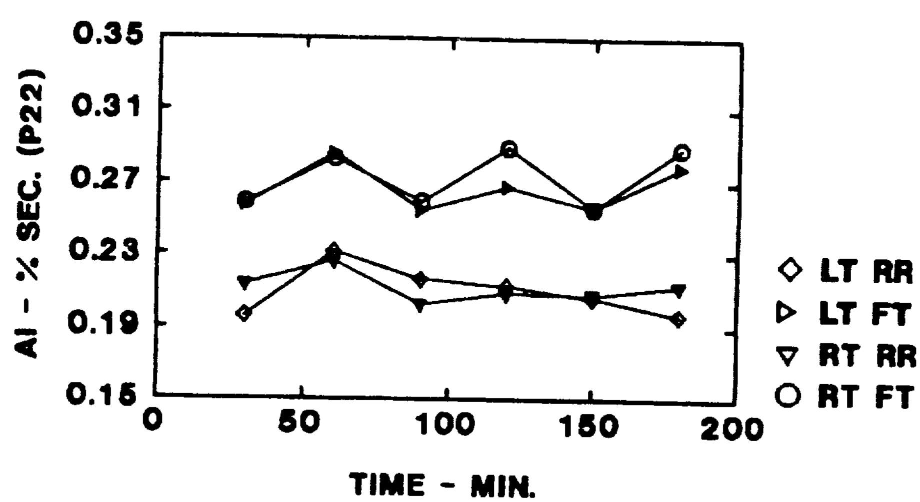

FIGURE VI.2.-62

REG MAX. AMP. PULSE TRANSIT TIME vs. TIME

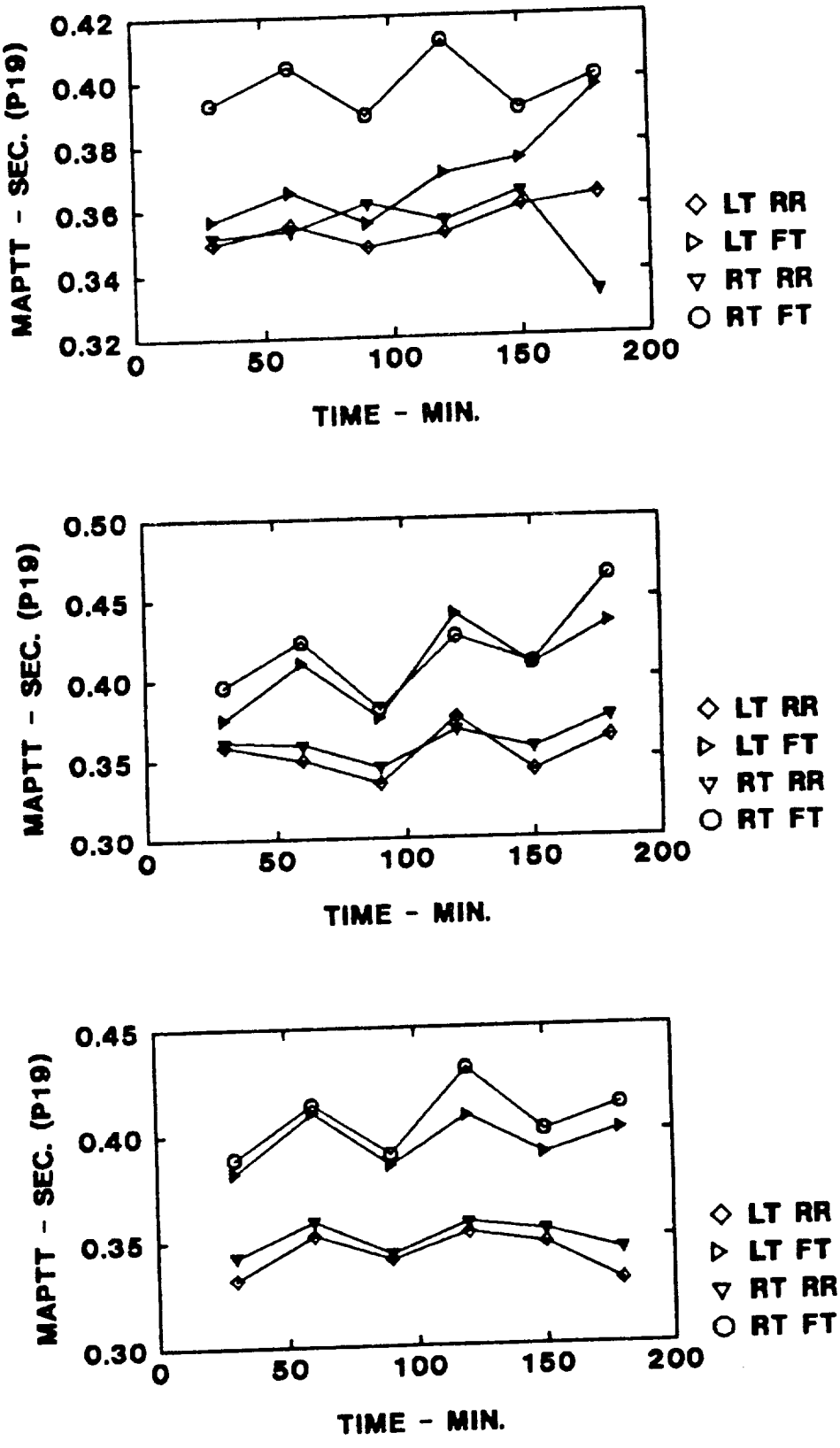

VII. DISCUSSION

ERP-based analysis of EEG data reveals not only peaks of activity localized to discrete cortical areas, but multi-electrode montages suggest the presence of systematic wave-form relations between electrodes, relations that can be obscured by observation of single time traces or frequency analysis. In order to explore this simultaneous inter-electrode relationship, we explored (during Phase I of this project) the use of state trajectories (Guisado, et. al., 1988) Although promising, this approach falls short of showing the entire picture: state trajectories can only view three electrode axes at a time, which limits the analysis of multi-electrode EEG montages. A better approach is given by constructing a three-dimensional picture of the whole voltage surface. This was obtained by fitting an equation to the data by least squares and then by rapidly displaying the series of surfaces corresponding to the fitted equations. The least squares fitted equations also facilitate vector-calculus transformations of the surfaces they represent. In this manner, gradients, Laplacians, etc., can be studied just as easily as the voltage surface itself. Others (Hjorth, 1980; Nunez, 1981) had used interpolation techniques to obtain a Laplacian and reveal charge density. The surface equations obtained by the least-squares fitting technique not only allow calculation of the Laplacian, but also of energy density, by multiplying voltage at each point by the charge density at that point.

Traditional methods of EEG analysis assume that EEG records "polarization currents" as they "flow up through the skull and onto the scalp" (Nunez, 1981). The high resistivity of the skull, however, makes it possible to measure the influence on scalp surface charges, of the electrical field radiated through the skull. The calculated energy density used in these experiments, is a reflection of the "work" done on scalp surface charges, by the underlying cortical electrical field.

The energy density equation offers two practical improvements over both charge density and voltage: it allows time integration (=power) and 2) it improves spatial resolution by producing single sharp peaks in the ERP surface.

The subject performance data, the energy density analysis and the REG data (Heart Rate Modulus-HRM), taken together suggests that the only cognitive task that equally and consistently stressed the experimental subjects was the VERB task. Subject performance and physiological indices showed less variance with difficulty level during the MATH task and it did not appreciably change during the SPAT task.

As shown under VI.1.1.1., (subjects' performance results), higher task levels did not necessarily correspond to

decreased level of performance. The reaction time appeared to be monotonically graded by task level, but the separations between task levels were not statistically significant. The other basic measure, percentage wrong, increased monotonically only for the Verbal task.

These results confirm the problematical nature of an a-priori approach to manipulation of task level (i.e., construction of tests that are thought to be at different levels of difficulty by design). The problem is that "difficult" is not a useful construct unless it is defined operationally. That is, a "difficult" task is simply one which a subject performs poorly. By this behavioral criterion, the level of difficulty of a particular task should be expected to vary from subject to subject and even from trial to trial, as a consequence of learning.

The experimental design attempted to accommodate this problem. The a-priori "LOW, MEDIUM, and HIGH" task-level classification was used only as a means of promoting a wide range of putative difficulty in testing sessions. However, rather than view these as experimentally controlled "treatment levels" (for an ANOVA or similar design), our attention was focussed on the correlation between selected features of a subjects' ERPs and their actual performance (averaged over the trials included in the ensemble-averaged ERP).

A remarkable cross-subject correlation of task performance with certain ERP features was indeed found. Individuals who generally perform a given type of task well (for whom the task is "easy") have quite different ERP amplitudes -- at certain sites and latencies -- than those individuals who generally perform poorly (for whom the task is "difficult").

This approach however, also implies a limitation with respect to causality. A high correlation between an EEG pattern (amplitude of a selected ERP peak, for instance) and task performance may result either from a direct effect of the nature of the task on neural function or because changes in neural function (such as learning or distraction) affect the performance outcome. One of the objectives of experimental designs based upon manipulation of "treatment levels" is to eliminate this ambiguity. For example, a finding of statistically significant differences in amplitude between a-priori task-levels would immediately invite the inference that task level differences "cause" EEG differences.

This limitation may be a weakness of our approach, depending upon how the results are used to facilitate monitoring in a work environment. The causal ambiguity of the results would be a weakness if the objective was to use EEG as a means of signalling that the operator had encountered a particular **pre-defined class** of tasks (eg. HIGH). On the other hand this

approach would be most useful if they were intended to facilitate monitoring of **actual performance.** Actual performance may deteriorate (under stress for example), even though the task level would be considered LOW according to a-prior or jury criteria.

This methodological limitation is due to the inherent ambiguity of non-operational definitions of "task difficulty". The implication is that it may not be possible to use EEG to signal occurrence of a pre-defined class of cognitive stimuli. Early psychometric research revealed that even a seemingly obvious categorization of stimuli, such as bright light versus dim light, may not necessarily correspond to individual subjects' sensation of brightness (or to that of a single subject from trial to trial). One should therefore expect even greater difficulty in "standardizing" categories of complex cognitive stimuli.

General Empirical Observations:

The utility of these procedures can be related directly to certain empirical observations regarding the kind of data likely to be generated by cognitive tasks. These observations and their implications for future research and applications of our techniques are summarized as follows:

a) The following pattern of good and poor correlations between types of data and features of the cognitive task experiments can be observed:

	REG-monitored blood flow parameters	Variance of continuous EEG data	Shape of stimulus-gated EEG
Subject state (fatigue, frustration, boredom)	GOOD (1)	GOOD (3)	POOR (4)
Changes in subject's own performance.	POOR (2)	POOR (3)	POOR (5)
Subject's performance relative to other subjects	POOR (2)	POOR (3)	GOOD (5)

(1): Section VI.2.3., pages 217 - 237
(2): Section VI.2.1., pages 166 - 201

(3): Section VI.1.2., pages 91 - 106
(4): Section VI.1.3., pages 107 - 165
(5): Section VI.1.1., pages 30 - 90

This matrix implies that REG and continuous EEG monitoring should be considered appropriate for monitoring subject state -- and ERP analysis should be viewed as mainly a tool for diagnosing differences in performance among subjects. ERPs might reveal changes in subject state for wider ranges of subject state than those explored in this project.

b) Subjects' EEG ERPs are highly stable across changes in the levels of difficulty of tasks and even from one type of task to another. However, by contrast, the shape of one subject's ERP is typically different from another subject's even for the same task level and type. This implies that it is not valid to speak of a generalized ERP (a general ERP shape characteristic of a given type of task, for example). Nor is it valid to pool subjects' ERPs.

c) On the other hand, differences in the shapes of subjects' ERPs (for the same task type) are evidently strongly related to differences in the subjects' capacities to perform the task. Almost all cross-subject performance variation can be accounted for by simple linear regression upon features of the ERP. This implies that such regression analysis offers a valuable tool for research into learning, specialization, cross-cultural differences in cognition, man-machine interfaces, and cognitive deficit syndromes associated with heredity, trauma, and disease.

d) In using the regression procedure, a significant improvement in statistical fit results when the ensemble-averaged ERPs are converted to "energy density ERPs". This is accomplished by 1) finding the Laplacian of the spatial distribution of the voltage field at each instant and then multiplying the negative of the Laplacian (charge density) at each spatial point, at each instant, by voltage at that point. This formula is commonly used to find the spatial distribution of potential energy of an electrical field, and the improvement in statistical fit implies that this conversion offers a means of improving the spatial resolution of EEG data.

e) The Laplacian required for the "energy density" transformation of ERPs was obtained by vector calculus performed directly upon an equation for the spatial distribution of voltage (at each instant). This was made possible by the discovery that such an equation could be obtained by multiple regression on the set of simultaneous electrode voltage readings (at each instant). A series of such fitted surfaces was found, on average, to capture ("explain") 92% of the actual variation in raw data response

montages; the fit is almost perfect for ensemble averaged ERPs, which are much smoother. This implies that such regression surfaces provide a picture of the spatial variation of voltage at least as good as interpolation, which is the currently used procedure for topographic EEG mapping. The regression approach also has at least three distinct advantages: it is far faster, it permits an animated 3D picture of the time evolution of the field to be reconstructed from the series of fitted surface equations, and it facilitates subsequent vector-calculus transformations (to view field gradients, Laplacians, etc.)

f) It was found that 32 scalp electrodes provide no significant improvement in spatial resolution of EEG data, over than obtained by regression on 21 electrodes. This implies that the spatial frequency of cortically generated electrical waves is so low that the length of most waves is less than the electrode spacing with 21 electrodes. This is consistent with the smooth shapes of ERPs observed (at any instant); it is contrary to the illusion of high frequency imparted by time traces recorded under conventional paper speeds.

Discussion of Rheoencephalographic Monitoring of Cognitive Tasks.

The specific objectives of the rheoencephalographic portion of this project were:

1. to develop and demonstrate equipment and procedures that allow the recording of multichannel cerebral blood flow during various experimental protocols,

2. to determine the effect of both stimulus gated and long term cognitive tasks upon cerebral and peripheral circulation, and

3. to compare the rheoencephalographic and frequency domain electroencephalographic responses of each test sequence as functions of duration and task content.

These objectives are described individually and by comparing the current status of rheoencephalography to that which existed prior to the Phase I SBIR project.

Instrument and Procedures

Prior to Phase I we employed a single channel bipolar impedance system to monitor head segment. Pulsatile impedance changes were recorded on a single channel strip chart. Quantification of cerebral blood flow responses to mental tasks was confined to hand graphical determination of maximum pulse height as an index of cerebral pulse volume.

During the Phase I effort a two channel tetrapolar REG was used to record right and left hemisphere blood flows on magnetic disk. Data analysis was still carried out by hand scoring to quantify cerebral blood flow, arterial and venous tone and cardiac dynamics.

The Phase II project provided the opportunity to utilize a four channel tetrapolar REG to measure right and left anterior and posterior quadrants of the head, forearm blood flow and a lead I electrocardiogram. Eight channels of analog signals were recorded on computer using a CODAS data acquisition system. This information was analyzed using the RHEOSYS computer program to quantify 30 indices of cerebral blood flow, volume, vasomotor reflexes, and cardiac function.

Cerebral Circulatory Responses to Cognitive Tasks

The three test sequences conducted during Phase II clearly demonstrate that regional cerebral blood flow and localized vasomotor responses are sensitive to both task content and duration. Each of the test sequences investigated a different aspect of cerebral circulation.

Mixed Tasks

Hemispheric cerebral blood flow was graded and varied in a statistically significant manner during the various Mixed tasks. Cerebral blood flow was predominantly affected by the MATH task, was less responsive during the VERB task, and remained unchanged during the SPAT task. Forearm blood flow was found not to change significantly during any of the three tests.

The Mixed task heart rate modulus (HRM) responses tend to support the hemodynamic responses found during the various tasks. These results suggest that the subject group was relaxed and not stressed during the initial periods of all three tasks. They also indicate that the subjects found the MATH task to be more stressful than the SPAT or VERB tasks, that the VERB task was somewhat stressful, and that the SPAT task was not stressful at all. An alternative explanation is that the MATH task was more engaging to the subjects than the other two tasks and that the SPAT task involved the least amount of thought to complete.

Tracking Task

The tracking task results suggest that the intracranial blood flow changes during a continuous task are the result of sympathetic and localized vasomotor responses, that tend to induce increased blood flow during the tracking task. These changes are independent of systemic blood flow changes. The mechanisms responsible for this differential response are primarily local vascular contractility, tone, and pulse

volume.

Long Term Task

The regional and temporal changes in blood flow, EEG percent and total band powers, and REG vasomotor indices found during the Long tests clearly illustrate how the test procedures developed during this investigation may be used in cognitive research. As a subject initiates and attends to a task he becomes relaxed or more confident during the first hour. As the task continues he becomes more aroused (or less relaxed) and has to mobilize his neural resources, particularly in the frontal segments of the head. The increased neural activity in the frontal segments during the midtask test sequences require a larger inflow of blood which is accomplished by increased heart rate and regionally active vasomotor reflexes.

The results of this task suggest that a close relationship exists between the neural activity and brain blood flow that may be task as well as time dependent. The regression analysis of blood flow and EEG activity showed that these variables are highly correlated.

Comparison of EEG and REG Responses to Mental Tasks

The fact that changes were found in both the REG and EEG power spectra during Phase I and Phase II mental tasks supports the notion that rheoencephalography monitors intracranial blood flow and not predominantly scalp blood flow, i.e. scalp effects would not alter the electro-encephalographic activity.

The extent of correlation between REG measures of cerebral blood flow and the 8 - 13 Hz electroencephalographic activity was very high ($r = 0.89 - 0.93$) for the frontal quadrants during the VERB/MAT task. These correlations decrease to approximately 0.70 during the MATH/MAT task. These results are quite similar to those of the Phase I project in which the REG index of venous tone was found to correlate with the EEG 0 - 8 Hz band power ($r=0.93$, $P < 0.01$) during mental arithmetic.

Based upon the results described in Section VI.2., the best application of REG may be for detection of cerebral circulatory changes during protracted experimental conditions. This is particularly true when serial measurements can be made on the same subject population over time. Rheoencephalography should be used on each subject using standardized methods and quantification procedures as described in this report.

REFERENCES

Action, W. H. and Crabtree, M.S. (1985) Users Guide for the Criterion Task Set. Armstrong Aerospace Medical Research Laboratory Report AAMRL-TR-85-034, Aerospace Medical Divison, Wright-Patterson Air Force Base, Ohio.

Arnegard, R.J., and Comstock, J.R., Jr. (1991) Multi-Attribute Task Battery: Applications in pilot workload and strategic behavior research. Proceedings of the Sixth International Symposium on Aviation Psychology, Columbus, Ohio, pp. 1118-1123.

Atefie, K. and Jenker, F.L. (1983) Matching results of rheoencephalography, 99m TC-scan and doppler. Medica Jadertina, Vol. XV (Supplementary Issue), pp 216-219.

Caplan, Roy S. and Essig, Alvin (1983) Bioenergetics and Linear Nonequilibrium Thermodynamics: The Steady State. Harvard U. Press: Cambridge.

Celesia, G. G. (1985) Visual Evoked Potentials: A Practical Approach Within the Guidelines for Clinical Evoked Potential Studies. American Journal of EEG Technnology, 5:93-113.

Chatrian, G. E., Lettich, E., and Nelson, P. E. (1988) 10% Electrode System. Journal of Clinical Neurophysiology, 5:183-6.

Cook, N. D. (1986) The Brain Code: Mechanisms of Information Transfer and the Role of the Corpus Callosum. Methuen Press.

Courchesne, E., Hillyard S., and Galambos, R. (1975) Stimulus Novelty, Task Relevance and the Visual Evoked Potential in Man. Electroencephalography and Clinical Neurophysiology, 39:131-143.

Churchland, P. S. (1986) Neurophilosophy. MIT Press: Cambridge, Mass.

Dekoninck W.J., Priaux A., Uytdenhoef P., Jacquy J. (1982) Relationship between EEG and cerebral blood flow in normal brain aging. Experimental Brain Research, Suppl. 5, pp. 208-215.

Doyle, J. C., Ornstein, R., and Galin, D. (1974) Lateral Specialization of Cognitive Mode: II. EEG Frequency Analysis. Psychophysiology, Vol. 11: 567-578.

Farah, Martha J. and Peronnet, F. (1989) Event-related Potentials in the Study of Mental Imagery. Journal of Psychophysiology, 3: 99-109.

Galambos, R. and Hillyard, S. (eds.) (1981) Electrophysiologicl Approaches to Human Cognitive Processing. Neurosciences Research Progress Bulletin, 20:1-270.

Gatlin, Lila L. (1972) Information Theory and the Living System. Columbia University Press: New York.

Gevins, A. S. and Cutillo, B. A. (1987) Signals and Cognition: Clinical Applications of Computer Analysis of EEG and other Neurological Signals. Chapter 11 of Handbook of Electoencephalography and Clinical Neurophysiology, Revised Series, Volume 2. Elsevier Science Publishers, New York, pp. 335-381.

Guisado, R., Montgomery, L. D., and Montgomery, R. W. (1988) Electoencephalographic Monitoring of Complex Mental Tasks, Final Report NASA Contract NAS1-18625.

Goldberger, Arthur S. (1968) Topics in Regression Analysis. Macmillan Company: New York.

Hadjiev D. (1968) A new method for quantitative evaluation of cerebral blood flow by rheoencephalography. Brain Research, Vol. 8, pp 213-215.

Hammond, P. (1981) Energy Methods in Electromagnetism. Clarendon Press: Oxford.

Hjorth, Bo. (1980) Source Derivation Simplifies EEG Interpretation. American Journal of EEG Technology, 20: 121-32.

Jacquy J., Dekoninck W.J., Piraux A., Calay R., Bacq J., Levy D., Noel G. (1974) Cerebral blood flow and quantitative rheoencephalography. Electroencephalography and Clinical Neurophysiology, Vol. 37, pp 507-511.

Jaynes, Julian (1976) The Origin of Consciousness in the Breakdown of the Bicameral Mind. Princeton University & Houton Mifflin Co.

Jenker F.L. (1962) Rheoencephalography: A method for the continuous registration of cerebralvascular changes. Charles C. Thomas, Springfield, Ill.

Kramer, A. F. (1983) Event Related Potentials. In: Gale, A. and Christie, B., (Eds) Psychophysiology and the Electronic Workplace. John Wiley and Sons Ltd.

Lehmann, D. (1984) EEG Assessment of Brain Activity: Spatial Aspects, Segmentation and Imaging. International Journal of Psychophysiology, 1:267-76.

Lehmann, D. (1987) Principles of Spatial Analysis. Gevins, A. and Remond, A., (Eds) Methods of Analysis of Brain Electrical and Magnetic Signals: EEG Handbook, (Revised Series, Vol. I). Elsevier Science Publishers.

Lehmann, D. and Skradies, W. (1984) Spatial Analysis of Evoked Potentials in Man: a Review. Progress in Neurobiology, 32:227-50.

Lovett-Doust J.W., Barchha R., Lee R.S.Y., Little M.H., Watkinson J.S. (1974) Acute effects of ECT on the cerebral circulation in man. Europ. Neurol., No. 12, pp 47-62.

Marble, T.N. (1988) Voluntary Cardiorespiratory Synchronization and Health Enhancement, M.S. Thesis. University of Minnesota.

Maxwell, J. C. (1891) Treatise on Electricity and Magnetism. Vol I, Part 1, Chapter 4. Clarendon University Press, (reprinted by Dover Publications, New York, 1954).

Moskalenko Y.E., Cooper R., Crow H.J., Walter G. (1964) Variations in blood flow and oxygen in the human brain. Nature, Vol. 4928, pp 159-161.

Nunez, Paul L. (1981) Electric Fields of the Brain: Neuro-Physics of EEG. Oxford University Press.

Nyboer J. (1970) Electrical impedance plethysmography, 2nd Edition. Charles C. Thomas, Springfield, Ill.

Plonsey, R. and Fleming, D. (1969) Bioelectric Phenomena. McGraw-Hill: New York.

Rao, N. N. (1977) Elements of Engineering Electromagnetics. Prentice-Hall, New York.

Rockstroh, B. et.al. (1982) Slow Brain Potentials and Behavior. Urban and Schwarzenberg, Baltimore.

Schey, H. M. (1973) Div, Grad, Curl and all that. Norton: New York.

Shadowitz, A., (1975) The Electromagnetic Field. Dover: New York.

Shingledecker, C. A. (1984) A Task Battery for Applied Human Performance Assessment Research. Air Force Aerospace Medical Research Laboratory Report AFAMRL-TR-84-071, Aerospace Medical Divison, Wright-Patterson Air Force Base, Ohio.

Snyder, E., HYillyard, S., and Galambos, R. (1980) Similarities and Differences among the P3 Waves to Detected Signals in Three Modalities. Psychological Physiology, 17: 112-22.

Sowerby, L. (1974) Vector Field Theory with Applications. Longman Group, Limited: New York.

Speckmann, E. J. and Elger, C. E. (1987) Introduction to the Neurophysiological Basis of the EEG and DC Potentials. In: Niedermeyer, E. and da Silva, F.L. Electroencephalography: Basic principles, clinical applications and related fields, 2nd Ed., pp.1-13. Urban and Schwarzenberg, Baltimore.

Spehr, W. (1976) Source Derivation after Hjorth: An Improved EEG Derivation Technique. Electromedica, 4:148-155.

Suprynowicz, V. A. (1966) Introduction to Electronics for Students of Biology, Chemistry and Medicine. Addison-Wesley: Reading, Mass.

Szentagothai, J. and Arbib, M. A. (1977) Conceptual Models of Neural Organization. Neuroscience Research Progress Bulletin, 12: 306-510.

Thompson, R. F. and Patterson, M. M. (1974) Biolectric Recording Techniques. Academic Press: New York.

Thompson, William. Lord Kelvin (1848) Article in Cambridge and Dublin Mathematical Journal (February) and entry in his diary, April 8, 1845.

Usochev V.V., Shinkarevskaya I.P. (1973) Functional changes in systemic and regional (intracranial) circulation accompanying low acceleration. Kosmich. Biol. Aviak. Med., Vol. 19, No. 1, pp 59-64.

Vaughan, H. G. and Arezzo, J. (1988) The Neural Basis of Event Related Potentials. Chapter 3 in Pitcon, T. W. (ed.), Human Event Related Potentials: EEG Handbook (revised series, Vol 3). Elsevier Science Publishers.

Vasilescu, V and Margineanu, D. G. (1982) Introduction to Neuro-Biophysics. Abacus Press: Tunbridge Wells, Kent.

Wonnacott, R. and Wonnacott, T. (1970) Econometrics. John Wiley and Son: New York.

Yarullin KK, et. al. (1980a) Studies of central and regional hemodynamics by isotope and impedance methods during LBNP. Kosmich. Biol. Aviak. Med., Vol. 14, No. 5, pp 99-104.

Yarullin KK, et. al. (1980b) Studies of prognostic significance of antiorthostatic position. Kosmich. Biol. Aviak. Med., Vol. 14, No. 3, pp 48-54.

Yarullin KK, et. al. (1972) Changes in cerebral, pulmonary, and peripheral blood circulation. Kosmich. Biol. Aviak. Med., Vol. 6, No. 4, pp 33-39.

APPENDIX A

SYSTEM CONTROL COMPUTER

Program requirements mandated a system capable of executing all monitoring, control and display functions to within a temporal resolution of about 1 msec. The system was designed to meet this requirement in an MS-DOS operating environment using a commercially available Analog-to-Digital Input/Digital-to-Analog Output expansion card with a programmable real-time pacer clock. A member of the 80386 class of desktop computers was identified as essential for this system in order to assure that the CPU will be capable of the required interrupt servicing at appropriately high-speeds. The system allows examination of response latencies not possible with earlier equipment and, because experimental control can be implemented in software, provides flexibility to accommodate altered or expanded experimental objectives that future results may motivate.

Data acquisition hardware and development of supporting system software are described below. The latter consists of custom application-specific modules that implement required I/O card functions using a software driver provided with the card, modified and re-compiled as required. The main run-time support modules, being written in BASIC, were compiled using Micro-Soft QUICK-BASIC and linked to the I/O card driver to obtain a stand-alone program able to run in the faster MS-DOS environment outside the BASIC Interpreter.

The time base of each run is driven by a programmable clock on the I/O card, set to trigger an A-D conversion scan of desired input channels and trip a real-time flag to pace operation of the control program every 1 msec. Each pulse of the I/O board clock can actually trigger only a single A-D conversion of analog data on a particular input channel. Consequently, forcing a scan of more than one channel for each clock pulse requires use of the I/O card ability to interrupt the CPU, where the main control program operates. The I/O board hardware can generate such interrupts by only two mechanisms: 1) after completion of each A-D conversion (one interrupt per channel scanned) or; 2) after transfering a fixed number of A-D conversion data (each triggered by a separate clock pulse) directly to a memory buffer; i.e., after terminal count for N DMA (Direct Memory Access) transfers. Only the first mechanism can be used in the present application.

Each clock pulse triggers an A-D conversion of the first channel in each scan. On completion of this conversion, an interrupt to the computer's CPU is issued. On receipt of this interrupt, the CPU suspends operation of the main program and runs an interrupt service routine that completes the

channel scan, sets a timing flag and returns control to the main program. The timing flag serves as the real-time pacer for the main control program, where the timing flag is reset for the next clock tick and the A-D data is read and processed. Scanned channels include the derivatized REG waveform (dR/dt), a single analog channel of the subject ECG and the analog output of a keyboard provided to the subject for registration of response to each presented cognitive task.

The I/O card driver as provided by the manufacturer required modification to implement the scheme of I/O board pacing of main program operation. Interrupt service routines in the original driver provided only limited real-time interfacing capability between the I/O card and the main program. As shipped, they can support such real-time interfacing only under control of the slower CPU clock. High speed data acquisition is achieved by data transfers commenced after a single I/O function call, where data is not available for processing in the main program until the data acquisition period has ended. Thus, required modifications entailed addition of the timing flag for main program pacing and the return of CPU control to the main program between each channel scan. Data write/reads using I/O data buffers were also modified to take advantage of the Direct Memory Access (DMA) capability of the I/O card to enhance execution speed of the program.

Different functions are performed during the period between each channel scan depending on the prevailing experimental state. A given experimental series consists of N runs. Each run entails presentation of a single cognitive task on a video display monitor to which the subject responds by pressing one of two buttons on the keyboard. After the series is parameterized and enabled by the operator, a randomized delay precedes presentation of each of the N tasks. Following each delay, detection of the next systolic peak in the dR/dt signal triggers the presentation of the cognitive task to the subject and the output of a signal to two separate D/A channels for a "task presented" marker on the EEG and REG records. These signals are held "high" until detection of a subject response on the keyboard. The dropping of this signal serves as a "task answered" marker on the EEG and REG records. The accuracy of the response can then be assessed, a "task response" marker is output to the EEG and REG records indicating the veracity of the answer, and the sequence recycles for the next task until completion of the series.

APPENDIX B

RHEOENCEPHALOGRAPHIC IMPEDANCE TRACE SCANNING SYSTEM

Typical display formats from the RHEOSYS program are attached to illustrate its application. As developed, RHEOSYS can be applied to simultaneously acquired rheoencephalo-graphic and electrocardiographic waveforms for the determination of pulse propagation times and other cardiac parameters in addition to numerous impedance indices.

Figure B-1 shows typical impedance data traces that may be used in the RHEOSYS computer program. The program permits the definition of specific traces from a multicolumn data array through a calibration file which asks the data columns to be displayed, the total number of data columns recorded, the digitization rate of the recorded signals, whether the displayed data is in the raw (recorded) format or to be the derivative of some other column, and the calibration factors of the recorded data. The automated calculated parameters are currently set up to utilize the format shown in Figure 11, with the blood flow pulse on the top, the derivative of the blood flow pulse (calculated by the program from the top trace) in the middle, and the ECG waveform at the bottom. Smoothing techniques or digital filters can be applied to the data to be analyzed as it is displayed on the computer monitor.

Figure B-2 shows the main working screen used by the RHEOSYS program. The options that can be invoked within the program are displayed at the top of the screen. Each option can be activated by depressing the appropriate terminal key as follows: R=REDO the current display resetting the calculations to the prior pulse, P=Pulses allows the cursor keys to select pulses that are to be analyzed, F=FLIP allows the operator to sequentially "flip" or page through the set of pulses selected for analysis, T=TIME can be used to select any trace segment to be displayed and to compress or expand the data traces, S=SCL is used to designate independent scaling factors for each data trace, V=VERT is used to change the baseline position of each of the displayed data traces on the computer monitor, E=END allows the operator to exit the program, A=AVE is used to calculate the average values for each parameter from the set of preselected pulses, and C=CHK may be used to display and check the set of parameter values for any single pulse from the preselected series.

The notation located at the lower left corner of the screen denotes the pulse number (P) that is currently displayed, the number of the pulse mark (M) that is being selected, and the point number (T) where the vertical cursor is located. PMARK OFF or PMARK ON tells the operator whether he is in the pulse select mode or the pulse calculate mode. The REG,

DERivative, and ECG fields at the bottom of the screen displays the actual voltage amplitude of each recorded signal (independent of the scaling factor and vertical positions used to display the data).

Figure B-3 shows a section of the waveforms from Figure B-1 which have been enlarged and positioned to facilitate selection of the pulse series to be analyzed.

Figure B-4 presents the first of a series of three pulses that have been selected for analysis usint the P option. As each pulse is selected it's number and location are displayed at the left margin of the screen. After a given number of pulses are selected the operator depresses the F option to sequentially display each of the selected pulse waveforms in an enlarged format for analysis.

A typical pulse that has been marked with predetermined points is shown in Figure B-5. As it is currently programmed, seven points are selected from the blood flow and ECG waveforms:

1. Peak of the first ECG QRS complex,
2. Start of systolic slope on the blood flow trace,
3. Maximum amplitude of the impedance pulse,
4. Position of the dicrotic notch,
5. Maximum amplitude of the postdicrotic segment,
6. Peak of the second ECG QRS complex, and
7. Start of the next blood flow pulse.

These points are used to calculate the various geometric and time related functions shown in Figure B-6 (from Lovett-Doust et. al., Acute effects of ECT on the cerebral circulation in man) which are then used to obtain each of the 32 impedance and cardiac cycle parameters by the RHEOSYS program.

This set of parameters include pulse amplitudes; areas; pulse propagation times; cardiac cycle times; and various measures of arterial and venous tone, contractility, and pulse volume.

The selected points are displayed on each of the displayed waveforms, including the point locations on the first derivative trace. In its present state of development, the program does not utilize any of the information provided on the first derivative data trace. It will be used in later versions of the program to potentially automate the point selection process (note that the blood flow points fall consistently at a baseline crossing of the first derivative data trace). In addition, this aspect will also be used to

calculate cardiac output according to presently used commercial algorithms.

Table B-I presents a typical set of average calculated parameters from a series of three pulses. This set of tabulated values can be saved as a two column ASCII file complete with header information that is compatible with most statistical programs.

The current version of the program may be recycled to include a second, third, etc. segmental blood flow pulse train using identical pulse times for analysis which facilitates comparison of multisegmental data under similar experimental conditions. This feature will be useful in the analysis of regional vasomotor responses to various types of environmental stress or in the comparison of interhemispheric blood flow during cognition.

The following parameters are calculated by the RHEOSYS computer program from the seven points that are selected on the ECG and REG pulsatile waveforms. The parameters are numbered according to the listing that is printed out by the RHEOSYS program (Jacquy, 1974; Lovett-Doust, 1974; Moskalenko, 1964; Nyboer, 1964; Usochev, 1973; Yarullin, 1980a, 1980b, 1972).

1. LI - DEG	Initial angle (between 0 and 10% of systolic amplitude) of REG systolic rise.
2. LA - DEG	Average angle (between 10 and 90% of systolic amplitude) of REG systolic rise.
3. HR - BPM	Heart rate as calculated from time between subsequent QRS peaks of the recorded ECG waveforms.
4. RI - (A) - OHMS	Rheographic Index of pulse volume as determined from the maximum height of the systolic portion of the REG waveform (A) when converted to ohms resistance.
5. B - OHMS	Height of the REG waveform at the dicrotic notch when converted to ohms resistance.
6. C - OHMS	Height of the maximum REG peak after the dicrotic notch when converted to ohms.

7. DCI - % OHMS	Dicrotic Index of arteriolar tone calculated as the ratio of C/A.
8. DSI - % OHMS	Diastolic Index of venular tone calculated as the ratio of B/A.
9. ST - OHM SEC	Total are under the REG waveform from the start of one pulse to the start of the next pulse.
10. SD - OHM SEC	Area of the diastolic portion of the REG waveform from the time of the dicrotic notch until the end of the pulse.
11. SS - OHM SEC	Area of the systolic portion of the REG waveform from the start of the pulse until the time of the dicrotic notch.
12. STFI - OHM	Average pulse amplitude during the cardiac cycle calculated as the ratio of ST/Cardiac Time-T.
13. SDST - % OHM SEC	Ratio of the diastolic area to the total pulse area.
14. SSST - % OHM SEC	Ratio of the systolic area to the total pulse area.
15. HRT - SEC	Cardiac cycle time as measured between two sequential QRS complexes of the ECG recording.
16. RT - SEC	Systolic rise time calculated between the times of the 10 and 90% systolic pulse amplitudes.
17. T - SEC	REG cycle time calculated as the time between the start of two sequential REG pulse waves.
18. PTT - SEC	Pulse transit time calculated as the time interval between the ECG QRS complex and the

	start of the REG pulse waveform.
19. MAPTT - SEC	Maximum amplitude pulse transit time calculated as the time interval between the ECG QRS complex and the maximum REG pulse amplitude.
20. DNPTT - SEC	Dicrotic notch pulse transit time calculated as the time interval between the ECG QRS complex and the time of the occurrance of the REG dicrotic notch.
21. PDNPTT - SEC	Post dicrotic notch pulse transit time calculated as the time interval between the ECG QRS complex and the time of the occurrance of the maximum REG pulse amplitude following the dicrotic notch.
22. AI - % SEC	Anacrotic Index of segmental vascular contractility. The ratio time from the start of the REG pulse until the occurrence of the maximum pulse amplitude to the total REG period.
23. THRT - % SEC	Ratio of the REG pulse duration to the ECG cardiac cycle time.
24. VOI - % SEC	Ratio of the time period between the maximum REG pulse amplitude and the dicrotic notch to the total REG cycle time.
25. BF - ML/MIN	Segmental blood flow calculated as [rho(Length squared)(pulse amplitude)/Ro squared]xHR.
26. AVE R - OHM	Average base resistance during the REG pulse duration.
27. EX HT - OHMS	Extrapolated REG pulse amplitude taken as the height from the start of systole to

	the backward line drawn tangent to the initial decline in the pulse waveform immediately following the maximum pulse amplitude.
28. VE - L	Segmental "electrical" volume calculated as rho(L sq)/Ro sq
29. F Index -	Jacquy's Rheographic - F Index 1/sec of grey matter blood flow.
30. C Index -	Jacquy's Capacitance - C Index 1/sec or regional vasomotor capacitance.
31. R Index -	Jacquy's Reserve - R Index of regional vasomotor reserve.
32. AMFAC -	Amplitude Calibration Factor, internally computed by REHOSYS and printed out as a functional check variable. It is not a regional hemodynamic parameter.

FIGURE 1

TYPICAL IMPEDANCE DATA TRACES USED IN THE RHEOSYS COMPUTER PROGRAM

PULSATILE IMPEDANCE CHANGES (TOP), FIRST DERIVATIVE (MIDDLE), ELECTROCARDIOGRAM (BOTTOM)

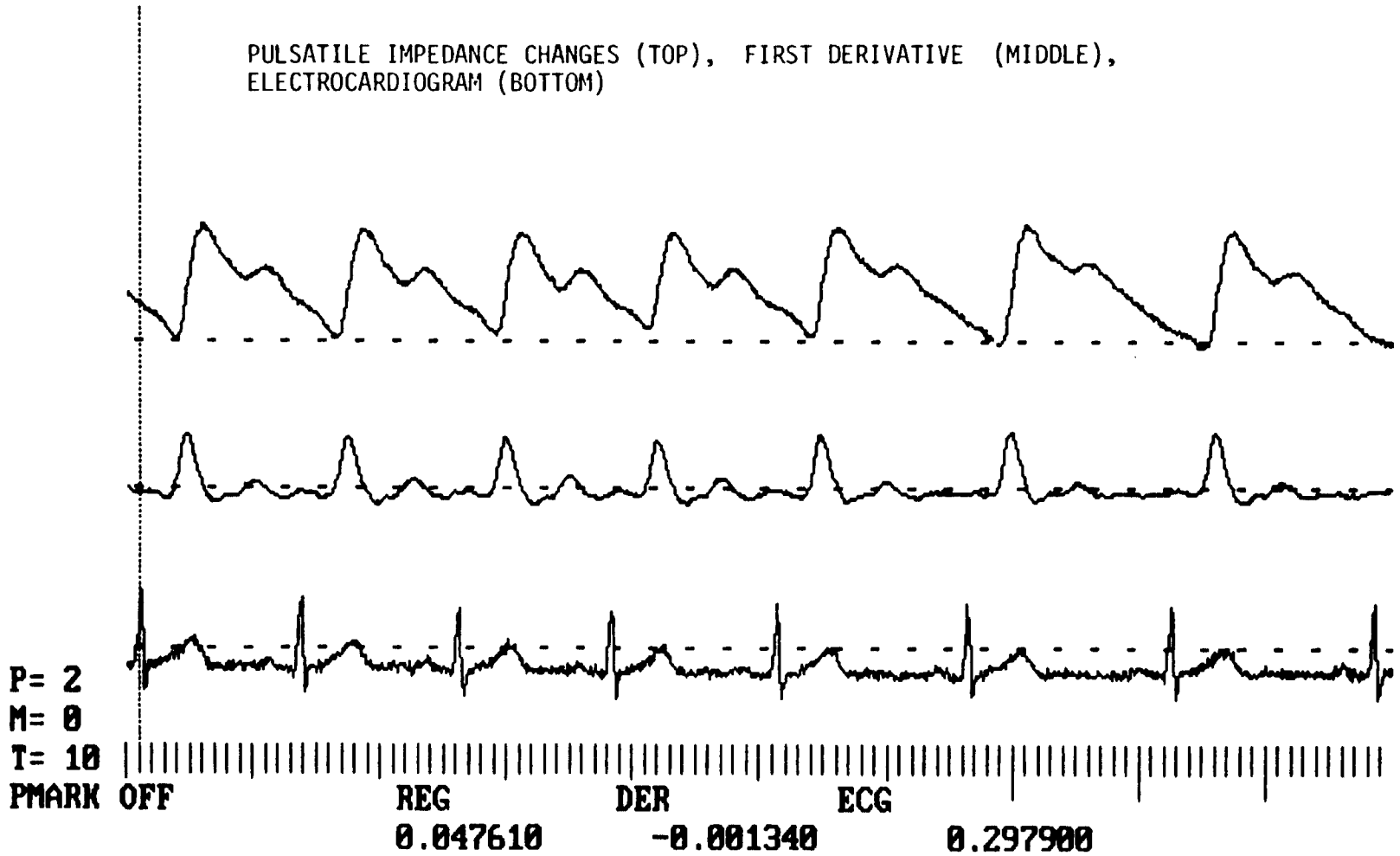

FIGURE 2

TYPICAL DISPLAY FORMAT USED BY THE RHEOSYS COMPUTER PROGRAM

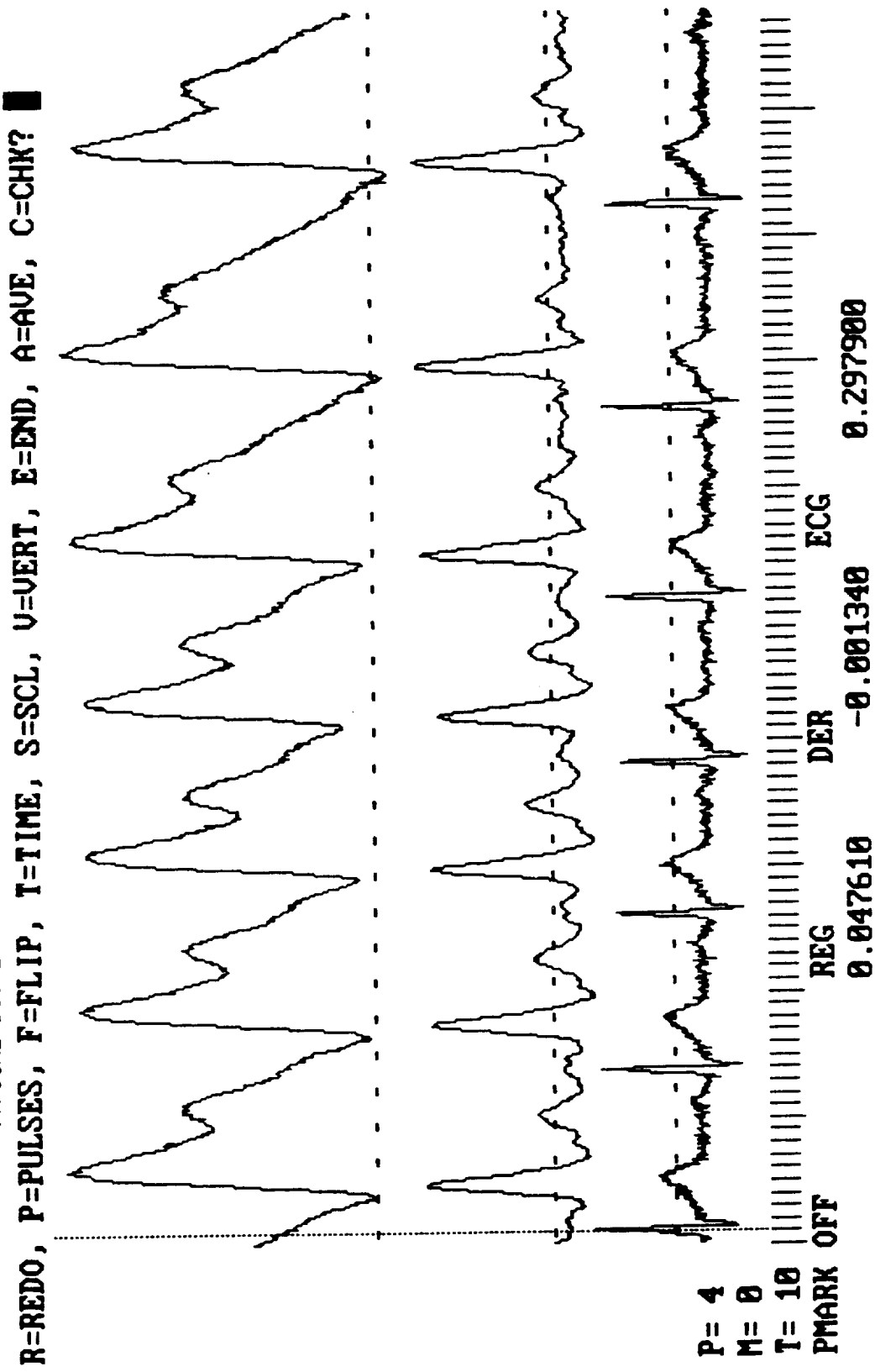

FIGURE 3

ENLARGED IMPEDANCE AND ECG WAVEFORMS USED TO SELECT SEGMENTS
FOR COMPUTERIZED ANALYSIS

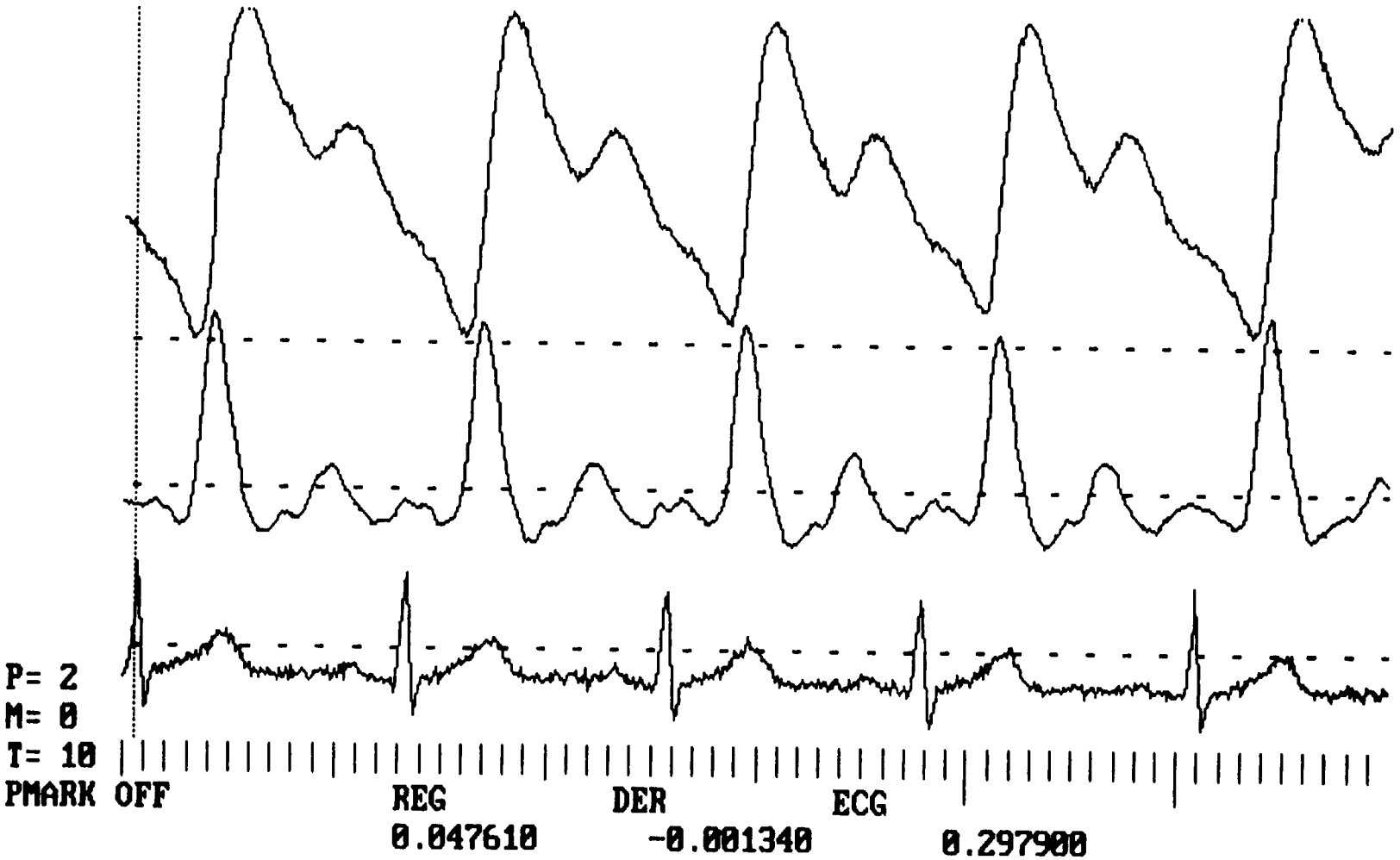

FIGURE 4

INDIVIDUAL PULSATILE SEGMENTS DISPLAYED THROUGH "FLIP" MODULE
PRIOR TO POINT SELECTION

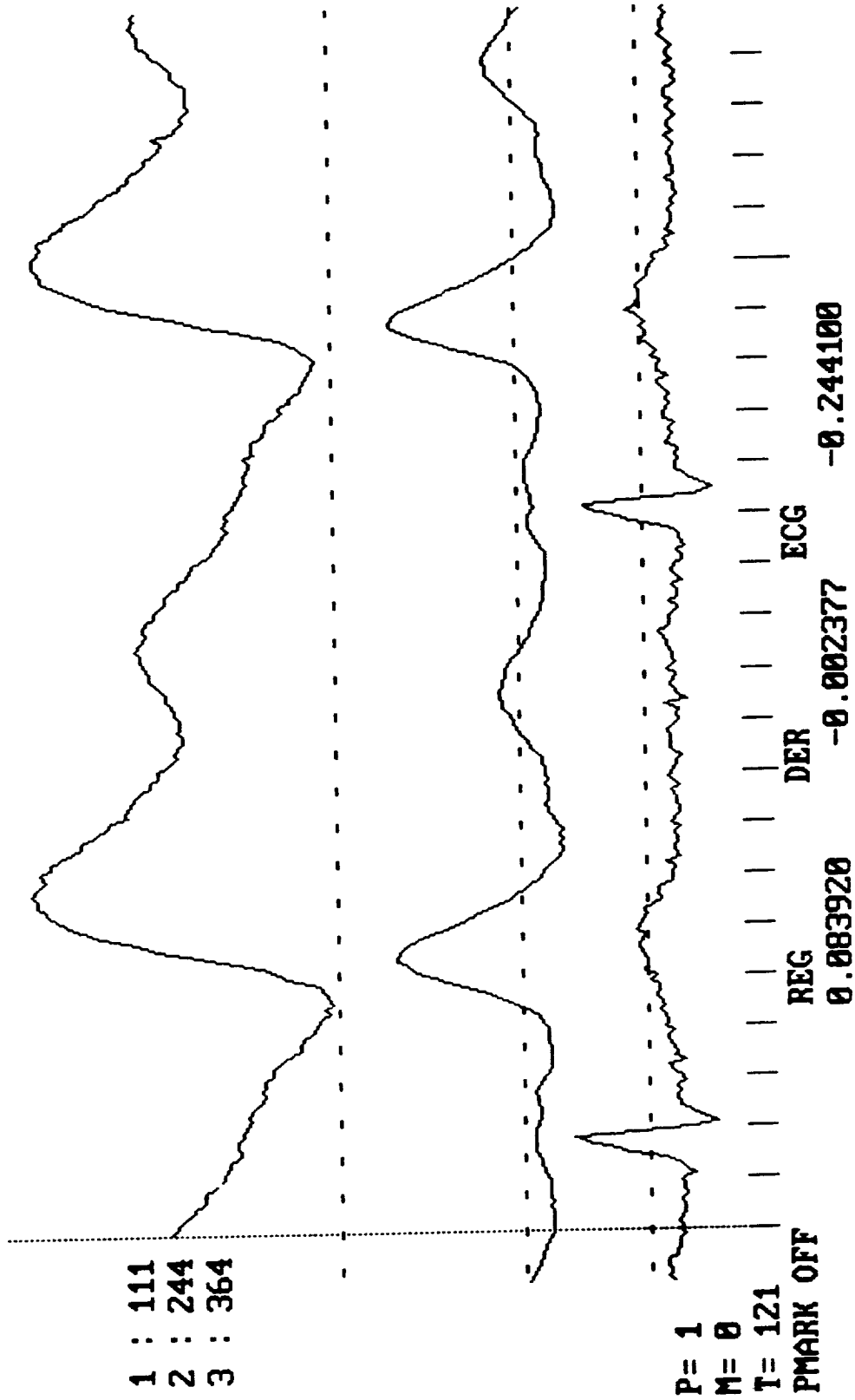

FIGURE 5

SELECTED POINTS ON IMPEDANCE AND ECG WAVEFORMS USED FOR PARAMETER CALCULATIONS

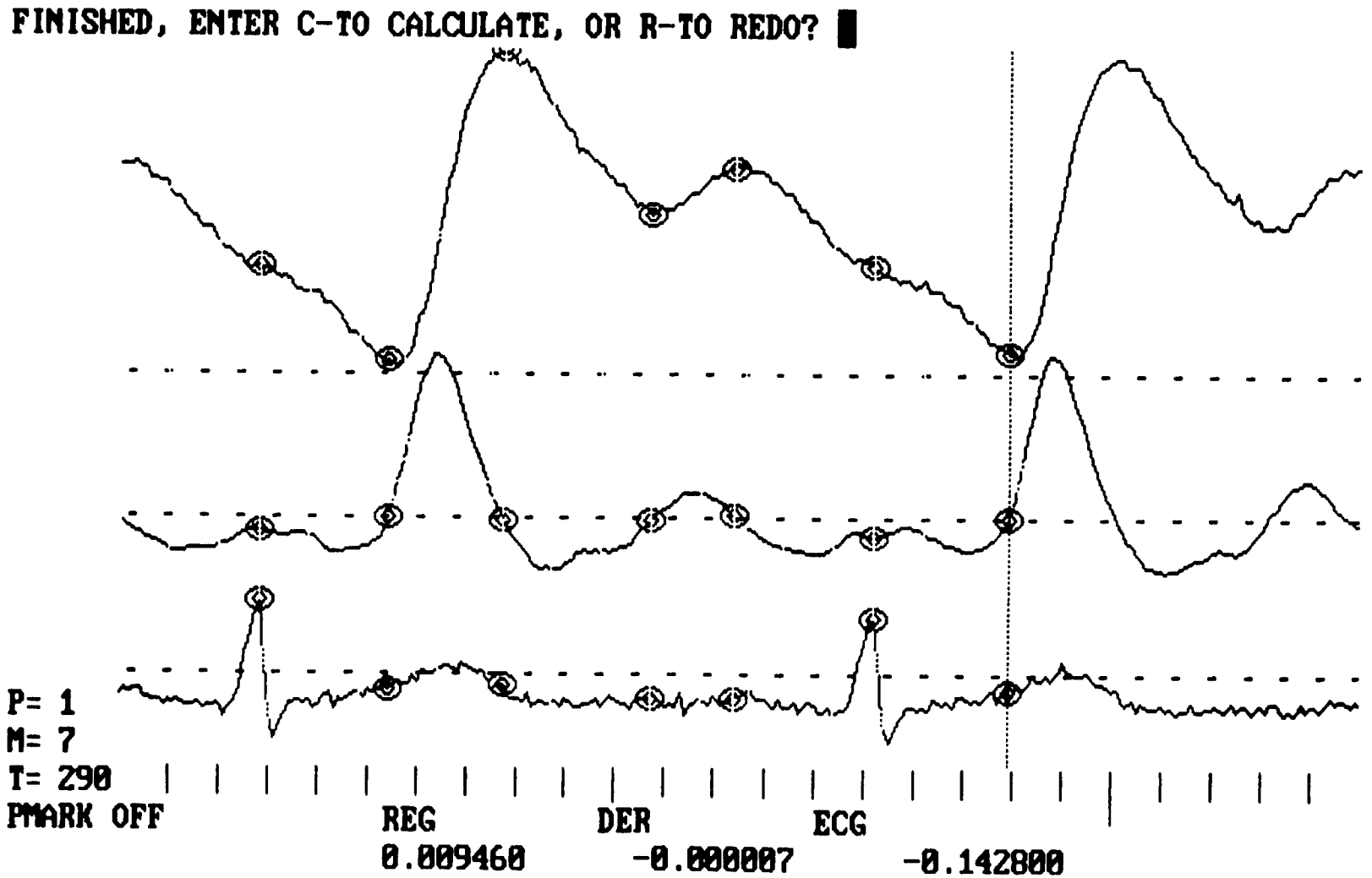

TABLE

TABULATED PARAMETERS CALCULATED BY RHEOSYS

AVERAGES FOR 1 PULSES FILE bmm11.rho CHANNEL 1

1 LI-DEG.....	0.1418	17 T-SEC.....	0.9400
2 LA-DEG.....	8.7892	18 PTT-SEC.....	0.1640
3 HR-BPM.....	63.5593	19 MAPTT-SEC....	0.3320
4 RI-(A)-OHMS..	0.0183	20 DNPTT-SEC....	0.5000
5 B-OHMS.....	0.0134	21 PDNPTT-SEC...	0.5800
6 C-OHMS.....	0.0147	22 AI-%SEC.....	0.1787
7 DCI-%OHMS....	0.7362	23 THRT-%SEC....	0.9958
8 DSI-%OHMS....	0.8057	24 VOI-%SEC.....	0.2638
9 ST-OHM SEC...	0.0093	25 BF-ML/MIN.....	573.2540
10 SD-OHM SEC...	0.0075	26 AVE R-OHMS....	12.0000
11 SS-OHM SEC...	0.0018	27 EX HT-OHMS....	0.0216
12 STFI-OHMS/SEC	0.0099	28 VE-L.....	5.0000
13 SDST-%OHM SEC	0.8067	29 F INDEX-1/SEC.	1356.4583
14 SSST-%OHM SEC	0.1933	30 C INDEX-1/SEC.	131.5951
15 HRT-SEC.....	0.9440	31 R INDEX-1/SEC.	6.3810
16 RT-SEC.....	0.0920	32 AMFAC (check)	0.0145

DO YOU WANT TO SAVE THESE AVERAGES AS A FILE (Y/N)?

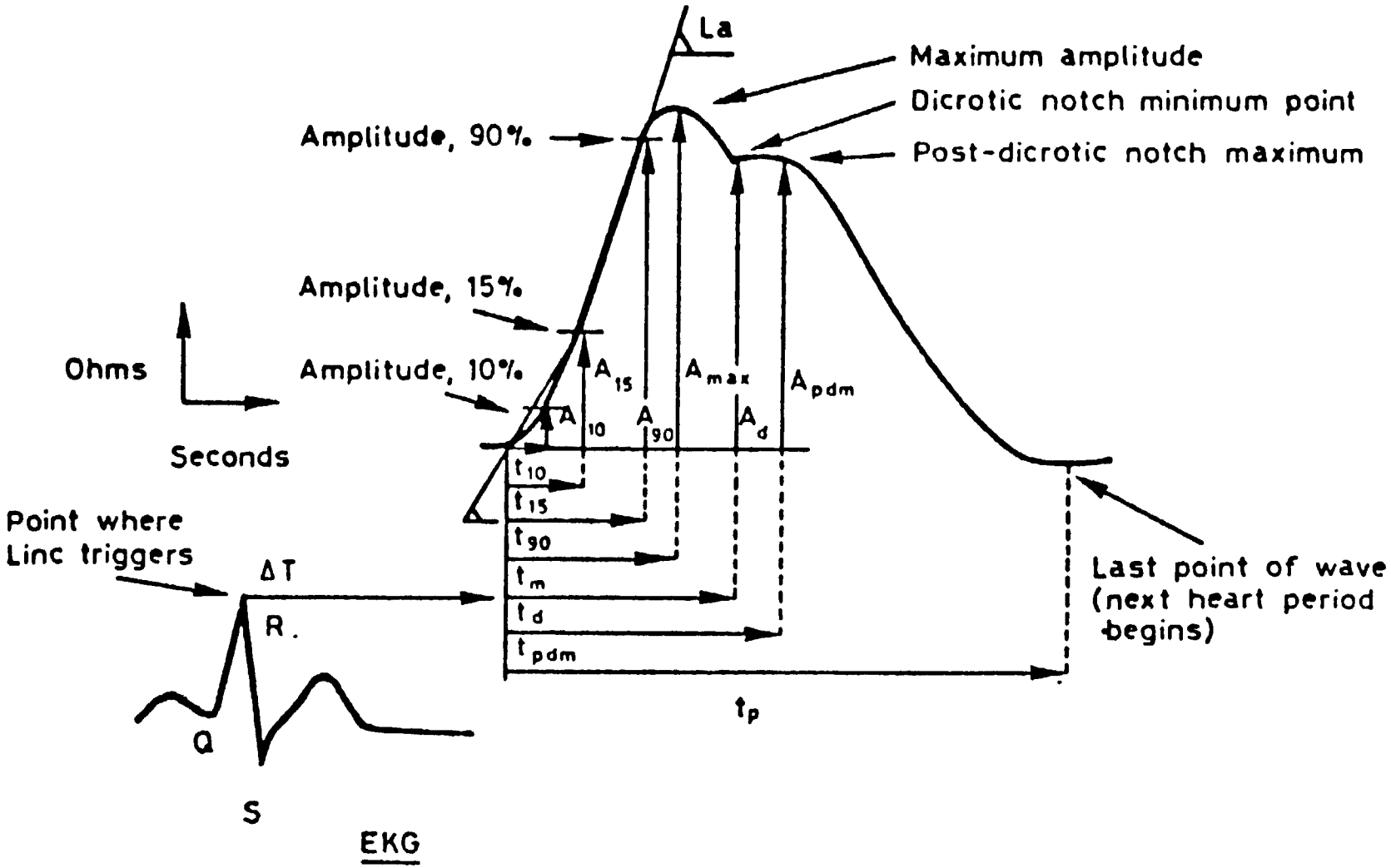
La
Maximum amplitude
Dicrotic notch minimum point
Post-dicrotic notch maximum
Amplitude, 90%
Amplitude, 15%
Amplitude, 10%
Ohms
Seconds
A15
Amax
Apdm
A10
A90
Ad
t10
t15
t90
tm
td
tpdm
tp
Point where
Linc triggers
ΔT
R
Q
S
Last point of wave
(next heart period
begins)
EKG

APPENDIX C

TABLE I

Performance Data for Mental Arithmetic Task

Subject	Low	Medium	High
Percent Wrong:			
00	25.3	30.0	13.3
03	29.5	24.4	20.8
07	25.3	33.7	21.3
08	34.8	27.3	12.5
09	29.7	28.6	25.3
Mean	28.9	28.8	18.6
Reaction Time:			
00	1.204	1.178	1.212
03	1.229	1.741	2.006
07	0.986	0.945	1.161
08	1.155	1.387	1.527
09	1.022	1.050	1.292
Mean	1.119	1.260	1.440
Error Index			
00	31.616	36.509	17.372
03	37.460	44.154	43.680
07	25.892	32.904	25.856
08	41.366	39.213	20.609
09	31.339	31.057	33.936
Mean	33.535	36.767	28.290

TABLE I (cont'd)

Performance Data for Word Pair Data

Subject	Low	Medium	High
Percent Wrong:			
00	12.2	21.4	30.3
03	3.8	11.5	32.1
07	7.4	13.8	27.5
08	10.0	14.8	30.0
09	6.2	10.0	21.0
Mean	7.9	14.3	28.2
Reaction Time:			
00	1.094	1.234	1.128
03	1.421	1.640	1.925
07	1.385	1.610	1.790
08	1.432	1.577	1.856
09	1.464	1.666	2.109
Mean	1.359	1.545	1.762
Error Index:			
00	14.465	27.575	35.348
03	6.820	20.561	63.621
07	11.648	23.751	51.024
08	15.580	24.926	57.521
09	10.495	18.126	46.339
Mean	11.802	22.988	50.779

TABLE I (cont'd)

Performance Data for Shape Matching Task

Subject	Low	Medium	High
Percent Wrong:			
00	7.3	3.2	2.1
03	7.5	17.7	11.4
07	7.1	2.4	6.0
08	12.2	11.2	15.7
09	9.7	4.4	4.4
Mean	8.8	7.8	8.0
Reaction Time:			
00	0.772	0.850	0.929
03	1.157	1.683	1.749
07	1.047	1.350	1.612
08	1.183	1.336	1.381
09	0.928	0.920	1.128
Mean	1.017	1.228	1.360
Error Index:			
00	6.400	3.537	2.889
03	9.835	31.504	21.675
07	8.440	4.564	11.205
08	15.634	16.355	23.096
09	9.914	4.921	6.037
Mean	10.045	12.176	12.980

TABLE II

MIXED TASK AVERAGES AND STANDARD ERRORS

CASE	%WRONG	R-TIME	ERROR INDEX
M L	28.90	1.1189	33.5345
	1.77	0.0488	2.6800
M M	28.78	1.2610	36.7676
	1.54	0.1406	2.3253
M H	18.63	1.4393	28.2905
	2.46	0.1548	4.7583
V L	7.90	1.3592	11.8017
	1.46	0.0674	1.5479
V M	14.27	1.5452	22.9877
	1.97	0.0793	1.6570
V H	28.18	1.7616	50.7786
	1.94	0.1671	4.8368
S L	8.75	1.0174	10.0448
	0.99	0.0761	1.5356
S M	7.77	1.2279	12.1763
	2.94	0.1535	5.3676
S H	7.91	1.3599	12.9802
	2.48	0.1509	4.0690

TABLE VI

C:TRAK-00.INT	LEFT	RIGHT	TOTAL
1	217.538	159.037	472.087
2	280.234	218.189	635.715
3	214.991	171.543	479.297
4	184.155	152.539	426.003
5	171.341	124.399	375.590
6	224.685	158.735	486.898
7	231.696	164.457	490.979
8	295.294	209.502	642.818
9	253.149	172.244	542.493
10	197.699	145.993	423.383
11	163.133	119.961	355.350
12	352.937	266.541	782.836
13	224.713	157.571	474.884
14	214.926	152.985	462.443
15	242.392	158.557	511.725
16	236.754	158.718	498.693
17	213.331	183.409	499.892
18	216.472	167.280	483.985
19	235.049	183.941	521.724
20	198.355	154.435	450.937
21	174.226	138.714	406.676
22	173.846	132.699	396.484
23	183.421	138.823	420.200
24	212.070	182.964	517.583
25	193.363	154.075	438.550
26	126.100	113.948	321.141
27	176.636	165.408	440.368
28	250.224	190.886	583.730
29	221.333	237.660	589.117
30	378.779	325.058	935.072
31	147.477	122.070	349.022
32	173.807	164.271	446.477
33	177.060	144.184	422.415
34	178.825	147.002	419.600
35	221.900	155.271	489.926
36	184.675	122.761	407.483
37	191.704	186.210	495.746
38	231.396	230.940	614.713
39	139.960	129.533	366.740
40	202.883	172.351	495.345

TABLE VI CONT.

C:TRAK-00.INT	LEFT	RIGHT	TOTAL
41	148.902	130.166	369.586
42	153.954	121.227	354.651
43	167.505	148.559	418.075
44	241.159	210.761	603.761
45	345.873	286.167	803.465
46	254.594	215.751	585.003
47	387.649	297.836	846.836
48	227.630	198.154	526.382
49	275.198	233.493	634.185
50	345.873	286.167	803.465
51	181.002	126.983	398.472
52	245.889	202.468	569.471
53	187.044	207.119	481.849
54	318.257	293.108	793.765
55	297.903	254.942	699.363
56	264.851	264.499	671.643
57	311.221	291.197	764.261
58	156.122	145.004	374.813
59	170.167	164.496	413.374
60	169.712	153.780	404.425
61	261.156	215.516	609.320
62	371.352	365.213	911.318
63	252.423	226.368	600.114
64	301.005	259.192	704.306
65	401.076	330.717	939.218
66	698.719	534.790	1479.841
67	680.332	586.348	1537.437
68	511.634	440.325	1157.754
69	639.629	611.239	1525.868
70	500.901	396.324	1084.080
71	292.033	248.259	658.022
72	357.945	293.424	837.441
73	357.799	320.092	855.560
74	374.579	328.282	881.741
75	347.272	252.195	747.578
76	159.242	143.083	397.986
77	184.758	148.968	441.359
78	150.404	138.208	384.820
79	189.930	185.706	498.835
80	152.253	129.767	367.651

TABLE VII

C:TRAK-03.INT	LEFT	RIGHT	TOTAL
1	166.724	127.070	379.489
2	162.403	129.365	379.828
3	101.517	92.572	252.058
4	206.695	215.625	542.203
5	97.256	95.493	254.517
6	106.835	111.371	280.401
7	179.675	197.400	498.266
8	181.888	191.957	487.801
9	127.867	134.839	343.486
10	152.981	139.036	370.664
11	144.234	158.512	383.749
12	283.899	221.226	653.499
13	123.427	131.429	334.668
14	149.334	144.211	370.929
15	154.133	155.751	402.777
16	133.403	116.431	321.453
17	113.211	126.343	307.701
18	170.108	169.006	419.520
19	363.658	298.958	873.029
20	162.326	152.431	412.507
21	140.465	143.556	359.386
22	205.655	207.352	526.909
23	153.685	164.106	399.349
24	181.760	176.646	446.417
25	213.907	169.418	485.590
26	158.533	131.485	382.529
27	204.656	192.492	522.858
28	177.293	150.213	418.809
29	167.445	184.415	449.594
30	381.420	278.293	834.593
31	266.336	250.478	654.163
32	204.656	192.492	522.858
33	149.952	189.543	456.149
34	258.597	210.022	627.941
35	208.051	190.659	506.013
36	214.973	240.667	580.879
37	197.872	208.667	507.770
38	279.637	270.841	693.860
39	334.145	300.811	810.710
40	516.177	409.363	1200.935

TABLE VII CONT.

C:TRAK-03.INT	LEFT	RIGHT	TOTAL
41	227.397	295.488	660.153
42	164.395	187.621	448.410
43	156.357	167.909	415.722
44	163.182	175.158	430.415
45	146.175	158.772	387.714
46	199.061	184.414	494.305
47	168.528	167.950	430.060
48	146.532	183.807	430.811
49	180.948	139.402	409.013
50	468.418	414.154	1182.335
51	240.696	264.237	642.794
52	222.746	262.190	625.680
53	241.514	258.606	631.615
54	253.918	275.513	667.688
55	327.471	330.011	832.080
56	117.932	124.837	316.728
57	147.447	142.739	367.910
58	130.342	120.456	322.366
59	105.963	127.325	302.295
60	159.634	175.625	431.800
61	121.899	88.962	281.791
62	183.097	143.746	422.545
63	179.581	156.513	431.357
64	128.054	108.676	315.222
65	187.750	168.547	466.122
66	186.204	214.771	520.399
67	259.379	236.005	642.303
68	194.829	191.199	491.457
69	291.430	294.137	751.099
70	202.706	224.283	543.089

TABLE VIII

C:TRAK-07.INT	LEFT	RIGHT	TOTAL
1	163.803	167.916	431.019
2	174.857	165.495	447.243
3	154.653	143.862	392.258
4	138.415	123.232	335.613
5	191.278	175.139	478.606
6	379.873	375.094	1025.133
7	427.123	406.225	1167.480
8	477.300	567.883	1381.383
9	278.810	297.621	783.668
10	472.030	355.713	1108.902
11	281.351	190.167	627.944
12	328.632	256.383	788.170
13	404.030	333.407	990.519
14	420.911	345.507	1024.042
15	300.902	314.985	802.279
16	152.915	166.046	420.167
17	406.138	273.708	905.732
18	162.333	135.594	397.030
19	215.910	170.124	513.909
20	340.313	288.014	869.262
21	333.518	225.115	743.491
22	269.019	231.351	669.789
23	404.300	280.147	944.290
24	338.782	216.973	738.207
25	356.933	274.226	850.547
26	318.966	288.841	832.069
27	490.898	429.385	1202.221
28	450.461	425.172	1182.460
29	271.729	214.491	663.952
30	429.766	290.975	978.188
31	463.174	411.503	1208.856
32	507.007	413.111	1205.077
33	472.705	362.151	1132.705
34	474.595	386.914	1127.219
35	401.862	363.503	1021.252
36	551.215	449.412	1376.525
37	452.127	339.392	1083.437
38	463.598	352.893	1102.915
39	346.025	314.350	888.329
40	419.286	327.117	1004.867

TABLE VIII CONT.

C:TRAK-07.INT	LEFT	RIGHT	TOTAL
41	424.052	347.895	1041.341
42	395.653	392.426	996.607
43	419.767	404.785	1065.664
44	644.050	517.484	1545.406
45	492.649	438.276	1282.671
46	413.269	337.695	988.396
47	858.754	568.953	1898.497
48	617.791	504.167	1467.529
49	248.645	223.672	611.646
50	434.692	396.391	1099.723
51	556.560	517.689	1436.951
52	632.787	450.350	1417.231
53	474.007	450.562	1239.591
54	460.742	375.328	1117.729
55	452.975	326.736	1064.719
56	290.850	283.373	743.591
57	369.675	318.689	928.380
58	313.391	318.728	835.579
59	408.346	284.830	937.461
60	438.764	369.181	1121.932
61	550.100	407.411	1284.064
62	471.120	390.436	1169.451
63	448.985	359.014	1084.650
64	492.677	342.942	1137.949
65	467.140	347.631	1118.668
66	467.034	353.435	1115.039
67	453.123	370.597	1112.495
68	610.481	500.223	1539.308
69	469.280	397.493	1200.179
70	568.007	483.496	1406.514
71	482.254	447.861	1290.558
72	510.575	385.286	1205.518
73	576.720	428.235	1347.555
74	424.310	326.229	1029.510
75	400.226	334.653	981.286
76	538.211	462.056	1342.425
77	470.382	378.242	1145.850
78	416.665	402.218	1126.438
79	706.191	507.622	1625.423
80	402.414	349.450	1002.906

TABLE IX

C:TRAK-08.INT	LEFT	RIGHT	TOTAL
1	191.048	156.557	457.304
2	151.098	106.960	338.520
3	165.451	120.624	362.945
4	121.559	86.743	266.299
5	133.592	111.519	313.182
6	229.720	169.513	515.256
7	120.105	88.046	270.547
8	168.072	108.986	364.695
9	152.892	107.888	338.016
10	145.517	99.306	315.161
11	223.334	228.148	582.177
12	198.139	156.168	458.312
13	166.689	120.090	364.586
14	152.566	113.427	347.762
15	134.363	114.182	326.323
16	218.486	173.457	524.322
17	182.244	171.176	461.708
18	230.971	141.034	476.758
19	374.200	310.441	932.963
20	163.688	116.128	365.899
21	146.591	109.177	333.427
22	195.042	183.996	484.012
23	207.337	151.387	468.248
24	180.312	116.195	383.247
25	203.303	152.751	466.100
26	237.935	173.458	537.933
27	292.318	249.649	706.067
28	227.443	183.367	531.326
29	231.707	184.260	537.750
30	236.613	171.871	529.954
31	297.215	212.829	648.449
32	291.763	226.761	658.514
33	316.895	261.146	743.021
34	386.511	260.785	849.389
35	410.192	311.898	926.695
36	140.892	130.165	355.752
37	399.429	294.792	936.238
38	310.488	292.962	796.990
39	291.864	197.641	633.253
40	322.717	258.965	749.192

TABLE IX CONT.

C:TRAK-08.INT	LEFT	RIGHT	TOTAL
41	411.930	321.608	992.772
42	209.593	144.979	463.647
43	230.912	194.880	562.030
44	250.326	188.832	576.902
45	197.620	155.887	470.623
46	300.754	271.786	727.632
47	353.392	333.501	898.355
48	259.254	239.028	634.452
49	323.988	343.370	864.365
50	221.838	216.137	562.761
51	346.814	213.028	727.422
52	396.257	277.514	858.148
53	311.645	200.904	669.215
54	291.941	193.392	621.149
55	305.959	235.962	696.572
56	696.462	711.899	1932.758
57	421.902	405.174	1054.093
58	458.212	359.082	1046.101
59	502.405	378.321	1117.766
60	558.791	454.545	1324.338
61	254.787	282.890	693.002
62	413.383	421.861	1067.341
63	282.766	310.093	736.540
64	306.401	305.620	772.131
65	267.952	283.192	702.353
66	441.285	446.049	1134.113
67	367.789	369.565	951.361
68	480.417	405.298	1126.596
69	464.180	369.773	1065.330
70	1635.041	1407.092	3764.837
71	287.541	259.551	693.788
72	212.432	193.789	522.729
73	461.175	398.534	1128.726
74	739.695	617.108	1838.070
75	519.404	415.087	1244.583
76	386.828	320.456	947.016
77	874.997	659.491	1896.045
78	194.583	177.610	486.439
79	171.647	158.224	430.943
80	208.257	146.193	475.780

TABLE X

C:TRAK-09.INT	LEFT	RIGHT	TOTAL
1	368.569	273.921	848.185
2	421.716	373.392	1040.876
3	353.713	352.852	918.475
4	452.530	475.951	1177.206
5	226.342	207.280	591.871
6	268.328	192.307	618.204
7	200.859	177.230	489.915
8	347.754	256.642	814.111
9	193.540	179.727	485.551
10	490.519	494.995	1271.500
11	292.766	277.288	750.149
12	241.743	231.430	619.731
13	254.159	203.797	599.542
14	384.773	382.720	1040.684
15	358.196	294.507	843.701
16	267.151	203.446	623.466
17	198.335	178.330	491.052
18	247.824	194.532	575.838
19	341.079	259.495	775.545
20	226.123	224.415	586.675
21	288.919	234.419	670.386
22	235.516	211.505	581.352
23	173.405	187.149	482.927
24	442.236	333.411	1014.418
25	592.387	533.589	1539.595
26	276.544	273.663	732.333
27	296.386	238.921	716.552
28	299.626	269.831	753.364
29	312.150	334.213	849.711
30	379.683	350.054	962.905
31	306.532	300.402	809.333
32	205.494	188.005	528.520
33	286.401	260.108	714.199
34	200.887	187.887	515.701
35	174.236	182.013	462.584
36	312.577	258.064	774.750
37	351.665	338.328	907.599
38	261.132	234.017	652.643
39	232.364	219.173	602.180
40	231.247	195.825	584.666

TABLE X CONT.

C:TRAK-09.INT	LEFT	RIGHT	TOTAL
41	253.117	247.632	673.532
42	189.231	163.679	462.142
43	188.543	183.142	479.811
44	364.199	359.726	938.909
45	220.173	290.820	676.080
46	457.918	407.866	1187.427
47	302.735	245.203	747.731
48	227.408	234.245	599.502
49	273.686	237.409	656.889
50	323.948	310.864	851.971
51	317.772	274.084	780.471
52	261.607	229.320	663.675
53	384.958	290.997	909.499
54	296.601	230.334	700.104
55	237.722	179.038	563.358
56	198.849	186.416	504.797
57	282.819	212.345	667.723
58	207.124	240.837	586.627
59	305.875	230.159	707.929
60	291.327	246.921	697.771
61	236.994	195.492	588.711
62	121.572	104.635	296.184
63	184.966	172.309	478.478
64	278.371	233.191	681.225
65	248.299	208.461	605.652
66	289.233	260.078	724.861
67	581.437	358.131	1267.898
68	275.921	237.605	670.618
69	247.724	204.186	595.044
70	210.578	177.017	493.473
71	412.147	348.082	1039.723
72	418.631	442.182	1148.930
73	305.889	277.323	781.043
74	371.683	321.974	892.395
75	436.548	487.638	1201.970
76	298.376	232.328	698.886
77	215.593	166.868	505.194
78	338.935	322.773	869.395
79	220.920	223.343	587.012
80	234.100	164.606	527.688

REPORT DOCUMENTATION PAGE

Form Approved
OMB No 0704-0188

1. AGENCY USE ONLY (Leave blank)	2. REPORT DATE	3. REPORT TYPE AND DATES COVERED
	February 1992	Contractor Report

4. TITLE AND SUBTITLE
Electroencephalographic Monitoring of Complex Mental Tasks

5. FUNDING NUMBERS
C NAS1-18847
WU 505-64-53-01

6. AUTHOR(S)
Raul Guisado, Richard Montgomery, Leslie Montgomery, and Chris Hickey

7. PERFORMING ORGANIZATION NAME(S) AND ADDRESS(ES)
Center for Neurodiagnostic Study, Inc.
275 Hospital Parkway
Suite 530
San Jose, CA 95119

8. PERFORMING ORGANIZATION REPORT NUMBER

9. SPONSORING / MONITORING AGENCY NAME(S) AND ADDRESS(ES)
National Aeronautics and Space Administration
Langley Research Center
Hampton, VA 23665-5225

10. SPONSORING / MONITORING AGENCY REPORT NUMBER
NASA CR-4425

11. SUPPLEMENTARY NOTES
Langley Technical Monitor: Alan T. Pope
Final Report

12a. DISTRIBUTION / AVAILABILITY STATEMENT
Unclassified - Unlimited

Subject Category 54

12b. DISTRIBUTION CODE

13. ABSTRACT *(Maximum 200 words)*

This final report outlines the development of neurophysiological procedures to monitor operators during the performance of cognitive tasks. Our approach included use of electroencephalographic (EEG) and rheoencephalographic (REG) techniques to determine changes in cortical function associated with cognition and REG in operator's state. A two channel tetrapolar REG, a single channel forearm impedance plethysmograph, a Lead I electrocardiogram (ECG) and a 21 channel EEG were used to measure subject responses to various visual-motor cognitive tasks. During the study period testing, analytical and display procedures for EEG and REG monitoring were developed, that extend the state of the art and provide a valuable tool for the study of cerebral circulatory and neural activity during cognition.

14. SUBJECT TERMS	15. NUMBER OF PAGES
Electroencephalography; Rheoencephalography; Human factors; Operator state	280
	16. PRICE CODE A13

17. SECURITY CLASSIFICATION OF REPORT	18. SECURITY CLASSIFICATION OF THIS PAGE	19. SECURITY CLASSIFICATION OF ABSTRACT	20. LIMITATION OF ABSTRACT
Unclassified	Unclassified		

NSN 7540-01-280-5500

Standard Form 298 (Rev 2-89)
Prescribed by ANSI Std. 239-18
298-102

*U.S. GOVERNMENT PRINTING OFFICE: 1992-627-064/60022

National Aeronautics and
Space Administration
Code NTT

Washington, D.C.
20546-0001